

# *Crustal Structure of Northeastern North America*

---

Results from the Ontario-New York-New England  
Seismic Refraction/Wide-Angle Reflection  
Experiment

A Thesis Submitted for the Degree of  
Doctor of Philosophy  
at the  
Department of Geology,  
Leicester University

by  
**Stephen Hughes B.Sc. (Durham)**

October, 1992

UMI Number: U041672

All rights reserved

INFORMATION TO ALL USERS

The quality of this reproduction is dependent upon the quality of the copy submitted.

In the unlikely event that the author did not send a complete manuscript and there are missing pages, these will be noted. Also, if material had to be removed, a note will indicate the deletion.



UMI U041672

Published by ProQuest LLC 2015. Copyright in the Dissertation held by the Author.  
Microform Edition © ProQuest LLC.

All rights reserved. This work is protected against  
unauthorized copying under Title 17, United States Code.



ProQuest LLC  
789 East Eisenhower Parkway  
P.O. Box 1346  
Ann Arbor, MI 48106-1346



7501128723



## *Abstract*

---

The Ontario-New York-New England seismic refraction/wide-angle reflection profile was acquired to investigate the deep structural inter-relationships between the southeastern Grenville province and the western New England Appalachians. The Grenville province is characterized by 45 km thick crust, with an average crustal seismic velocity of 6.6 km/s and a Poisson's ratio of  $0.28 \pm 0.01$ . In the mid-crust a laminated dome-like body is inferred to be composed of mafic cumulate sills on the basis of its high velocity (7.1 km/s) and Poisson's ratio (0.27). The lower crust is characterized by a velocity of 7.0 km/s which suggests a strongly mafic composition such as garnet pyroxene granulite. The Moho is a variable feature, characterized by en-echelon reflections suggestive of compositional interlayering. An anomalous mantle layer with a velocity of 8.6 km/s is proposed to represent an eclogized basaltic layer added to the lithosphere during Grenvillian orogenesis. The boundary between the Grenvillian craton and the western New England Appalachians is marked by an eastward dipping ramp structure which penetrates to a depth of 25 km where it soles out above a transitional mid-lower crustal interface. The New England Appalachians are characterized by an average crustal velocity of 6.4 km/s and a sharply reflective Moho delineating crustal thinning from 41 km to 37 km towards the Atlantic margin. The lower crustal velocity is 6.8 km/s, with a Poisson's ratio of  $0.26 \pm 0.01$ . In contrast to the Grenvillian craton the seismic properties of the Appalachian lower crust are consistent with an intermediate composition interlaced with mafic sills related to extensional underplating and intrusion during the rifting of the Atlantic Ocean.

# *Table of Contents*

---

Title Page	
Frontispiece.....	ii
Abstract .....	iii
Acknowledgments .....	iv
Table of Contents.....	v
List of Illustrations .....	x
List of Tables .....	xiii
List of Plates .....	xiv
<b>Introduction.....</b>	<b>1</b>
<b>Chapter 1: Crustal Structure of the Western New England Appalachians and the Adirondack Mountains</b>	
1.1 Abstract.....	4
1.2 Introduction.....	6
1.3 Profile Geology.....	7
1.4 Crustal Structure and Geophysical Framework.....	9
1.5 The Experiment .....	11
1.6 Description of the Principal Seismic Phases.....	12
1.7 Seismic Modeling.....	13
Description of the New England Model .....	15
Description of the Grenvillian Model.....	21
Description of the Ramp Structure.....	22
1.8 Shear Wave Analysis .....	24
1.9 Discussion .....	25

# *Acknowledgments*

---

The completion of this thesis owes much to the contributions of others who kindly assisted my research efforts and helped to make my time at the USGS both productive and stimulating. Special thanks are due to my supervisors at the US Geological Survey Jim Luetgert and Walter Mooney. Thanks Jim for putting up with my A-Z of things to complain about when it all got to much to handle (America to Zelt?). To Walter Mooney, surely the only person I know, who when suggesting that it was time to get on with some work would leave me a line from Richard III, 'I've wasted time, now doth time waste me'.

My thanks are due to Peter Maguire for allowing me the freedom to abandon ship and pursue my research interests at the USGS.

To my two drinking buddies, Harley for the coffee, and Tom for the beer (I owe you one or two!) I can not thank you enough. I owe thanks to Jill McCarthy, Tom Brocher, Dave Stewart, Rolfe Stanley, Steve Bohlen, and Bob Simpson for their interest and encouragement. In addition, I'd like to thank all the people with whom I participated on the many fieldwork projects at the USGS.

John Cipar, US Air Force Geophysics Laboratory, provided financial support for my sojourn at the USGS, and funding for the collection of a suite of rock samples from Vermont. In this endeavor I would also like to thank Nic Christensen and Dean Ballotti at Purdue University for sample preparation and laboratory measurements.

## Table of Contents

---

Structure of the Grenvillian Ramp.....	26
Composition of the Grenvillian Crust.....	28
Composition of the Appalachian Crust.....	29
1.10 Acknowledgments.....	35
1.11 References.....	36
1.12 Captions.....	43
1.13 Figures.....	49

## Chapter 2: Crustal Structure of the Southeastern Grenville Province

2.1 Abstract.....	65
2.2 Introduction.....	68
2.3 Regional Geology.....	69
2.4 Crustal Structure and Geophysical Framework.....	72
2.5 The Experiment.....	75
2.6 Description of the Principal Seismic Phases.....	76
2.7 Seismic Modeling.....	78
The Upper Crust.....	81
The Mid-Crust.....	85
The Lower Crust and Moho.....	89
The Upper Mantle.....	91
2.8 Discussion.....	92
The Tahawus Complex.....	94
The Mid-Lower Crustal Reflector.....	96
The Lower Crust.....	97
The Moho and Upper Mantle.....	99
Tectonic Model.....	100
2.9 Acknowledgments.....	103
2.10 References.....	104
2.11 Captions.....	110
2.12 Table.....	117

## Table of Contents

---

2.13 Figures.....	118
-------------------	-----

### **Chapter 3: Is the Moho a Late-Stage Feature?**

#### **Evidence for Structural Variations Beneath the Ontario-New York-New England Seismic profile**

3.1 Abstract.....	133
3.2 Introduction.....	135
3.3 Results - Structure of the Lower Crust and Upper Mantle.....	136
The Southeastern Grenville Province.....	137
The Western New England Appalachians.....	138
3.4 Discussion - Evolution of the Lower Crust and Upper Mantle..	138
Underplating and Eclogization of the Grenvillian Crust.....	139
Rifting of the Iapetan Margin.....	141
The Grenvillian Ramp.....	141
The Appalachian Lower Crust.....	142
3.5 Conclusion.....	144
3.6 Acknowledgments.....	145
3.7 References.....	146
3.8 Captions.....	150
3.9 Figures.....	151

### **Chapter 4: Seismic Anisotropy and Structural Inter-Relationships across the Grenvillian-Appalachian Boundary in New England**

4.1 Abstract.....	154
4.2 Introduction.....	156
4.3 Structural Framework of the Grenvillian-Appalachian Boundary.....	157
4.4 Geophysical Constraints on the Deep Crustal Structure.....	159
4.5 Rock Samples.....	162
4.6 Discussion.....	164

## Table of Contents

---

Composition .....	164
Structure and Anisotropy .....	165
Spatial Sampling.....	166
4.7 Conclusions .....	167
4.8 Acknowledgments .....	168
4.9 References .....	169
4.10 Captions.....	173
4.11 Table .....	176
4.12 Figures.....	177

## Appendix A: Data Report for the Ontario-New York-New England

### Seismic Refraction/Wide-Angle Reflection Experiment

A.1 Introduction.....	184
A.2 Background.....	185
A.3 Description of the Survey.....	185
A.4 Instrumentation and Data Reduction .....	187
The Seismic Recorders.....	187
Data Reduction.....	188
Record Sections .....	189
A.5 Description of the Plates .....	189
A.6 Acknowledgments.....	192
A.7 References.....	193
A.8 Captions.....	194
A.9 Table.....	195
A.10 Figures .....	196

## Appendix B: Travel-time Modeling of Seismic Refraction/Wide-Angle

### Reflection Data: Forward and Inverse Methods

B.1 Introduction.....	203
B.2 Assumptions and Restrictions.....	204

## Table of Contents

---

B.3 Reduction of the Seismic Data.....	204
B.4 The Forward Method - Iterative Ray Trace Modeling.....	205
Model Parameterization.....	205
The Raytrace Algorithm.....	206
Errors and Model Uniqueness .....	207
The Lateral Position of the Grenvillian Ramp Structure.....	208
The Dipping Geometry of the Grenvillian Ramp Structure.....	211
Internal Structure of the Grenvillian Ramp Structure.....	212
Practical Application .....	214
B.5 The Inverse Method - Linearized Travel Time Inversion.....	214
Least Squares Inversion Theory .....	215
Resolution.....	217
Errors and Model Uniqueness .....	218
Practical Application .....	218
B.6 Discussion and Conclusions.....	219
B.7 References.....	221
B.8 Captions.....	222
B.9 Table.....	223
B.10 Figures.....	224

## **Appendix C: Rock Sample Data**

C.1 Introduction.....	230
C.2 Description of the Rock Samples.....	230
C.3 Reference .....	232
C.4 Caption.....	232
C.5 Table.....	233

# *List of Illustrations*

---

## **Chapter One:**

1.1 Geologic Map of Western New England.....	49
1.2 Seismic Velocity Model of Western New England.....	50
1.3 Record Section for Shotpoint 1.....	51
1.4 Record Section for Shotpoint 10 West.....	52
1.5 Record Section for Shotpoint 7 East.....	53
1.6 The Upper Crustal Low Velocity Zone.....	54
1.7 Evidence for the Mid-Lower Crustal Interface.....	55
1.8 Record Section for Shotpoint 10 East.....	56
1.9a Enlarged Portion of Record Section for Shotpoint 10 East.....	57
1.9b Enlarged Portion of Record Section for Shotpoint 10 East.....	58
1.10 Record Section for Shotpoint 7 West.....	59
1.11 The Appalachian-Grenvillian Transition.....	60
1.12 Poisson's Ratios at the Edge of the Adirondack Mnts.....	61
1.13 Geologic Interpretation of the Velocity Model.....	62
1.14 Comparison of Ramp Structures.....	63
1.15 The Composition of the Lower Crust.....	64

## **Chapter Two:**

2.1 Geologic Map of the Southeastern Grenville Province.....	118
2.2 Geophysical Experiments in the Central Granulite Terrane.....	119
2.3 Record Section for Shotpoint 16 West.....	120
2.4 Record Section for Shotpoint 10 West.....	121
2.5 Seismic Velocity Model.....	122
2.6 One-Dimensional Model for Shotpoint 20.....	123
2.7 Inversion for Upper Crustal Velocity and Interfaces.....	124

## List of Illustrations

---

2.8 The Tahawus Complex.....	125
2.9 Inversion for Mid-Crustal Interfaces .....	126
2.10 The Lower Crustal Reflector.....	127
2.11 Inversion for Lower Crust and Upper Mantle.....	128
2.12 The Upper Mantle.....	129
2.13 Interpretive Deep Crustal Section .....	130
2.14 The Composition of the Lower Crust.....	131
2.15 Tectonic Scenario .....	132

### Chapter Three:

3.1 Location Map.....	151
3.2 Velocity model.....	152
3.3 Moho Reflections.....	153

### Chapter Four:

4.1 Geologic map of the Grenvillian-Appalachian Boundary.....	177
4.2 Cross section through the Grenvillian Ramp .....	178
4.3 Seismic Refraction and Reflection Images .....	179
4.4 Samples from the Adirondacks and the Appalachians.....	180
4.5 Rock Samples at 100 MPa .....	181
4.6 Effect of Retrogressive Metamorphism on Seismic Velocity.....	182
4.7 Anisotropic Properties of Mylonitized Gneisses.....	183

### Appendix A:

A.1 Shotpoints Fired During the Experiment.....	196
A.2 Recording Sites and Shotpoints for Deployment 1 .....	197
A.3 Recording Sites and Shotpoints for Deployment 2 .....	198
A.4 Recording Sites and Shotpoints for Deployment 3 .....	199
A.5 The High Density, Wide-Angle Reflection Experiment .....	200
A.6 Recording Sites for Reflection Experiment.....	201
A.7 Response Curves for Instruments .....	202

**Appendix B:**

B.1 Model Parameterization .....	224
B.2 Travel time diagrams for the Grenvillian Ramp.....	225
B.3 Travel time diagrams for Ramp 1 and Ramp 2.....	226
B.4 Travel time diagrams for Ramp 3 and Ramp 4.....	227
B.5 Linearized Inversion .....	228
B.6 Trade-off Between Resolution and Damping.....	229

# *List of Tables*

---

## **Chapter Two:**

2.1 Final Results of the Travel Time Inversion.....	117
-----------------------------------------------------	-----

## **Chapter Four:**

4.1 Location and composition of samples .....	176
-----------------------------------------------	-----

## **Appendix A:**

A.1 Master Shot List.....	195
---------------------------	-----

## **Appendix B:**

B.1 Comparison of Forward and Inverse Methods.....	223
----------------------------------------------------	-----

## **Appendix C:**

C.1 Seismic velocity measurements of rock samples .....	233
---------------------------------------------------------	-----

# *List of Plates*

---

## **Plate 1**

Shotpoints 1, 2, 3 and 4 recorded on deployment 1.

## **Plate 2**

Shotpoints 5, 6 and 7 recorded on deployment 1.

Shotpoints 7, 8 and 9 recorded on deployment 2.

## **Plate 3**

Shotpoints 10 and 14 recorded on deployments 1,2 & 3.

Shotpoints 11, 12 and 13 recorded on deployment 2.

## **Plate 4**

Shotpoints 15, 16, 17 and 18 recorded on deployment 3.

## **Plate 5**

Shotpoints 19, 20, 21 and 22 recorded on deployments 2 and 3.

## **Plate 6**

Shotpoint 4, 7, 8 and 9 recorded on deployment 2 [fan].

Shotpoint 11 recorded on deployment 2.

Shotpoint 23 recorded on deployment 1.

## **Plate 7**

Shotpoint 12, 13, 14, 17, 20, 21 and 22 recorded on deployment 2.

## **Plate 8**

Shotpoint 4, 5 and 7 recorded on the reflection experiment.

## *-Introduction-*

---

Geologic investigations in northeastern North America began around the turn of the century. These early endeavors paved the way for a succession of investigators to establish a geologic literature that is renowned in both its scope and intricacy. Fundamental conceptual advances in understanding the mechanisms of crustal formation awaited the development of tectono-stratigraphic principles which saw the amalgamation of stratigraphic, metamorphic and structural studies into a sequential tectonic framework. This framework seeks to coalesce a complex mosaic of interwoven crustal fragments upon the North American craton through successive accretionary episodes spanning more than a billion years of crustal orogenesis in northeastern North America. The acquisition of regional-scale seismic data provides the fundamental means of examining large-scale crustal features left as remnants of the orogenic processes which bound the crust together during the Grenvillian and Appalachian orogenies.

Seismic studies of the lithosphere are large and expensive projects which by necessity involve numerous people through the various stages of project inception to successful acquisition of the seismic data set. The principle data set used in this thesis consists of 650 km of seismic refraction/wide-angle reflection data spanning the southeastern Grenvillian craton into the Adirondack massif and extending across the western New England Appalachians. The Ontario-New York-New England seismic profile was acquired by the US Geological Survey (USGS) in collaboration with the Geological Survey of Canada (GSC) and the US Air Force Geophysics Laboratory (AFGL). I present an interpretation of this seismic

## Introduction

---

data, together with complementary geophysical and rock sample data, in order that the deep crustal structure of northeastern North America may be resolved, and thereby provide constraints for studies of the tectonic evolution in North America. Four manuscripts are presented together with three appendices summarizing technical information not contained within the body of the individual manuscripts. Each manuscript was co-authored by my colleague Dr. J.H. Luetgert (USGS), and further aided and abetted by Dr. W.D. Mooney (USGS). The contributions of these scientists in initiating the projects, collecting the data, and by providing the impetus necessary for a complete interpretation of the data warrant co-authorship. In each case, however, the analysis, writing and principal interpretations are my own.

The first two chapters contain detailed descriptions of the modeling procedures used to interpret the Ontario-New York-New England seismic refraction/wide-angle reflection data set. Chapter one contains a manuscript published in the *Journal of Geophysical Research* that describes raytrace forward modeling of the eastern portion of the seismic data set in the western New England Appalachians and the adjacent Adirondack Highlands. Interpretation of this seismic velocity model provides evidence for the obduction of the allochthonous western New England Appalachians upon the Grenvillian craton above a zone of detachment that penetrates at least to mid-crustal depths and was the locus of successive Paleozoic thrusting.

In chapter two the application of a simultaneous travel time inversion to the western portion of the seismic data set is described. The velocity model provides important evidence for underplating and mafic intrusion of the lower crust during the Grenvillian orogeny. Remnants of these magmatic processes survive in the mid-lower crust as a layered cumulate body and as a lens of eclogite in the upper mantle, possibly delaminated from the over-thickened crust prior to exhumation of the Adirondack

## Introduction

---

massif. This manuscript has been accepted for publication in the *Journal of Geophysical Research*.

Chapter three presents a geologic synthesis of the principal seismic results, with emphasis placed on characterizing the role of the lower crust and lithospheric mantle during orogenesis and subsequent post-orogenic equilibration. The seismic expression of the lower crust and Moho is interpreted as a post-orogenic feature, which reflects thermal and extensional processes in the lower crust and upper mantle. This manuscript is presently in review, pending publication in *Geology*.

In chapter four an integrated petro-physical and geophysical approach is applied to re-examine the seismic structure of the Grenvillian-Appalachian boundary. Laboratory measurements of seismic velocity for a suite of rock samples collected from the western New England Appalachians are used to show that resolution of the imbricated basement structures is inhibited by the anisotropic properties of the polydeformed and retrogressive paragneisses. Co-authorship with Dr. N.I. Christensen (Purdue University) is acknowledged with respect to laboratory measurements. This manuscript is presently in review, pending publication in *Tectonophysics*.

Appendix A presents the seismic refraction/wide-angle reflection data on enlarged pullout plates to facilitate inspection of the data. This appendix is an abbreviated version of the US Geological Survey Open File Report, and was co-authored by J.H. Luetgert (USGS), J. Cipar (AFGL), S. Mangino (AFGL), D. Forsyth (GSC) and I. Asudeh (GSC). Appendix B presents a technical description of the forward and inverse methodologies employed to model the seismic data. Appendix C presents high pressure laboratory measurements of seismic velocity for the rock samples used in chapter 4.

## **Crustal Structure of the Western New England Appalachians and the Adirondack Mountains**

### **1.1 Abstract**

We present an interpretation of the crustal velocity structure of the New England Appalachians and the Adirondack mountains based on a seismic refraction/wide-angle reflection experiment in eastern North America extending from the Adirondacks in New York State, through the northern Appalachians in Vermont and New Hampshire to central Maine. Modeling of the eastern portion of the profile within the New England Appalachians shows a sub-horizontal layered crust with upper-crustal velocities ranging from 5.5 to 6.2 km/s, a mid-crustal velocity of 6.4 km/s, and a lower crustal velocity of approximately 6.8 km/s. Crustal thickness increases from 36 km beneath Maine to 40 km in Vermont. Little evidence is seen for structures at depth directly related to the White mountains or the Green mountains. A major lateral velocity change in the upper and mid-crust occurs between the Appalachians and the Adirondacks. This boundary, projecting to the surface beneath the Champlain Valley, dips to the east beneath the Green mountains and extends to a depth of ~25 km below the eastern edge of the Connecticut Valley Synclinorium in Vermont. The Tahawus complex, a series of strong horizontal reflections at 18 to 24 km depth beneath the Adirondack Highlands is seen to dip

eastwards beneath Vermont. Upper crustal rocks in the Adirondack mountains have Poisson's ratios of  $0.28 \pm 0.01$  that can be correlated with the Marcy Anorthosite. Poisson's ratios of  $0.24 \pm 0.01$  calculated for rocks of the Connecticut Valley Synclinorium indicate a siliceous upper crust in Vermont. The lower crust is considered to be best represented by intermediate to mafic granulites; a high Poisson's ratio (0.26-0.27) tends to support a mafic lower crust in the New England Appalachians. This seismic refraction/wide-angle reflection experiment provides further evidence for the obduction of the allochthonous western Appalachian units onto Grenvillian crust above a zone of detachment that penetrates at least to mid-crustal depths and was the locus of successive Paleozoic thrusting.

## 1.2 Introduction

The New England Appalachians are characterized by a series of tectono-stratigraphic terranes accreted to North America during multiple Paleozoic orogenic events. Three major terranes are identified across the northern Appalachians; (1) a western terrane underlain by Grenvillian crust and overthrust by allochthons that contain Grenvillian basement with Lower Paleozoic shelf sediments, (2) a central terrane typified by island arc volcanics of the Bronson Hill Anticlinorium and miogeoclinal lithologies of the Merrimack Synclinorium, and (3) an Avalonian terrane with distinctive Precambrian and Mid-Paleozoic faunas. It is increasingly recognized that such terranes are in fact a complex composite collage of smaller (suspect) terranes.

The deeply eroded Appalachian orogen is the center of numerous controversies relating to the mechanisms and extent of terrane accretion during the Lower Paleozoic. Seismic refraction/wide-angle reflection experiments are capable of resolving deep continental structures, and provide a means of inferring relationships between the surface geology and the underlying crust. This paper reports on recently acquired seismic refraction/wide-angle reflection data collected across the western New England Appalachians, and attempts to answer the following questions; (1) What is the velocity structure of the New England crust? (2) What is the structural relationship between the Grenville province and the allochthonous New England Appalachians? (3) What constraints can be applied to the inference of lower crustal composition from compressional and shear-wave data? We begin with an overview of the regional geology observed along the profile and present a summary of the interpreted crustal structure from previous geophysical studies in New England, before moving on to a description of the two-dimensional seismic velocity model.

Finally, an interpretation of the crustal velocity structure and the inferred crustal composition is presented.

### **1.3 Profile Geology**

The refraction/wide-angle reflection profile discussed here extends from the Grenville province exposed in northern New York State, across the western New England Appalachians and on into central Maine (Figure 1.1). The profile crosses six tectono-stratigraphic units, which are from west to east; (1) the Mid-Proterozoic Grenvillian basement exposed in the Adirondack mountains (northern New York), (2) autochthonous platformal sediments and allochthonous slope-rise sediments of the Taconic sequence, (3) imbricated and metamorphosed Lower Paleozoic flysch deposits and underlying Grenvillian basement of the Green mountains (central Vermont), (4) Silurian to Lower Devonian meta-pelites of the Connecticut Valley Synclinorium (eastern Vermont), (5) Ordovician forearc sediments and volcanics of the Bronson Hill Anticlinorium (New Hampshire), and (6) metamorphosed and deformed Silurian to Devonian turbidites of the Merrimack Synclinorium. Numerous articles have been written discussing the tectonic evolution of the northern New England region (Osberg, 1978; Robinson and Hall, 1979; Williams and Hatcher, 1982; Bradley, 1983; Zen, 1983; Taylor, 1989). However, for the purposes of our study we present a generalized overview of the litho-tectonic units traversed by the profile and describe the nature of the contacts between these units.

Our transect begins in the Proterozoic domal massif of the Adirondack mountains, which forms an anomalous topographic feature extending southeastwards from the Grenville province of eastern Canada. The Adirondack Highlands expose an oblique section through the Proterozoic mid-lower crust (Selleck, 1980; McLelland and Isachsen, 1986). A complex

assemblage of ductily deformed and interleaved granulite facies meta-pelites, marbles and quartzites are exposed in the Adirondack Highlands (Wiener *et al.*, 1984; McLelland and Isachsen, 1986). Intruding the gneisses are meta-anorthosite bodies, the largest of which is the Marcy Anorthosite (Figure 1.1). The Adirondack dome is surrounded by Cambrian platformal carbonates and quartzites which lie unconformably upon the Grenvillian basement. This autochthonous wedge of Cambrian sediments lies *in situ* between Grenvillian basement and the allochthonous Taconic (Mid-Upper Ordovician) units of the western Appalachians.

The contact between the Appalachian and Grenville provinces lies beneath the Champlain Valley. In the Champlain Valley Cambrian to Lower Ordovician continental shelf sediments and deep marine clastics (Foreland Thrust Belt) lie unconformably on the Grenvillian autochthon. These sediments have been interpreted as an accretionary complex developed above the eastward subducting Grenvillian margin during the Mid-Ordovician Taconic orogeny (Rowley and Kidd, 1980; Stanley and Ratcliffe, 1985). Subsequent closure of the Taconic subduction system resulted in the obduction of allochthonous slices of Grenvillian 'basement' which now form the core of the Green Mountain Anticlinorium exposed in central Vermont. To the east of the Green mountains, the Taconic 'suture' is traced by the Vermont Ultramafic Belt which is interpreted as altered slivers of oceanic crust and upper mantle imbricated with accretionary prism sediments (Osberg, 1978; Bradley, 1983; Stanley and Ratcliffe, 1985).

From the eastern edge of the Green mountains the profile proceeds eastwards across the Connecticut Valley Synclinorium. Silurian to Lower Devonian meta-pelites and carbonates attain chlorite grade metamorphism (Rodgers, 1970). These post-Taconic sediments are interpreted to be a shallow thrust sheet juxtaposed against the Bronson Hill Anticlinorium by the Ammonoosuc fault. The Bronson Hill island arc complex accreted in

the Taconic orogeny is exposed as a linear belt of volcanics stretching through eastern Vermont and western New Hampshire. The Bronson Hill Anticlinorium can be traced through the central New England Appalachians as an aligned chain of elliptical gneissic domes (Oliverian Plutonic Series) mantled by a series of Mid-Ordovician meta-volcanics and meta-sediments. Metamorphic grades vary from greenschist facies to upper amphibolite facies at the cores of the Oliverian gneissic domes (Rodgers, 1970). Overlying these eugeoclinal lithologies is a series of Silurian to Lower Devonian meta-pelites and carbonates belonging to the Connecticut Valley Synclinorium to the west, and the Merrimack Synclinorium to the east.

The Merrimack Synclinorium lies to the east of the Bronson Hill Anticlinorium. This broad structural low contains a thick sequence of Silurian to Devonian deep marine clastics, and locally calc-silicates and meta-volcanics typically attaining upper amphibolite grade metamorphism. At least three phases of nappe emplacement and associated regional metamorphism in the Acadian (Mid-Devonian) orogenic events have resulted in widespread ductile deformation of these mid-crustal rocks now exposed at the present erosion surface (Chamberlain and England, 1985; Eusden *et al.*, 1987). The Merrimack Synclinorium has been extensively intruded by Acadian granites of the New Hampshire Plutonic Series and by the Jurassic White Mountain Magma Series which forms a north-south elongate batholith composed predominantly of syenite, granite and monzonite (McHone and Butler, 1984).

#### **1.4 Crustal Structure and Geophysical Framework**

A recent synthesis of geophysical data collected through the Appalachian orogen indicates that significant differences exist in the deep crust between the northern Appalachians and the adjacent Grenville

province (Taylor, 1989). The New England Appalachians are characterized by a relatively thick crust (~40 km) with an average seismic velocity of 6.4 km/s, whereas the Adirondacks have a somewhat thinner crust (36 km), and high velocities ( $\geq 6.6$  km/s) are observed throughout the crust in this region (Taylor and Töskoz, 1982; Taylor, 1989). Previous deep crustal studies in the New England orogen have included seismic refraction/wide-angle reflection profiles collected in northern Maine and Quebec, and seismic reflection profiles collected across southern Vermont and northern New York State. Interpretation of these data sets suggests that the autochthonous Grenvillian basement extends beneath at least the western portion of the allochthonous Appalachian orogen.

Seismic reflection and refraction profiles were obtained in 1984 by the US Geological Survey (USGS) and the Geological Survey of Canada (GSC) across and along strike to the northern Appalachians in Maine and Quebec (Figure 1.1-line 1). Analysis of the seismic data from the Quebec-Maine transect provides evidence for the eastward extension of Grenvillian basement beneath the northern Appalachians. A major zone of reflections can be traced over some 200 km from shallow depths beneath the St. Lawrence Lowlands to approximately 25 km below the Chain Lakes massif (Stewart *et al.*, 1986; Spencer *et al.*, 1987; Spencer *et al.*, 1989). These reflections have been interpreted as a 'décollement' separating the Grenvillian basement from the allochthonous Appalachians (Spencer *et al.*, 1989).

In central Maine, a 180-km-long cross profile shot along the axis of the Merrimack Synclinorium reveals a 38 km thick crust (Figure 1.1-line 2). In the region where line 2 crosses the seismic refraction/wide-angle reflection profile discussed herein the upper crust has velocity between 6.0 and 6.3 km/s, and is characterized by strong lateral and vertical seismic velocity variations. The base of the Merrimack Synclinorium at 15 km depth is

marked by an increase in velocity to 6.4 km/s. The lower crust has a velocity of 6.8 km/s (Hennet *et al.*, 1991). Normal moveout corrections applied to Moho reflections in the vicinity of our profile (Shotpoint 2) indicate that the crust is 37-38 km thick in eastern Maine (Luetgert *et al.*, 1987).

Deep seismic reflection profiles in southern Vermont (Figure 1.1-line 3) display the seismically transparent Grenvillian basement extending eastwards beneath the 'thin skin' of the Taconic sequence to approximately 25 km beneath the Connecticut Valley Synclinorium (Brown *et al.*, 1983; Ando *et al.*, 1984). The buried edge of the Grenville province was interpreted to be a highly deformed thrust-imbricated zone passing eastwards into a transitional lower crust of undetermined basement type. The Green mountains were identified as an imbricated thrust slice obducted above the lower crustal penetrating ramp. Reflection profiling across the southern Adirondacks revealed a striking band of high reflectivity between 6 and 8 seconds two-way travel-time, or approximately 18-26 km in depth (Brown *et al.*, 1983; Klemperer *et al.*, 1985). These authors applied the name Tahawus complex to this set of reflections and this name is retained here.

## 1.5 The Experiment

Seismic refraction/wide-angle reflection data were acquired by the US Geological Survey (USGS), the US Air Force Geophysical Laboratory (AFGL) and the Geological Survey of Canada (GSC) during the fall of 1988. This profile is 650 km long and traverses the central New England Appalachians before extending west through the Adirondacks and into the Proterozoic craton of southern Ontario. The results of analysis of the easternmost 300 km of this profile are presented below. Exceptionally high quality seismic data were obtained at offsets ranging from 0 to 450 km along a continuous linear refraction profile recorded in three separate deployments. Data were recorded by 120 USGS portable FM cassette recorders (Murphy, 1989) and 150

GSC digital instruments (I. Asudeh, *personnel communication*, 1988). In each case 2 Hz geophones were deployed. The seismometer spacing was nominally 800 m with an estimated survey location error of 25 m. In total 32 shots, ranging in size from 900 kg to 2700 kg, were detonated along the entire profile length; 3 fan shots were also recorded. The shotpoint spacing was 30 to 40 km (Luetgert *et al.*, 1990).

### 1.6 Description of the Principal Seismic Phases

The data set gathered by this seismic experiment provides a unique opportunity to derive the seismic velocity structure of the New England Appalachians and the adjacent Grenville province. We present a brief description of the principal phases observed on the seismic record sections. Emphasis will be placed on broad generalities, although it should be borne in mind that lateral variations do exist along the length of the profile. Subsequently, the major features of the derived two-dimensional model are highlighted, and a detailed description of the travel-time and synthetic amplitude modeling used to derive the final model shown in Figure 1.2 is presented.

The record section for shotpoint 1 is representative of the seismic data gathered in New England; principally it shows four characteristic phases labeled  $P_g$ ,  $P_{1VZ}P$ ,  $P_iP$ ,  $P_mP$  on Figure 1.3. The upper crust in New England is characterized by a laterally extensive and impulsive first arrival branch ( $P_g$ ) with apparent velocity 6.0-6.1 km/s. Significantly, no crustal first arrival phases are observed with apparent velocities exceeding 6.2 km/s. The relatively low amplitude of the first arrival branch at offsets exceeding 50 km is a result of plotting normalized traces, where the amplitude of the first arrival branch is relative to the amplitude of the secondary arrivals. In Maine, localized high-amplitude wide-angle reflections ( $P_{1VZ}P$ ) are observed at offsets from the source of 20-60 km. Prominent mid-crustal wide-angle

reflections ( $P_tP$ ) are the most striking feature of this data set. In western Maine and New Hampshire, strongly coherent wide-angle reflections appear at post-critical offsets between 70-120 km. Evidence for phases refracted within the lower crust in New England are tenuous. The seismic velocity structure of the lower crust must be indirectly inferred from analysis of Moho reflections ( $P_mP$ ) as they asymptotically approach the lower crustal refracted phase. In New England the upper mantle is characterized by emergent direct arrivals ( $P_n$ ) at offsets exceeding 160 km, and by segmented en-echelon  $P_mP$  reflections, possibly indicative of complex lamination around the crust/mantle transition. The apparent velocity of the upper mantle is  $8.0 \pm 0.1$  km/s.

The record section for shotpoint 10 west is characteristic of data collected across the Grenvillian Adirondack massif (Figure 1.4). Exceptionally high upper crustal velocities (6.6 km/s) are associated with the Grenvillian crust. Conspicuous high amplitude, wide-angle reflections ( $P_tP$ ) are observed at offsets between 50 and 90 km. Strongly coherent en-echelon reflection segments ( $P_tP$ ) suggest a laminated mid-crustal body beneath the Adirondack massif, referred to previously as the Tahawus complex.

### 1.7 Seismic Modeling

Two-dimensional ray-trace modeling, asymptotic ray-theory synthetics and full-waveform reflectivity synthetic seismograms were used to derive a seismic velocity model from this data set. The two-dimensional seismic velocity model is comprised of two discrete and independently derived 'blocks' which are connected by a mid-crustal penetrating ramp structure (Figure 1.2). The New England Appalachian crust is essentially composed of three sub-horizontal planar layers, (1) an upper crust with apparent velocities in the range 6.0-6.2 km/s, (2) a 10 km thick mid-crustal layer

modeled with a negative gradient between 6.5-6.4 km/s, and (3) a lower crustal layer with an estimated velocity of 6.7-7.0 km/s. In northern New York State the Grenvillian Adirondack mountains are represented by a model consisting of a two layer crust. High upper crustal velocities of 6.6 km/s and a mid-crustal reflecting interface are the most prominent features of the model in this region. Once modeling was completed for the Appalachian and Adirondack 'blocks', the contact between these two terranes was analyzed. The high velocity Adirondack 'block' was imaged in the form of a ramp extending to mid-crustal depths beneath the Appalachian upper crust in Vermont (Figure 1.2). Crustal thickness varies from 36 km in western Maine to 40 km in Vermont.

Modeling of this Appalachian data set was completed in successive phases, each used to constrain subsequent iterations and so to improve the resolution of the final model. Initially, seismic velocity functions for each shotpoint were calculated using one-dimensional raytrace modeling assuming a plane homogeneous layered Earth (Luetgert, 1988b; Luetgert, 1988c). Reference was made to reciprocal travel-times to aid in the identification and correlation of phases. The shotpoint spacing is insufficient to resolve individual igneous bodies, and consequently minor travel-time perturbations associated with localized variations in the surface geology have not been modeled. The one-dimensional models were extensively used to minimize the number of iterations required in successive two-dimensional raytrace modeling described in the following section.

An initial composite two-dimensional seismic velocity model was constructed by contouring one-dimensional homogeneous layer solutions computed at each shotpoint. Iterative two-dimensional raytracing was used to constrain the velocity boundaries (Cerveny *et al*, 1977; Luetgert, 1988a). Topography was included in the model. Incorporation of wide-angle and

near-vertical reflections for each shotpoint significantly increased the resolution of the model. Identification of critical points for the major reflected phases ( $P_mP$ ,  $P_iP$ ) allowed velocity contrasts across interfaces to be estimated. Seismic velocity gradients and velocity contrasts were estimated by means of amplitude modeling. In the eastern part of the profile the model is approximately one-dimensional, and full-waveform reflectivity modeling was used to determine the relative amplitude characteristics of the observed phases.

Generally, observed and calculated travel-times for the model presented in Figure 1.2 match to 0.1 s or less, with no mismatches greater than 0.2 s. The sensitivity of the model is greatest in the uppermost 10 km where the ray density is greatest. Within the upper crust (layers 2/3) the error in depth to interfaces is probably no greater than several hundred meters, and the corresponding precision in the derived velocity is  $6.05 \pm 0.05$  km/s. The velocity gradient in the upper crust is  $0.01 \text{ s}^{-1}$ , this value is tightly constrained by the lateral persistence of the first arrival phase ( $P_g$ ). The magnitude of the mid-crustal velocity discontinuity (layers 3/5) is inferred from amplitude modeling to be precise to  $\pm 0.1$  km/s. Considerably more uncertainty exists for the velocity structure of the lower crust as this has largely been indirectly inferred from secondary arrivals. The precision of the modeled lower crustal velocity is probably no better than  $6.8 \pm 0.2$  km/s; beyond these limits acceptable travel-time and amplitude constraints are exceeded. In view of the poorly constrained lower crustal velocity structure, a 2 km uncertainty in the Moho depth may be expected, although the dipping geometry is unlikely to be affected by this. Uncertainties introduced by the interpretive step of phase correlation are usually much larger than the quantifiable uncertainties listed above (Mooney, 1989).

*Description of the New England Model:* A detailed description of the compressional-wave velocity model shown in Figure 1.2 is presented below.

Justification for each layer in terms of its apparent velocity and structure is related to the key phases identified on the record sections. The upper crust is represented by a model consisting of three layers. The near surface (layer 1) has seismic velocities in the range 5.5-5.7 km/s. An additional 'cover' layer is modeled along the eastern portion of the profile, with a seismic velocity of 5.0 km/s. The upper crust (layer 2) is characterized by a seismic velocity of 6.05 km/s increasing to 6.1 km/s at the base of the layer. The 6.05 km/s refracted phase is observed extending to offsets of 120 km, requiring a vertical seismic velocity gradient in layer 2 of  $0.01 \text{ s}^{-1}$  ( $P_g$  in Figure 1.3). Throughout New England the first arrival phase ( $P_g$ ) is laterally continuous indicating that near surface velocity variations (statics) do not affect the data. Between shotpoints 7 and 10 layer 2 thickens and somewhat lower velocities are included in the model in this region (5.95-6.1 km/s). The incorporation of slower velocities into the model provides a travel-time delay observed in the first arrival refracted branch from shotpoint 4. Immediately east of shotpoint 10, a 6.1 km/s near-surface velocity is incorporated within layer 2.

Layer 3, with a seismic velocity of 6.1-6.2 km/s, varies laterally in thickness and occurs between depths of 5 to 15 km. First arrivals from layer 3 are observed at offsets exceeding 120 km and signify a continuous increase in velocity with depth in the uppermost crust, rather than a first-order velocity discontinuity (Figure 1.5). Between shotpoints 7 and 9 the velocity of layer 3 is increased to 6.2-6.3 km/s. A first-order velocity discontinuity in this region of the model satisfies near offset reflections from shotpoint 7 east (Figure 1.5) and additionally allows refracted arrivals from shotpoint 7 west to successfully turn through the ramp structure. The velocity structure of the ramp is discussed more fully in the following sections.

Large amplitude reflections ( $P_{1vz}P$ ) are observed on shotpoints 1, 2, and 3 at offsets of 20-60 km. These reflections are delayed in arrival time by as

much as 0.5 seconds, and are best modeled by a low velocity zone with velocity 5.8 km/s as shown by layer 4 in Figure 1.2. One-dimensional travel-time modeling enabled the geometry of this upper crustal reflector to be determined. Integration of the one-dimensional models into the two-dimensional model produced a 1 km thick low velocity zone with velocity 5.8 km/s (Figure 1.6). The velocity of the low velocity zone (5.8 km/s) is determined by amplitude modeling and by the abrupt termination of this set of reflections from shotpoint 1 at an offset of ~80 km ( $P_{lvz}P$  in Figure 1.3). Amplitude modeling of this discontinuous low velocity body produces a good match with the observed reflected phases, although it is hard to determine the magnitude of the seismic gradient within this layer. One-dimensional full-waveform reflectivity solutions were calculated for shotpoint 1 producing an exceptionally close correlation to the relative amplitudes observed along the profile.

The mid-crust has been modeled with a negative gradient; the vertical seismic velocity gradient decreases from 6.5 km/s to 6.4 km/s over a 10 km depth interval in layer 5 (Figure 1.2). The top of layer 5 rises from 14.5 km in the east to 11.5 km in the west before merging with the ramp beneath shotpoint 9. Large amplitude post-critical reflected arrivals observed at 70-120 km offsets define this mid-crustal interface ( $P_iP$  in Figure 1.5). Full-waveform reflectivity modeling indicated that a seismic velocity step from 6.2 km/s to 6.5 km/s at the top of layer 5 would satisfy critical point and amplitude constraints. Reflections originating from the top of layer 5 are not all equally as coherent or large in amplitude, yet the model predicts laterally continuous high amplitude reflections. Clearly, two-dimensional ray-tracing can only produce an approximate first-order representation of complex layered and laterally varying interfaces within the Earth. No refracted first arrivals are observed from layer 5. Two possible models were considered to fulfill the above described mid-crustal reflections without a

corresponding refracted phase; (1) a thin high velocity layer and (2) a negative gradient layer. First, a thin positive gradient high velocity layer, where refractions are terminated, and limited refracted energy returns to the surface was rejected because of the added complexity of determining the velocity between such a thin layer and the top of the lower crust. The second option of a negative gradient layer was chosen in preference as it produced the simplest solution to the observed phases. Since negative gradients cannot be resolved by amplitude modeling; this is an inferred structure. It is not necessary to have a negative gradient through the entire thickness of layer 5; an intermediate layer of, say, 6.45 km/s with a positive gradient is not ruled out although arrivals from such a layer would have to be 'hidden'. Immediately east of the Grenvillian ramp layer 5 has a positive velocity gradient; this is an essential feature of the model, as without it rays originating from within the Adirondacks and propagating to mid-crustal depths would never be refracted towards the surface (Figure 1.2).

The lower crust is modeled as a 'hidden' layer and lies below 25 km depth (layer 6 in Figure 1.2). Refracted first arrivals are not observed from the lower crust because of longer travel-times for direct arrivals from the lower crust than for the upper crustal refractions. Estimates of the lower crustal velocity must be indirectly inferred. We have three principal constraints on the velocity of the lower crust; (1) an estimate of 6.8 km/s for the lower crustal velocity was obtained from  $P_mP$  reflections as they asymptotically approached the lower crustal refracted phase, (2) travel-time modeling of critical  $P_mP$  reflection hyperbolae indicates a high velocity, high gradient lower crust, and (3) estimates of crustal thickness in the vicinity of our profile of around 38 km support a high velocity (6.8 km/s) in the lower crust (Luetgert *et al.*, 1987; Hennet *et al.*, 1991). The lower crust has been modeled with velocity 6.7 km/s increasing to 7.0 km/s at the base of the crust. The velocity gradient modeled in the lower crust is constrained by

the curvature of the  $P_mP$  hyperbola. Reflectivity modeling necessitates a minimum velocity discontinuity between layers 5 and 6. Perturbations in the modeled lower crustal velocities exceeding  $\pm 0.2$  km/s significantly degrade travel-time fits for Moho reflections.  $P_mP$  does not bottom any further east than shotpoint 3. Between shotpoints 1 and 3 the model is constrained by the USGS refraction profile along the axis of the Merrimack Synclinorium (Hennet *et al.*, 1991).

The top of the lower crust is represented in the model by a first-order velocity discontinuity. A first-order velocity discontinuity is presented as the simplest possible model which fits the observed travel-time constraints. The shallowest possible depths to the top of the lower crust is given by modeling lower crustal refractions so that they are coincident with the picked first arrivals (Figure 1.7a). The geometry of the lower crustal interface is poorly constrained because reflections from the top of the lower crust are indistinct (Figure 1.7b). The modeled  $P_{ij}P$  reflection shown on 1.5 is an artifact of modeling a hidden lower crust rather than a correlatable reflected phase. The top of the lower crust is modeled with a 6.7 km/s seismic velocity. Velocities as low as 6.5 km/s at the top of the lower crust are incompatible with prior estimates of crustal thickness in Maine and New Hampshire (Luetgert *et al.*, 1987; Hennet *et al.*, 1991), whilst velocities as high as 6.9 km/s for the top of the lower crust would produce large amplitude lower crustal reflections relative to  $P_mP$  and  $P_iP$  which are not observed. Ray-theory synthetic models of the lower crustal reflection ( $P_{ij}P$ ) are inconsistent with observed lower crustal reflectivity (Figure 1.3), suggesting that this interface is more complex than the first-order velocity discontinuity used for travel-time modeling. The primary observation of crustal thickness obtained from critical  $P_mP$  reflections is satisfied in preference to information obtained from synthetic models necessitating a high velocity in the lower crust. The top of the lower crust is considered to

be best represented by a gradational velocity interface, incapable of generating coherent reflections.

The geometry of the crust/mantle transition is constrained by Moho reflections ( $P_mP$ ) and direct arrivals from the upper mantle ( $P_n$ ). Together these indicate that the crust thickens from 36 km beneath western Maine to 40 km beneath Vermont. In the eastern portion of our model between shotpoints 1 and 7, a tightly constrained crust/mantle geometry is determined from complementary and reciprocal crust/mantle phases (Figure 1.7a). Greater emphasis was placed on modeling critical Moho reflections than low-amplitude emergent direct arrivals from the mantle. Although lower crustal velocities are relatively poorly constrained, thinning of the crust towards the east is a primary feature of the data set as indicated by the relative  $P_n$  crossover distances on shotpoints 1 and 7.

Exceptionally coherent large amplitude Moho reflections ( $P_mP$ ) observed from shotpoint 10 east, provide information on the crust/mantle transition beneath Vermont and New Hampshire. Compelling evidence for a 40 km thick crust beneath Vermont is provided by strongly coherent post-critical  $P_mP$  reflections observed at offsets between 90-140 km on shotpoint 10 (Figure 1.8). At wider angles delayed en-echelon  $P_mP$  reflection segments are observed (Figure 1.8-arrows a and b). Three possible explanations are considered for this feature (1) a step in the Moho, (2) complex lamination at the base of the crust, and (3) out of plane reflections. Firstly, the delay observed at an offset of 150 km from shotpoint 10 in the  $P_mP$  arrivals, can be modeled by a step in the Moho (Figure 1.9b). High upper mantle gradients are required to avoid a shadow zone in the  $P_n$  arrivals. Although such a model adequately satisfies travel-time constraints it is rejected on the basis that it is thought to be geologically less likely. The later two suggestions cannot be readily qualified. However, compositional lamination at the base of the crust may be invoked on the basis that

estimates of crustal thickness obtained from post-critical  $P_mP$  reflections are incompatible with those obtained from  $P_n$  arrivals from shotpoint 10. The delayed large amplitude reflections on shotpoint 10 may be caused by out of plane effects (Figure 1.8-arrow b).

Reflections observed on shotpoint 10 at offsets greater than 240 km with an apparent velocity exceeding 8.1 km/s are interpreted as an upper mantle reflection (Figure 1.8- $P_{um}P$ ). These upper mantle reflections tend to dominate the low-amplitude emergent  $P_n$  arrivals on shotpoint 10, adding further complexity to the determination of crustal thickness in New England. These upper mantle reflections ( $P_{um}P$ ) are unreversed and are tentatively modeled by a small velocity step in the upper mantle.

*Description of the Grenvillian Model:* The easternmost edge of the Adirondack massif is incorporated within the model as shown in Figure 1.2. The Grenvillian upper crust is characterized by exceptionally high upper crustal velocities (6.55-6.65 km/s). A thin surface layer is modeled with velocity 6.1 km/s. The top of a mid-crustal interface is sharply defined by prominent mid-crustal reflections at offsets of 50-90 km (Figure 1.4). This mid-crustal body is referred to by Klemperer *et al.*, 1985 as the Tahawus complex, and has been modeled by a planar mid-crustal velocity discontinuity dipping to the east within the Grenvillian crust. Pre-critical reflections from the eastern extent of the Tahawus complex observed on shotpoint 7 west provide important new evidence for the continuation of the Tahawus complex beneath Vermont ( $P_tP$  on Figure 1.10). Amplitude modeling of shotpoint 7 west is severely restricted due to the combination of upper crustal reflections resulting in a complex summation of phases. Shotpoint 10 west lacks any upper crustal reflections, and this facilitates amplitude modeling of this mid-crustal feature. A velocity contrast of 6.65 km/s to 6.8 km/s at 17 km depth adequately satisfies the observed travel-time constraints. Improved amplitude matching may be obtained by a

somewhat higher velocity contrast at the top of the Tahawus complex, although the velocity at the top of the lower crust may not exceed 6.8 km/s, because higher apparent velocities will result in an advanced arrival time relative to the observed first-arrival phase in the Adirondacks. The lower crust beneath the Adirondack massif is modeled with a velocity of 6.8-7.0 km/s, this adequately satisfies the previously discussed constraints imposed by critical  $P_mP$  reflections from shotpoint 10.

*Description of the Ramp Structure:* The contact between the Appalachian and Grenvillian provinces is marked by a lateral change in apparent velocity. This lateral transition in apparent velocity is observed at the same receiver position for all shotpoints traversing the Appalachian-Grenvillian boundary (Figure 1.11). Because this lateral change in apparent velocity occurs at a fixed receiver position it marks a steeply dipping interface in the seismic velocity model. Constraints on the geometry of the Appalachian-Grenvillian contact are imposed by the apparent velocity and travel-time paths of phases traversing the boundary. Shotpoints 9 and 10 situated immediately adjacent to the seismic velocity boundary provide critical reverse control on the discontinuity in the uppermost crust. The upper edge of the seismological boundary is located ~10 km east of shotpoint 10, this point is marked 'Hinge' on Figure 1.11. The boundary separating the low velocity Appalachian crust from the high velocity Grenvillian crust is therefore defined by the position of lateral transition in apparent velocity and by travel-time modeling of upper and mid-crustal phases traversing the boundary.

A steeply dipping interface which extends to mid-crustal depths beneath Vermont separates the high velocity Grenvillian 'block' from the lower velocities observed in the Appalachian upper crust. This velocity interface, referred to as the Grenvillian ramp, is reversed at all depths. Progressively deeper portions of the ramp are sampled by shotpoints at

successively greater offsets from the Appalachian-Grenvillian contact. Rays originating from the west are refracted through the ramp structure and are transmitted through the lower velocity Appalachian crust. Shotpoints west of the ramp therefore characteristically show high apparent Grenvillian velocities, followed by a rapid transition to a lower apparent velocity at offsets beyond the 'Hinge' (shotpoint 11 in Figure 1.11). East of the ramp the mirror image of this effect is observed; low Appalachian velocities give way to high Grenvillian velocities at offsets beyond the 'Hinge' (shotpoint 8 in Figure 1.11). The dipping structure of the ramp is determined by the modeling of apparent velocity and travel-times for raypaths from several different shotpoints which traverse the ramp. The travel-times of raypaths originating from shotpoints east of the ramp in Vermont can be integrated together to provide information on the dipping geometry of the ramp (Figure 1.11). If the boundary is too steeply dipping then modeled arrivals will be too early and have too high an apparent velocity (and vice-versa).

Constraints on the modeled geometry are imposed by reversing shotpoints in the Adirondacks. The deep geometry of the ramp structure is controlled by refracted first arrivals that have sampled Grenvillian velocities at their refracting horizon. Rays that are refracted through the deepest portions of the Grenvillian ramp are attenuated, on shotpoint 10 for example, the first arrival branch is emergent at offsets exceeding 100 km. The apparent velocity of refracted first arrivals that have been transmitted down the ramp to mid-crustal depths is characteristic of the high velocity (6.6 km/s) Grenvillian crust. Because high velocity 'Grenvillian' first arrivals are observed extending into the Appalachians at offsets of 200 km from the Appalachian-Grenvillian contact the ramp must continue to mid-crustal depths. This effect can be seen on shotpoint 10 which lies almost directly above the ramp and whose refracted arrivals have a phase velocity of 6.6 km/s ( $P_r$  on Figure 1.9a). High apparent velocity discontinuous

reflections are observed from the top of the ramp. Although these reflections cannot be satisfactorily resolved by two-dimensional raytrace modeling, they indicate that the ramp is likely to be a complex laminated/imbricated structure.

### 1.8 Shear Wave Analysis

Shear-wave velocities used in conjunction with compressional-wave velocities provide important constraints on estimates of crustal composition. In this section shear-wave arrival times are qualitatively compared with those of compressional-waves, and Poisson's ratio are calculated for phases traversing the upper and lower crust. Extended length travel-time plots were produced to determine the strength of the recorded shear-waves. Qualitative analysis was first carried out by overlaying shear-wave data reduced at 3.46 km/s and plotted on a time axis compressed by  $\sqrt{3}$  to allow compressional and shear-wave sections to be overlain and compared one to one. Such comparisons are in effect a measure of the relative compressional and shear-wave velocities of the crust, and for a 'normal' crustal  $V_p/V_s$  ratio of 1.732 shear-wave arrivals should align exactly with those of the compressional-waves. A delayed shear-wave arrival indicates a high  $V_p/V_s$  ratio, and vice-versa.

Prominent shear-wave arrivals produced by shotpoint 10 enable  $V_p/V_s$  ratios to be determined for the rocks of the Appalachian and Grenvillian crustal blocks. An estimate of the average crustal shear-wave velocity can be obtained by inspection of crust/mantle reflections. Large amplitude wide-angle reflections from the base of the crust show delayed  $S_mS$  compared to that which would be expected for a 'normal'  $V_p/V_s$  ratio indicating that the New England Appalachians have a high average crustal  $V_p/V_s$  ratio (Figure 1.9b). In the Appalachian upper crust shear-waves are advanced by up to 0.3 seconds compared to that which would be expected for

a 'normal'  $V_p/V_s$  ratio ( $S_r$  in Figure 1.12a). In comparison, the upper crustal shear-wave phase in the Adirondacks is delayed by at least 0.5 seconds ( $S_7$  in Figure 1.12a). Reflections from the Tahawus complex are delayed by almost a second ( $S_tS$  in Figure 1.12a). These qualitative observations show relatively slow shear-wave velocities in the Adirondacks (high  $V_p/V_s$  ratio) and somewhat higher shear-wave velocities in the Appalachians (low  $V_p/V_s$  ratio).

A useful criterion for determining crustal compositions is the calculation of Poisson's ratio. Arrival times of compressional and shear-wave phases at a given receiver location were picked enabling Poisson's ratio to be calculated for any particular travel-time path (Luetgert, 1990). For a given rayset (arrival branch) multiple calculations of Poisson's ratio may be made, which when averaged together provide information on the region of the crust through which the rayset has penetrated. For raypaths originating from shotpoint 10 and traversing the Appalachian upper crust normal Poisson's ratios of  $0.24 \pm 0.01$  were obtained, while higher ratios of  $0.28 \pm 0.01$  were obtained for the upper crust in the Adirondacks (Figure 1.12b). Somewhat more coherent results were obtained for the upper crust than for Moho reflections, where lower signal to noise ratios hampered precise shear-wave arrival time picks. A Poisson's ratio of  $0.26 \pm 0.01$  was obtained by picking travel-times for  $P_mP$  and  $S_mS$  arrivals on shotpoint 10. The derived Poisson's ratios are discussed more fully in terms of their relation to crustal composition in the following sections.

## 1.9 Discussion

The compressional-wave velocity model derived for the western New England Appalachians and the Adirondack mountains provides important new constraints on the deep crustal structure of the juxtaposed Proterozoic/Lower Paleozoic terranes in northeastern North America. In

the present study, seismic refraction/wide-angle reflection data are interpreted to show a steeply dipping ramp structure that separates the Proterozoic craton of North America from the obducted Appalachian allochthons. Recent compilations of geologic and geophysical data collected in the northern Appalachians include studies by Taylor, 1989; Hatcher *et al.*, 1990; Costain, 1990 and Stewart *et al.*, 1991. We present a synthesis of the most recent seismic experiments traversing the Appalachian-Grenvillian boundary in New England. The integration of compressional and shear-wave velocity information obtained in this study with geologic and physical property data is used to infer the deep crustal composition of these juxtaposed terranes.

*Structure of the Grenvillian Ramp:* The Grenvillian ramp imaged by forward modeling of this seismic data set separates the autochthonous Grenvillian rocks and their 'cover' sequence of the Adirondack region from the allochthonous Appalachian terranes. The relatively low resolution of the Ontario-New England-New York seismic refraction profile means that only broad features of the seismic velocity structure of the crust are resolved. In short, we can trace a velocity interface that separates high seismic velocities characteristic of the Grenvillian upper crust from those of the lower velocity rocks of the western Appalachians (Figure 1.13). The simplicity of this velocity interface belies the geological complexity of the basement-cover relationship of the Grenvillian crustal block. In the Champlain Valley autochthonous platformal carbonates and quartzites lie *insitu* above the Grenvillian basement. These platformal rocks are imbricated with allochthonous slope-rise lithologies of the Foreland Thrust Belt. Further east the Green Mountain Anticlinorium exposes obducted slices of Grenvillian basement interposed between the allochthonous 'cover' sequence in the Taconian orogeny. This imbricated wedge of allochthonous and autochthonous rocks is at its narrowest, and most

structurally complex, at the point where the Ontario-New England-New York seismic profile crosses into the Grenvillian crust. We interpret the Grenvillian ramp as the basal detachment of the allochthonous thrust rocks of the Appalachians. The Grenvillian ramp is likely to be a highly complex thrust imbricated and mylonitized remnant of the pre-Taconian (Ordovician) margin of proto-North America, upon which the accreted Bronson Hill island arc complex was obducted in Mid-Upper Ordovician times. Subsequent reactivation of the ramp in the Acadian orogeny (Devonian) is strongly suggested by tectonic syntheses in the New England region (Rowley and Kidd, 1980; Stanley and Ratcliffe, 1985).

In the vicinity of our profile the transition from autochthonous Grenvillian lithologies to the accreted allochthons of the western Appalachians is delineated by the Champlain thrust (Logan's Line). Comparison of results obtained from recent seismic experiments traversing the Appalachian-Grenvillian boundary may be usefully illustrated by aligning the models obtained from these experiments with respect to Logan's Line (Figure 1.14). In northern Maine, a major zone of reflections extends from shallow depths beneath the Foreland Thrust Belt to 25 km depth beneath the Chain Lakes massif (Stewart *et al.*, 1986; Spencer *et al.*, 1987; Spencer *et al.*, 1989). This reflection package has been interpreted as a 'décollement' surface separating the allochthonous upper crustal units of the Appalachians from the autochthonous Grenvillian crust which underlies much of the western Appalachians (Figure 1.14a). Comparison of the Quebec-Maine 'décollement' surface with the ramp model presented herein suggests that a remarkable degree of similarity exists along strike between these two models (Figure 1.14b). In the Ontario-New England-New York seismic experiment the subcrop of the ramp structure lies approximately at the position of the Champlain thrust. The resolution of the data does not allow us to definitively link these two features. Deep

seismic reflection profiling in southern Vermont images a 'thin skin' detachment beneath the Taconic allochthon which extends in the form of a steep 'step-like' thrust imbricated structure beneath the Bronson Hill Anticlinorium to a depth of 30 km as shown in Figure 1.14c (Brown *et al.*, 1983; Ando *et al.*, 1984, Phinney and Roy-Chowdhury, 1989). Recent reprocessing of the southern Vermont profiles, has resulted in a re-interpretation which suggests that the Appalachian-Grenvillian boundary is delineated by a series of steep planar imbricated fault zones extending into the lower crust (Thigpen, 1989). Despite the relatively low resolution of the Ontario-New-York-New England seismic refraction profile a consistent image of the buried edge of the Grenville province emerges from comparison of the Quebec-Maine transect, the Vermont reflection profiles, and the present study. The variations observed in the near-surface geometry of the ramp structure most likely owe their origin to lateral geologic discontinuities in the allochthonous Appalachian units. In the light of these results, we suggest that the buried edge of the Grenville province may be mapped extending beneath the Appalachians to a depth of around 25 km, at least as far as the eastern boundary of the Connecticut Valley Synclinorium.

*Composition of the Grenvillian Crust:* In the present study the Grenvillian upper crust is characterized by high compressional-wave velocities (6.6 km/s) and high Poisson's ratios ( $0.28 \pm 0.01$ ). Laboratory measurements of compressional-wave velocities and Poisson's ratios for samples of Adirondack granulites and meta-anorthosites at elevated pressures are consistent with the derived velocity model shown in 1.15a (Birch, 1960; Christensen and Fountain, 1975). The Marcy Anorthosite is exposed at the western end of our profile as it crosses the meta-igneous Adirondack massif. Gravity modeling of the Marcy Anorthosite indicates that it is tabular in shape and extends to a depth of 4 km, possibly with roots

extending to 10 km (Simmons, 1964). A suitable seismological analogue of the gravity model would be a 4 km thick anorthosite layer with a velocity of 6.6 km/s, underlain by a layer composed of granulitic gneisses (exposed in the Adirondacks). Samples of granulitic gneisses in the high pressure laboratory generally have upper crustal velocities less than those of anorthosite (Birch, 1960; Christensen, 1965; Christensen and Fountain, 1975). Thus, if the Marcy Anorthosite were a shallow sheet-like intrusion as suggested by gravity modeling, a decrease in signal amplitude and a simultaneous delay in the arrival time branch from the lower velocity gneissic crust would be observed. The absence of such features indicates that at the base of the Marcy Anorthosite similar compressional-wave velocities are observed for both the anorthosite and the underlying gneisses. At depths exceeding 10 km meta-anorthosite and granulitic gneisses have similar compressional-wave velocities and as such are seismically indistinguishable. The Marcy Anorthosite is likely to be around 10 km thick (Figure 1.13).

*Composition of the Appalachian Crust:* The New England Appalachian upper crust is composed of upper greenschist to middle amphibolite facies sediments/volcanics and numerous intermediate to acidic meta-igneous bodies. No identifiable reflections or travel-time anomalies were observed from such major bodies as the Green mountains, the Bronson Hill Anticlinorium or the White Mountain Batholith. High amplitude upper crustal reflections observed beneath the easternmost extent of our profile may be explained by the presence of gneissic layering, or by the subcrop of the New Hampshire Series granites exposed along the profile and this would certainly fit with extrapolations of gravity models derived for the New Hampshire granites (Nielson *et al.*, 1976; Hodge *et al.*, 1982). The modeled upper crustal velocities of around 6.1-6.2 km/s are consistent with laboratory measurements for a compositionally diverse set

of gneisses, schists, meta-gabbros, and granodiorites (Birch, 1960; Christensen, 1965; Christensen and Fountain, 1975; Holbrook *et al.*, 1992).

The two-dimensional seismic velocity model for the New England Appalachian crust significantly lacks lateral velocity variations which might be correlated with terrane boundaries (Figure 1.13). This must, in part, be a consequence of the extensive obduction that formed the western Appalachians, where terrane boundaries are interpreted as highly imbricated structures (Rowley and Kidd, 1980; Stanley and Ratcliffe, 1985). We envisage successive high grade thermal 'pulses' associated with at least three orogenic episodes resulting in regional amphibolite metamorphism, widespread plutonic intrusion, migmatization and, at deeper levels, whole-scale melting and mixing resulting in a largely homogenized Appalachian crustal block. Removal of the upper crust through successive periods of unroofing/isostatic uplift (Eusden *et al.*, 1985; Chamberlain *et al.*, 1987; Harrison *et al.*, 1989) reveals a window into highly deformed and altered mid-crustal rocks which appear seismically homogeneous. The apparent seismic homogeneity of the New England upper crust is thus a possible indication of the overall mineralogical similarity of the constituents of the present day upper crust. It is thus the case that although widely differing lithologies are observed at outcrop through the New England Appalachians we are unable to resolve their seismological heterogeneity in the present study.

In this study, the mid-crust (layer 5) is represented by a 10 km thick layer which has been modeled with a negative seismic velocity gradient (Figure 1.13). This feature of the model may be related to compositional and thermal properties of the mid-crust. Zones of velocity reversal can be produced by the anisotropic thermal expansion of the individual mineral constituents of the crust (Christensen, 1979; Kern and Richter, 1981). In the eastern United States the geothermal gradient is ~15 °C/km (Blackwell,

1971). High thermal coefficients for likely constituents of the mid-crust (amphibolitic granitic gneisses) mean that critical thermal gradients will be exceeded, and a velocity reversal will result (Christensen, 1979; Kern and Richter, 1981). The magnitude of the velocity reversal produced by high temperatures is dependent on the thermal gradient and the mineralogy of the crust, but is unlikely to exceed  $0.01 \text{ s}^{-1}$  (Christensen, 1979). At the top of the mid-crust a planar reflecting horizon marks an abrupt increase in seismic velocity. The appearance of prominent mid-crustal reflections over regional dimensions is a noticeable feature of this data set and of others collected in the vicinity (Klemperer and Luetgert, 1987; Luetgert and Mann, 1990; Hennet *et al.*, 1991). Mid-crustal reflectivity may be related to gneissic lamination, igneous 'ponding', fluid rich zones in the mid-crust, or bulk compositional changes. Whilst all of the above may be considered as suitable proponents the associated increase in seismic velocity observed in this study is most likely representative of bulk compositional change across the mid-crustal interface. We consider that the mid-crustal reflector delineates an increase in the mafic content of the crust.

Uncertainties in the derived velocity structure of the lower crust mean that lower crustal compositions cannot be unequivocally determined. In this study, shear-wave velocity information is used to reduce the uncertainty in inferring the composition of the lower crust from compressional-wave velocities alone, since shear-wave velocities are sensitive to the felsic content of the crust. The incorporation of shear-wave velocities into models of crustal composition enables the calculation of Poisson's ratio, a parameter which may be most usefully thought of as an indication of the relative quartz/feldspar content of the crust. Regions which exhibit low Poisson's ratios (low  $V_p/V_s$ ) are typically quartz rich, since quartz has high shear-wave velocities (Christensen and Fountain, 1975). An estimate of Poisson's ratio for the lower crust may be obtained by

removing the observed upper crustal Poisson's ratios from values obtained from phases traversing the whole crust. The delayed  $S_mS$  phase relative to a 'normal'  $V_p/V_s$  ratio of 1.732 indicates an average crustal Poisson's ratio of  $0.26 \pm 0.01$  (Figure 1.9b). Upper crustal rocks in New England have 'normal' Poisson's ratios ( $0.24 \pm 0.01$ ). The travel-time delay observed for phases traversing the entire crust must be restricted to the lower crust. Poisson's ratio for lower crustal rocks beneath the New England Appalachian are then likely to exceed 0.26.

A recent compilation of laboratory measured rock velocities enables both compressional and shear-wave velocities to be calculated for a particular rock type (Holbrook *et al.*, 1992). Although the assignment of seismic velocity to rock type is highly dependent on the samples chosen to represent a particular compositional range, this data set provides a useful means of specifying end members of a compositional series beyond which constraints imposed by *in situ* seismic velocities can not be satisfied. The high compressional-wave velocities (6.7-7.0 km/s) and high Poisson's ratios (0.26-0.27) observed for rocks of the lower crust tends to favor an intermediate-mafic composition. Possible constituents of the lower crust include anorthosite, intermediate-mafic granulites and amphibolitic assemblages. Laboratory determinations of Poisson's ratios for samples of anorthosites of around 0.29 (Holbrook *et al.*, 1992) suggests that anorthosite is an unlikely constituent of the lower crust in New England. Amphibolitic assemblages (meta-gabbro/hornblende, feldspar, pyroxene) at elevated pressures generally have compositional-wave velocities exceeding those derived herein, whilst felsic granulites generally have compressional-wave velocities much less than those observed beneath the New England Appalachians (Birch, 1960; Christensen, 1965; Holbrook *et al.*, 1992). The most favorable composition for the lower crust is a mafic granulite facies assemblage containing feldspar, pyroxene and garnet (Figure 1.15b).

Xenoliths provide direct evidence of lower crustal composition and can be used to reduce the non-uniqueness inherent in inferring composition from seismic velocities alone. Lamprophyre dike suites at Ayres Cliff, Quebec, and North Hartland, Vermont contain granulite facies xenoliths (Williams and McHone, 1984; Trzcieski and Marchildon, 1989). The xenoliths from Ayres Cliff are relatively unaltered and are commonly of two types; (a) meta-pelitic assemblages originating from mid-crustal depths, which are interpreted as Cambrian meta-sediments, and (b) mafic assemblages and anorthosite fragments which are readily correlated to Grenvillian exposures in the Adirondacks. The North Hartland xenoliths are relatively unaltered lower-crustal/upper-mantle ultramafics and quartz-plagioclase granulites. These xenoliths support the existence of Grenvillian crust extending beneath the Appalachians, at least as far as the western edge of the Connecticut Valley Synclinorium.

The obduction of the western Appalachians against the Grenvillian crustal block in the Taconic orogeny has resulted in the juxtaposition of allochthonous Lower Paleozoic continental sediments and volcanics against the Proterozoic protolith of North America. The seismic refraction data set obtained in this study allows us to characterize the seismic velocity structure of the accreted terranes in the New England orogen. We can trace a steeply dipping ramp structure that divides the Grenvillian crust from the allochthonous Appalachian units emplaced during the Taconic orogeny. The Grenvillian ramp extends to mid-crustal depths at least as far as the western portion of the New England Appalachians. The Grenvillian lower crust appears seismically indistinguishable from the lower crust beneath the accreted Appalachian allochthons in spite of profound differences in the upper crustal structures and lithologies. This suggests that the lower crust may have been largely re-formed, homogenized and annealed during

successive Lower Paleozoic orogenic events and subsequent Mesozoic extension.

### 1.10 Acknowledgments

The data presented in this paper were collected by the US Geological Survey, the Geological Survey of Canada, and the US Air Force Geophysics Laboratory. We thank Walter Mooney (USGS), Jill McCarthy (USGS) and Bruce Beaudoin (Stanford University) for constructive reviews of earlier drafts of this manuscript. S.H. gratefully acknowledges financial support provided by the National Environmental Research Council, UK (GT4/88/GS/64) and thanks his colleagues at the USGS, Menlo Park, California for their assistance and encouragement. Reviews by Dave Stewart (USGS) and two anonymous reviewers greatly enhanced this manuscript.

**1.11 References**

- Ando, C.J., B.L. Czuchra, S.L. Klemperer, L.D. Brown, M.J. Cheadle, F.A. Cook, J.E. Oliver, S. Kaufman, T. Walsh, J.R. Thompson, J.B. Lyons, J.L. Rosenfeld, Crustal profile of a mountain belt: COCORP deep seismic reflection profile in New England and implications for architecture of convergent mountain chains, *Am. Assoc. Pet. Geol.*, 68, 819-837, 1984.
- Birch, F., The velocity of compressional waves in rocks at 10 Kbars part 1, *J. Geophys. Res.*, 65, 1083-1102, 1960.
- Blackwell, D.D., The thermal structure of the continental crust, in *The Structure and Physical Properties of the Earth's crust*, edited by J.G. Heacock, Am. Geophys. Un. Geophys. Monogr. Ser. 14, pp. 169-184, 1971.
- Bradley, D.C., Tectonics of the Acadian orogeny in New England and adjacent Canada, *Journal of Geology*, 91, 381-400, 1983.
- Brown, L.D., C.J. Ando, S. Klemperer, J.E. Oliver, S. Kaufman, B. Czuchra, T. Walsh, and Y.W. Isachsen, Adirondack-Appalachian crustal structure: The COCORP northeast traverse, *Geol. Soc. Am. Bull.*, 94, 1173-1184, 1983.
- Cerveny, V., I.A. Molotkov, I. Psencik, *Ray Method in Seismology*, Karlova Univ. Press, Prague, 214 pp., 1977.
- Chamberlain, C.P. and P.C. England, The Acadian thermal history of the Merrimack Synclinorium in New Hampshire, *Journal of Geology*, 93, 593-602, 1985.
- Christensen, N.I., Compressional-wave velocities in rocks at high temperatures and pressures, critical thermal gradients, and crustal low velocity zones, *J. Geophys. Res.*, 84, 6849-6857, 1979.
- Christensen, N.I. and D.M. Fountain, Constitution of the lower continental crust based on experimental studies of seismic velocities in granulite, *Geol. Soc. Am. Bull.*, 86, 227-236, 1975.

- Christensen, N.I., Compressional-wave velocities in metamorphic rocks at pressures to 10 Kbars, *J. Geophys. Res.*, 70, 6147-6164, 1965.
- Costain, J.K., R.D. Jr. Hatcher, C. Coruh, T.J. Pratt, S.R. Taylor, J.J. Litehiser, I. Zietz, Geophysical characteristics of the Appalachian crust, in *The Appalachian-Ouachita orogen in the United States*, edited by R.D. Jr. Hatcher, W.A. Thomas, G.W. Viele, pp. 385-416, *The Geology of North America*, Geol. Soc. Am. F-2, 1990.
- Eusden, J., W.A. Bothner, A.M. Hussey, The Kearsarge-Central Maine synclinorium of southeast New Hampshire and southwestern Maine: stratigraphic and structural relations of an inverted section, *Am. J. Sci.*, 287, 246-264, 1987.
- Harrison, M.T., F.S. Spear, M.T. Heilzer, Geochronologic studies in central New England II: Post-Acadian hinged and differential uplift, *Geology*, 17, 185-189, 1989.
- Hatcher, R.D. Jr., P.H. Osberg, A.A. Jr. Drake, P. Robinson, W.A. Thomas, Tectonic Map of the US Appalachians, in *The Appalachian-Ouachita orogen in the United States*, edited by R.D. Jr. Hatcher, W.A. Thomas G.W. Viele, plate 1, *The Geology of North America*, Geol. Soc. Am. F-2, 1990.
- Hennet, C.G., J.H. Luetgert, R.A. Phinney, Coherency processing and structural analysis of refraction data from central Maine, *J. Geophys. Res.*, 1991.
- Hodge, D.S., D.A. Abbey, M.A. Harbin, J.L. Patterson, M.J. Ring and J.F. Sweeney, Gravity studies of subsurface mass distributions of granitic rocks in Maine and New Hampshire, *Am. J. Sci.*, 282, 1289-1324, 1982.
- Holbrook, W.S., W.D. Mooney and N.I. Christensen, The seismic velocity structure of the deep continental crust, in *The Continental Lower Crust*, edited by D.M. Fountain, R. Arculus and R. Kay, pp. 5-44, Elsevier, Holland, 1992.

- Klemperer, S.L., L.D. Brown, J.E. Oliver, C.J. Ando, B.L. Czuchra and S. Kaufman, Some results of COCORP's seismic reflection profiling in the Grenville-age Adirondack mountains, New York State, *Can. J. Earth Sci.*, 22, 141-153, 1985.
- Klemperer, S. L. and J.H. Luetgert, A comparison of reflection and refraction processing and interpretation methods applied to conventional refraction data from coastal Maine, *Seismological Soc. Am. Bull.*, 77, 614-630, 1987.
- Kern, H. and A. Richter, Temperature derivatives of compressional and shear wave velocities in crustal and mantle rocks at 6 Kbars confining pressure, *Journal of Geophysics*, 49, 47-56, 1981.
- Luetgert, J.H., S. Hughes, J. Cipar, S. Mangino , D. Forsyth, and I. Asudeh, Data report for O-NYNEX, the 1988 Grenville-Appalachian seismic refraction experiment in Ontario, New York and New England, *US Geological Survey Open File report 90-426*, 1990.
- Luetgert, J.H., C.E. Mann, S.L. Klemperer, Wide-angle crustal reflections in the northern Appalachians, *Geophys. J. R. Astro. Soc.*, 89, 183-188, 1987.
- Luetgert, J.H., C.E. Mann, Avalon terrane in eastern coastal Maine: Seismic refraction-wide-angle reflection data, *Geology*, 18, 878-881, 1990.
- Luetgert, J.H., Users Manual for RAY83/R83PLT: Interactive two-dimensional raytracing/synthetic seismogram package, *US Geol. Surv. Open File Report 88-238*, 1988a.
- Luetgert, J.H., Users manual for RSEC88: Interactive computer program for plotting seismic refraction record sections, *US Geol. Surv. Open File Report 88-262*, 1988b.
- Luetgert, J.H., Users manual for R1D84: Interactive modeling of one-dimensional velocity depth functions, *US Geol. Surv. Open File Report 88-262*, 1988c.

- Mooney, W.D., Seismic methods for determining earthquake source parameters and lithospheric structure, in *Geophysical Framework of the Continental United States*, edited by L.C. Pakiser and W.D. Mooney, pp. 11-34, Geol. Soc. Am. Memoir 172, 1989.
- McHone, J.G. and J.R. Butler, Mesozoic igneous provinces of New England and the opening of the North Atlantic Ocean, *Geol. Soc. Am. Bull.*, 95, 757-765, 1984.
- McLelland, J.M. and Y.W. Isachsen, Synthesis of geology of the Adirondack mountains, New York, and their tectonic setting within the southwestern Grenville province, in *The Grenville Province*, edited by J.M. Moore, A. Davidson and A.J. Baer, Geological Association of Canada special paper 31, pp. 75-94, 1986.
- Murphy, J.M., USGS FM cassette seismic-refraction recording system, *US Geol. Surv. Open File Report 89-570*, 1989.
- Nielson, D.L., R.G. Clark, J.B. Lyons, E.J. Englund and D.J. Boris, Gravity models and mode of emplacement of the New Hampshire Plutonic Series, *Geol. Soc. Am. Memoir 146*, 301-318, 1976.
- Osberg, P.H., Synthesis of the geology of the Northeastern Appalachians, USA, in *Caledonian-Appalachian orogen of the North Atlantic Region* edited by E.T. Tozer *et al.*, pp. 137-147, Geol. Surv. Canada, I.G.C.P., 27, 1978.
- Phinney, R.A. and K. Roy-Chowdhury, Reflection seismic studies in the eastern United States, in *Geophysical Framework of the Continental United States*, edited by L.C. Pakiser and W.D. Mooney, Geol. Soc. Memoir 172, pp. 613-653, 1989.
- Robinson, P and L.M. Hall., Tectonic synthesis of southern New England, in *The Caledonides in the USA*, edited by D.R. Wones, pp. 73-81, I.G.C.P. 27, 1979.

- Rogers, J., *The Tectonics of the Appalachians*, pp. 270, Regional Geology Series, Willey-Interscience, New York, 91-115, 1970.
- Rowley, D.B. and W.S.F. Kidd, Stratigraphic relationships and detrital composition of the medial Ordovician flysch of western New England: Implications for the tectonic evolution of the Taconic orogeny, *Journal of Geology*, 89, 199-218, 1980.
- Selleck, B.W., Post orogenic history of the Adirondack region; a review, *Geol. Soc. Am. Bull.*, 91, 120-124, 1980.
- Simmons, G., Gravity survey and geologic interpretation, northern New York, *Geol. Soc. Am. Bull.*, 75, 81-98, 1964.
- Spencer, C., A. Green, P. Morel-a-l'Huissier, B. Milkereit, J.H. Luetgert, D.B. Stewart, J.D. Unger, and J.D. Philips, Allochthonous units in the Northern Appalachians: Results from the Quebec-Maine seismic reflection and refraction surveys, *Tectonics*, 8, 667-696, 1989.
- Spencer, C., A. Green, and J.H. Luetgert, More seismic evidence on the location of the Grenvillian basement beneath the Appalachians of Quebec-Maine, *Geophys. J. R. Astro. Soc.*, 89, 177-182, 1987.
- Stanley, R.S. and M.N. Ratcliffe, Tectonic synthesis of the Taconic orogeny in western New England, *Geol. Soc. Am. Bull.*, 96, 1227-1250, 1985.
- Stewart, D.B., Unger J.D., Philips J.D., Goldsmith R., Poole W.H., Spencer C.P., Green A.G., Loiselle M.C., St-Julien P., The Quebec-Western Maine seismic reflection profile: Setting and first year results, in *Reflection Seismology: The Continental Crust*, edited by M. Barazangi and L.D. Brown, pp. 189-199, Am. Geophys. Un. Geodynamics series 14, 1986.
- Stewart, D.B., B.E. Wright, J.D. Unger, J.D. Phillips, D.R. Hutchinson, J.H. Luetgert, W.A. Bothner, K.D. Klitgord, L.M. Liberty, C. Spencer, The Quebec-Maine-Gulf of Maine Transect, Southeastern Canada,

Northeastern United States of America, Global Geoscience Transect 8, *US Geological Survey Open File Report 91-353*, 1991.

Taylor, S.R., Geophysical framework of the Appalachians, in *Geophysical Framework of the Continental United States*, edited by L.C. Pakiser and W.D. Mooney, *Geol. Soc. Am. Memoir 172*, pp. 317-348, 1989.

Taylor, S.R. and M.N. Toksoz, Crust and upper-mantle velocity structure in the Appalachian orogenic belt: Implications for tectonic evolution, *Geol. Soc. Am. Bull.*, 93, 315-329, 1982.

Thigpen, J.T., Seismic reflection evidence for imbricate basement slices in central New England, *unpublished Msc. Thesis, Cornell University*, pp. 95, 1989.

Trzcieski, W. E. and N. Marchildon, Kyanite-garnet bearing Cambrian rocks and Grenville granulites from the Ayer's Cliff, Quebec, Canada, lamprophyre dike suite: Deep crustal fragments from the northern Appalachians, *Geology*, 17, 637-640, 1989.

Wiener, R.W., J.M. McLelland, W.I. Isachsen, L.M. Hall, Stratigraphy and Structural Geology of the Adirondack mountains, New York: Review and Synthesis, in *The Grenville Event in the Appalachians and Related Topics*, edited by M.J. Bartholomew, *Geol. Soc. Am. Special Paper 194.*, pp. 1-55, 1984.

Williams, H., Tectonic lithofacies map of the Appalachian orogen, Map 1a, The Appalachian-Caledonides orogen, Canadian contribution 5, I.G.C.P. 27, Memorial University of Newfoundland, 1978.

Williams, H. and R.D. Hatcher, Suspect terrains and the accretionary history of the Appalachian orogen, *Geology*, 10, 530-536, 1982.

Willams, N.A. and J.G. McHone, Mantle and crustal xenoliths from the North Hartland dike, Vermont, *Geol. Soc. Am. Abstr. with Programs*, 16, 71, 1984.

Zen, E-an, Exotic terranes in the New England Appalachians-limits, candidates, and ages: a speculative essay, in *Contributions to the tectonics and geophysics of mountain chains*, edited by R.D. Jr. Hatcher, H. Williams and I. Zietz, pp. 55-81, Geol. Soc. Am. Memoir 158, 1983.

### 1.12 Captions

**Figure 1.1:** Simplified geologic map showing the location of the eastern portion of the 1988 Ontario-New York-New England seismic refraction /wide-angle reflection profile. Inset map shows regional location of the entire profile. Inline shotpoints are marked by dots along the profile, and fanshots are shown offset to the south. Previous seismic profiles are shown by the dashed lines; (1) the Quebec-Maine seismic reflection and refraction profiles (Spencer *et al.*, 1989), and (2) the USGS refraction profile along the axis of the Merrimack Synclinorium (Hennet *et al.*, 1991), (3) the southern Vermont and Adirondack deep seismic reflection profiles collected by COCORP (Ando *et al.*, 1984). The geologic map is simplified after Williams [1975] and McLelland and Isachsen [1986].

**Figure 1.2:** Seismic velocity model derived from the eastern portion of the Ontario-New York-New England seismic refraction/wide-angle reflection data. Velocity interfaces are consistent with the observed phases; well constrained reversed control is achieved throughout the upper and mid-crust. The model is a first-order representation of complex layered and gradational interfaces within the New England Appalachians and Adirondack mountains. Topography is included in the model. Layer numbers are referenced in the text, and in subsequent ray diagrams. All velocities are shown in km/s. Distance is plotted relative to shotpoint 10 (Figure 1.1).

**Figure 1.3:** Trace normalized seismic refraction data from shotpoint 1 (SP1) and ray-synthetic seismogram (top) calculated for the eastern portion of the model in Figure 1.2. Shotpoint 1 is representative of data collected across the New England Appalachians and shows characteristically large amplitude coherent mid-crustal reflections ( $P_iP$ ). The model predicts strongly coherent PmP reflections, which are not observed in the data; the Moho may be laminated beneath the central New

England Appalachians. Data is plotted using a reducing velocity of 6.0 km/s. No filtering has been applied to the data. Key to phase identification (used throughout);

$P_g$ , the diving or continuously refracted P-wave in the upper crustal layers, with an apparent velocity between 6.0 to 6.2 km/s.

$P_r$ , the refracted P-wave through the Grenvillian ramp structure.

$P_7$ , the refracted P-wave in the Grenvillian upper crust (layer 7), with an apparent velocity of 6.6 km/s.

$P_n$ , the uppermost mantle refracted P-wave phase, with an apparent velocity between 8.0 to 8.1 km/s.

$P_iP$ , the wide-angle reflection from the mid-crustal interface (layers 3/5), no corresponding refracted first arrival is observed from layer 5.

$P_{ii}P$ , the wide-angle reflection from the lower crustal interface (layers 5/6), no corresponding refracted first arrival is observed from layer 6.

$P_mP$ , the wide-angle reflection from the crust-mantle boundary.

$P_tP$ , the wide-angle reflection from the top of the Tahawus complex (layers 7/6).

**Figure 1.4:** Record section for shotpoint 10 west (SP10 west) plotted in trace normalized format with distances plotted relative to the shotpoint. Seismic refraction data collected across the Adirondack mountains characteristically show high upper crustal velocities (6.6 km/s), compared to those observed in the Appalachians. Large amplitude coherent reflections ( $P_tP$ ) observed at offsets between 50-90 km are related to a laminated mid-crustal interface referred to by *Klemperer et al.*, [1985], as the Tahawus complex.

**Figure 1.5:** Trace normalized seismic refraction data from shotpoint 7 east (SP7 east) and ray-diagram (bottom) for the eastern portion of the model shown in Figure 1.2. The New England seismic velocity structure is fully reversed by SP7 east. Mid-crustal reflections ( $P_iP$ ) show an

advanced travel-time relative to that observed for shotpoint 1. Critical points are marked on the data by the black dots, and the corresponding critical distances are marked on the model. Distances are plotted relative to shotpoint 7. See Figure 1.3 for key to phase identification.

**Figure 1.6:** Near-offset trace normalized seismic refraction data from shotpoint 1 (top) and shotpoint 3 (middle). Large-amplitude upper-crustal reflections ( $P_{1vz}P$ ) observed from shotpoints in western Maine, are best modeled by a thin low-velocity layer. Ray-diagram for shotpoint 3 (bottom) shows pre-critical reflections from the base of the low-velocity layer. Distances are plotted relative to the shotpoint.

**Figure 1.7:** Trace normalized record sections from (a) shotpoint 7 east showing refracted direct arrivals from the lower crust ( $P_{1rcr}$ ) modeled so that they are coincident with the first arrival around the  $P_n$  crossover, and (b) shotpoint 5 showing weakly coherent critical reflections from the top of the lower crust ( $P_{ii}P$ ) that are observed only in the absence of strong mid-crustal reflections ( $P_iP$ ). Note, the first arrival branch is observed at offsets of 120 km with an apparent velocity of 6.1 km/s. Distances are plotted relative to shotpoint in each case.

**Figure 1.8:** Trace normalized seismic refraction data from shotpoint 10 east (SP10 east) and ray diagram (bottom) for the model shown in Figure 1.2. Large amplitude  $P_mP$  reflections dominate the record section. Offset and segmented  $P_mP$  reflections (arrow a and b) may be the result of compositional lamination at the base of the crust or out of plane effects. The Grenvillian ramp structure is highlighted by the dotted line. For clarity, only every second seismic trace is plotted. Distances are plotted relative to shotpoint 10.

**Figure 1.9:** Enlarged portions of the record section for shotpoint 10 east (Figure 1.8) showing (a) the refracted phase through the Grenvillian ramp  $P_r$  and (b) segmented and en-echelon Moho reflections. The delayed

$P_mP$  arrivals at 150 km can be modeled by a small step in the Moho although this geometry is regarded as geologically less likely. Predicted travel-times (solid lines) are plotted on the S-wave section, assuming a Poisson's ratio of 0.25. The delayed  $S_mS$  phase provides evidence for a mafic lower crust beneath the New England Appalachians. On the S-wave section the reduction velocity is 3.46 km/s, and the time axis is compressed by  $\sqrt{3}$  relative to the P-wave time axis.

**Figure 1.10:** Trace normalized seismic refraction data from shotpoint 7 west (SP7 west) and ray diagram (bottom) for the western portion of the model shown in Figure 1.2. A lateral velocity transition is marked by the abrupt increase in apparent velocity at -80 km. Pre-critical reflections ( $P_tP$ ) from SP7 west provide important new evidence for the continuation of the Tahawus complex beneath western Vermont. Distances are plotted relative to shotpoint 7. The Grenvillian crust is shown stippled and the ramp structure is high-lighted by the dotted line.

**Figure 1.11:** The Appalachian-Grenvillian contact is characterized by a lateral velocity transition. This velocity transition is located at the same receiver position for all shotpoints traversing the boundary and is labeled 'Hinge'. West of the 'Hinge' in the Adirondack upper crust high velocities are observed, while east of the 'Hinge' low Appalachian velocities are observed. The record section for shotpoint 8 (top) shows an increase in apparent velocity at offsets beyond the 'Hinge'. Shotpoint 11 (middle) shows a decrease in apparent velocity beyond the 'Hinge'.

**Figure 1.12:** Variations in Poisson's ratio in upper crustal rocks near the edge of the Adirondack mountains. Record sections for shotpoint 10 (a) show delayed S-wave arrivals for ray paths through the Grenvillian crust, and advanced S-wave arrivals in the Appalachians. Predicted travel-times (solid lines) for the model shown in Figure 1.2 are plotted on the S-wave section, assuming a Poisson's ratio of 0.25. Upper crustal  $P_g$  and  $S_g$

arrival times at each receiver station have been used to calculate Poisson's ratio from shotpoint 10 (b). High Poisson's ratios observed in the Adirondack Highlands can be correlated with the Marcy Anorthosite, and normal Poisson's ratios observed for the upper crust in Vermont indicate the predominance of quartz-rich lithologies.

**Figure 1.13:** Geologic interpretation of the first-order velocity model shown in Figure 1.2. A mid-crustal penetrating ramp separates the Grenvillian crustal block from the accreted Appalachian terranes. A ramp structure divides the high velocity Grenvillian terrane from the lower velocity sub-horizontally layered Appalachian crust. The lower crust is shown as a continuous layer, but may be divided into discrete Appalachian-Grenvillian units. Solid lines indicate first-order velocity discontinuities, dashed lines indicate complex laminated gradational interfaces. Prominent mid-crustal reflective interfaces are highlighted by the wavy lines.

**Figure 1.14:** Comparison of recent seismic experiments across the Appalachian-Grenvillian terrane boundary in New England. From north to south the results obtained from these seismic experiments are (a) the Quebec-Maine seismic reflection/refraction experiment in southern Quebec (Stewart *et al.*, 1986; Spencer *et al.*, 1987; Spencer *et al.*, 1989), (b) the New England seismic refraction profile discussed herein, and (c) deep seismic reflection profiling across the Taconic Allochthon in southern Vermont (Brown *et al.*, 1983; Ando *et al.*, 1984). The boundary between the Grenville province and the accreted Appalachians is characterized by a noticeably similar planar ramp structures extending to mid-crustal depths beneath the thrust allochthons of the western Appalachians.

**Figure 1.15:** Comparison of one-dimensional velocity-depth functions (bold line) for (a) the Adirondacks (SP11), and (b) the Appalachians (SP4) with laboratory velocity measurements of samples at elevated pressures. Average seismic velocities are presented for possible

constituents of the lower crust, ranges shown are one standard deviation (Holbrook *et al.*, 1992). The lower crustal velocities beneath the central Appalachians are inferred to be best represented by mafic granulites (anhydrous feldspar, pyroxene, garnet assemblages). Laboratory data have been corrected for temperature using a geotherm of 15 °C/km (Blackwell, 1971) and an average thermal coefficient of  $2.0 \times 10^{-4} \text{ km/s}^\circ\text{C}^{-1}$  (Christensen, 1979; Kern and Richter, 1981). Samples referenced are from *Christensen* [1965] and *Holbrook et al.*, [1992].

1.13 Figures

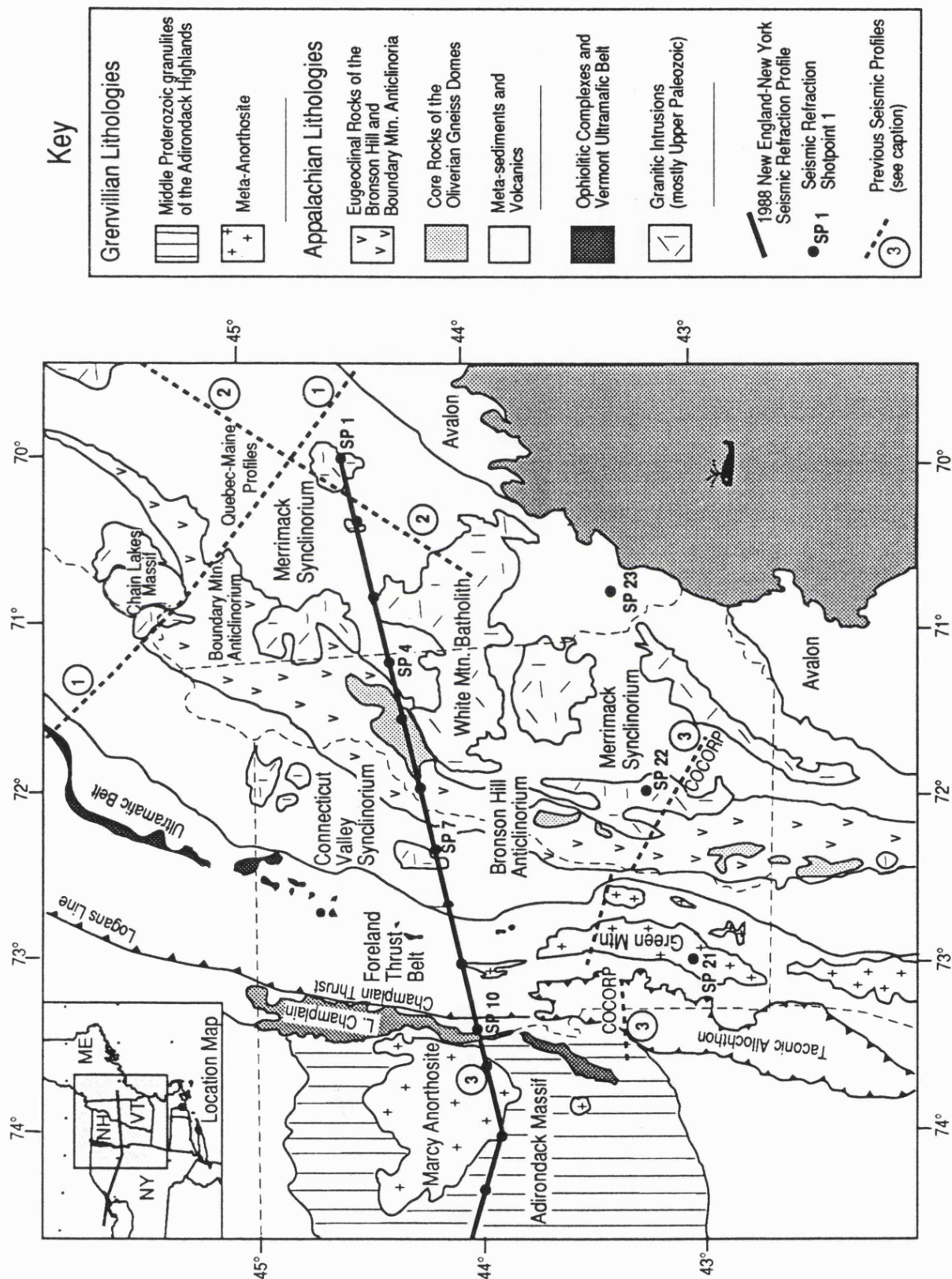


Figure 1.1



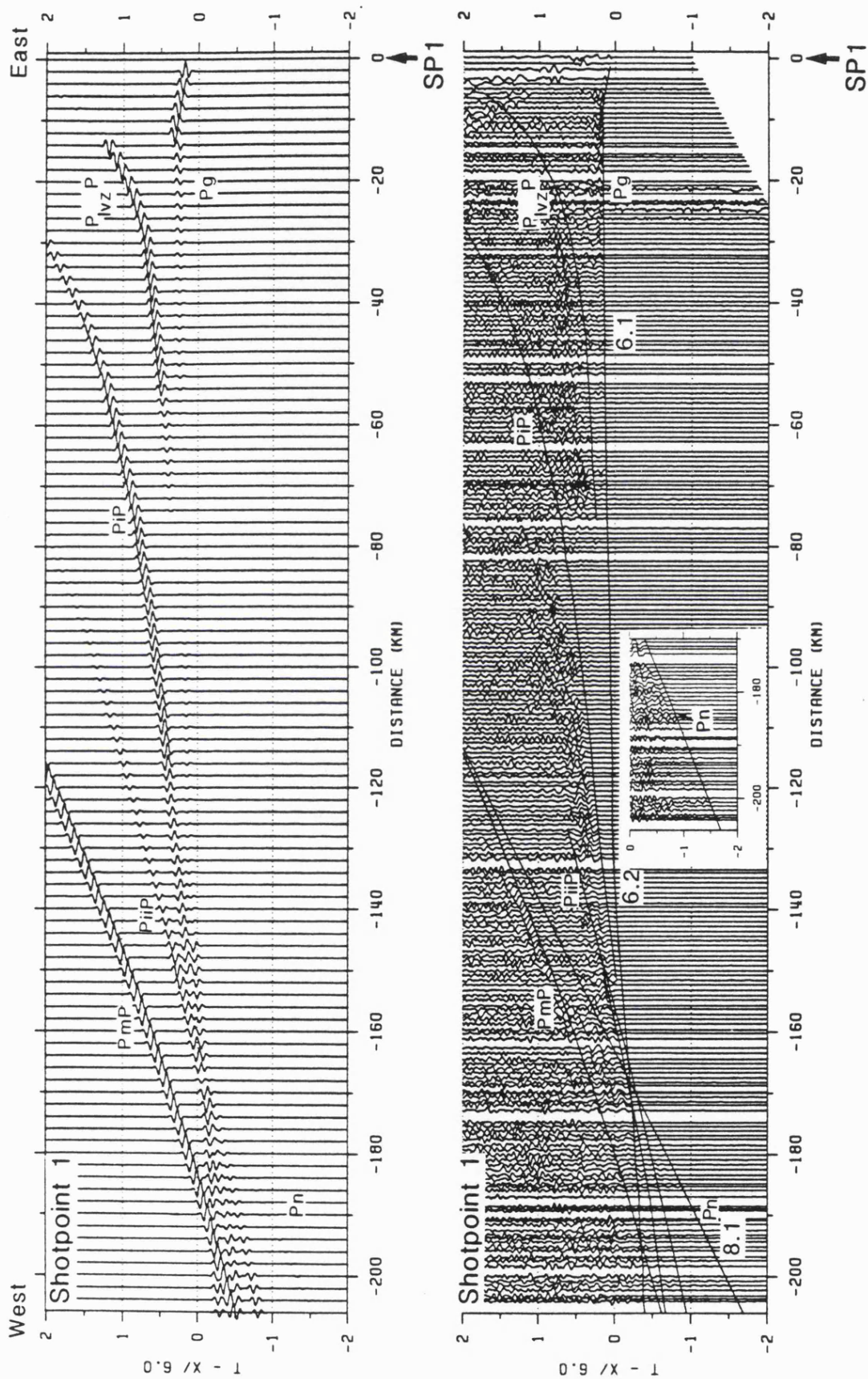


Figure 1.3

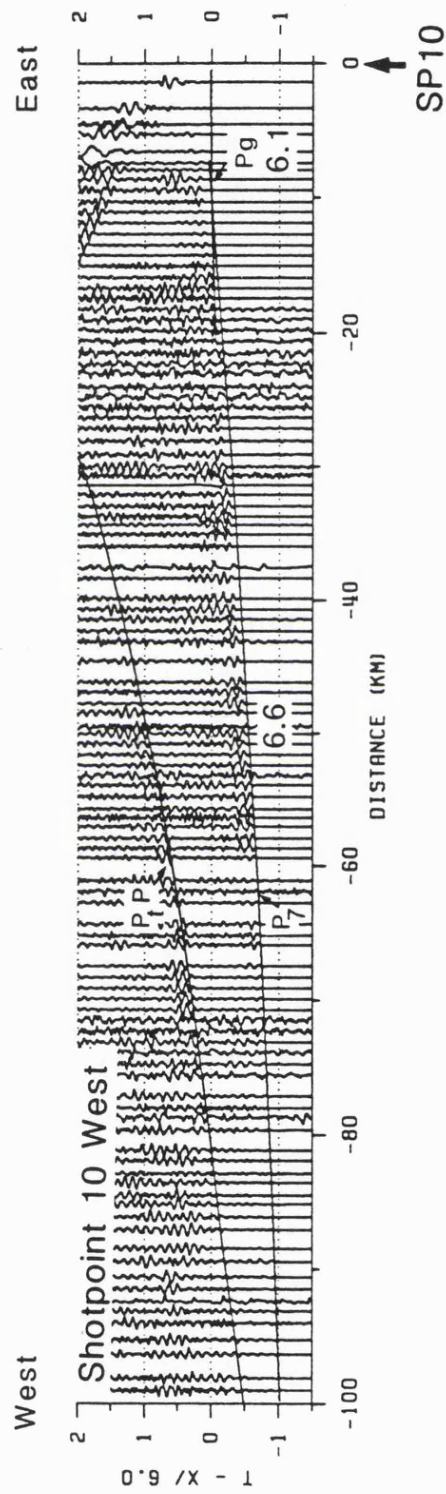


Figure 1.4

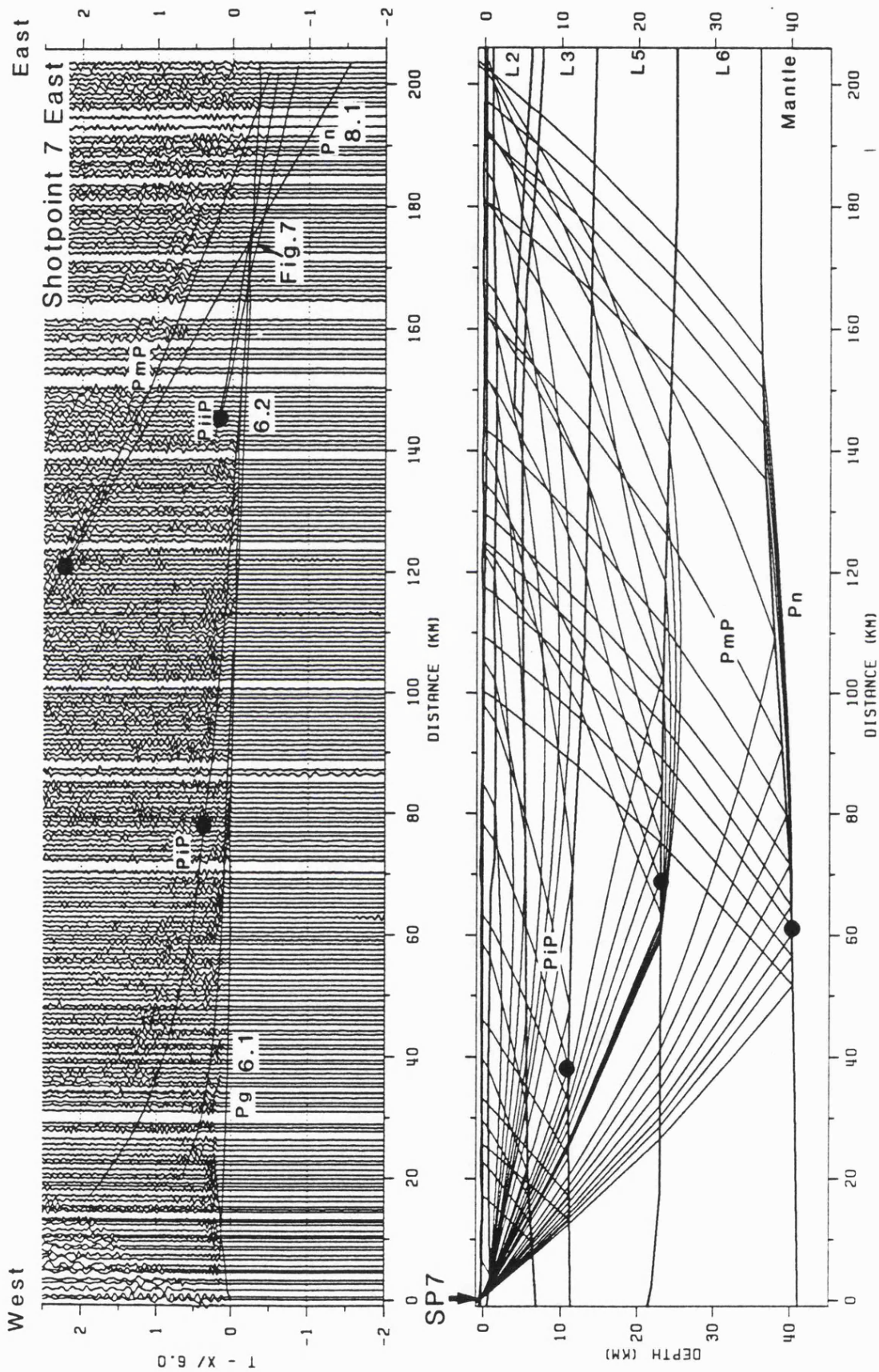


Figure 1.5

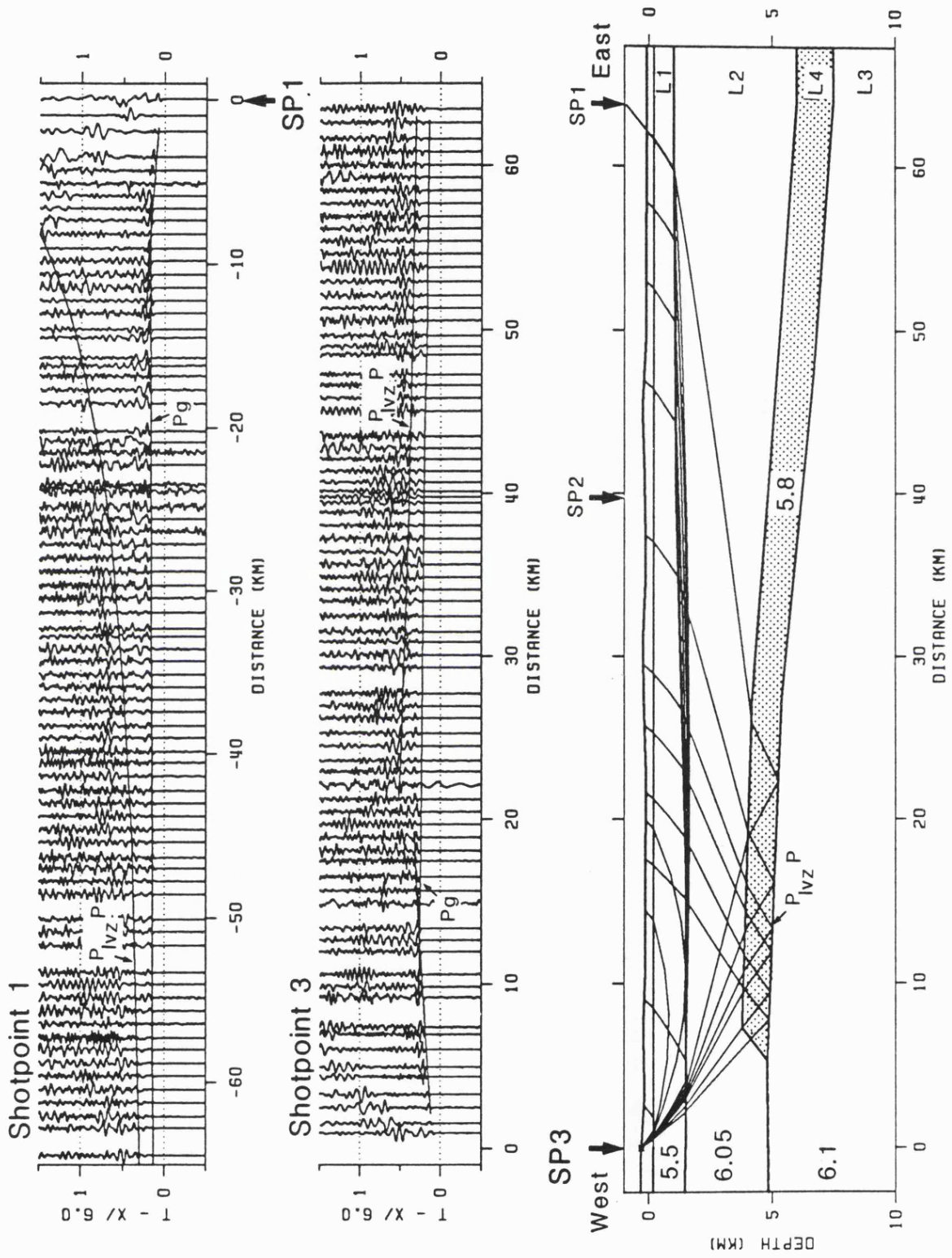


Figure 1.6

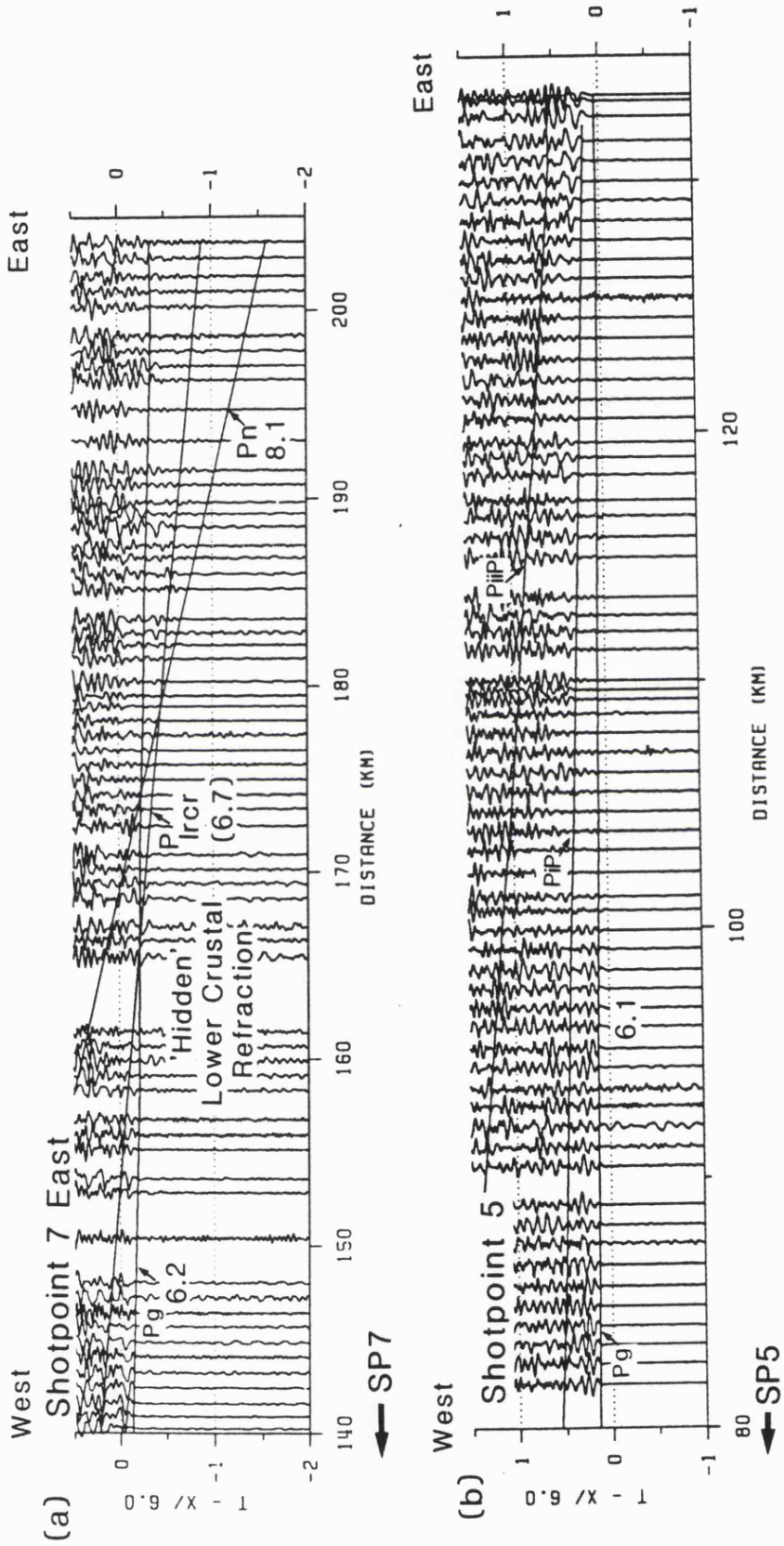


Figure 1.7

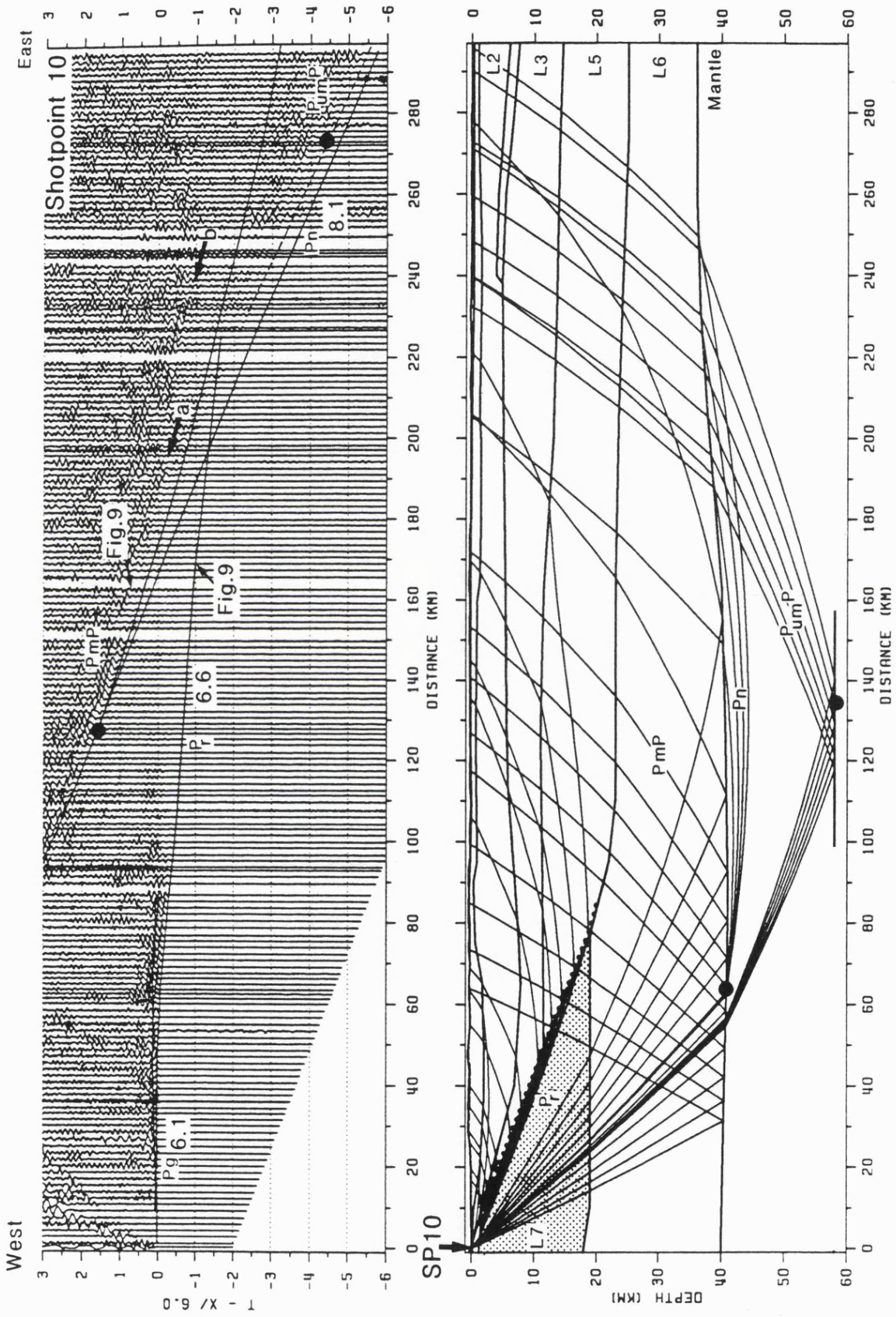


Figure 1.8

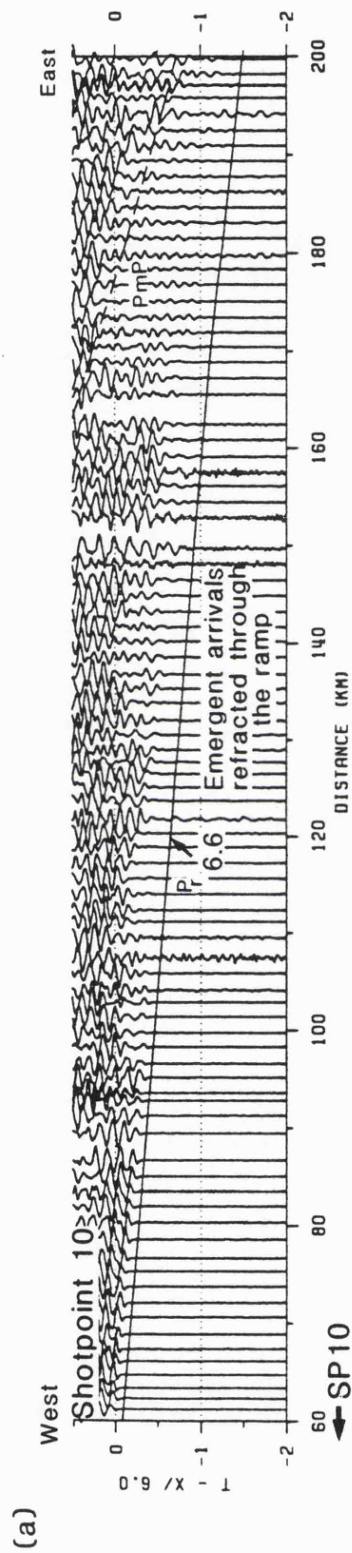


Figure 1.9a

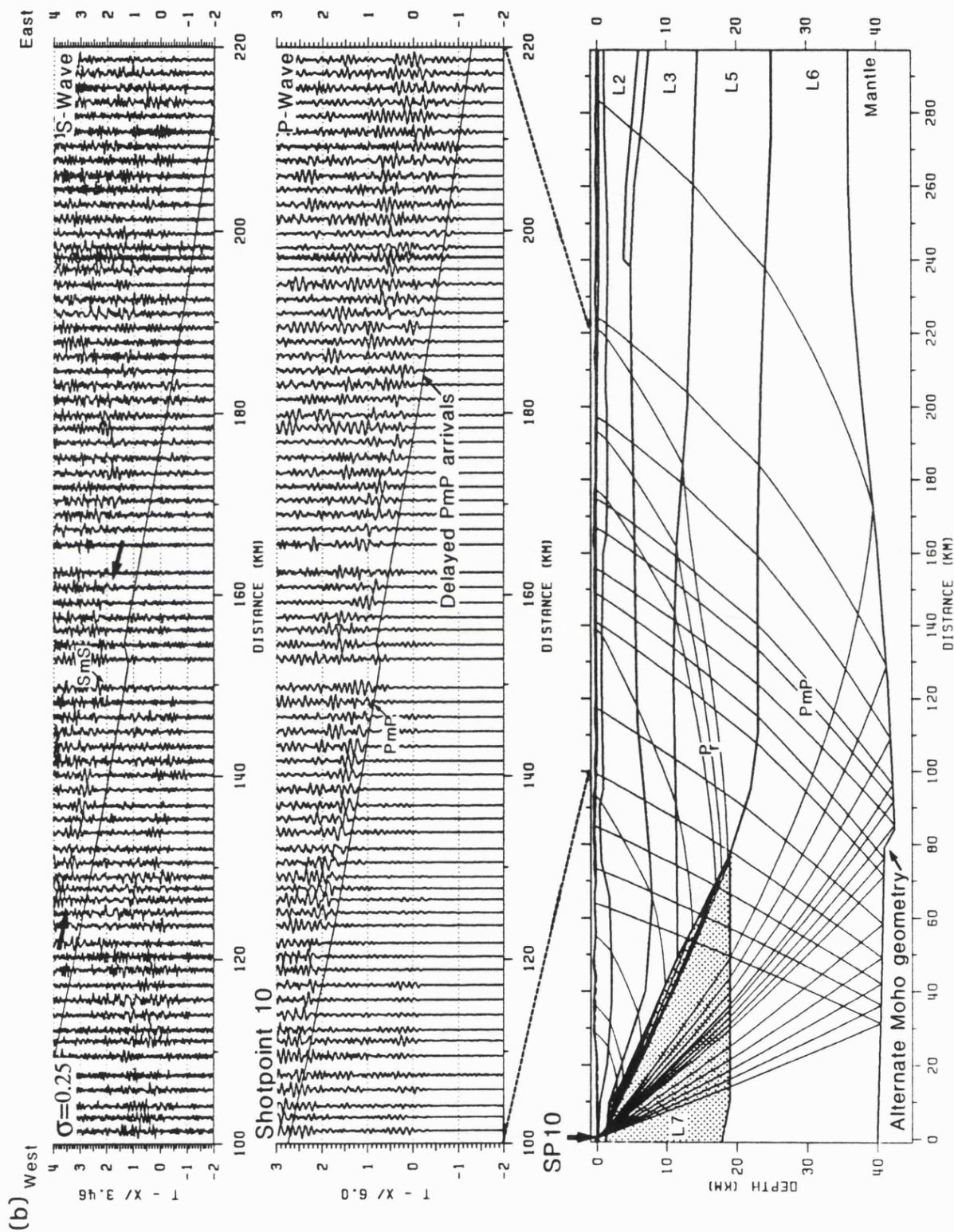


Figure 1.9b

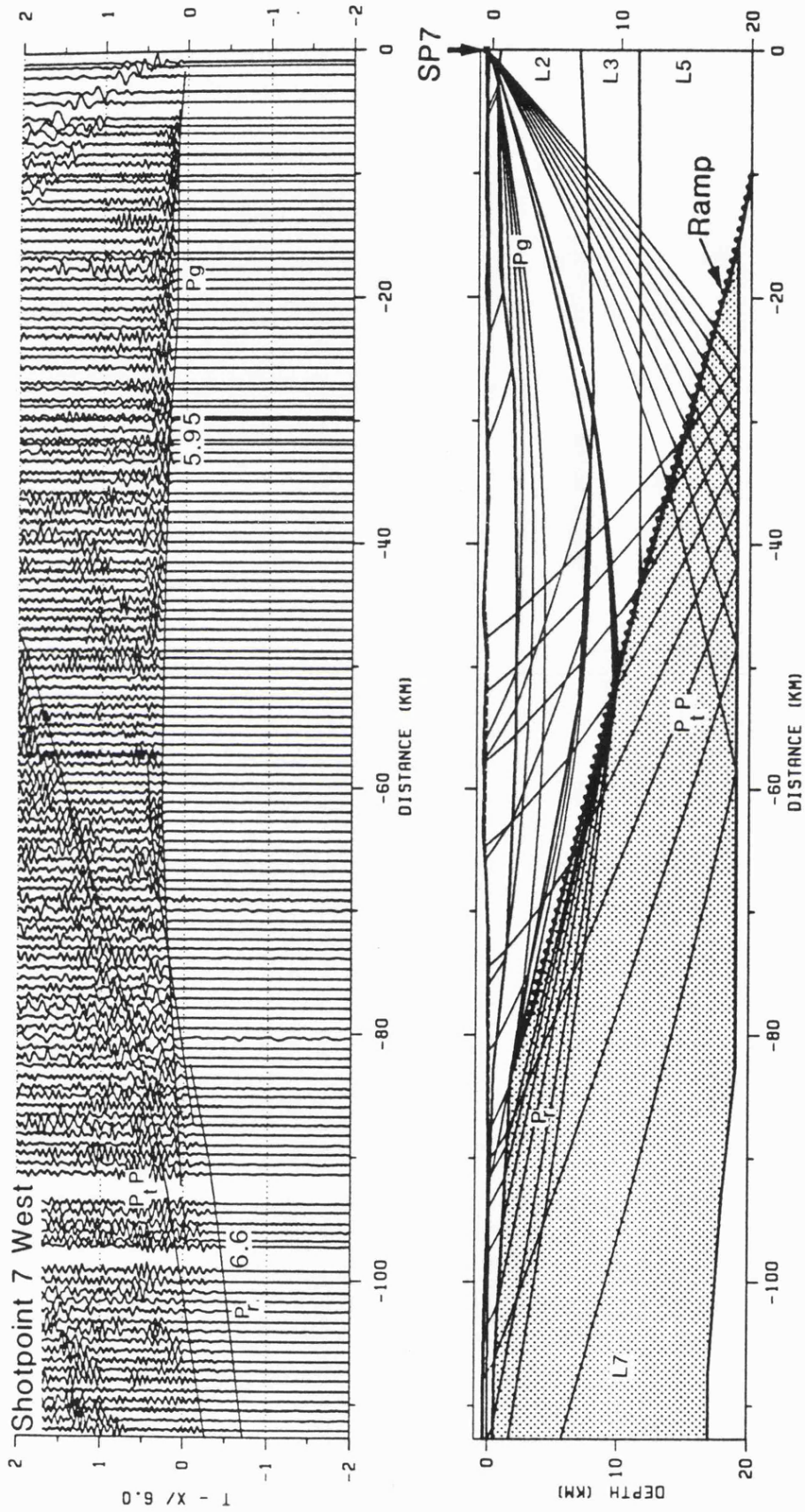


Figure 1.10

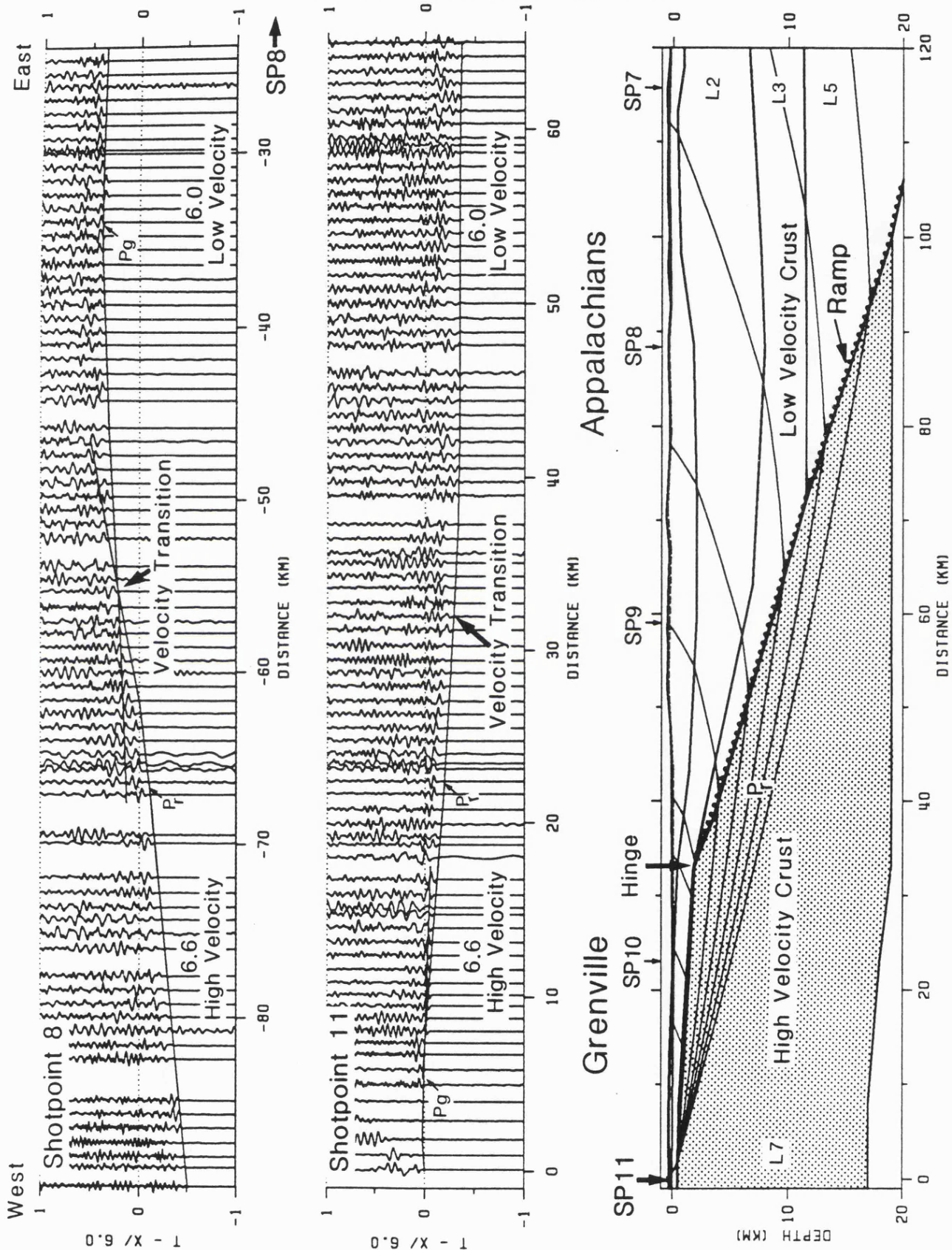


Figure 1.11

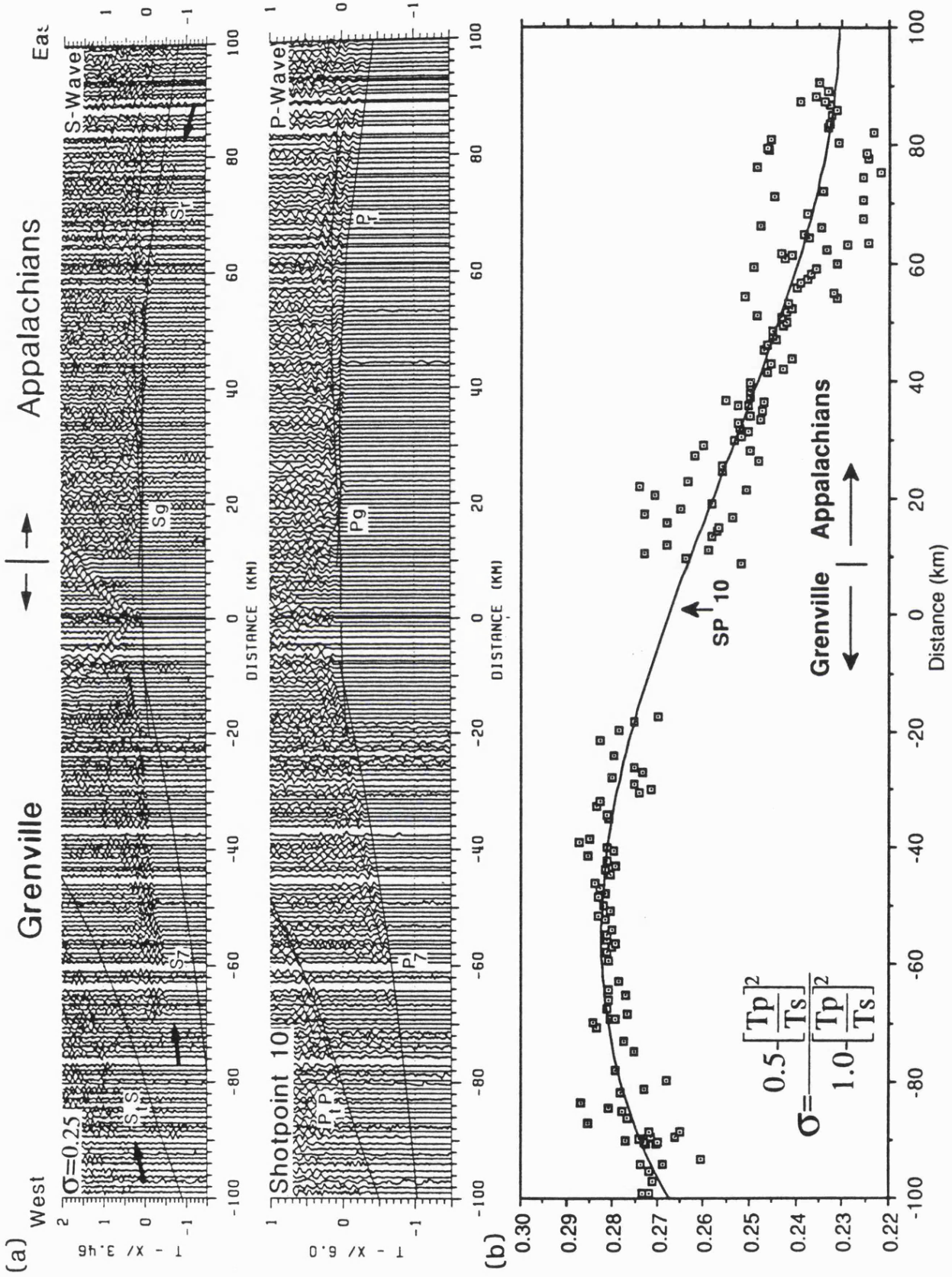


Figure 1.12

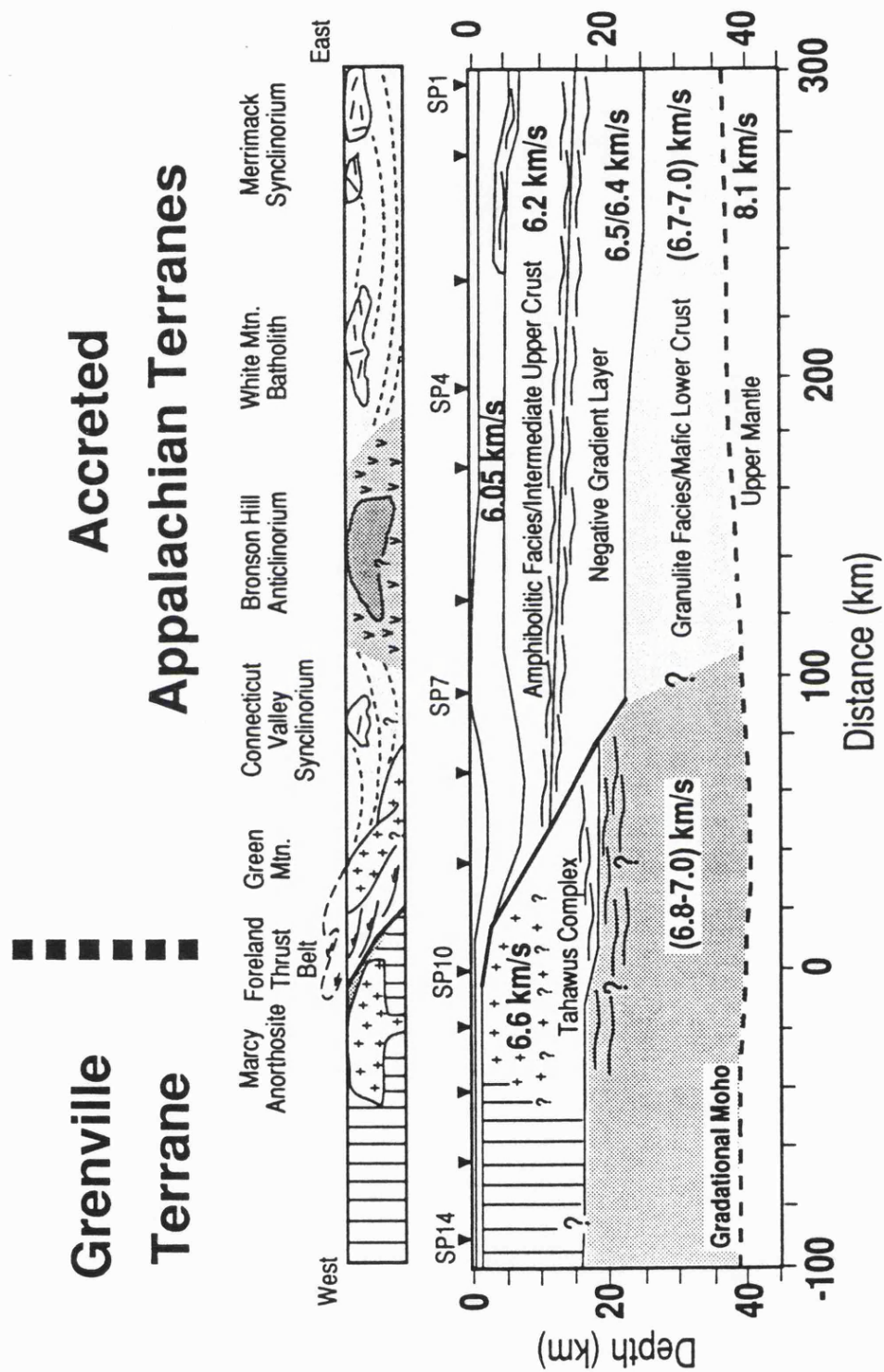
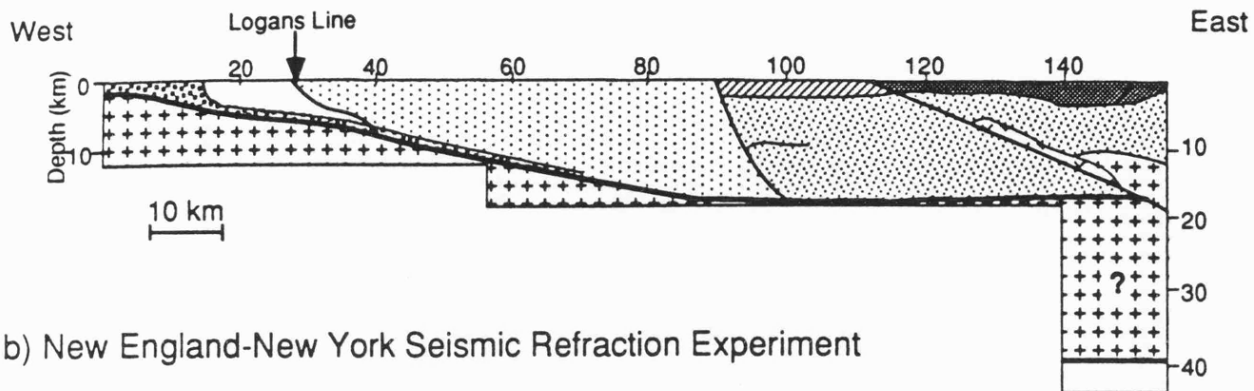
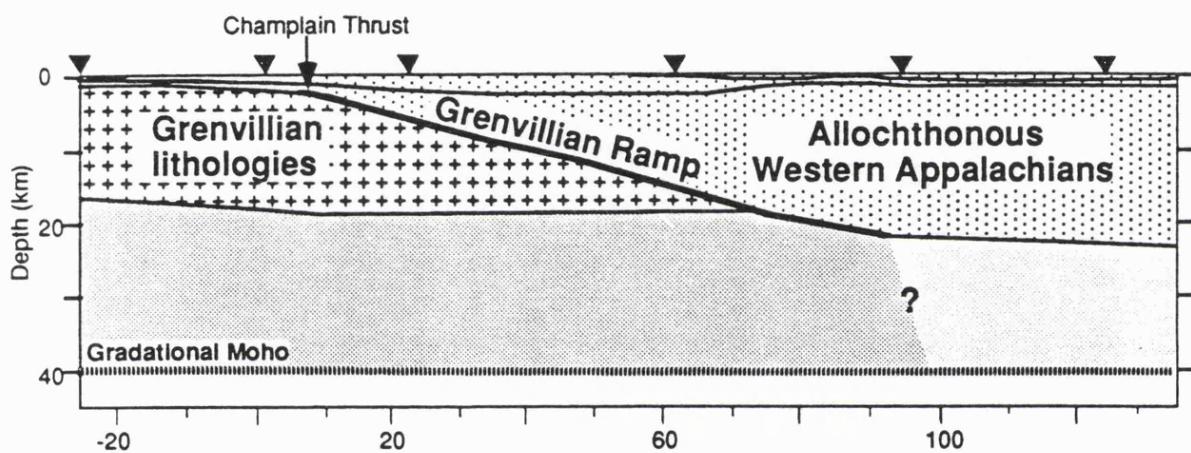


Figure 1.13

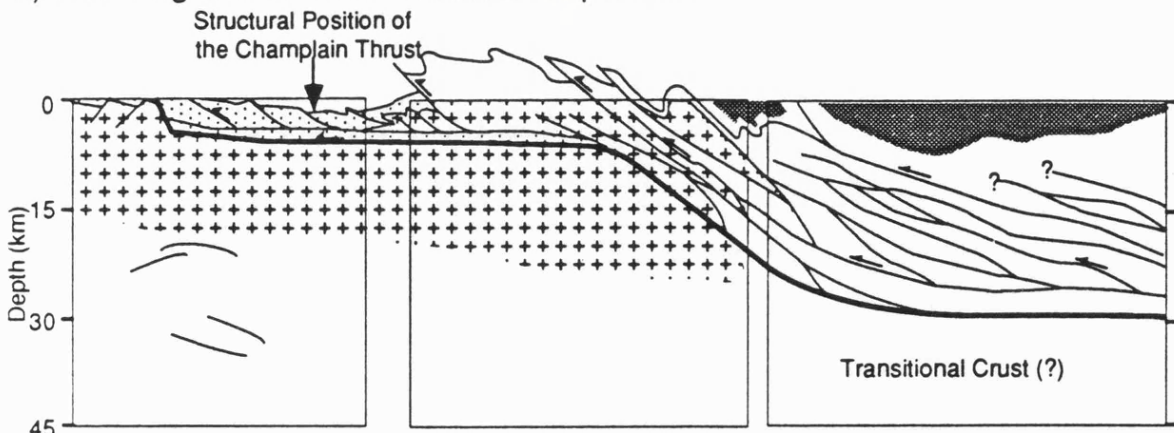
a) Quebec-Maine Seismic Reflection/Refraction Experiment



b) New England-New York Seismic Refraction Experiment



c) New England Seismic Reflection Experiment



Key

- |                                     |                                                   |                                                            |
|-------------------------------------|---------------------------------------------------|------------------------------------------------------------|
| Grenvillian Basement                | Allochthonous Continental Sediments and Volcanics | Connecticut Valley Synclinorium and Merrimack Synclinorium |
| Basement of the Chain Lakes Terrane | Magmatic Arc Complex                              | St. Lawrence Platform                                      |

Figure 1.14

Comparison of Insitu Seismic Velocity Measurements with those obtained from Laboratory Samples

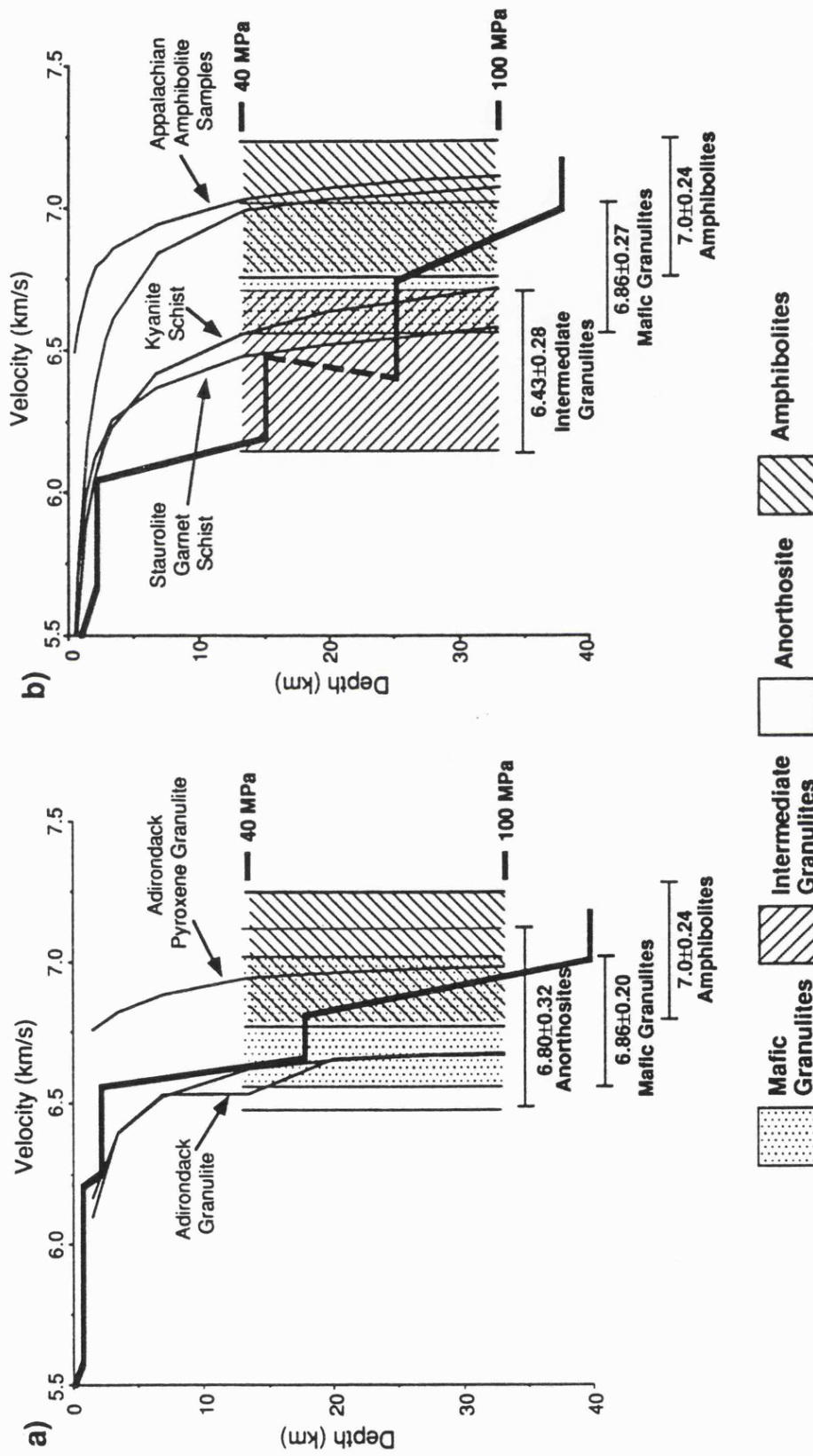


Figure 1.15

## Crustal Structure of the Southeastern Grenville Province

### 2.1 Abstract

The Grenville province exposes an oblique cross section through mid-lower crustal lithologies that were pervasively deformed and subjected to regional thermal overprinting during the Grenvillian orogeny (1.1 Ga.). The southeastern Grenville province is divided into two sub-terrane by the Carthage-Colton mylonite zone, a 110-km-long lineament characterized by intense ductile shear and igneous intrusion, which separates the amphibolite facies metasediments of the Central Metasedimentary Belt to the west, from the granulite facies metaplutonics of the Central Granulite Terrane to the east. The recognition of distinct litho-tectonic domains separated by zones of intense ductile shear in the Grenville province raises questions concerning the deep structure of these sub-terrane and in particular, the means by which the mid-lower crustal rocks exposed in the Grenville province were emplaced. Seismic refraction/wide-angle reflection data were acquired to investigate the deep structural inter-relationships within the southeastern Grenville province. A travel time inversion for velocity and interface depth was applied to the seismic data, together with constraints from amplitude modeling to produce a seismic velocity model of the crust in the southeastern Grenville province. In the

Central Metasedimentary Belt the upper crust is characterized by velocities in the range 6.3-6.4 km/s and a Poisson's ratio of  $0.26 \pm 0.01$  which are attributed to quartzofeldspathic rocks. Further east in the Central Granulite Terrane, upper crustal velocities of 6.55 km/s and a Poisson's ratio of  $0.28 \pm 0.01$  are associated with the Marcy Anorthosite. The seismic homogeneity of the upper crust in the region of the Carthage-Colton mylonite zone suggests that this boundary is a shallow feature, limited to the upper 2-3 km of the crust. The deep crustal structure of the southeastern Grenville province is characterized by two discrete and laterally discontinuous seismic interfaces. In the Central Metasedimentary Belt the top of the lower crust is delineated by an eastward dipping interface at 24-28 km depth. In the Central Granulite Terrane prominent en-echelon reflections, referred to as the Tahawus complex, form a gently arched dome at 17-22 km depth. Interpretation of the Tahawus complex as a zone of layered mafic cumulates is supported by its high velocity (7.1 km/s) and Poisson's ratio ( $0.27 \pm 0.02$ ). The lower crust is characterized by a velocity of 7.0-7.2 km/s and an anomalously high Poisson's ratio of  $0.30 \pm 0.02$ , which are representative of pyroxene-garnet granulites. In contrast velocities of 6.8-7.0 km/s are modeled beneath the Central Granulite Terrane and appear to signify a lateral change in composition. The Moho lies at 44-45 km depth and is characterized by pronounced en-echelon reflection segments suggesting compositional interlayering around the crust-mantle boundary. The velocity of the upper mantle is 8.0-8.2 km/s. An anomalous upper mantle layer with a reversed velocity of 8.6 km/s dips eastwards from 50 to 60 km depth beneath the southeastern Grenville province. Our results indicate that remnants of magmatic intrusions that mobilized and thickened the crust during the Grenvillian orogeny are preserved in the mid-lower crust as a layered cumulate body (Tahawus complex) and in the

upper mantle as an eclogitic lens, possibly delaminated from the over-thickened crust during uplift of the southeastern Grenville province.

## 2.2 Introduction

The Grenville province is the focus of intense debate concerning the application of modern plate-tectonic concepts to the evolution and genesis of the Proterozoic crust (Dewey and Burke, 1973; McLelland and Isachsen, 1980; Baer, 1981; Windley, 1986; Kroner, 1986; Durrheim and Mooney, 1991). The recognition of distinct litho-tectonic domains within the Grenville province suggests that the crust is composed of remnant fragments of an Early Proterozoic orogen (Wynne-Edwards, 1972; Davidson, 1986; Moore, 1986). In the southeastern Grenville province two sub-terrane are distinguished on the basis of lithologic, metamorphic and structural characteristics. In the west of the study area, the Central Metasedimentary Belt exposes a suite of amphibolite facies metasediments and metavolcanics, while to the east the Central Granulite Terrane is dominated by granulite facies metaplutonics (Figure 2.1). Isotopic age dating across the Central Metasedimentary Belt and Central Granulite Terrane suggests that these sub-terrane were contemporaneous prior to the Grenvillian orogeny (Corriveau, 1990; McLelland *et al.*, *in press*). During the Mid-Proterozoic Grenvillian orogeny the crust was pervasively deformed and thermally overprinted. Subsequent cooling and exhumation of the crust in the Late-Proterozoic exposed an oblique cross section through amphibolite-granulite facies lithologies that equilibrated at mid-lower crustal depths (McLelland and Isachsen, 1980; Wiener *et al.*, 1984; Bohlen *et al.*, 1985; Davidson, 1986). The Grenville province is of particular relevance to studies of the continental crust because the present-day erosion surface provides a window into deep seated crustal processes active during the Grenvillian orogeny. In this study seismic refraction/wide-angle reflection data are used to provide constraints on the structure and composition of the deep crust in the southeastern Grenville province. Fundamental questions concerning the evolution of the Proterozoic crust addressed by this study are; (1) What

is the structural inter-relationship between the Central Metasedimentary Belt and the Central Granulite Terrane? (2) What evidence is there for magmatic or compressional events in the deep crust which can be related to the Grenvillian orogeny? and (3) How were the mid-lower crustal lithologies exposed in the Grenville province emplaced?

The Ontario-New York-New England seismic refraction/wide-angle reflection profile was acquired by the US Geological Survey as part of a collaborative effort with the Geological Survey of Canada and the US Air Force Geophysics Laboratory to investigate the lithospheric velocity structure of the southeastern Grenville province and the adjacent western New England Appalachian orogen (Luetgert *et al.*, 1990; Hughes and Luetgert, 1991). A new method for inverting seismic refraction travel time data (Zelt and Smith, 1992) is used to obtain a two-dimensional seismic velocity model of the lithosphere from the western portion of the Ontario-New York-New England seismic refraction/wide-angle reflection profile. We begin by presenting the geologic and geophysical features which distinguish the Central Metasedimentary Belt and the Central Granulite Terrane. A detailed description of the travel time and synthetic amplitude modeling is presented, before moving on to an interpretation of the composition and evolution of the deep crust in the southeastern Grenville province.

### 2.3 Regional Geology

The seismic refraction/wide-angle reflection profile discussed in this paper traverses the southeastern promontory of the Grenville province (Figure 2.1). The profile extends from eastern Ontario across the Frontenac Arch into the Adirondack massif of northern New York State. The seismic velocity information derived from this seismic refraction/wide-angle reflection profile is intimately related to the compositional and structural

properties of the lithologies which comprise the southeastern Grenville province. Of particular significance to this study is the recognition of distinctive lithologic, metamorphic and structural features associated with the Central Metasedimentary Belt and the Central Granulite Terrane, respectively. These regional geologic characteristics are presented here in order to highlight the geophysical information presented in the following sections.

In eastern Ontario the Central Metasedimentary Belt is characterized by a series of highly sheared calc-silicate marbles, quartzites, meta-evaporites and pelitic migmatitic gneisses belonging to the Grenville supergroup (Lonker, 1980; Davidson, 1986; Carl *et al.*, 1990). During the Grenvillian orogenic cycle the Central Metasedimentary Belt was pervasively deformed, intruded, and metamorphosed to amphibolite/granulite facies suggestive of paleopressures and temperatures of 400-600 MPa/600°C (Wynne-Edwards, 1972; Wiener *et al.*, 1984; McLelland and Isachsen, 1986). On a crustal scale, the Central Metasedimentary Belt is characterized by a series of curvilinear sub-domains separated by a series of mylonitic shear zones which reflect deep level tectonic interleaving with major displacements occurring primarily by ductile flow (Davidson, 1986). Unconformably overlying the Grenville supergroup a Cambrian sandstone and limestone cover sequence denotes the exhumation of the mid-crustal Grenville supergroup lithologies.

The Frontenac Arch, a narrow corridor of Central Metasedimentary Belt lithologies, forms a bridge between the Grenville province exposed in the Canadian Shield and the Grenvillian lithologies which form the anomalous topographic dome of the Adirondack massif (Figure 2.1). The prevailing metamorphic grades diminish somewhat in the Frontenac Arch, where amphibolite facies marbles predominate over the pelitic gneisses and quartzites of the Grenville supergroup (Wiener *et al.*, 1984; McLelland and

Isachsen, 1986). Quartzofeldspathic gneisses exposed in the core of the Frontenac Arch are possible candidates for the basement of the Grenville supergroup (Davidson, 1986). Lithologies belonging to the Central Metasedimentary Belt traverse the St. Lawrence River and extend into the Adirondack Lowlands of northern New York State.

Physiographically, the Adirondack massif is divided into the Adirondack Lowlands, underlain by metasedimentary rocks of the Central Metasedimentary Belt, and the Adirondack Highlands consisting mainly of metaplutonic rocks with intervening synclines of metasediments of the Central Granulite Terrane (McLelland and Isachsen, 1986). The boundary between the Central Metasedimentary Belt and the Central Granulite Terrane is marked by the 110-km-long Carthage-Colton mylonite zone (Figure 2.1). The Carthage-Colton mylonite zone is characterized by intense ductile strain and igneous intrusion synonymous with pervasive mid-lower crustal deformation (McLelland and Isachsen, 1986). A gradational metamorphic facies transition occurs across the Carthage-Colton mylonite zone from the amphibolitic facies metasediments of the Central Metasedimentary Belt to the granulite facies metaplutonic rocks of the Central Granulite Terrane (Bohlen *et al.*, 1985). The continuity of structural and stratigraphic features across the 'boundary' implies that no major displacement has occurred along the Carthage-Colton mylonite zone since the intrusive episode (Wiener, 1983).

In the Adirondack Highlands the Central Granulite Terrane exposes a complex assemblage of polydeformed granitic gneisses, syenites, charnockites and migmatites, interleaved with quartzites and marbles (Wynne-Edwards, 1972; Wiener *et al.*, 1984; McLelland and Isachsen, 1986). Upper granulite facies metamorphism is widely attained within the Central Granulite Terrane, corresponding to lower crustal conditions (800 MPa/800°C) and suggestive of a double crustal thickness at the time of

formation (McLelland and Isachsen, 1980; Wiener *et al.*, 1984; Bohlen *et al.*, 1985). Five phases of deformation are recognized in the Adirondack massif which produce highly complex fold interference patterns rendering stratigraphic correlations across the Adirondacks extremely complex. However, the 'basal units' are believed to be composed of granitic, charnockitic and hornblende gneisses with localized mafic and amphibolitic interlayering (Wiener *et al.*, 1984; McLelland and Isachsen, 1986).

Several large intrusions of meta-anorthosite occur within the Central Granulite Terrane. The largest of these is the Marcy Anorthosite, which is crossed by the seismic profile at its southern tip (Figure 2.1). The Marcy Anorthosite forms a plutonic complex that was emplaced at shallow crustal levels during mild abortive rifting or anorogenic magmatism prior to the Grenvillian orogeny (Moore, 1986; McLelland and Chiarenzelli, 1990). The granitic gneisses, syenites and charnockites that mantle the Marcy Anorthosite are believed to result from widespread melting in the mid-lower crust (Wiener *et al.*, 1984; McLelland and Isachsen, 1986). Field relations, isotopic ages and rare earth element patterns indicate that the granitic envelope that surrounds the Marcy Anorthosite is contemporaneous, but not comagmatic with the anorthosite (McLelland and Isachsen, 1986; McLelland and Chiarenzelli, 1990).

## 2.4 Crustal Structure and Geophysical Framework

In this section we review the results obtained from previous geophysical studies in the southeastern Grenville province, with emphasis placed on characterizing the geophysical features which distinguish the Central Metasedimentary Belt from the Central Granulite Terrane. A broad overview of the deep crustal structure of these sub-terrane is presented by collating previous studies which include seismic reflection experiments, a

teleseismic receiver experiment and geo-conductivity measurements (Figure 2.1).

In 1982 the Geological Survey of Canada conducted a seismic refraction/wide-angle reflection experiment in the Grenville province of eastern Ontario (COCRUST in Figure 2.1). The results obtained from a 320 km long profile which traverses the Central Metasedimentary Belt suggest that the crust is 40 km thick and is characterized by anomalously high seismic velocities (Mereu *et al.*, 1986). The upper crust has a relatively low vertical gradient with velocities of 6.4 km/s at the surface increasing to 6.7 km/s at 23 km depth. The lower crust lies below 23 km and has a velocity of 6.7-7.1 km/s. Previous results obtained from regional seismic surveys in the southeastern Grenville province suggests that these velocity results are broadly applicable across the Central Metasedimentary Belt. *Berry and Fuchs* [1973] found that the crust in the Central Metasedimentary Belt is composed of two layers with velocities of 6.2-6.4 km/s and 6.6-7.1 km/s for the upper and lower crust respectively. In their study the Mohorovicic discontinuity was modeled by a thick transitional zone across which the seismic velocity increases from 7.1-8.5 km/s between a depth of 36 to 50 km. Analysis of converted shear wave phases at the Moho ( $S_p$ ) from long-period seismograms recorded on a regional seismic network in eastern Canada suggests that the average crustal shear wave velocity is  $3.65 \pm 0.15$  km/s, and that the lower crust is characterized by shear wave velocities as low as 3.4 km/s (Jordan and Frazer, 1975). This low shear wave velocity signifies that the lower crust is characterized by an anomalous Poisson's ratio.

Early seismic studies in the Adirondack Highlands utilizing quarry blasts were interpreted to show a 36 km thick crust, with an average seismic velocity of 6.4 km/s (Katz, 1955). An anomalous upper crustal seismic velocity of 6.6 km/s was correlated with the Marcy Anorthosite. *Taylor and Tosköz* [1982] were able to refine this interpretation by analysis of regional

teleseismic travel time data; they found that the crust in the Central Granulite Terrane is relatively homogeneous, about 37 km thick with an average seismic velocity of 6.6 km/s. More recently geophysical studies in the Central Granulite Terrane have concentrated on characterizing a zone of high reflectivity, high shear wave velocities, and high conductivity anomalies in the mid-lower crust (Figure 2.2). Deep seismic reflection profiles collected across the Adirondack massif have enabled a detailed image of the crust in the Central Granulite Terrane to be obtained (COCORP in Figure 2.1). The upper crust is characterized by relatively weak cross-cutting and discontinuous reflections which were interpreted to be consistent with the interlayered meta-igneous/gneissic lithologies exposed at the surface (Brown *et al.*, 1983; Klemperer *et al.*, 1985). A conspicuous band of high amplitude reflections at 18-26 km depth form a wedge-shaped body dipping to the west beneath the Marcy Anorthosite (Figure 2.2a). This band of mid-crustal reflectivity was referred to as the Tahawus complex (Brown *et al.*, 1983). Incomplete resolution of the subcrop of the Tahawus complex resulted in a rather ambiguous definition of its geometry, and hence suggestions concerning its genesis are necessarily unresolved. Beneath the Tahawus complex the lower crust is weakly reflective. Reflections from the Moho are weakly coherent, suggesting a broad transitional crust-mantle discontinuity. This is consistent with results obtained from a teleseismic receiver station.

Analysis of broadband recordings of 31 teleseismic events in the central Adirondack Highlands (RSNY in Figure 2.1) has enabled detailed shear wave velocity information for a localized region of the Adirondack crust to be calculated (Owens, 1987). The principal feature obtained from inversion of the teleseismic receiver functions is a zone of anomalous shear wave velocities of 3.9-4.0 km/s in the mid-crust (Figure 2.2c). This velocity anomaly is underlain by a velocity inversion in the lower crust. Controlled

source electromagnetic sounding in the Central Granulite Terrane suggests the presence of a highly conductive lower crust (Figure 2.1). A hundred-fold increase in the conductivity of the crust was determined for a 5 km thick mid-crustal layer overlying a conductive lower crust (Connerney *et al.*, 1980). This highly conductive zone in the lower crust appears to lie beneath the Tahawus complex (Figure 2.2d).

In summary, the deep crustal structure of the Central Metasedimentary Belt and the Central Granulite Terrane are characterized by profoundly dissimilar geophysical features. These geophysical observations are in accordance with the distinctive lithologic, structural and metamorphic relationships which distinguish the Central Metasedimentary Belt from the Central Granulite Terrane. The western portion of the Ontario-New York-New England seismic profile provides a means to examine the inter-relationship between these two juxtaposed sub-terrane in the southeastern Grenville province.

## 2.5 The Experiment

During the fall of 1988 a 650-km-long seismic refraction/wide-angle reflection profile was deployed across the western New England Appalachian mountains extending through the Adirondack mountains of northern New York State into the Grenvillian craton of southeastern Ontario (Figure 2.1-inset). This seismic profile was acquired by the US Geological Survey, in collaboration with the Geological Survey of Canada and the US Air Force Geophysical Laboratory. Details of the experiment are contained in *Luetgert et al.* [1990]. Results obtained from interpretation of the eastern portion of this seismic profile are presented by *Hughes and Luetgert* [1991].

The western portion of the Ontario-New York-New England seismic profile was recorded in two separate deployments. Full reverse coverage

was obtained by recording shotpoints 10, 14, 17 and 20 in both deployments (Figure 2.1). Following digitization final record sections were plotted in trace normalized and true amplitude format, with a 2-12 Hz filter applied to remove high frequency noise. The most prominent arrivals (first arrivals and reflected phases) were picked. Reciprocal travel times were matched to ensure that all picks were internally consistent. Reciprocity calculations were hindered by low signal to noise ratios at offsets exceeding 50 km on shotpoints 17 and 18. Estimates of travel time pick uncertainties were made for each of the arrival phases as shown in Table 2.1. In general the impulsive nature of the first arrivals and 8-10 Hz dominant frequency of the data ensured that phases were accurately picked and correlated across the record sections. At offsets beyond 170 km diminishing signal strength made picking arrival times somewhat more subjective, and this is reflected in the estimated pick uncertainties.

## 2.6 Description of the Principal Seismic Phases

The record section for shotpoint 16 is characteristic of the seismic refraction/wide-angle reflection data collected across the Central Metasedimentary Belt (Figure 2.3). It shows a first arrival branch ( $P_g$ ) with an apparent velocity of 6.0-6.1 km/s. At an offset of 50 km a crossover to upper crustal ( $P_3$ ) velocities of 6.3-6.4 km/s is observed. Although the profile is 170 km long no refracted first arrivals are observed with apparent velocities exceeding 6.4 km/s. Thus refracted first arrivals from the lower crust must be 'hidden', and have later travel times than those for first arrivals from the upper crust. Weakly coherent reflections ( $P_1P$ ) observed at offsets of 100 km are suggestive of a velocity step into higher mid-crustal velocities (>6.4 km/s). The most striking feature of data collected in the Central Metasedimentary Belt is the observation of multiple coherent wide-angle reflection segments from the lower crust. The lower crustal wide-

angle reflection labeled  $P_{ii}P$  on Figure 2.3 may be correlated laterally within the Central Metasedimentary Belt. The large amplitude of the  $P_{ii}P$  reflection suggests a sharp velocity discontinuity at the top of the lower crust. Reflections from the Moho ( $P_mP$ ) are typically strongly coherent at critical offsets of 130 km. In the Central Metasedimentary Belt Moho reflections are multi-cyclic suggesting compositional interlayering around the crust-mantle boundary (Figure 2.3-arrows).

The record section for shotpoint 10 west is representative of the seismic data gathered across the Central Granulite Terrane. Four principal crustal phases labeled  $P_g$ ,  $P_3$ ,  $P_4$  and  $P_tP$  on Figure 2.4 can be identified and correlated laterally within the Central Granulite Terrane. In addition four crust-mantle phases labeled  $P_mP$ ,  $P_n$ ,  $P_{um}$  and  $P_{um}P$  are observed at offsets exceeding 170 km (Figure 2.4b). In the Central Granulite Terrane the upper crust is characterized by a first arrival ( $P_g$ ) with an apparent velocity of 6.1 km/s, proceeded at a crossover distance of 10 km by a first-arrival branch ( $P_3$ ) with an anomalous apparent velocity of 6.5 km/s. At an offset of 170 km a crossover is observed to first arrivals with an apparent velocity of 6.6 km/s ( $P_4$  in Figure 2.4b). Conspicuous coherent wide-angle reflections ( $P_tP$ ) are observed at offsets between 50 and 150 km that suggest a sharp velocity increase in the mid-crust. Segmented and en-echelon reflections observed behind the  $P_tP$  reflections suggest that the mid-crust is laminated. On shotpoint 10 a broad swath of crust-mantle reflections are observed at offsets greater than 170 km (Figure 2.4b-arrows). Moho reflections ( $P_mP$ ) are typically weakly coherent, indicating a gradational velocity transition into the mantle beneath the Central Granulite Terrane. The  $P_mP$  travel time picks shown on Figure 2.4b delineate the earliest arrival times of these crust-mantle reflections beneath the Central Granulite Terrane. First arrivals from the mantle ( $P_n$ ) are observed at offsets exceeding 240 km with an apparent velocity of 8.0 km/s. The apparent velocity of first-arrivals from

the upper mantle increases dramatically at an offset of 280 km to a velocity of 8.6 km/s ( $P_{um}$ ). This velocity discontinuity in the upper mantle produces a reflected phase labeled  $P_{um}P$ .

## 2.7 Seismic Modeling

We present a two-dimensional seismic velocity model of the crust in the southeastern Grenville province of eastern Ontario and northern New York State. One-dimensional travel time modeling, reflectivity synthetic amplitude modeling, and a two-dimensional linearized travel time inversion were used to derive the seismic velocity model shown in Figure 2.5. The two-dimensional seismic velocity model presented herein is characterized by two discrete and laterally discontinuous mid-lower crustal interfaces. These lateral variations in the model are described below in terms of sub-horizontally layered crustal 'blocks' referred to as the Central Metasedimentary Belt and the Central Granulite Terrane.

The Central Metasedimentary Belt lies at the western end of the profile; between shotpoints 20 and 16 (Figure 2.5). In the Central Metasedimentary Belt the upper crust is represented by three sub-horizontal planar layers. Near surface velocities increase from 5.4 km/s to 6.15 km/s at around 2 km depth. Velocities in the range 6.35-6.45 km/s characterize the upper crust which extends to a depth of 10 km. The base of the upper crust is marked by a weakly reflecting interface, which is modeled by a small velocity step in the model (Figure 2.5a). A 15-km-thick mid-crustal layer is modeled with a velocity of 6.5-6.65 km/s. The transition into the lower crust is delineated by a prominent reflecting interface which dips eastwards from 24 to 28 km depth. The lower crust is modeled with a velocity of 7.0-7.2 km/s. The Moho lies at 44-45 km depth. To the east of shotpoint 16 the profile traverses the Central Granulite Terrane that is represented by a model composed of four layers; (1) a surface layer with apparent velocities

in the range 5.4 km/s to 6.15 km/s, (2) an upper crustal layer characterized by lateral velocity variations associated with the outcrop of the Marcy Anorthosite and velocities in the range 6.45-6.55 km/s, (3) a 5-km-thick mid-crustal layer with a velocity of 7.1 km/s, and (4) a lower crustal layer with an estimated velocity of 6.8-7.0 km/s. In the Central Granulite Terrane the Moho forms a gradational interface with the upper mantle. The upper mantle is characterized by velocities of 8.05-8.2 km/s. A reversed upper mantle layer with a velocity of 8.6 km/s lies at a depth of 50 km beneath the Central Metasedimentary Belt and dips eastwards to a depth of 60 km beneath the Central Granulite Terrane.

Modeling of the western portion of the Ontario-New York-New England seismic refraction/wide-angle reflection data set was completed in successive phases, each used to constrain subsequent iterations. Initially, seismic velocity functions for each shotpoint were calculated using one-dimensional ray trace modeling assuming a plane homogeneous layered Earth (Luetgert, 1988a; Luetgert, 1988b). One-dimensional models of the seismic travel time data acquired across the southeastern Grenville province provide important information on the gross crustal velocity structure. Prominent Moho reflections ( $P_mP$ ) observed on shotpoint 20 at offsets in excess of 300 km enables constraints to be placed on the lower crustal velocity. This is because a significant portion of the total travel time for these far offset  $P_mP$  arrivals is contained within the lower crust, thus the velocity of the lower crust is effectively sampled by the  $P_mP$  phase. A salient point resulting from one-dimensional modeling of shotpoint 20 is that the lower crust is required to have a seismic velocity greater than 7.0 km/s if the  $P_mP$  reflections at offsets exceeding 300 km are to be satisfactorily modeled (Figure 2.6). This is a primary feature of the travel time data acquired in the southeastern Grenville province and must be satisfied in the following two-dimensional analysis.

A simultaneous travel time inversion for interface position and velocity was applied to the seismic data obtained from the western portion of the Ontario-New York-New England seismic refraction/wide-angle reflection experiment. The inversion was completed in three successive steps; (1) inversion for the upper crustal velocity structure from the first arrivals ( $P_g$ ,  $P_3$ ,  $P_4$ ), (2) incorporation of reflections ( $P_iP$ ,  $P_tP$ ,  $P_{ii}P$ ) to define the middle and lower crustal interfaces, and (3) inversion of the crust-mantle boundary phases ( $P_mP$ ,  $P_n$ ) to define the lower crustal velocity and Moho structure. The upper mantle phases ( $P_{um}P$ ,  $P_{um}$ ) were forward modeled to determine the velocity structure of the upper mantle. Each layer in the model is correlated with a particular first arrival branch or reflected phase. For each successively deeper layer results obtained from the above described one-dimensional analyses were contoured to obtain a two-dimensional starting model. The incorporation of reflected phases enhanced the stability of the inversion scheme, by adding additional ray coverage to the deeper portions of the model. Where inadequate ray coverage was available, velocity gradient information obtained from synthetic amplitude modeling aided the inversion procedure. The velocity gradients in each layer were in general fixed prior to the inversion in order to minimize the number of independent parameters. To obtain the best possible final model, the number and position of the velocity and interface nodes were iteratively adjusted to optimize the nodal resolution and travel time fits. The model is intentionally under-parameterized in order to ensure stability in the inversion algorithm, while maximizing the nodal resolution.

In this study we have attempted to quantify the uncertainties involved in deriving the seismic velocity model shown in Figure 2.5. The interpretive step of phase correlation usually introduces much larger uncertainties than those associated with actual travel time modeling of the

correlated phases (Mooney, 1989). The high nodal resolutions obtained herein suggest that the phases selected for travel time modeling are internally consistent. The RMS travel time residuals are on average less than 0.1 seconds. The maximum misfit is associated with the upper mantle where an RMS travel time residual of 0.17 seconds is obtained (Table 2.1). Absolute errors associated with travel time modeling are difficult to quantify. An estimate of the error in depth to interfaces and velocity was sought by applying a series of perturbations to the final model and observing the corresponding deviation in the travel time fit. We estimate that the error in depth to interfaces in the upper crust is probably no greater than several hundred meters, and the corresponding precision in the derived velocity is  $\pm 0.05$  km/s. Considerably more uncertainty exists for the velocity structure of the lower crust as this has been indirectly inferred from later reflected phases. The geometry of the lower crustal and Moho interfaces is probably no better than  $\pm 2$  km. The velocity of the lower crust is likely to be precise to  $\pm 0.2$  km/s; beyond these limits acceptable travel time and amplitude constraints are exceeded.

*The Upper Crust:* The upper crust is represented by a model consisting of three sub-horizontal continuous layers lying above 10 km depth (Figure 2.5a). Topography was included in the model. The near surface (layer 1) is characterized by a homogeneous seismic velocity of 5.4-5.6 km/s. The near offset arrivals ( $P_s$ ) were inverted to estimate the velocities in the near surface layer. The relatively short length of the  $P_s$  arrival branch did not allow the velocity in layer 1 to be resolved laterally between the shotpoints. An inversion for the velocity of the near surface layer was obtained by placing a single velocity node in layer 1. The inclusion of additional velocity nodes into the layer 1 did not provide a justifiable refinement to the inverted velocity structure of this near surface layer. The thickness of layer 1 was specified by an interface node beneath each shotpoint, whose

depth had been previously determined by one-dimensional travel time modeling of the near offset arrivals.

The starting model for layer 2 is characterized by a uniform seismic velocity of 6.0 km/s increasing to 6.1 km/s at 2 km depth. A velocity inversion of layer 2 was then performed by associating this layer with the  $P_g$  arrival branch. During the inversion undesirable velocity oscillations at the base of layer 2 were eliminated by inserting a fixed velocity gradient into layer 2, thus limiting the number of independent parameters and increasing the stability of the inversion. The inversion was run with a series of different vertical velocity gradients fixed into layer 2 to select an optimum value. In this manner the starting velocity was adjusted to a value of 6.0-6.05 km/s because it enabled rays to be traced to a maximum number of travel time observations, while also ensuring a minimum travel time residual. The number of nodes used to specify the velocity structure in layer 2 was increased iteratively and the resulting inverted model was compared to that obtained from the previous inversion. The final model was selected by ensuring that; (1) a minimum RMS travel time residual was obtained, (2) nodal resolutions exceeded 0.6, and (3) by ensuring that rays were traced to a maximum number of travel time picks. Once a suitable model parameterization had been selected, an interface between layers 2 and 3 was inserted into the model. At this point in the modeling procedure the interface between layers 2 and 3 was obtained from one-dimensional modeling which indicated that layer 2 is approximately 2 km thick, but pinches out between shotpoints 13 and 10. The inversion was re-run in order to check that all the observed travel time picks could be ray traced once the interface between layers 2 and 3 had been inserted. The final model obtained from inverting the  $P_g$  arrival has 6 independent velocity nodes evenly divided across the model, and 11 interface nodes, one beneath each shotpoint (Figure 2.5a). A RMS travel time residual of 0.06 seconds

was obtained for the velocity inversion of layer 2. All the parameters had a resolution exceeding 0.8, except a single velocity node beneath shotpoint 10 which was poorly constrained due to the limited extent of the  $P_g$  branch in this location (Table 2.1).

The starting model for layer 3 has a seismic velocity of 6.3-6.4 km/s and extends to a depth of 10 km. First arrivals from the  $P_3$  arrival branch are first observed at crossover offsets of between 20-40 km, and signify a velocity discontinuity in the upper crust (Figure 2.5). The interface between layers 2 and 3 was obtained by smoothing the one-dimensional interface depths, used above, to ensure that rays could be traced to all the  $P_3$  travel time observations (Figure 2.7). Once the interface between layers 2 and 3 was established an inversion for the velocity in layer 3 was performed. The vertical seismic velocity gradient was selected in a similar fashion to that described previously for layer 2, and additional constraints are provided by synthetic amplitude models, described in the following section. The number of velocity nodes incorporated into layer 3 was carefully chosen to maximize the 'goodness of fit' (*i.e.*, the trade-off between RMS residual and nodal resolution). An artifact of this inversion algorithm is that when a layer becomes over-parameterized an unrealistic lateral velocity oscillation is often introduced into the inverted model (Zelt and Smith, 1992). Velocity heterogeneities associated with such an over-parameterized model will characteristically scatter and focus rays resulting in shadow zones at the surface. The final model must therefore be chosen to reflect the geologic complexities inherent in the data, while simultaneously avoiding the introduction of poorly constrained lateral velocity undulations. The velocity model for layer 3 is parameterized by 11 interface nodes and 8 velocity nodes (Figure 2.5a). The first arrivals from layer 3 ( $P_3$ ) were fitted with an RMS travel time residual of 0.09 seconds.

In the Central Metasedimentary Belt a series of weak reflections delineate a velocity step at around 10 km depth ( $P_iP$  in Figure 2.3). Although these reflections are not observed in the Central Granulite Terrane the boundary between layers 3 and 4 was extended across the model to facilitate the travel time modeling procedure. The  $P_iP$  reflections in the Central Metasedimentary Belt were inverted by specifying 5 interface nodes unequally distributed through the model at a depth of 10 km (Figure 2.5a). The number and spacing of these interface nodes were selected to maximize nodal resolution, while ensuring that the interface remained relatively smooth across the model to allow rays to be traced to all observations. The low amplitude and poor coherency of the upper crustal reflections ( $P_iP$ ) did not justify the inclusion of additional nodes into the model. The  $P_iP$  reflections are fitted with an RMS travel time residual of 0.09 seconds (Table 2.1). The inclusion of this reflecting interface had the affect of altering the velocity gradient within layer 3. It was thus necessary to make minor adjustments to the velocity gradients within layer 3 to ensure that all travel time picks could be ray traced once this reflecting interface was included in the model. The final nodal velocity values for layer 3 are shown in Figure 2.5a. The inversion for velocity in layer 3 was run with an RMS travel time residual of 0.09 seconds (Table 2.1).

First arrivals at offsets exceeding 170 km ( $P_4$ ) were used to invert for velocity in layer 4. The starting model for layer 4 has a seismic velocity of 6.5 km/s increasing to 6.6 km/s at 15 km depth. The velocity of layer 4 was obtained by performing an inversion on 6 velocity nodes unequally distributed through the model (Figure 2.5a). The  $P_4$  arrivals are fitted with an RMS travel time residual of 0.09 seconds. The velocity nodes have a resolution in excess of 0.9 except at the edges of the model where there is limited ray coverage from these long offset arrivals (Figure 2.7).

The final velocity model for the upper crust is shown in Figure 2.5a. The upper crustal model is parameterized with 21 velocity nodes and 27 interface nodes. Rays were traced through the upper crustal model using all the first arrivals ( $P_s$ ,  $P_g$ ,  $P_3$  and  $P_4$ ) resulting in an RMS travel time residual of 0.08 seconds for the 1862 first arrival travel time picks used to constrain the velocity structure of the upper crust (Table 2.1). Rays were traced to all travel time observations (Figure 2.7).

*The Mid-Crust:* A fundamental problem encountered in modeling the western portion of the Ontario-New York-New England seismic travel time data is the discontinuous nature of phases associated with the deeper portions of the crust. Reflections from the Tahawus complex ( $P_tP$ ) are only observed within the Central Granulite Terrane, while reflections from the top of the lower crust ( $P_{ij}P$ ) are restricted to the Central Metasedimentary Belt. The velocity gradient in the mid-crust became unrealistic if it was allowed to vary during the inversion, this is because the limited extent of the mid-lower crustal reflection hyperbolae ( $P_tP$  and  $P_{ij}P$ ) do not constrain the velocity of the mid-crust sufficiently to allow a stable velocity inversion. In the following sections we attempt to place constraints on the vertical velocity gradient within the mid-crust by generating synthetic amplitude models for the mid-crustal phases. The information gained from these synthetic amplitude models is then incorporated into the inversion procedure to form a fully reversed model of the mid-crust in the southeastern Grenville province.

In the Central Granulite Terrane the mid-crust is characterized by a series of exceptionally prominent and coherent reflections ( $P_tP$ ) which delineate the top surface of the Tahawus complex (Figure 2.8). Reflectivity synthetic amplitude models were calculated to estimate the vertical seismic gradient in the mid-crust. In the synthetic amplitude model shown in Figure 2.8 we have not attempted to model the intrinsic attenuation of the

crust, rather by adjusting the seismic gradient and the velocity step in the mid-crust we have sought to replicate the amplitude characteristics of the first arrival and reflected phases. The coherent character of the  $P_tP$  reflections suggests a sharp velocity interface in the mid-crust. A velocity step of 0.4 km/s at a depth of 17 km is required to generate sufficiently large amplitude  $P_tP$  reflections at critical offsets of 70-80 km. The seismic velocity gradient of the upper crust is constrained by the decay of the first arrival branch ( $P_3$ ) at offsets greater than 70 km. This necessitates maintaining a minimal vertical velocity gradient ( $\leq 0.01s^{-1}$ ) in the mid-crust, and a velocity step of 6.65 km/s to 7.1 km/s at the top of the Tahawus complex (Figure 2.8-inset).

Once the seismic velocity gradient of the mid-crust had been estimated, an inversion for the interface at the top of the Tahawus complex was performed. The velocity of the mid-crust was fixed prior to running the inversion using the results obtained from the synthetic amplitude modeling. The top of the Tahawus complex was inverted for by specifying 7 interface nodes unevenly distributed across the model. The results obtained from the inversion procedure suggest that the Tahawus complex forms a dome-like feature which dips to the west beneath shotpoint 15 as shown by layer 5 in Figure 2.9. The most westerly reflections which can be correlated with the Tahawus complex lie at 22 km depth beneath shotpoint 15. These westernmost reflections from the Tahawus complex are reversed by shotpoints 14 and 16, and provide important information on the lateral extent of the Tahawus complex (Figure 2.9). Reflections from the top of the Tahawus complex ( $P_tP$ ) are fitted with an RMS travel time residual of 0.08 seconds, and the interface nodes are well resolved (Table 2.1).

The internal structure of the Tahawus complex is poorly constrained by this seismic data set, but significant inferences can be made which allow us to estimate the thickness of the Tahawus complex. In the coda of the  $P_tP$

reflections, which define the top of the Tahawus complex, a series of en-echelon reflection segments characterize the internal structure of the Tahawus complex (Figure 2.8-arrows). These en-echelon reflection segments are likely to be caused by internal laminations and scattering effects within the Tahawus complex itself. An attempt was made to model these reflection segments using a reflectivity model composed of alternating high (7.1 km/s) and low (6.8 km/s) velocity lamellae. The thickness of the velocity lamellae were adjusted to fit the arrival times of the reflection segments from the Tahawus complex. Although it is not possible to resolve the magnitude of the velocity inversion between adjacent layers, such a laminated velocity model allows a qualitative estimate of 22 km to be placed on the deepest reflection segments from the Tahawus complex. A second constraint on the thickness of the Tahawus complex can be obtained from critical  $P_mP$  reflections observed on shotpoint 10. A 7.1 km/s mid-crustal layer which is thicker than 10 km is not permitted by the  $P_mP$  data from shotpoint 10 because it necessitates modeling either an unacceptably thick crust (50 km), or a velocity inversion (<6.6 km/s) in the lower crust beneath the Central Granulite Terrane (discussed fully in the lower crust and Moho section). In the model shown in Figure 2.9 the base of the Tahawus complex is modeled at 22 km depth. In this model the western edge of the Tahawus complex (layer 5) pinches out beneath shotpoint 15 where the westernmost reflections from the Tahawus complex are observed. Layer 5 extends across the model, but further west than shotpoint 15 it has no velocity discontinuity across it and is negligibly thick. This is because reflections from the Tahawus complex are not observed within the Central Metasedimentary Belt.

Modeling of the lower crustal reflections ( $P_{ii}P$ ) within the Central Metasedimentary Belt started by first estimating the vertical seismic velocity gradient of the mid-crust. The seismic velocity gradient of the mid-crust is

constrained by the decay of the first arrival branch ( $P_4$ ). In addition a trade-off is observed between the amplitude of the first arrivals with the magnitude of the velocity step in the lower crust. A velocity step of 0.3 km/s at 25 km depth is required to satisfy the observed  $P_{ii}P$  amplitudes. This necessitates that the velocity gradient in the mid-crust does not exceed  $0.01s^{-1}$  (Figure 2.10). The apparent dip of the lower crustal reflections ( $P_{ii}P$ ) can not be modeled with one-dimensional reflectivity synthetics (Figure 2.10). This feature of the synthetic model indicates that a dipping geometry is required for the interface at the top of the lower crust within the Central Metasedimentary Belt.

Once the velocity in the mid-crust was satisfactorily resolved, an inversion was performed for the mid-lower crustal interface using the  $P_{ii}P$  reflections. The velocity of the mid-crust in the Central Metasedimentary Belt was fixed with a velocity of 6.5-6.65 km/s prior to performing the inversion. In the model, the mid-crust in the Central Metasedimentary Belt is dissected by layer 5. The nodal velocity values in the mid-crust were carefully adjusted above and below layer 5 to ensure that no velocity discontinuity occurred across this model interface in the Central Metasedimentary Belt. Five interface nodes were used to define the mid-lower crustal interface (layers 6/7) in the Central Metasedimentary Belt (Figure 2.9). The lowr crustal reflections ( $P_{ii}P$ ) are fitted with an RMS travel time residual of 0.12 seconds (Table 2.1).

The final model for the mid-crust contains two discontinuous velocity layers which extend across the model (layers 5 and 6 in Figure 2.9). This model parameterization enables rays to be traced to all travel time observations without introducing the added complexity associated with abrupt layer terminations, or sub-vertical interfaces which result in shadow zones and diffractions. An inversion for the  $P_tP$  and  $P_{ii}P$  reflections was performed on the final mid-crustal model to ensure that the above

described reflections and velocity discontinuities could be replicated once these features had been merged across the entire model. Rays were traced through the mid-crustal model using all the  $P_tP$  and  $P_{ii}P$  arrivals resulting in an RMS travel time residual of 0.09 seconds for the 395 travel time picks used to constrain the structure of the mid-crustal interfaces (Figure 2.9).

*The Lower Crust and Moho:* The lower crust is modeled as a 'hidden' layer (layer 7 in Figure 2.11). Estimates of the lower crustal velocity must be indirectly inferred because no first arrivals are observed from the lower crust. In the Central Metasedimentary Belt the velocity structure of lower crust is reversed by Moho reflections ( $P_mP$ ) observed on shotpoints 14 through 20. In the Central Granulite Terrane however, the velocity of the lower crust is poorly constrained because  $P_mP$  reflections are only observed on shotpoint 10, resulting in limited ray coverage for the lower crust in the eastern portion of the model. Constraints on the velocity structure of the lower crust are provided by; (1) one-dimensional travel time modeling of the  $P_mP$  reflection hyperbolae which requires a velocity of 7.0-7.2 km/s in the lower crust as shown in Figure 2.6, (2) iteratively adjusting the velocity in the lower crust until a minimum RMS travel time residual is obtained for the  $P_mP$  phase, and (3) synthetic amplitude modeling of the lower crustal reflections ( $P_{ii}P$ ) which provide evidence for a large velocity step at the top of the lower crust (Figure 2.10).

A simultaneous inversion for velocity and interface position in the lower crust and upper mantle (layers 7 and 8) was performed using the  $P_mP$  and  $P_n$  arrivals (Figure 2.11). The inversion procedure began by considering a homogeneous velocity model for the lower crust and inserting two interface nodes at 45 km for the Moho. A fixed velocity gradient of 7.0-7.2 km/s was inserted into the lower crust to improve the stability of the inversion. The vertical velocity gradient in the lower crust is constrained by the curvature of the  $P_mP$  hyperbola which requires a velocity gradient of 0.01

$s^{-1}$  if rays are to be traced out to offsets of 350 km. This homogeneous lower crustal velocity inversion resulted in a 50 km thick crust beneath the Central Granulite Terrane. This is because the inversion for lower crustal velocity is effectively dominated by the  $P_mP$  phases in the Central Metasedimentary Belt which constrain the lower crust to a velocity of 7.0-7.2 km/s. Consequently, the Moho was forced to a depth of 50 km beneath the Central Granulite Terrane in order to adequately fit the  $P_mP$  phase observed on shotpoint 10. *Hughes and Luetgert* [1991] presented evidence for a 41 km thick crust immediately east of shotpoint 10. The homogeneous lower crustal velocity model was rejected because a 50 km thick crust beneath the Central Granulite Terrane creates an unrealistic Moho topography between the Central Granulite Terrane and the Western New England Appalachians. In order to alleviate this problem two velocity nodes were inserted into the lower crustal model and the inversion was performed again. This time the inversion resulted in a lateral velocity transition in the lower crust from a velocity of 7.15 km/s in the west to a velocity of 6.8 km/s in the east. In this inversion the Moho lies at 44-45 km across the model which is considered geologically more reasonable. The upper mantle (layer 8) was parameterized by 2 velocity nodes at either end of the model, which resulted in a velocity of 8.05-8.2 km/s for the uppermost mantle. An acceptable RMS travel time residual of 0.1 seconds was obtained for the  $P_mP$  and  $P_n$  phases. However, it was not possible to trace rays to the furthest offset  $P_mP$  arrivals using this parameterization.

At this point the number of nodes used to represent the Moho and the velocity of the lower crust were adjusted in an iterative fashion to determine the uniqueness and stability of the inversion. Six interface nodes were selected to represent the Moho. The insertion of more than 6 nodes for the Moho produced unrealistic vertical undulations in this interface (Figure 2.11). The insertion of additional velocity nodes into the model

caused the velocity of the lower crust to become unstable beneath the Central Granulite Terrane, so it was necessary to fix the velocity at the eastern end of the model with the value obtained by the two node inversion. The addition of a third lower crustal velocity node beneath the Central Metasedimentary Belt allowed rays to be traced to all the  $P_mP$  arrivals (Figure 2.11). This third velocity node exploits the  $P_mP$  travel time observations from within the Central Metasedimentary Belt. In the Central Metasedimentary Belt the lower crust has been modeled with vertical velocity gradient of 7.0-7.2 km/s, while to the east in the Central Granulite Terrane the lower crust is modeled with a velocity of 6.8-6.95 km/s. The final model for the lower crust and Moho consists of 3 velocity nodes and 6 interface nodes unevenly spaced across the model (Figure 2.11). The resolution of each interface node is greater than 0.9, and the velocity nodes are similarly well resolved. The RMS travel time residual was 0.11 seconds for the  $P_mP$  and  $P_n$  arrivals (Table 2.1).

*The Upper Mantle:* The velocity structure of the upper mantle was determined by forward modeling of the first arrival and reflected phases ( $P_{um}$  and  $P_{umP}$ ) observed on shotpoints 10 and 20. Although these mantle phases allow a fully reversed forward model to be constructed there is insufficient ray coverage to permit a stable travel time inversion. A velocity of 8.6 km/s is modeled in the upper mantle (layer 9) from reversed first arrivals ( $P_{um}$ ). The position of the interface within the upper mantle (layers 8/9) was iteratively forward modeled to optimize the travel time fit to the  $P_{um}$  and  $P_{umP}$  phases. A dipping interface is required in the upper mantle because of the extreme asymmetry in the  $P_{um}$  first arrival branch. On shotpoint 20 first arrivals from the mantle crossover to a velocity of 8.6 km/s at an offset of 220 km (Figure 2.12a), whereas on shotpoint 10 the  $P_n/P_{um}$  crossover is observed at an offset of 280 km (Figure 2.12b). Two interface nodes were used to define an eastward dipping interface between

50 km to 60 km which allowed rays to be traced to all the travel time picks (Figure 2.12c). The RMS travel time residual was 0.17 seconds for the  $P_{um}$  and  $P_{um}P$  arrivals (Table 2.1).

## 2.8 Discussion

The seismic velocity model derived from the travel time inversion of the western portion of the Ontario-New York-New England seismic refraction/wide-angle reflection profile provides important insights into many geologic and tectonic features of the southeastern Grenville province. In the upper crust a transitional boundary separates the amphibolite facies metasediments of the Central Metasedimentary Belt from the metaplutonic rocks of the Central Granulite Terrane (Figure 2.14). This boundary, known as the Carthage-Colton mylonite zone, forms a regional NNE trending structural lineament characterized by a diffuse zone of steep northwesterly dipping mylonites and metaplutonic intrusives (Wiener *et al.*, 1983; McLelland and Isachsen, 1986). The tectonic significance of the Carthage-Colton mylonite zone is problematic, and remains to be placed in the overall context of the Grenvillian orogenic cycle. However, the continuity of metamorphic isograds and the similarity of stratigraphic sequences across this mylonitic boundary zone implies that it is unlikely to be a crustal penetrating suture (Wiener *et al.*, 1984; Moore, 1986). In concordance with this observation, recent isotopic age and thermobarometry studies across the southeastern Grenville province suggest that the Carthage-Colton mylonite zone is a late-stage extensional fault which developed in response to crustal over thickening and collapse of the Grenville orogen (Corriveau, 1990; McLelland *et al.*, *in press*). Conclusive seismic evidence for the deep crustal expression of the Carthage-Colton mylonite zone is elusive. The velocity structure of the upper crust is remarkably homogeneous in the region of the Carthage-Colton mylonite zone (Figure 2.14). The absence of a resolvable

velocity anomaly or of a seismic reflector associated with the Carthage-Colton mylonite zone suggests that this boundary zone is relatively shallow, probably not penetrating deeper than 2-3 km of the upper crust (Figure 2.14). This interpretation is in accordance with a seismic reflection profile acquired across the northwestern Adirondacks which imaged sparse, discontinuous reflections in the upper crust around the Carthage-Colton mylonite zone (Brown *et al.*, 1983; Klemperer *et al.*, 1985). These seismological observations tend to corroborate many of the observed petrologic, thermobarometry and structural features which distinguish the Central Metasedimentary Belt from the Central Granulite Terrane. In particular, the proposed late-stage extensional down-throw of the Adirondack Lowlands is sufficiently small (3-4 km) to inhibit the resolution of this feature by regional seismic refraction or deep seismic reflection techniques. While simultaneously providing enough displacement to allow the structurally higher and colder amphibolite facies rocks of the Adirondack Lowlands to attain the same structural level as the metaplutonic granulites of the Highlands without suffering granulite facies thermal overprinting.

In the Central Metasedimentary Belt the upper crust is characterized by velocities in the range 6.35-6.45 km/s, and a Poisson's ratio of  $0.26 \pm 0.01$  which are attributable to the amphibolite facies quartzofeldspathic gneisses that underlie this sub-terrane. In the eastern portion of the study area upper crustal velocities of 6.45-6.55 km/s are associated with the granulite facies metaplutonics exposed in the Central Granulite Terrane (Figure 2.14). The Marcy Anorthosite is characterized by an anomalously high compressional-wave velocity of 6.55 km/s. A Poisson's ratio of  $0.28 \pm 0.01$  was obtained for the Marcy Anorthosite from analysis of the eastern portion of the Ontario-New York-New England seismic profile which overlaps with this study (Hughes and Luetgert, 1991). Conclusive seismic evidence for the base of

the Marcy Anorthosite is not resolved by this study. However, the absence of upper crustal reflections or zones of low velocity originating from a change in lithology beneath the anorthosite implies that the Marcy Anorthosite is a thick tabular body possibly extending to a depth of as much as 10 km (Hughes and Luetgert, 1991). The Marcy Anorthosite is overlain by a prominent gravity low, presumably due to its low density relative to the mantling charnockitic and syenitic gneisses (Simmons, 1965; Taylor, 1989). Gravity modeling of the Marcy Anorthosite suggests that it is a 4-5 km thick tabular body, with localized roots extending to 10 km depth (Simmons, 1965). The gravity low coupled with the absence of upper crustal reflections suggests that the Marcy Anorthosite is unlikely to be soled by a gabbroic 'parental' root.

*The Tahawus Complex:* The most prominent feature of the Ontario-New York-New England seismic refraction/wide-angle reflection experiment is the identification of a 5-km-thick layered body in the mid-lower crust, referred to previously as the Tahawus complex (Brown *et al.*, 1983; Klemperer *et al.*, 1985). Correlation of the conspicuous reflections from the Tahawus complex allow us to delineate the top of the Tahawus complex at 17 km dipping gently to the west to a depth of 22 km (Figure 2.14). Hughes and Luetgert [1991] recently reported evidence for the eastward extension of the Tahawus complex dipping from 18 to 20 km beneath the Green Mountains of Vermont. The regional extension of the Tahawus complex is further confirmed by a teleseismic receiver station situated approximately 60 km northwest of the profile (Owens, 1987). The Tahawus complex is characterized by a compressional wave velocity of 7.1 km/s, which when combined with an estimated shear wave velocity of 3.9-4.0 km/s (Owens, 1987) provides an estimate for Poisson's ratio of  $0.27 \pm 0.02$ . Rock types which satisfy these velocity criteria include intermediate-mafic granulites, amphibolites and anorthosite (Fountain and Christensen, 1989;

Holbrook *et al.*, 1992). Important constraints on the origin of the Tahawus complex are provided by the characteristic en-echelon reflection segments which suggest interlayering in the mid-crust. Resolution of the internal structure of the Tahawus complex is enhanced by coincident seismic reflection data which image a westward dipping wedge of short sub-horizontal reflection segments at 18-26 km (Brown *et al.*, 1983; Klemperer *et al.*, 1985). Comparison of the seismic reflection data with the seismic velocity model presented herein, suggests that the Tahawus complex is a 5 km thick laminated body tapering at its edges, so that it appears to form a gently arched dome beneath the Central Granulite Terrane (Figure 2.14).

Layering in the mid-lower crust may be produced by a variety of igneous and structural processes related to the tectono-thermal evolution of the Central Granulite Terrane. Previously proposed candidates include; (1) igneous cumulates deposited as a residue during the genesis of the anorthosite, (2) underthrust metasedimentary strata produced in a continental collision, (3) mafic sills intruded into the mid-lower crust during the rifting of the Iapetus ocean, or (4) gneissic stratification related to the development of large scale nappes in the Adirondack massif (Klemperer *et al.*, 1985; Taylor, 1989; Culotta *et al.*, 1990). We do not favor a relationship between the Marcy Anorthosite and the Tahawus complex, as geologic evidence points to direct fractionation of the anorthosite from a mantle source, without significant crustal contamination resulting from magmatic ponding in the mid-lower crust prior to the emplacement of the Marcy Anorthosite at shallow crustal levels (McLelland and Chiarenzelli, 1989). The dome-like structure coupled with the apparent absence of crustal penetrating shear zones within the Adirondack massif implies that the Tahawus complex is unlikely to be a zone of mylonitized metasediments caught up in a continental collision. Indeed, the high velocity (7.1 km/s) modeled for the Tahawus complex refutes the suggestion that the Tahawus

complex is a mylonitized shear zone. The absence of significant volumes of Precambrian mafic intrusives or a thermal disturbance related to the opening of the Iapetus ocean implies that the Tahawus complex is unlikely to be associated with rift magmatism and the intrusion of mafic sills. Furthermore, the large scale nappe structures in the Adirondack massif produce only a sparsely reflective upper crust on the seismic reflection data (Brown *et al.*, 1983), so that gneissic stratification seems an unlikely candidate for mid-crustal reflectivity within the Adirondack massif.

We propose that the Tahawus complex is related to the intrusion of a series of syn-late orogenic magmas into the mid-lower crust which ponded and differentiated to produce a sequence of alternating felsic layers interspersed with mafic cumulate sills. The development of sub-horizontal recumbent nappes in the Grenvillian orogeny may have provided a favorable rheology to promote stratified layering of the intruded magmas. If this inference is correct, then given the apparent regional dimensions and thickness of the Tahawus complex, a corresponding thermal signature would be expected in the metamorphic record of the exposed metaplutonic granulites. In the Central Granulite Terrane concentric isotherms radiating outwards from the eastern Adirondack Highlands have been correlated with peak Grenvillian metamorphism (Bohlen *et al.*, 1985). The intrusion of successive syn-late orogenic magmas into the deep crust is the most likely source for this radial isotherm pattern. Thus, we believe the Tahawus complex is a laminated mafic cumulate body related to widespread igneous activity coupled with the generation of regional granulite facies conditions during the Grenvillian orogeny (Figure 2.14).

*The Mid-Lower Crustal Reflector:* The lower crust beneath the Central Metasedimentary Belt is characterized by an interface which dips eastwards from 24 to 28 km depth. This interface does not extend eastwards beyond the boundary of the Central Metasedimentary Belt (Figure 2.14). The

seismic character of this interface in the Central Metasedimentary Belt is noticeably dissimilar to that observed for reflections from the Tahawus complex. The mid-lower crustal interface delineates a sharp velocity increase in the crust indicating a bulk compositional change in the lower crust. The structural significance of this dipping lower crustal interface is unclear, but may be an expression of a discontinuity separating the Central Metasedimentary Belt from a deeper underthrust (?) crustal block (Figure 2.14).

*The Lower Crust:* The lower crust beneath the southeastern Grenville province is characterized by compressional-wave velocities in the range 7.0-7.2 km/s, a high Poisson's ratio, and a high conductivity anomaly. Abundant wide-angle Moho reflections from the Central Metasedimentary Belt permit the velocity of the lower crust to be tightly constrained at 7.0-7.2 km/s. In the Central Granulite Terrane however, estimates of the velocity of the lower crust are less well resolved due to the indistinct character of the Moho. Travel times of wide-angle Moho reflections from shotpoint 10 necessitate modeling either; (1) a lateral velocity transition in the lower crust, or (2) a 50 km thick crust beneath the Central Granulite Terrane. The latter alternate is discounted as this requires modeling an unacceptable topography on the Moho, given that the crust is 41 km thick beneath the Champlain Lowlands immediately east of shotpoint 10 (Hughes and Luetgert, 1991). The lower crust is consequently modeled with a lateral velocity transition from 7.0 km/s decreasing to 6.8 km/s at the eastern edge of the model. *Taylor* [1989] summarized previously reported estimates of the lower crustal shear wave velocity which he found to lie in the range 3.4-4.0 km/s. A surprisingly low shear wave velocity of 3.4 km/s was estimated for the lower crust beneath eastern Canada from a study of Moho converted shear wave phases (Jordan and Frazer, 1975). The extension of this anomalously low shear wave velocity beneath the southeastern Grenville

province seems unlikely as shear wave Moho reflections from shotpoint 20 provide evidence of a Poisson's ratio of  $0.28 \pm 0.01$  for the whole crust. An estimate of Poisson's ratio for the lower crust can be made by combining a shear wave velocity of 3.6-3.7 km/s obtained from inversion of teleseismic receiver functions (Owens, 1987) with the compressional wave velocity model which yields a high Poisson's ratio of  $0.30 \pm 0.02$ . This estimate utilizes velocities obtained from two fundamentally different techniques, so precise specification of the lower crustal Poisson's ratio is not possible.

Constraints on the composition of the lower crust can be sought from high pressure laboratory measurements of seismic velocity for typical samples of Adirondack granulites collected in the vicinity of the profile (Birch, 1960; Manghnani *et al.*, 1974; Christensen and Fountain, 1975). These Adirondack rock samples reflect the inherent non-uniqueness of compositional estimates of the lower crust; a sample of anorthosite may have similar seismic properties to a sample of hornblende-pyroxene granulite (Figure 2.14). Broad estimates of lower crustal composition may be obtained by referring to the average seismic properties for a particular suite of rock samples with a similar bulk composition (Holbrook *et al.*, 1992). This analysis suggests that mafic granulites, anorthosite, or amphibolites (meta-gabbros) may be representative of the lower crust (Figure 2.14). Additional geologic and geophysical information must be sought to constrain the composition of the lower crust. *Christensen and Fountain* [1975] noted that laboratory samples at elevated pressures commonly display lower vertical velocity gradients than those typically reported for the lower crust. This observation implies that compositional and metamorphic phase changes are important in the lower crust. Compositional heterogeneity is strongly implied by geo-conductivity measurements in the Adirondack massif which suggest that hydrated minerals such as amphibolite, or alternatively interstitial electrolytes may exist in the lower crust (Connerney

*et al.*, 1980). In the Adirondack massif a typical felsic granulite contains only a few percent garnet, but within a column of granulite 45 km thick, as the velocity model implies, the proportion of garnet should increase corresponding to the breakdown of feldspars with depth. This suggests that the lower crust is likely to be composed of anhydrous garnet-rich granulite lithologies, possibly associated with eclogites. In the following section we will show that a plausible explanation for the high Poisson's ratio lies in the intrusion of substantial volumes of mantle-derived mafic magmas into the lower crust during the Grenvillian orogeny.

*The Moho and Upper Mantle:* The Moho is a variable feature beneath the southeastern Grenville province, and is characterized by short en-echelon reflection segments which denote a gradational velocity increase into the upper mantle. The transitional nature of the Moho is particularly marked beneath the Central Granulite Terrane, where compositional interlayering near the crust-mantle boundary is strongly implied by a broad swath of en-echelon Moho reflection segments. The granulite-eclogite phase transition is a mechanism capable of producing such heterogeneous interlayering. We suggest that the crust-mantle boundary is composed of an interlayered assemblage of garnet-pyroxene granulites, eclogites and peridotites.

In the southeastern Grenville province the upper mantle is characterized by an anomalous seismic velocity of 8.6 km/s, which forms an eastward dipping layer beneath the southeastern Grenville province (Figure 2.14). Fully reversed ray coverage of this mantle layer allows the seismic velocity of 8.6 km/s together with the eastward dip from 50 km to 60 km depth to be well constrained ( $\pm 0.2$  km/s). This anomalous upper mantle velocity is most readily explained by the presence of eclogites (Christensen, 1974; Fountain and Christensen, 1989). Anisotropic alignment of olivine (dunite) in the mantle can not be unequivocally dismissed as a plausible

explanation for the anomalous mantle velocity. The base of this anomalous mantle layer is not resolved by this study, but on the basis of maintaining isostatic equilibrium we suggest that the 8.6 km/s layer is unlikely to extend to the base of the lithosphere. In the following section we propose a possible tectonic mechanism for the generation of eclogites in the upper mantle.

*Tectonic Model:* The geologic vestiges of the Grenvillian orogenic cycle are commonly placed in one of two tectonic models, either continental-continental collision (Dewey and Burke, 1973; Davidson, 1986; Windley, 1986), or ensialic hot spot orogeny (Wynne-Edwards, 1972; Baer, 1981; Bohlen and Mezger, 1989), but as yet resolution of the Grenville problem remains enigmatic. Important constraints on the tectonic evolution of the Grenville province are provided by estimates of cooling rates and inferred uplift histories from thermochronology and thermobarometry studies (Bohlen *et al.*, 1985; Cosca *et al.*, 1991). Paleopressures of 400-600 MPa indicate burial depths of 10-15 km for the amphibolite facies lithologies exposed in the Central Metasedimentary Belt, while in the Central Granulite Terrane paleopressures of 700-800 MPa suggest that the granulite lithologies were exhumed from depths of up to 20 km following the Grenvillian orogeny (Bohlen *et al.*, 1985; McLelland and Isachsen, 1986). These once deeply buried rocks now exposed at the surface are underlain by a 45 km thick crust. This implies that the crust was anomalously thickened ( $\geq 65$  km) during the Grenvillian orogeny, given that there is no evidence for a major crustal thickening event in the period following the Grenvillian orogeny and prior to the exhumation and equilibration of the crust.

Magmatic heating coupled with a high degree of compressive stress appears to be a prerequisite for any tectonic model for the Grenvillian orogeny. The generation of regional granulite facies conditions necessitates high crustal temperatures (750-800°C) during the Grenvillian orogeny.

Burial of the crust by underthrusting alone is unlikely to provide sufficient heat to generate the granulite facies conditions given the low radiogenic component of typical granulites (Taylor and McLennan, 1985). The additional heat necessary for the generation of regional scale granulite facies conditions may be provided by the intrusion of large volumes of early or syn-tectonic magmas of basaltic composition into the Proterozoic crust (Bohlen and Mezger, 1989). The most likely source region for the episodic fractionation and intrusion of these felsic magmas is from a mantle-derived basaltic underplate which formed early in the Grenvillian orogenic cycle (Figure 2.15a). These hot felsic intrusions promoted the progressive anatectic melting and dehydration of the crust resulting in the formation of a thick refractory mass of felsic granulites, charnockites, and syenites (Wynne-Edwards, 1972; Bohlen and Mezger, 1989).

Interpretation of this model for the formation of granulite facies conditions implies that the underplated magmas which ponded near the base of the over-thickened Grenvillian crust would crystallize as eclogites with densities near that of spinel or garnet peridotite. The formation of eclogite facies assemblages in the lower crust would initially retard regional uplift, allowing the penetration of granulite facies conditions on a regional scale. Eclogization of the lower crust is strongly implied by thermo-barometry studies which indicate that slow isobaric cooling preceded exhumation of the crust (Bohlen *et al.*, 1985; Bohlen and Mezger, 1989). However, with the ensuing thermal relaxation, delamination of the dense underplated crustal root would initiate differential isostatic uplift (Figure 2.15b). Thus, in the period following the Grenvillian orogeny the dense underplated crust would be recycled back into the mantle by means of gravitational differentiation. We suggest that the anomalous 8.6 km/s layer in the upper mantle may be surviving evidence of Mid-Proterozoic magmatic underplating of the crust (Figure 2.15b). Once the Proterozoic

crust began to delaminate, the lighter upper crust would tend to rise isostatically. The rate of uplift is controlled by many factors including the prevailing compressional regime, the thermo-rheology and the density of the crust and upper mantle. Interpretation of the velocity model suggests that the lower crust and upper mantle is more mafic and hence denser beneath the Central Metasedimentary Belt than beneath the Central Granulite Terrane (Figure 2.14). We propose that on a macro-scale the exhumation of the crust was controlled by the petro-physical properties of the deep crust which influenced the rate and degree of uplift of the mid-lower crustal rocks exposed in the southeastern Grenville province.

The Grenvillian orogeny was a major metamorphic, tectonic and magmatic mountain building episode that accreted older crystalline basements to the Proterozoic craton of North America. In the southeastern Grenville province ductile interleaving and magmatic reworking of the crust has acted to homogenize and anneal the boundary separating the Central Metasedimentary Belt from the Central Granulite Terrane. The structures that we observe in the deep crust beneath the southeastern Grenville province are remnants of Proterozoic crustal formation processes, which likely owe their origin to successive northwest directed compressional events coupled with the intrusion of large volumes of syn-tectonic mantle-derived magmas.

**2.9 Acknowledgments**

The data presented in this paper were collected by the US Geological Survey, the Geological Survey of Canada, and the US Air Force Geophysics Laboratory. The authors would like to thank the field crew for their Herculean efforts, with special mention going to Ed Criley without whom the experiment would not have been a success. Penetrating and constructive discussions with our colleagues at the USGS helped to enhance our appreciation of the data and our understanding of its tectonic significance. Walter Mooney, Steve Bohlen and Harley Benz provided reviews of earlier versions of this paper. We thank John Ebel and Colin Zelt for their reviews of the manuscript prior to publication. Support from the US Air Force Geophysical Laboratory and the USGS Deep Continental Studies program is gratefully acknowledged.

**2.10 References**

- Baer, A.J., A Grenvillian model of Proterozoic plate tectonics, in *Precambrian Plate Tectonics*, edited by A. Kroner, pp. 353-385, Elsevier, Holland, 1981.
- Berry, M.J. and K. Fuchs, Crustal structure of the Superior and Grenville provinces of the northeastern Canadian Shield, *Bull. Siesmo. Soc. Am.*, 63, 1393-1432, 1973.
- Birch, F., The velocity of compressional waves in rocks at 10 Kbars part 1, *J. Geophys. Res.*, 65, 1083-1102, 1960.
- Blackwell, D.D., The thermal structure of the continental crust, in *The Structure and Physical Properties of the Earth's crust*, edited by J.G. Heacock, Am. Geophys. Un. Geophys. Monogr. Ser. 14, pp. 169-184, 1971.
- Bohlen, S.R., J.W. Valley, and E.J. Essene, Metamorphism in the Adirondacks I petrology, pressure and temperature, *Journal of Petrology*, 26, 971-992, 1985.
- Bohlen, S.R. and K. Mezger, Origin of granulite terranes and the formation of the lowermost continental crust, *Science*, 244, 326-329, 1989.
- Brown, L.D., C.J. Ando, S. Klemperer, J.E. Oliver, S. Kaufman, B. Czuchra, T. Walsh, and Y.W. Isachsen, Adirondack-Appalachian crustal structure: The COCORP northeast traverse, *Geol. Soc. Am. Bull.*, 94, 1173-1184, 1983.
- Carl, J.D., W.F. DeLorraine, D.G. Mose, and Y. Shieh, Geochemical evidence for a revised Precambrian sequence in the northwest Adirondacks, New York, *Geol. Soc. Am. Bull.*, 102, 182-192, 1990.
- Christensen, N.I., Compressional-wave velocities in possible mantle rocks to pressures of 30 Kbars, *J. Geophys. Res.*, 79, 407-412, 1974.

- Christensen, N.I., Compressional-wave velocities in rocks at high temperatures and pressures, critical thermal gradients, and crustal low velocity zones, *J. Geophys. Res.*, *84*, 6849-6857, 1979.
- Christensen, N.I. and D.M. Fountain, Constitution of the lower continental crust based on experimental studies of seismic velocities in granulite, *Geol. Soc. Am. Bull.*, *86*, 227-236, 1975.
- Connerney, J.E.P., A. Nekut and A.F. Kuckes, Deep crustal electrical conductivity in the Adirondacks, *J. Geophys. Res.*, *85*, 2603-2614, 1980.
- Corriveau, L., Proterozoic subduction and terrane amalgamation in the southwestern Grenville province, Canada: Evidence for ultrapotassic to shoshontic plutonism, *Geology*, *18*, 614-617, 1990.
- Cosca M.A., J.F. Sutter and E.J. Essene, Cooling and inferred uplift/erosion history of the Grenville orogeny, Ontario: constraints from  $^{40}\text{Ar}/^{39}\text{Ar}$  thermochronology, *Tectonics*, *10*, 959-977, 1991.
- Culotta, R.C., T. Pratt and J.E. Oliver, A tale of two sutures: COCORP's deep seismic surveys of the Grenville province in the eastern US mid-continent, *Geology*, *18*, 646-649, 1990.
- Davidson, A., New interpretations in the southwestern Grenville province, in *The Grenville province*, edited by J. M. Moore, A. Davidson and A. J. Baer, pp. 61-74, Geol. Assoc. Can. Special Paper 31, 1986.
- Dewey, J.F. and K.C.A. Burke, Tibetan, Variscan, and Precambrian basement reactivation: products of continental collision, *Journal of Geology*, *81*, 683-692, 1973.
- Durrheim R.J. and W.D. Mooney, Archean and Proterozoic crustal evolution: Evidence from crustal seismology, *Geology*, *19*, 606-609, 1991.
- Fountain, D.M. and N.I. Christensen, Composition of the continental crust and upper mantle; a review, in *Geophysical Framework of the*

*Continental United States*, edited by L.C. Pakiser and W.D. Mooney, pp. 711-742, Geol. Soc. Am. Memoir 172, 1989.

Holbrook, W.S., W.D. Mooney and N.I. Christensen, The seismic velocity structure of the deep continental crust, in *The Continental Lower Crust*, edited by D.M. Fountain, R. Arculus and R. Kay, pp. 5-44, Elsevier, Holland, 1992.

Hughes, S. and J.H. Luetgert, Crustal structure of the western Appalachians and the Adirondack Mountains, *J. Geophys. Res.*, 96, 16471-16494, 1991.

Jordan, T.H., and L.N. Frazer, Crustal and upper mantle structure from S<sub>p</sub> phases, *J. Geophys. Res.*, 80, 1504-1518, 1975.

Katz, S., Seismic study of crustal structure in Pennsylvania and New York, *Bull. Seismo. Soc. Am.*, 45, 303-325, 1955.

Klemperer, S.L., L.D. Brown, J.E. Oliver, C.J. Ando, B.L. Czuchra and S. Kaufman, Some results of COCORP seismic reflection profiling in the Grenville-age Adirondack Mountains, New York State, *Can. J. Earth Sci.*, 22, 141-153, 1985.

Kroner, A., Composition, structure and evolution of the early Precambrian lower continental crust: constraints from geological observations and age relationships, in *Reflection Seismology: The continental crust, Geodynamics series 14*, edited by M. Barazangi and L.D. Brown, pp. 107-119, AGU, Washington D.C., 1986.

Lonker, S., Conditions of metamorphism in high-grade pelitic gneisses from the Frontenac Axis, Ontario, Canada, *Can. J. Earth Sci.*, 17, 1666-1684, 1980.

Luetgert, J.H., S. Hughes, J. Cipar, S. Mangino, D. Forsyth, and I. Asudeh, Data report for O-NYNEX, the 1988 Grenville-Appalachian seismic refraction experiment in Ontario, New York and New England, *US Geological Survey Open File report 90-426*, 1990.

- Luetgert, J.H., Users manual for RSEC88: Interactive computer program for plotting seismic refraction record sections, *US Geol. Surv. Open File Report 88-262*, 1988a.
- Luetgert, J.H., Users manual for R1D84: Interactive modeling of one-dimensional velocity depth functions, *US Geol. Surv. Open File Report 88-262*, 1988b.
- Manghnani, M.H., R. Ramananantoandro and S.P. Clark, Compressional and shear wave velocities in granulite facies rocks and eclogites to 10 Kbars, *J. Geophys. Res.*, 79, 5427-5446, 1974.
- McLelland, J.M., J.S. Daly and J. Chiarenzelli, Sm-Nd and U-Pb isotopic evidence of juvenile crust in the Adirondack Lowlands and implications for the evolution of the Adirondack Mountains, *Journal of Geology*, in press.
- McLelland, J.M. and J. Chiarenzelli, Isotopic constraints on emplacement age of anorthositic rocks of the Marcy Massif, Adirondack Mountains, New York, *Journal of Geology*, 98, 19-41, 1990.
- McLelland, J.M. and Y.W. Isachsen, Structural synthesis of the southern and central Adirondacks: A model for the Adirondacks as a whole and plate tectonics interpretations, *Bull. Geol. Soc. Am.*, 91, 208-292, 1980.
- McLelland, J.M. and Y.W. Isachsen, Synthesis of Geology of the Adirondack Mountains, New York and their tectonic setting within the southwestern Grenville province, in *The Grenville province*, edited by J.M. Moore, A. Davidson and A.J. Baer, pp. 61-74, Geol. Assoc. Can. Special Paper 31, 1986.
- Mereu, R., D. Wang , and O. Kuhn, Evidence for an inactive rift in the Precambrian from a wide-angle reflection survey across the Ottawa-Bonnechere graben, in *Reflection Seismology: The continental crust, Geodynamics series 14*, edited by M. Barazangi and L.D. Brown, pp. 127-134, AGU, Washington D.C., 1986.

- Mooney, W.D., Seismic methods for determining earthquake source parameters and lithospheric structure, in *Geophysical Framework of the Continental United States*, edited by L.C. Pakiser and W.D. Mooney, pp. 11-34, Geol. Soc. Am. Memoir 172, 1989.
- Moore, J.M., Introduction: The Grenville problem then and now, in *The Grenville province*, edited by J.M. Moore, A. Davidson and A.J. Baer, pp. 1-11, Geol. Assoc. Can. Special Paper 31, 1986.
- Owens, T.J., Crustal structure of the Adirondacks determined from broadband teleseismic waveform modeling, *J. Geophys. Res.*, 92, 6391-6401, 1987.
- Simmons, G., Gravity survey and geological interpretation, northern New York, *Geol. Soc. Am.*, 75, 81-98, 1964.
- Taylor, S.R. and S.M. McLennan, *The Continental Crust: its composition and evolution*. pp. 75-81, Blackwell, Oxford, 1985.
- Taylor, S.R., Geophysical framework of the Appalachians and Adjacent Grenville province, in *The Geophysical Framework of the Continental United States*, edited by L.C. Pakiser and W.D. Mooney, pp. 317-348, Geol. Soc. Am. Memoir 172, 1989.
- Taylor, S.R. and M.N. Tosköz, Crust and upper-mantle velocity structure in the Appalachian orogenic Belt: Implications for tectonic evolution, *Geol. Soc. Am. Bull.*, 93, 315-329, 1982.
- Wiener, R.W., J.M. McLelland, Y.I. Isachsen, and L.M. Hall, Stratigraphy and structural geology of the Adirondack Mountains, New York: review and synthesis, in *The Grenville Event in the Appalachians and Related Topics*, edited by M.J. Bartholomew, pp. 1-55, Geol. Soc. Am. Special Paper 194, 1984.
- Wiener, R.W., Adirondack Highlands-Northwest lowlands 'boundary': a multiply folded intrusive contact with associated mylonitization, *Geol. Soc. Am. Bull.*, 94, 1081-1108, 1983.

Windley, B.F., Comparative tectonics of the western Grenville and the western Himalayas, in *The Grenville province*, edited by J.M. Moore, A. Davidson and A.J. Baer, pp. 341-348, Geol. Assoc. Can. Special Paper 31, 1986.

Wynne-Edwards, H.R., The Grenville province, in *Variations in Tectonic Styles in Canada*, edited by R.A. Price and R.J.W. Douglas, pp. 263-334, Geol. Assoc. Can. Special Paper 11, 1972.

Zelt, C.A. and Smith R.B., Seismic travel time inversion for two-dimensional crustal velocity structure, *Geophysical Journal International*, 108, 16-34, 1992.

## 2.11 Captions

**Table 2.1:** Final results obtained from the travel time inversion of the Ontario-New York-New England seismic refraction/wide-angle reflection data. The RMS travel time residual indicates the misfit between the observed data and the predicted travel times by the final model shown in Figure 2.5. Chi-squared is the normalized (to the number of observations) misfit with an expected value of 1. The resolution indicates the relative amount of ray coverage that samples each model parameter, and varies between 0 and 1 with values greater than 0.5 considered well resolved and reliable (Zelt and Smith, 1992).

**Figure 2.1:** Simplified geologic map of the southeastern Grenville province, showing the location of the western portion of the Ontario-New York-New England seismic refraction/wide-angle reflection profile (O-NYNEX). The inset map shows regional location, and the extent of the entire seismic profile. Mylonitic shear zones (gray lines) divide the southeastern Grenville province into the Central Metasedimentary Belt and the Central Granulite Terrane (Davidson, 1986; McLelland and Isachsen, 1986). The following sub-domains; F-Frontenac Arch, L-Adirondack Lowlands, and H-Adirondack Highlands are referred to in the text. The figure shows the locations of previous geophysical experiments in the southeastern Grenville province (Connerney *et al.*, 1980; Brown *et al.*, 1983; Mereu *et al.*, 1986; and Owens, 1987).

**Figure 2.2:** A comparison of geophysical experiments in the Central Granulite Terrane. The Tahawus complex, a thick laminated body in the mid-crust beneath the Central Granulite Terrane, has been imaged by (a) vertical reflection profiling (Brown *et al.*, 1983; Klemperer *et al.*, 1985), (b) the present study, (c) teleseismic receiver studies (Owens, 1987). Geoelectrical measurements (d) indicate that the lower crust is anomalously conductive (Connerney *et al.*, 1980).

**Figure 2.3:** Record section for shotpoint 16 west plotted in trace normalized format with distances plotted relative to the shotpoint. Seismic refraction/wide-angle reflection data collected across the Central Metasedimentary Belt characteristically show an upper crustal velocity of 6.1 km/s ( $P_g$ ) with a crossover at 50 km to a velocity of 6.4 km/s ( $P_3$ ). Weakly coherent reflections ( $P_iP$ ) at offsets of 80-110 km signify a velocity step into the mid-crust. The top of the lower crust is defined by prominent reflections ( $P_{ij}P$ ) observed at offsets between 140-170 km. En-echelon reflection segments from the Moho suggest compositional interlayering around the crust-mantle boundary (arrows). Travel time picks used in the inversion are shown by the dots, and critical points are indicated on the seismic data. The data are plotted with a reduction velocity of 6.0 km/s. A 2-12 Hz band-pass filter has been applied to the data.

**Figure 2.4:** Record section for shotpoint 10 west plotted in trace normalized format with distances plotted relative to the shotpoint. Seismic refraction/wide-angle reflection data collected across the Central Granulite Terrane show characteristic upper crustal velocities of 6.5 km/s ( $P_3$ ) and prominent coherent mid-crustal reflections ( $P_tP$ ) of the Tahawus complex (a). Segmented and en-echelon Moho reflections ( $P_mP$ ) suggest a transitional crust-mantle boundary beneath the Central Granulite Terrane (b-arrows). Travel time picks for  $P_mP$  delineate the earliest reflections from the base of the crust. First arrivals from the upper mantle ( $P_n$ ) are observed at offsets up to 240 km with an apparent velocity of 8.0 km/s. A crossover to an apparent velocity of 8.6 km/s ( $P_{um}$ ) is observed at 280 km (b). Travel time picks used in the inversion are shown by the dots. Plotting parameters as in Figure 2.3.

**Figure 2.5:** Seismic velocity model derived from the western portion of the Ontario-New York-New England seismic refraction/wide-angle reflection profile. The upper crust is shown in (a), and the complete

model is shown below (b). The velocity model is parameterized by a series of velocity nodes indicated by the circles, and interface nodes shown by the squares. All velocity nodes are labeled in km/s. Prominent reflecting interfaces are shown by the bold lines, and model interfaces are shown dashed. The Tahawus complex is shown stippled (Layer 5). Topography is included in the model. Layer numbers are referenced in the text, and in subsequent figures. Distance is plotted relative to shotpoint 20 (Figure 2.1).

**Figure 2.6:** A one-dimensional velocity model for shotpoint 20 (Figure 2.1). The upper crustal arrival ( $P_3$ ) with a velocity of 6.4 km/s may be traced laterally for over 200 km. Reflections from the top of the lower crust ( $P_{ii}P$ ) are modeled by a velocity step at 25 km depth. A high velocity layer (7.0-7.2 km/s) in the lower crust is required to adequately fit the wide-angle Moho reflections ( $P_mP$ ) at offsets exceeding 300 km. Note, the far offset  $P_mP$  arrivals cannot be fitted with a velocity of 6.8 km/s in the lower crust (stippled travel-time hyperbola).

**Figure 2.7:** Results obtained from the travel time inversion of the upper crustal first arrival phases  $P_s$ ,  $P_g$ ,  $P_3$  and  $P_4$  related to layers 1, 2, 3 and 4 respectively. A total of 1862 travel time picks were used in the inversion, whose estimated travel time uncertainty is proportional to the height of the vertical bars (a). Rays are traced to all the picks in the final model which yields an RMS travel time residual of 0.08 seconds (b). The nodal parameterization of the velocity model (b) is shown in Figure 2.5a. Interfaces are shown by the bold lines for clarity. Every third ray is shown, so actual ray density is three times greater than shown.

**Figure 2.8:** Reflectivity synthetic (a) and trace normalized seismic refraction/wide-angle reflection data from shotpoint 13 east (b) showing reflections from the Tahawus complex ( $P_tP$ ). The velocity model used to calculate the synthetic is shown (inset). A P-wave attenuation ( $Q_\alpha$ ) of 1000 was used to calculate the synthetics. The arrows show pre-critical reflections

that were not modeled, but are probably caused by internal laminations and scattering within the Tahawus complex (b). Travel time picks are shown by the dots, and the critical point is indicated on the  $P_tP$  phase. Plotting parameters as in Figure 2.3.

**Figure 2.9:** Results obtained from the travel time inversion of the mid-crustal phases  $P_tP$  and  $P_{ii}P$  used to invert for the interfaces 4/5 and 6/7 respectively. The Tahawus complex is shown stippled (layer 5). The nodal velocity parameterization is shown in Figure 2.5b. A total of 395 travel time picks were used in the inversion, with an estimated pick uncertainty of  $\pm 0.05$  s for  $P_tP$  and  $\pm 0.075$  s for  $P_{ii}P$  (a). Rays are traced to all picks in the final model (b) which yields an RMS travel time residual of 0.09 seconds. Interface nodes used in the inversion are shown by the squares. Every third ray is shown, so actual ray density is three times greater than shown.

**Figure 2.10:** Reflectivity synthetic (a) and trace normalized seismic refraction/wide-angle reflection data from shotpoint 15 west (b) showing reflections from the top of the lower crust ( $P_{ii}P$ ). The velocity model used to calculate the synthetic is shown (inset). A P-wave attenuation ( $Q_\alpha$ ) of 1000 was used to calculate the synthetics. Travel time picks are shown by the dots. Plotting parameters as in Figure 2.3.

**Figure 2.11:** Results obtained from a simultaneous travel time inversion for velocity and interface in the lower crust (layer 7) and upper mantle (layer 8) using the  $P_mP$  and  $P_n$  phases. The lower crust is shown shaded, velocity and interface nodes used in the inversion are shown by the circles and squares respectively. The Tahawus complex is shown by the stipple pattern. See Figure 2.5b for the nodal velocity parameterization. A total of 589 travel time picks were used in the inversion, with an estimated pick uncertainty of  $\pm 0.05$  s for  $P_mP$  phase and  $\pm 0.1$  s for  $P_n$  phase (a). Rays are traced to all picks in the final model (b) which yields an RMS travel time

residual of 0.11 seconds. Every third ray is shown, so actual ray density is three times greater than shown.

**Figure 2.12:** Results obtained from forward modeling of the upper mantle (layers 8 and 9) using the  $P_n$ ,  $P_{um}$  and  $P_{um}P$  phases. The record section for shotpoint 20 east shows refracted first arrivals from the upper mantle with an apparent velocity of 8.6 km/s (a). The travel time picks used in the forward modeling are shown by the dots on the data and in the travel time diagram (b). The ray diagram shows reversed control on the dipping mantle interface (c). Rays are traced to all picks in the final model which yields an RMS travel time residual of 0.17 seconds. Every third ray is shown, so actual ray density is three times greater than shown. The seismic data are plotted using a reducing velocity of 8.0 km/s (a), and travel-time data are plotted with a reduction velocity of 6.0 km/s (b). A 2-12 Hz band-pass filter has been applied to the data.

**Figure 2.13:** Interpretive deep crustal section for the southeastern Grenville province obtained from the western portion of the Ontario-New York-New England seismic refraction/wide-angle reflection profile (Figure 2.1). The homogeneous velocity structure of the upper crust in the vicinity of the Carthage-Colton mylonite zone suggests that this boundary is a shallow feature. The Tahawus complex, a laminated dome-like body in the mid-crust, is interpreted as a zone of mafic cumulate sills on the basis of its high velocity (7.1 km/s) and Poisson's ratio ( $0.27 \pm 0.02$ ). The lower crust is characterized by a velocity of 7.0 km/s and a Poisson's ratio of  $0.30 \pm 0.02$  indicating mafic granulites, possibly grading into eclogites in the lower portions of the crust and upper mantle. Velocity variations in the lower crust appear to signify a lateral change in composition, possible reflecting a decrease in the mafic content of the lower crust beneath the Central Granulite Terrane. The Moho is a transitional zone of interlayered mafic granulites, eclogites and peridotites. The anomalous upper mantle layer

with a velocity of 8.6 km/s is interpreted as a lens of eclogite associated with extensive underplating and fractionation of mantle-derived melts during the Grenvillian orogeny. Inferred layer compositions are illustrated with their associated compressional and shear wave velocities ( $V_p$  and  $V_s$ ) and Poisson's ratio ( $\sigma$ ), in each case the average layer velocity is allotted. The velocity suffixes refer to; (1) *Hughes and Luetgert* [1991] and (2) *Owens* [1987].

**Figure 2.14:** The composition of the lower crust is estimated by comparing its seismic velocity (dark stipple) with laboratory velocity measurements of rock samples at elevated pressures. The average seismic velocities for possible constituents of the lower crust are plotted and keyed to the patterns on the left; ranges shown are one standard deviation (*Holbrook et al.*, 1992). Rock samples from the Adirondack massif are plotted with a temperature correction using a geotherm of 15°C/km (*Blackwell*, 1971) and an average thermal coefficient of  $2.0 \times 10^{-4}$  km/s°C<sup>-1</sup> (*Christensen*, 1979). Samples are from *Manghnani et al.* [1974] and *Christensen and Fountain* [1975]. The seismic velocity of the lower crust is inferred to be best represented by mafic granulites (anhydrous feldspar, pyroxene, garnet assemblages).

**Figure 2.15:** Interpretative tectonic scenario for the southeastern Grenville province. At the time of the Grenvillian orogeny the crust was over-thickened by the development of large scale northwestward verging nappes coupled with magmatic underplating of the crust (a). The mid-lower crust was intruded by hot felsic magmas derived from the mantle underplate which provided the heat for the production of regional granulite facies conditions. Ponding and fractionation of these intruded magmas may have produced the Tahawus complex. Subsequent isostatic and thermal adjustments initiated by the eclogization and delamination of the dense underplated crustal root has exposed an oblique slice through the mid-lower

crust (b). The delaminated magmatic underplate survives as a lens of eclogite in the upper mantle.

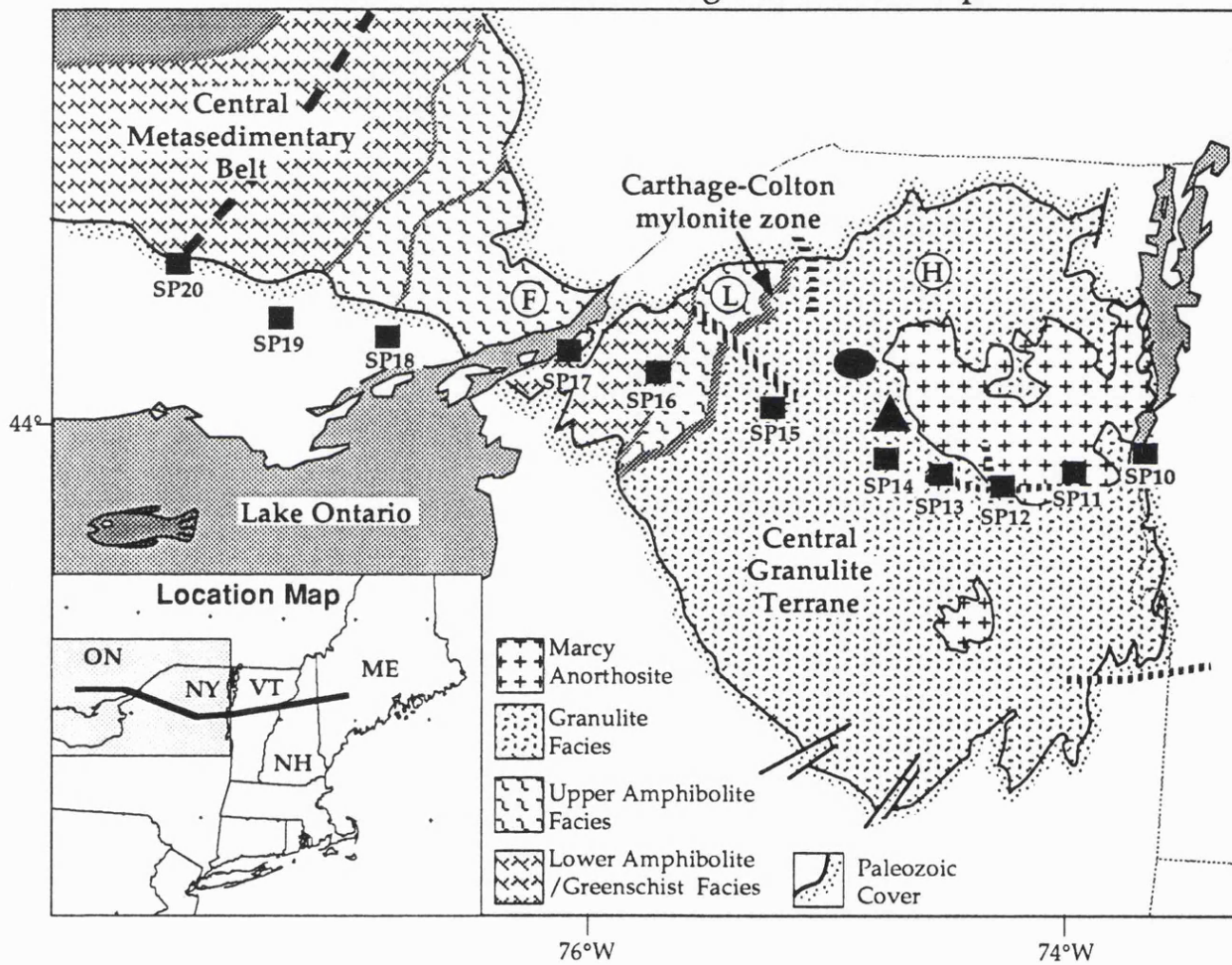
2.12 Table

INVERSION	Data			Final Model			Parameters	
	PHASES USED (layer no.)	Number of Picks (Uncertainty, s)	Number of Picks used	RMS TRAVEL TIME RESIDUAL, S	Chi-Squared	Velocity Nodes (Resolution)	Interface Nodes (Resolution)	
Upper Crustal Velocity and Interface	P <sub>s</sub> (1)	74 (±0.02)	68	0.03	2.26	1 (>0.9)	14	
	P <sub>g</sub> (2)	419 (±0.05)	417	0.06	1.42	6 (>0.8)	11 (>0.9)	
	P <sub>3</sub> (3)	1206 (±0.05)	1191	0.09	3.04	8 (>0.9)	11 (>0.9)	
	P <sub>1</sub> P (3/4)	76 (±0.075)	76	0.09	1.47	-	5 (>0.8)	
	P <sub>4</sub> (4)	163 (±0.05)	163	0.09	1.47	6 (>0.9)	-	
Upper Crustal Model	P <sub>s</sub> , P <sub>g</sub> , P <sub>3</sub> , P <sub>4</sub> (1, 2, 3, 4)	1862	1836	0.08	2.50	21 (>0.8)	-	
Tahawus Complex	P <sub>t</sub> P (4/5)	270 (±0.05)	266	0.08	2.25	-	7 (>0.9)	
Lower Crustal Reflector	P <sub>ii</sub> P (6/7)	131 (±0.075)	119	0.12	1.48	-	5 (>0.6)	
Mid-Crustal Model	P <sub>t</sub> P, P <sub>ii</sub> P (4/5, 6/7)	395	387	0.09	1.96	-	12 (>0.6)	
Lower Crust/ Upper Mantle Velocity and Moho	P <sub>m</sub> P (7/8)	528 (±0.05)	573	0.11	4.96	3 (>0.7)	6 (>0.9)	
	P <sub>n</sub> (8)	61 (±0.1)				2 (>0.8)		
Mantle Velocity and Interface	P <sub>um</sub> P (8/9) P <sub>um</sub> (9)	61 (±0.15) 185 (±0.1)	232	0.17	2.34	1 (>0.9)	4 (>0.4)	

Table 2.1

2.13 Figures

The Ontario-New York-New England Seismic Experiment



Key to Symbols

- |           |                                         |   |                                                           |
|-----------|-----------------------------------------|---|-----------------------------------------------------------|
| ■<br>SP10 | Seismic Refraction Shotpoints (O-NYNEX) | ▲ | Location of Source Loop for Geo-Conductivity Measurements |
| ---       | Deep Seismic Reflection Line (COCORP)   | ● | Broad Band Teleseismic Receiver Station (RSNY)            |
| ---       | Seismic Refraction Profile (COCRUST)    |   |                                                           |

Figure 2.1



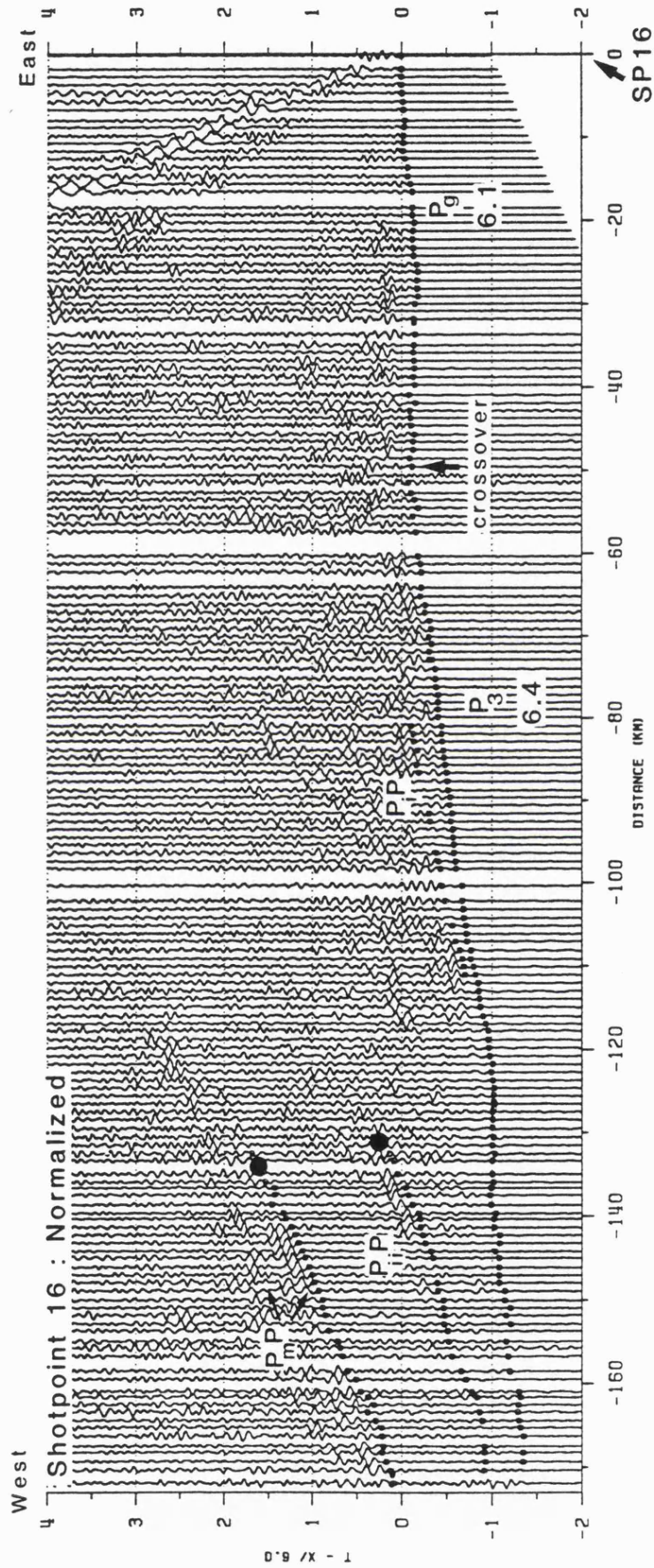


Figure 2.3

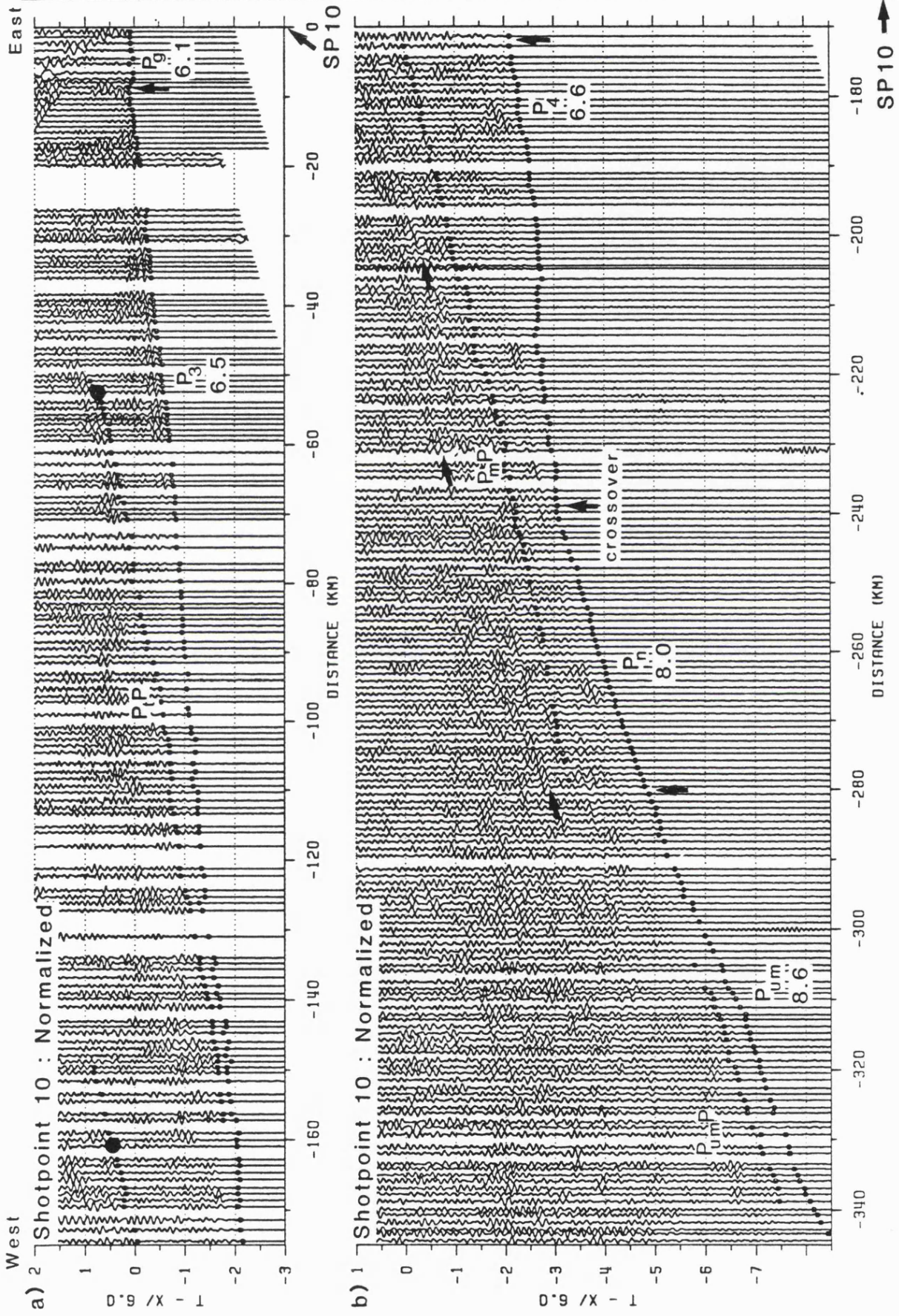


Figure 2.4

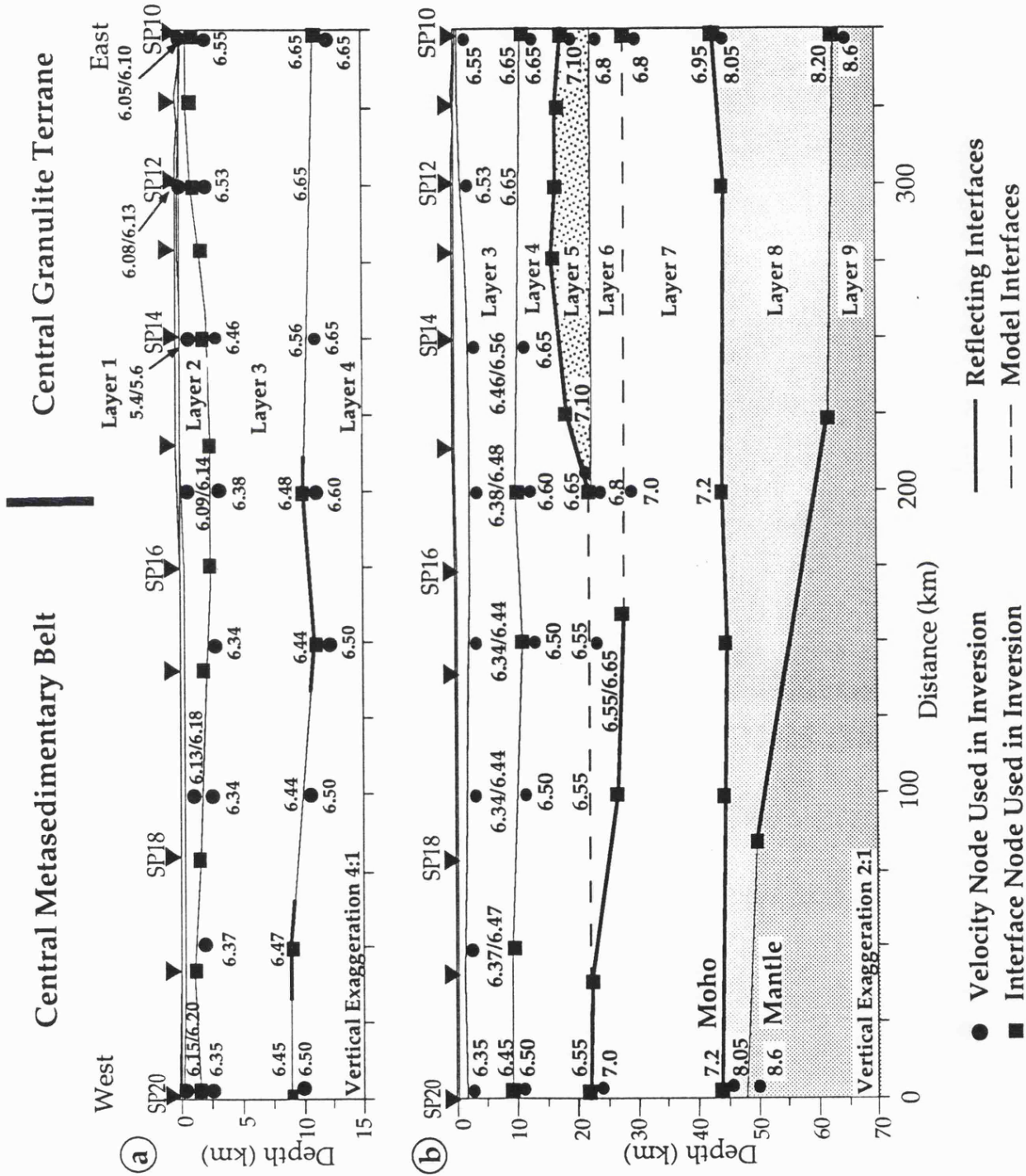


Figure 2.5

One Dimensional Travel Time Model for Shotpoint 20

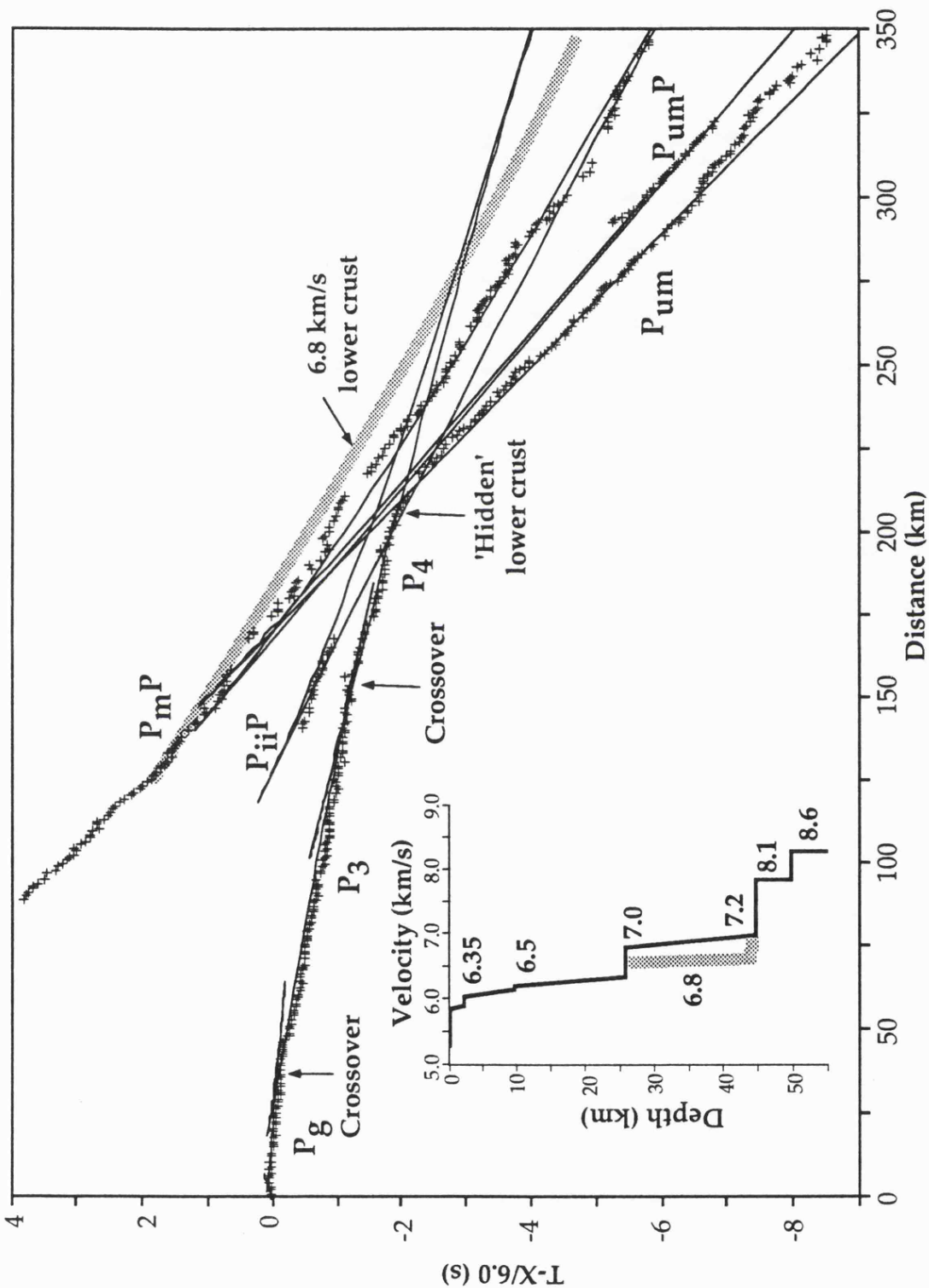


Figure 2.6

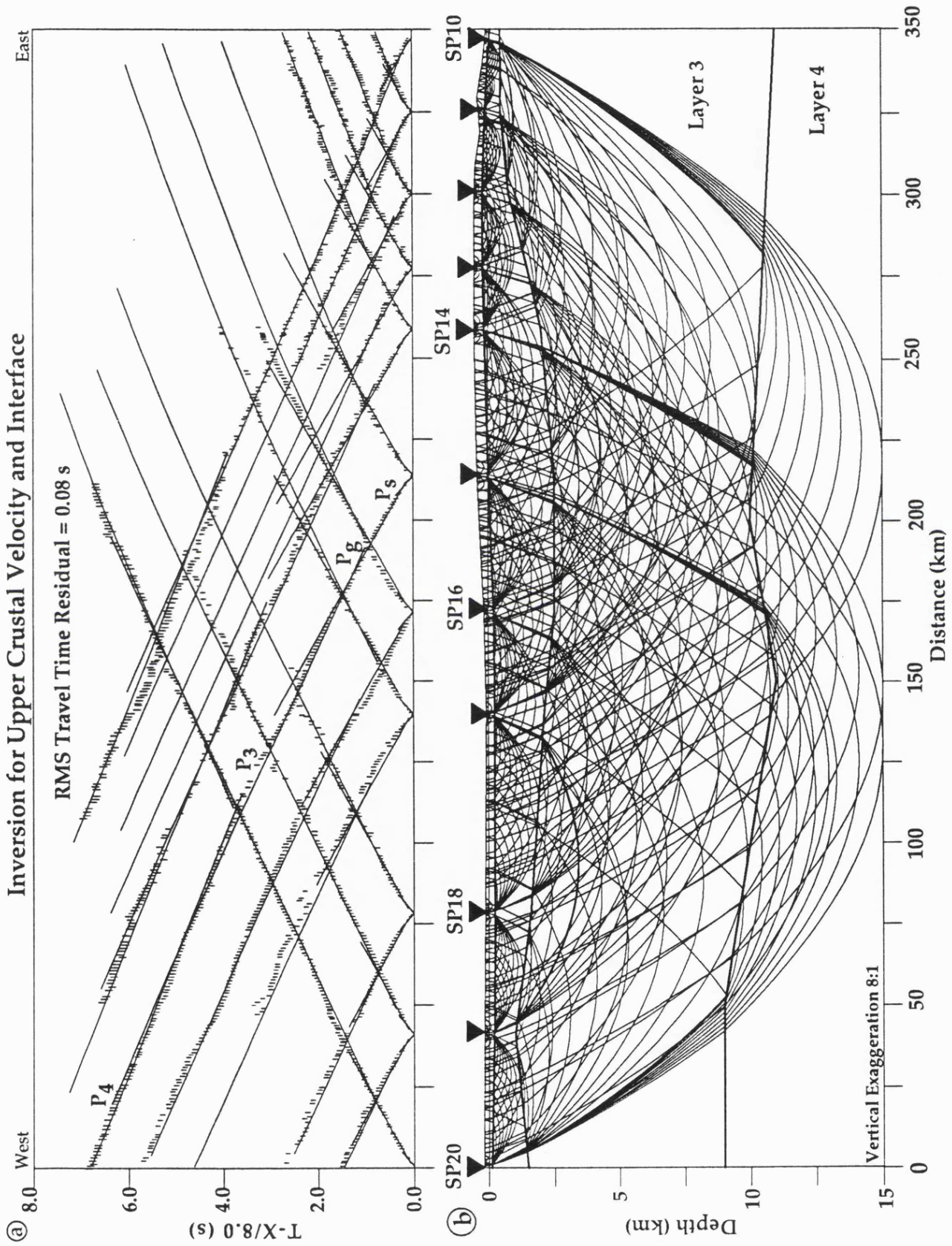


Figure 2.7

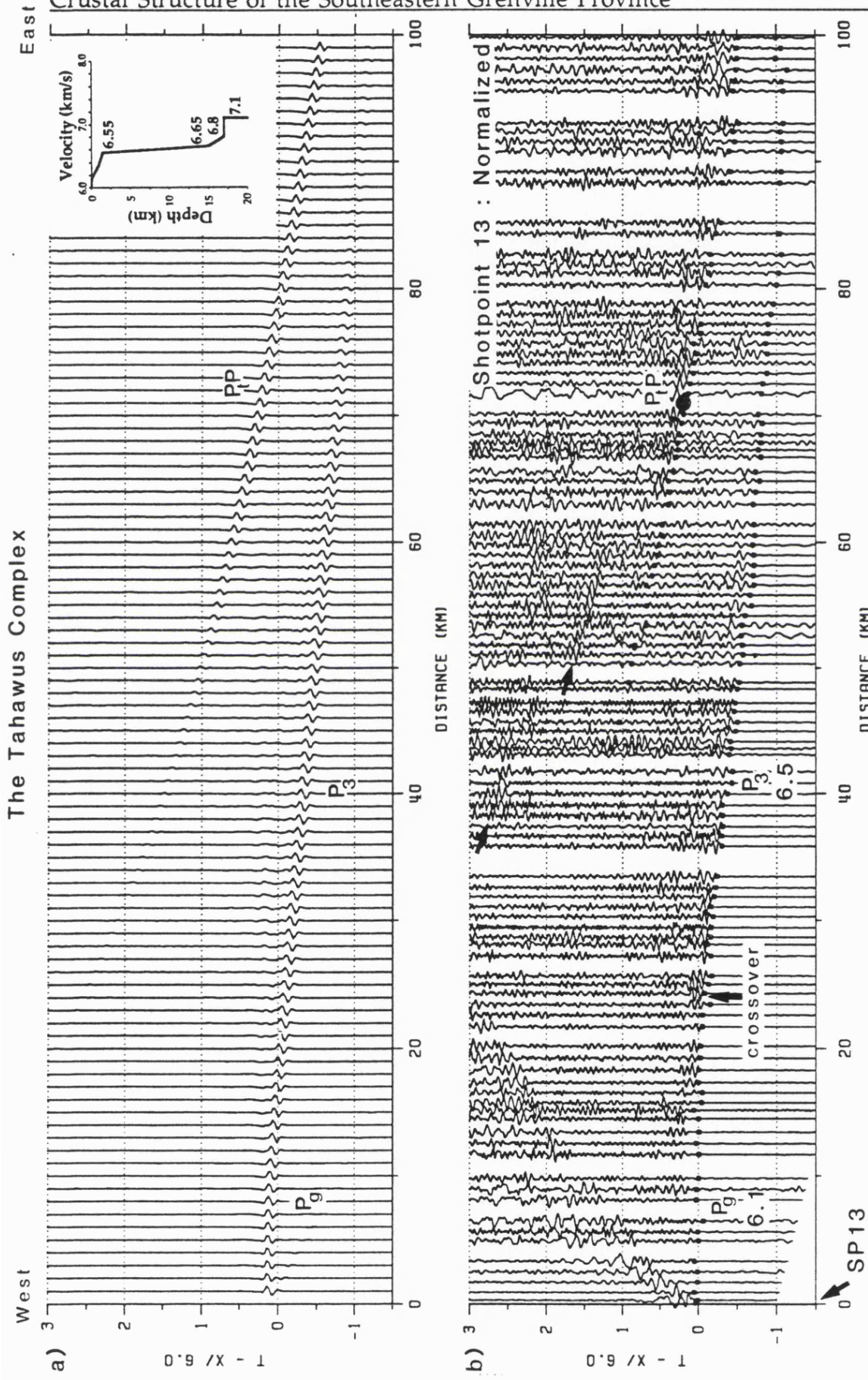


Figure 2.8

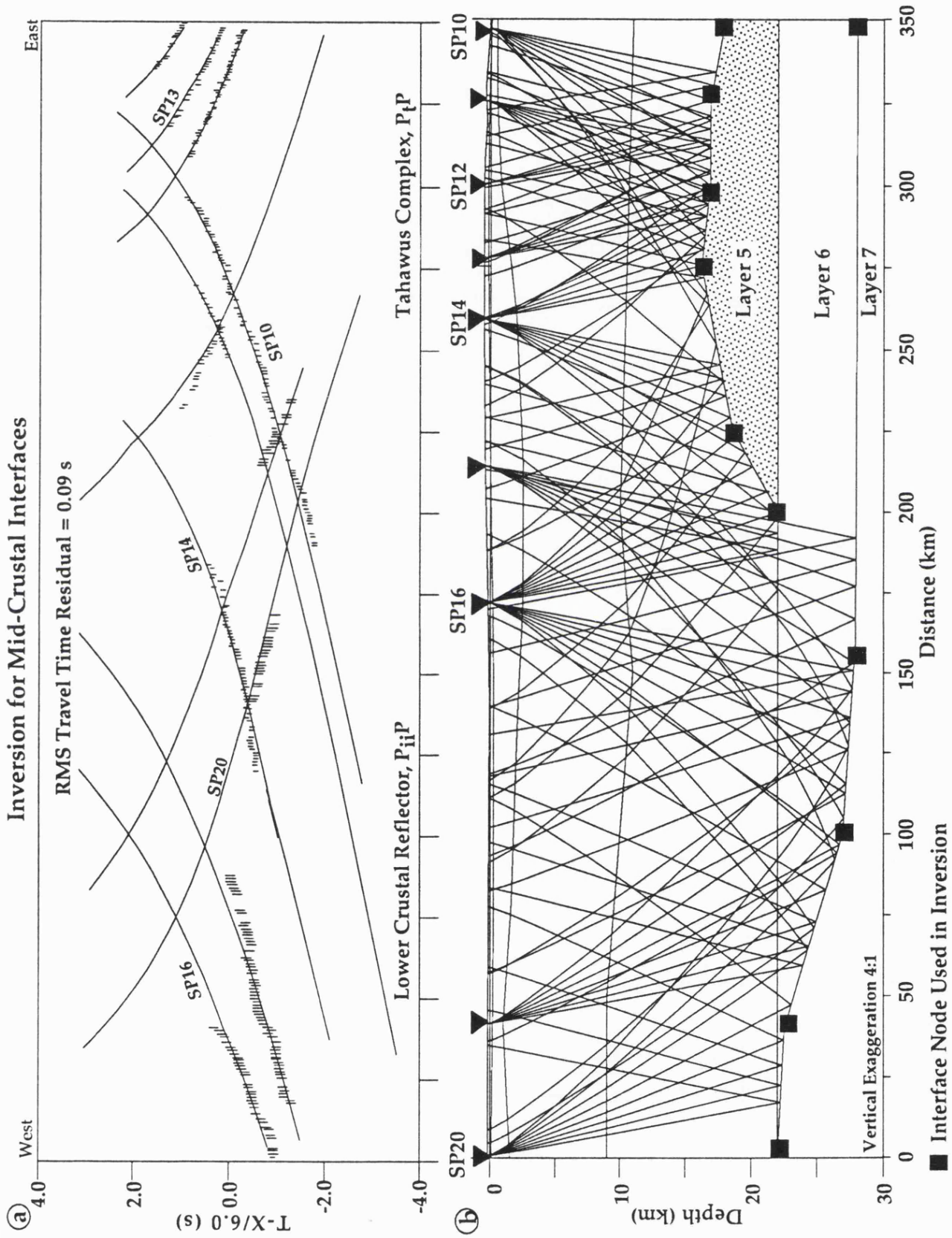


Figure 2.9

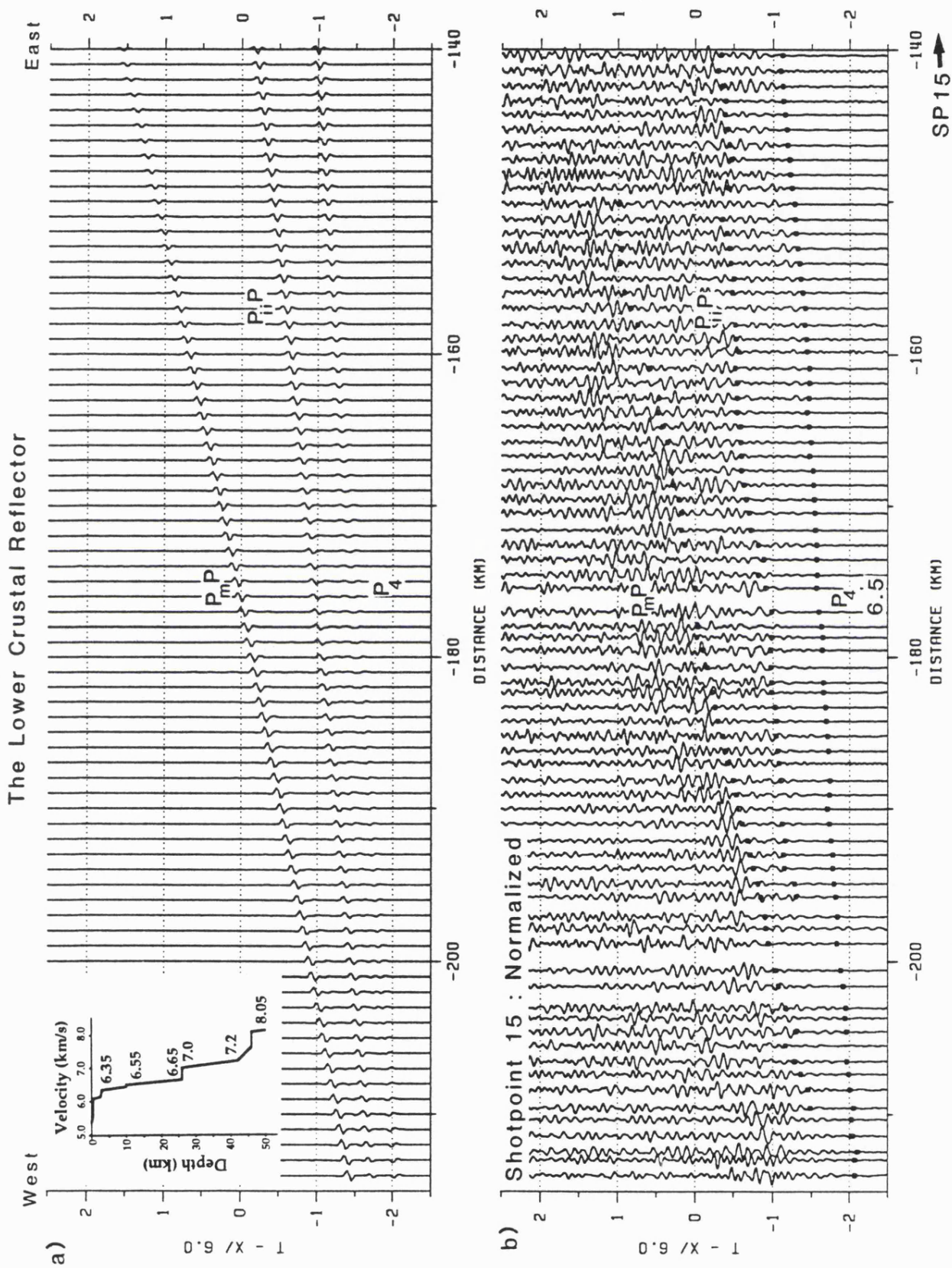


Figure 2.10

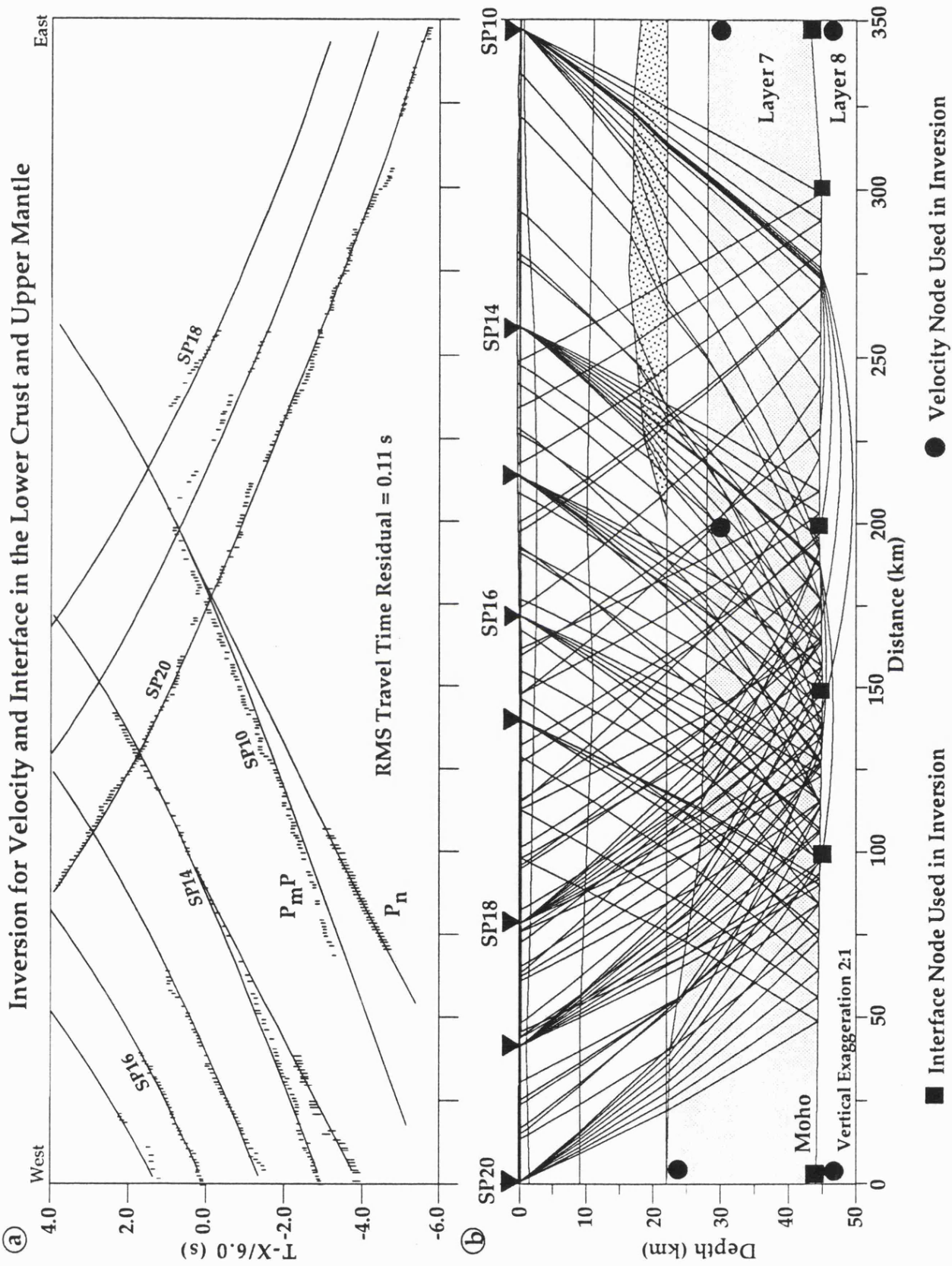


Figure 2.11

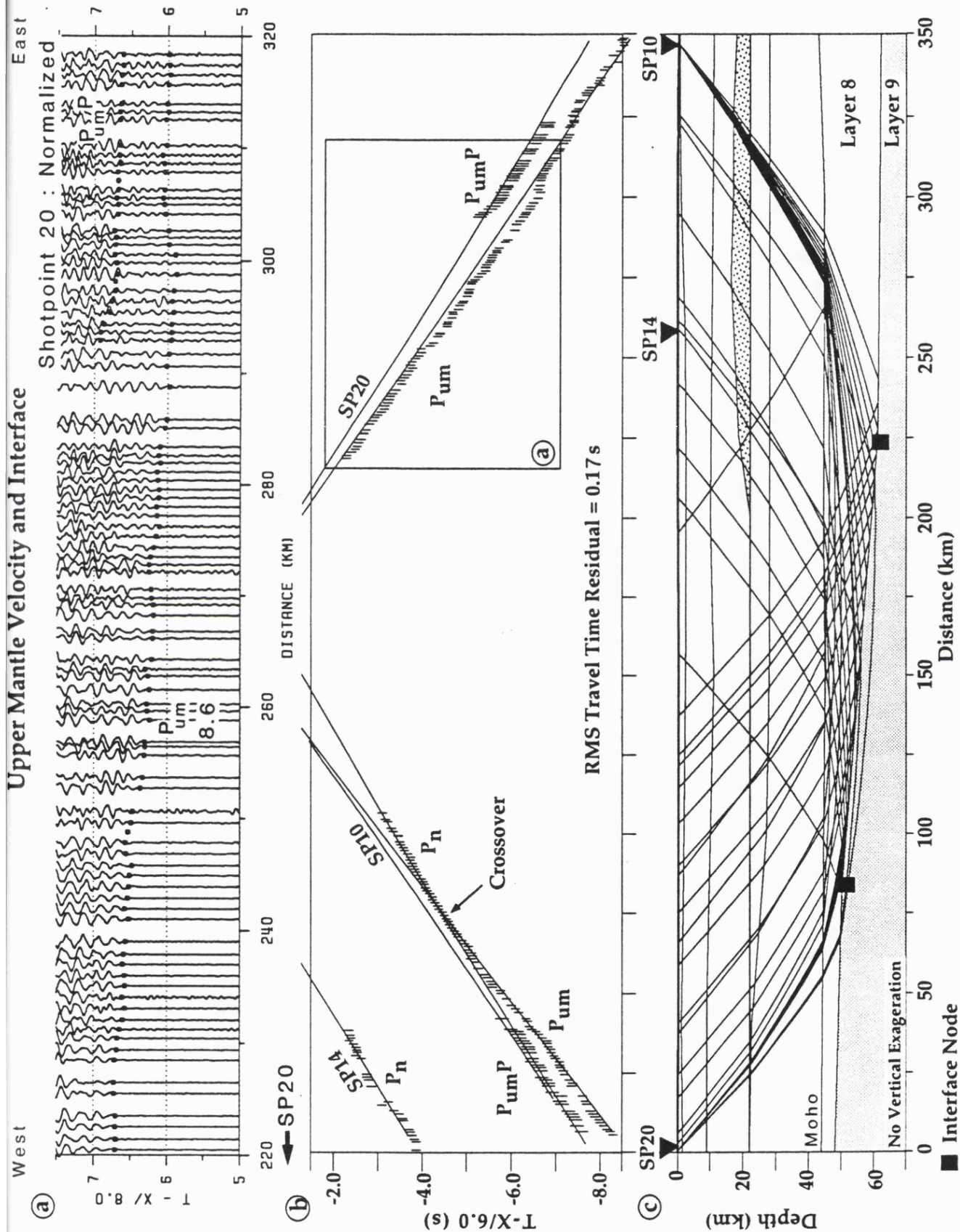


Figure 2.12

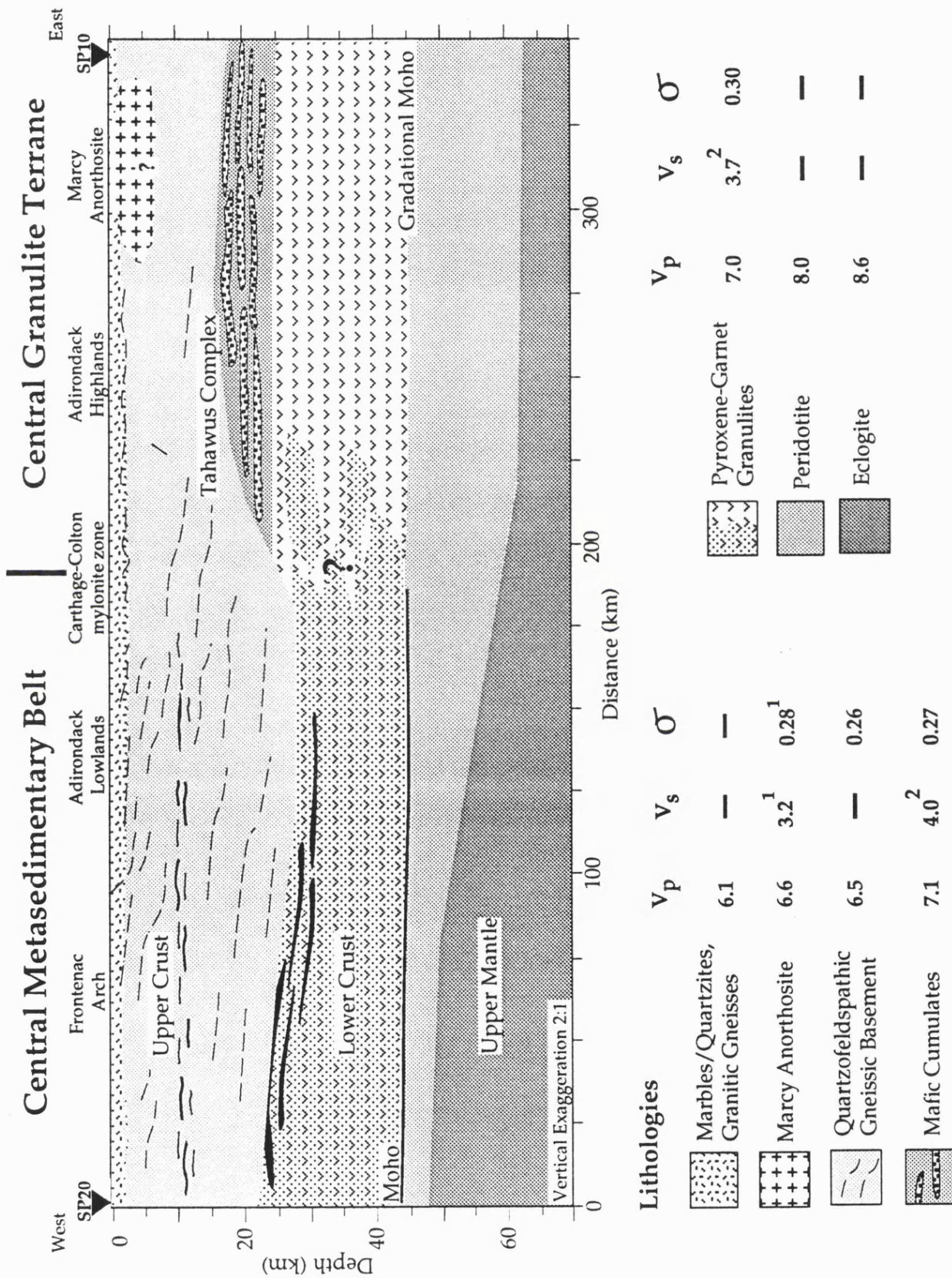


Figure 2.13

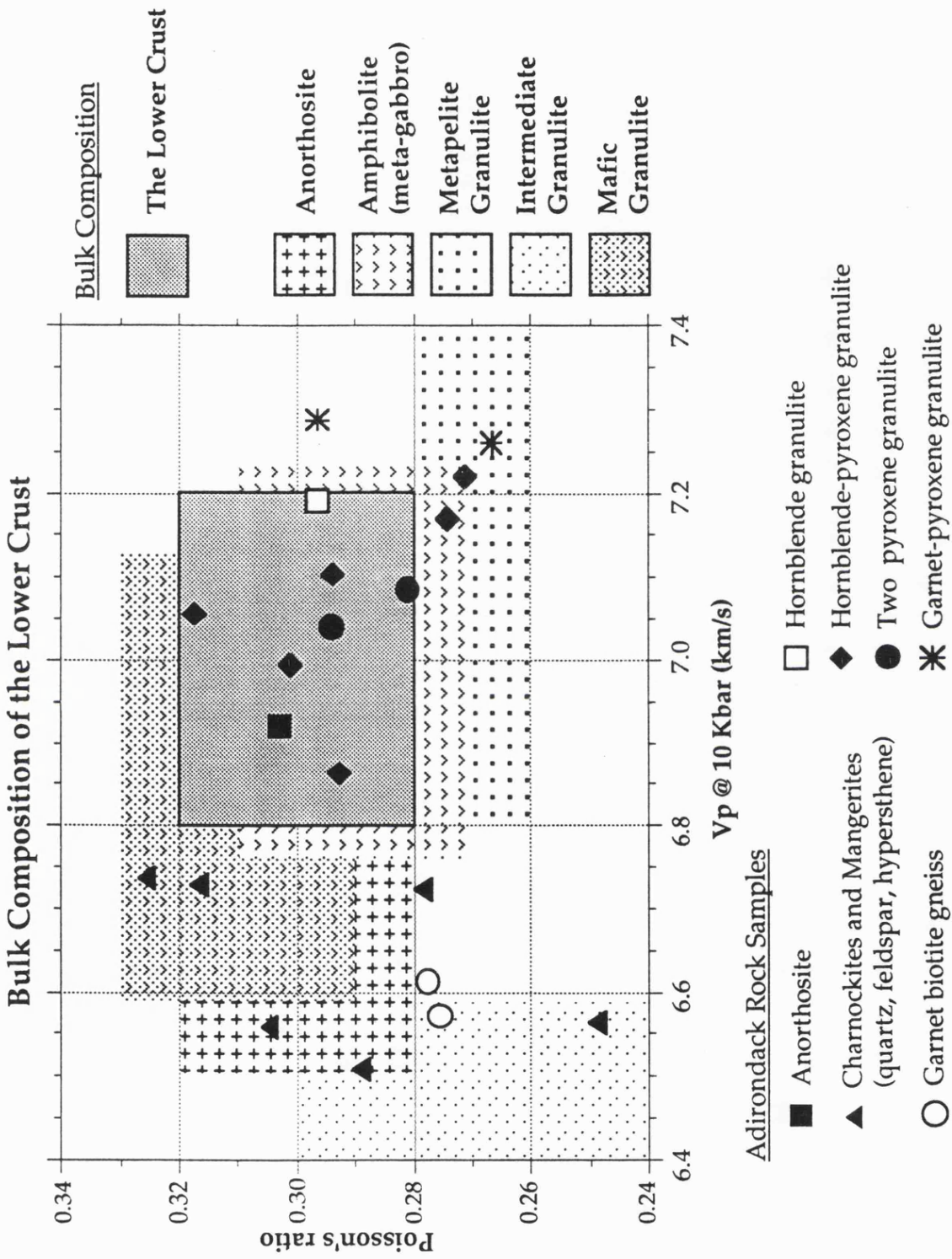


Figure 2.14

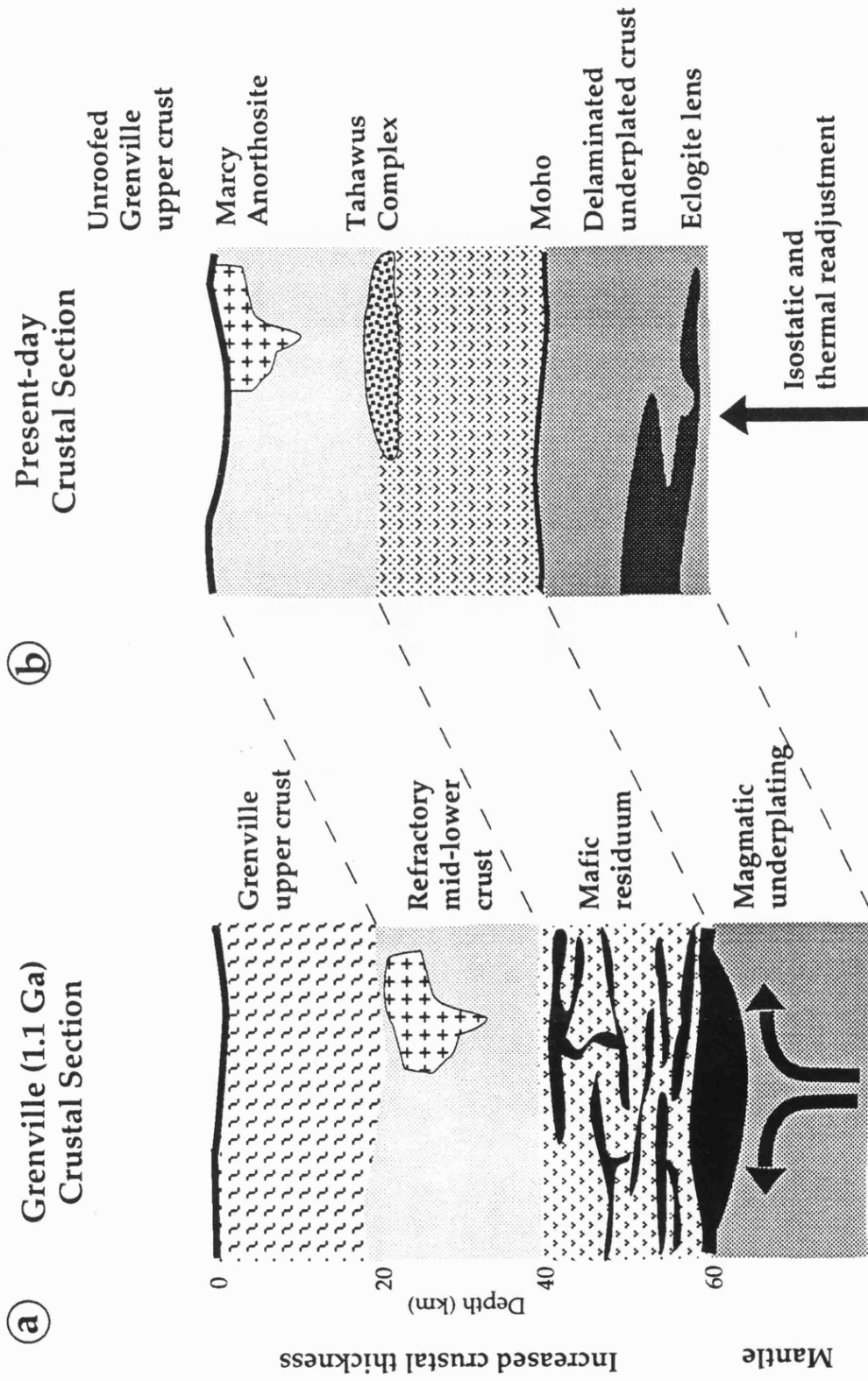


Figure 2.15

**Is the Moho a Late-Stage Feature ?  
Evidence for Structural Variations Beneath the  
Ontario-New York-New England Seismic Profile**

**3.1 Abstract**

Variations in the seismic structure of the lower crust and upper mantle across the Mid-Proterozoic Grenvillian craton and the Paleozoic Appalachian mountains can be related to successive tectono-thermal processes which have modified the deep crust. The Grenvillian craton is characterized by 45 km thick crust, with a lower crust whose seismic properties are representative of garnet-pyroxene granulites. The Grenvillian Moho is an indistinct feature suggesting compositional interlayering and gradation into the mantle. An anomalous mantle layer which dips eastwards from 50 km to 60 km beneath the Grenvillian craton is proposed to represent a layer of eclogite. The New England Appalachians are characterized by a sharp reflection Moho rising from 40 km to 35 km towards the Atlantic margin. In contrast to the Grenvillian craton the seismic properties of the Appalachian lower crust are consistent with an intermediate bulk composition, such as amphibolite or felsic granulite. Beneath the New England Appalachians the top of the lower crust is a sub-horizontal planar feature that demarcates increased reflectivity. This suggests that the lower crust/Moho attained its reflective character

synchronously with the extension of the crust in the Late Paleozoic/Early Mesozoic. We ascribe the dissimilar lower crustal/Moho features of the Grenville and Appalachian provinces to ductile flow induced by extensional rifting of thermally elevated crust beneath the Appalachians, compared to the cold stabilized cratonic crust beneath the Grenville province.

### 3.2 Introduction

Geologic studies of continental evolution are underpinned by uniformitarian principles. Recent deep seismic studies across Proterozoic cratons (e.g., Green *et al.*, 1988; Fountain *et al.*, 1990) and bounding Phanerozoic mountain belts (e.g., Ando *et al.*, 1984; Spencer *et al.*, 1989; Phinney and Roy-Chowdhury, 1989) suggest that significant differences exist in the structure of the lower crust and upper mantle between these two crustal provinces. Cratonic Proterozoic crust is commonly 40-45 km thick, has an average seismic velocity of 6.6 km/s, and a variable reflective character often with an indistinct Moho. Phanerozoic crust on the other hand is commonly 30-35 km, has a lower average seismic velocity of 6.4 km/s, a highly reflective laminated lower crust, and a sharp reflection Moho (Meisner, 1986; Braile *et al.*, 1989; Nelson, 1991). Are these dissimilarities intrinsically related to differences in the tectono-thermal regimes which operated in the Proterozoic and Phanerozoic eons? Or is the laminated fabric of the lower crust/sharp Moho commonly observed beneath collapsed Phanerozoic mountain belts a late-stage feature and hence primarily related to extensional processes? If indeed this is the case, then why aren't similar structures observed beneath Proterozoic cratons that have also suffered late-stage extensional collapse? A seismic refraction/wide-angle reflection profile acquired across the Proterozoic Grenvillian craton to the Paleozoic New England Appalachian mountains provides an excellent opportunity to explore these fundamental issues which lie at the heart of the uniformitarian paradigm.

In northeastern American a series of crustal fragments are exposed that were juxtaposed over a billion years of tectonic activity that includes the Grenvillian and the Appalachian orogenies (Figure 3.1). The Grenvillian orogenic cycle was a major tectonic, plutonic, and metamorphic mountain building episode that deformed and reworked older crustal remnants during

the Mid-Proterozoic (Wynne-Edwards, 1972). Characteristic features of the Grenville province include pervasive ductile deformation, granulite facies thermal overprinting and paleopressures of up to 8 Kbars suggesting a double crustal thickness during peak orogenesis (McLelland and Isachsen, 1980; Bohlen *et al.*, 1985). Slow isobaric cooling and isostatic equilibration followed the Grenvillian orogeny resulting in the unroofing of 10-15 km of the crust in the Central Metasedimentary Belt (Cosca, 1991), and up to 20 km of the crust in the Central Granulite Terrane (Bohlen *et al.*, 1985; Mezger *et al.*, 1990). During the Late Proterozoic a protracted period of extensional tectonism resulted in the formation of the Iapetus ocean along the rifted margin of the Grenvillian craton (Coish *et al.*, 1991). Compressional activity was renewed in the Lower Paleozoic with the episodic accretion of a multifarious assemblage of allochthonous crustal fragments to the Grenvillian continental margin (Stanley and Ratcliffe, 1985; Stewart *et al.*, 1991; Thompson *et al.*, *in press*). These compressional episodes were punctuated by the development of foreland basins receiving sediment from the converging orogenic belts. The New England Appalachian orogen is characterized by amphibolite facies metamorphism and widespread igneous intrusion (McHone and Butler, 1984). Appalachian tectonism ceased in the Early Mesozoic with rifting of the Atlantic continental margin.

### 3.3 Results - Structure of the Lower Crust and Upper Mantle

The Ontario-New York-New England seismic refraction/wide-angle reflection profile allows the seismic structural inter-relationships between the Grenvillian and Appalachian provinces to be investigated (Figure 3.2). A seismic velocity model was derived by a combination of raytrace forward modeling, linearized travel time inversions, and synthetic amplitude modeling techniques (Hughes and Luetgert, 1991; Hughes and Luetgert, *in press*). Herein we focus upon the lower crust whose velocity was obtained by

adjusting the velocity model until the calculated travel times matched those observed from Moho reflections. Determination of the lower crustal velocity to within  $\pm 0.2$  km/s is facilitated by Moho reflections recorded at offsets of up to 350 km (Hughes and Luetgert, 1991; Hughes and Luetgert, *in press*). Furthermore, the character of the Moho reflections provides subtle but important clues to the nature of the crust-mantle transition. In general, a thin (<2 km) laterally continuous Moho is indicated by impulsive, coherent Moho reflections, whereas a thick irregular or laminated crust-mantle transition is recognized by diffuse, poorly coherent reflections with a long coda (Zelt and Ellis, 1989). Support for our contention that the deep crustal structure of the Grenvillian and Appalachian provinces is significantly different is illustrated by the character of Moho reflections beneath the two provinces (Figure 3.3).

*The Southeastern Grenville Province:* A typical Moho reflection from the Grenville province is shown in Figure 3.3a, where a series of en-echelon reflection segments suggest broad-scale compositional inter-layering around the crust-mantle boundary. Travel time modeling of these Moho reflections constrains the velocity of the lower crust to be 7.0-7.2 km/s, and the crustal thickness to be  $45 \pm 3$  km (Figure 3.2). Comparison of compressional and shear wave Moho reflections indicate a Poisson's ratio of  $0.28 \pm 0.01$  suggesting the predominance of mafic granulites in the lower crust (Fountain and Christensen, 1989). The absence of laterally coherent Moho reflections in the Grenville province is a notable feature of the Ontario-New York-New England seismic data set (Hughes and Luetgert, *in press*) and is also characteristic of seismic reflection profiles acquired across the Adirondack Highlands (Brown *et al.*, 1983) and the Quebec reentrant (Spencer *et al.*, 1989). This gradational Moho feature is corroborated by teleseismic receiver functions which suggest a 10-km-thick velocity transition at the base of the crust (Owens, 1987). First arrivals refracted from

the upper mantle are observed with a velocity of 8.6 km/s (Hughes and Luetgert, *in press*). The top of this anomalously high velocity dips eastward from 50 km to 60 km (Figure 3.2). Both the velocity and the geometry of this layer are well constrained by reversed shotpoints 10 and 20.

*The Western New England Appalachians:* In the western New England Appalachians wide-angle reflections from the Moho are impulsive and strongly coherent suggesting a sharp velocity transition across the crust-mantle boundary (Figure 3.3b). The lower crust has a velocity of 6.7-6.9 km/s, and a Poisson's ratio in excess of 0.26 which tends to favor an intermediate bulk composition for the lower crust such as amphibolite or felsic granulite (Hughes and Luetgert, 1991). The effects of extensional processes are particularly evident in the lower crust and Moho where a gradual crustal thinning from 41 km to 37 km is observed (Figure 3.2). The extended Appalachian crust is characterized on seismic reflection profiles by a laminated reflective lower crust and a sharp reflection Moho (Brown *et al.*, 1983; Hutchinson *et al.*, 1988; Phinney and Roy-Chowdhury, 1989; Spencer *et al.*, 1989). Refracted first arrivals from the upper mantle are impulsive with a velocity of 8.0 km/s. A reflection within the upper mantle at 60 km depth beneath the Bronson Hill Anticlinorium may be the easternmost expression of the anomalous mantle layer observed beneath the Grenville province (Figure 3.2).

### **3.4 Discussion - Evolution of the Lower Crust and Upper Mantle**

The Grenvillian and Appalachian provinces have broadly similar evolutionary histories. Both regions underwent multiple episodes of compressional tectonism, magmatic underplating and over-thickening terminating in extensional collapse. Furthermore, oceanic rifting was the last pervasive thermo-tectonic process to have impinged upon both the Grenvillian and Appalachian provinces. The structure of the lower

crust/Moho, however, is distinctly different beneath these two provinces, raising the question how does the lower crust/Moho evolve with time?

*Underplating and Eclogization of the Grenvillian Crust:* Important constraints on the tectonic evolution of the Grenville province are provided by estimates of cooling rates and inferred uplift histories from thermochronology and thermobarometry. These studies provide evidence for a preferentially thickened crust beneath the Central Granulite Terrane (>65 km) relative to the Central Metasedimentary Belt (50-55 km) during the Grenvillian orogeny (Bohlen *et al.*, 1985; Mezger *et al.*, 1990; Cosca *et al.*, 1991). Crustal thickening was most likely produced by northwestward directed stacking of a series of fold/thrust nappes accompanied by voluminous intrusions of felsic melts (McLelland and Isachsen, 1980). In concordance with these studies, magmatic underplating of the crust was postulated as a means of generating the elevated thermal conditions (750-800°C) necessary for the formation of regional granulite facies metamorphism (Bohlen and Mezger, 1989). From this tectono-thermal scenario we propose that the preferentially over-thickened crust beneath the Central Granulite Terrane was supported by a crustal root which indented the upper mantle. This crustal root was likely the locus of mantle-derived basaltic underplating which initiated anatexic melting and dehydration of the mid-lower crust. Evidence for this hypothesis is provided by successive episodes of felsic intrusions which are exposed in the Central Granulite Terrane and testify to large scale melting in the lower crust during the Grenvillian orogeny (Chiarenzelli and McLelland, 1990). The Tahawus complex, a laminated dome-like body, may be an expression of one of these intrusions that fractionated to produce a mafic cumulate body in the mid-crust (Figure 3.2). We ascribe the mafic and homogenous structure of the lower crust to pervasive intrusion, wide-spread melting and mobilization of the crust during the Grenvillian orogeny.

We propose that thermal relaxation allowed the mantle-derived basaltic melts that intruded the over-thickened crust to crystallize as eclogites, with densities near that of the mantle. These dense eclogite facies assemblages would initially retard regional uplift, thus allowing isobaric cooling to precede uplift (Martignole, 1986; Mezger *et al.*, 1990). However, by the Late Proterozoic the crust had attained isostatic equilibrium resulting in the unroofing of mid-lower crustal lithologies through a combination of thermal, petro-physical and extensional adjustments which juxtaposed rocks from different structure levels at the same erosional horizon (Richardson and England, 1979; Cosca *et al.*, 1991; Hughes and Luetgert, *in press*; McLelland *et al.*, *in press*). Isostatic uplift of the buoyant felsic upper crust may have been facilitated by delamination of the dense eclogitic lower crust (stoping of the lower crust). However, we do not imply whole lithosphere delamination here, as there is little evidence to support rapid late-stage uplift or the intrusion of large volumes of late-melts that would be generated by decompressive melting of rising asthenospheric mantle.

Interpretation of the velocity model shown in Figure 3.2 suggests that remnants of these magmatic processes are retained in the upper mantle. The incorporation of the over-thickened and underplated lower crust into the upper mantle is a natural outcome of our eclogization hypothesis. In tandem with the eclogization of the lower crust, we would expect the Moho to rise dynamically through the cooling crustal column and consequently attain its present planar geometry (Figure 3.2). By this mechanism we argue for an indistinct crust-mantle boundary beneath the southeastern Grenville province whose properties are an aggregate of both lower crustal and mantle-derived material. It thus follows that ultra-mafic residuals, differentiated during the Grenvillian orogeny, now reside in the upper mantle and contribute to the gradational nature of the crust-mantle boundary beneath the Grenville province. We interpret the anomalous mantle layer with

velocity 8.6 km/s as a fractionated basaltic layer that ponded in the upper mantle and crystallized as eclogite following the Grenvillian orogeny (Hughes and Luetgert, *in press*). The dipping geometry of this eclogitic lens may be a fossilized template of the Grenvillian crustal root.

*Rifting of the Iapetan Margin:* The nature and extent of Late Proterozoic Iapetan rifting along the edge of the Grenvillian continental margin is somewhat enigmatic. Rift-related features preserved along the Late Proterozoic cratonic margin include mafic dikes, block faulting, and autochthonous syn-rift clastics and volcanics (Coish *et al.*, 1991). In the lower crust, however, characteristic extensional features (laminated lower crust/sharp Moho) are absent (Brown *et al.*, 1983; Hughes and Luetgert, 1991). In part, this absence may be related to the confinement of rift-related magmatism and extension to a narrow zone beneath the Late Proterozoic cratonic margin. The most compelling evidence for rift magmatism in the deep crust is the correlation of the Appalachian gravity high with a high density 'transitional' zone which lies beneath the easternmost exposure of the Grenvillian craton in the Green Mountains, Vermont (Thompson *et al.*, *in press*). We believe that this 'transitional' zone is a remnant of Late Proterozoic rifting with associated intrusion of mafic dike swarms into the lower crust at the edge of the Late Proterozoic cratonic margin. Seismic velocity evidence for this 'transitional' zone is sparse, although it may possibly have an expression in the apparent travel time advance observed for Moho reflections at the edge of the Grenville province (see alternate Moho geometry in Hughes and Luetgert, [1991]). Perhaps the most significant clue to the absence of extensional lower crustal/Moho features at the edge of the Grenvillian craton lies in the consumption of the Iapetus ocean in the Taconian orogeny.

*The Grenvillian Ramp:* Seismic studies across the New England orogen reveal the Grenvillian crust extending in the form of a tapered wedge

beneath the western New England Appalachians (Ando *et al.*, 1984; Spencer *et al.*, 1989; Phinney and Roy-Chowdhury, 1989; Hughes and Luetgert, 1991). Results from the Ontario-New York-New England seismic refraction/wide-angle reflection experiment indicate that the Grenvillian crust dips beneath the Green Mountains in the form of a crustal ramp extending to a depth of at least 20 km, where it soles out to a planar mid-lower crustal interface (Figure 3.2). Interpretation of the Grenvillian ramp suggests that it is an imbricated and mylonitized remnant of the Late Proterozoic cratonic margin that was the locus of successive Paleozoic accretionary episodes (Hughes and Luetgert, 1991). The Grenvillian lower crust extends eastwards beneath the ramp into a diffuse transitional zone where seismic velocities are indistinguishable from those observed beneath the western New England Appalachians (Figure 3.2). Comparison of the Appalachian collisional margin with present day analogues in the Alpine and Pyrenean convergent belts suggests that compressive stresses associated with the closure of the Iapetus ocean were likely to have been transmitted through the crust resulting in large scale lower crustal imbrication (Nelson, 1991). Seismic reflection images of the Moho beneath the apex of Appalachian convergence are noticeably planar (Ando *et al.*, 1984; Spencer *et al.*, 1989) which suggests that important post-collisional processes have modified the deep crust beneath the New England Appalachians.

*The Appalachian Lower Crust:* In the New England Appalachians a sharp laterally continuous reflection Moho appears to be a ubiquitous feature (Ando *et al.*, 1984; Hutchinson *et al.*, 1988; Phinney and Roy-Chowdhury, 1989; Spencer *et al.*, 1989). This 'sharp' Appalachian Moho extends from the Gulf of Maine to the easternmost tip of the Grenvillian ramp and corresponds to an increase in the reflectivity of the lower crust suggesting a genetic relationship between the reflectivity of the lower crust and the 'sharp' Appalachian Moho. Increased reflectivity in the lower crust may be

correlated with a sub-horizontal velocity interface at 25 km depth which delineates an increase in the mafic content of the Appalachian crust (Figure 3.2). The internal structure of the lower crust is not readily resolved with wide-angle seismic reflection data, nonetheless an important observation can be made from examination of the coda of Moho reflections across the Grenville and Appalachian provinces. Wide-angle Moho reflections recorded from shotpoint 10, situated at the edge of the Adirondack mountains, display a distinctly more energetic wavetrain for Moho reflections from the Appalachians than from the Grenville. This suggests that lower crust beneath the New England Appalachians is finely laminated and hence capable of producing complex multi-path and scattering effects. A likely source for these laminations is the intrusion of mafic sills into the lower crust during late-stage collapse and extension of the Appalachian orogen (Stewart *et al.*, 1991). We suggest that the mid-lower crustal interface at 25 km depth delineates the extent of Late Paleozoic/Early Mesozoic anatexis related to the intrusion of basaltic sills and the subsequent extraction of siliceous melts to form the granitic and syenitic batholithic rocks of New England (McHone and Butler, 1984; Stewart *et al.*, 1991). Multiple extensional episodes and the accompanying development of thick sedimentary basins in the Late Paleozoic/Early Mesozoic (Hutchinson *et al.*, 1988; Stewart *et al.*, 1991) suggests extensive stretching of the crust and by analogy ductile flow in the mobile thermally elevated lower crust. In this manner, we propose that the reflective Appalachian lower crust/sharp Moho is coeval with underplating and extensional processes in the Late Paleozoic/Early Mesozoic. Thus the lower crust has attained a 'new' composite identity which can no longer be related to the allochthonous upper crustal terranes. If this inference is correct, then the Appalachian lower crust has been wholly reformed through a combination of large-scale

lower plate imbrication, magmatic intrusion and subsequent lower crustal flow which appear to be characteristic processes of collisional orogens.

### 3.5 Conclusion

Iapetan rifting of the Grenville province occurred some 600 Ma after peak orogenesis; a time span that is ten times longer than the perturbation of elevated crustal isotherms arising from the tectono-thermal events of the Grenvillian orogeny. In the New England Appalachians, however, Atlantic rifting followed the last convergent episode (Alleghenian) by about 60 Ma; the lower crust would thus remain in a thermally elevated state prior to rifting of the Atlantic margin. The laminated lower crust/sharp reflection Moho commonly observed beneath Phanerozoic mountain belts is likely a product of mantle-derived underplating and anatectic melting in the lower crust (Mooney and Meisner, 1992). Enhancement of the reflective character of such mafic intrusions is strongly implied in the thermally elevated lower crust beneath the New England Appalachians during Late Paleozoic/Early Mesozoic extension. Although the Grenvillian craton suffered a similar extensional episode, we believe it is unlikely that these effects were as pervasive in the thermally stabilized crust of the Grenville province. We conclude that variations in the seismic structure of the lower crust/Moho beneath the Proterozoic Grenvillian craton and the Paleozoic Appalachians are related to intrusive and underplating processes that may have been augmented by ductile extension of the thermally elevated lower crust beneath the New England Appalachians.

---

### 3.6 Acknowledgments

The seismic data presented in this paper were acquired by the US Geological Survey, the Geological Survey of Canada, and the US Air Force Geophysics Laboratory. We thank Steve Bohlen (USGS), Tom Brocher (USGS), Ray Durrheim (University of Witwatersrand), Jill McCarthy (USGS), Jim McLelland (Colgate College), Walter Mooney (USGS), Doug Nelson (Cornell) and Dave Stewart (USGS) for reviews and challenging ideas during the composition of this paper. Support from the US Air Force Geophysical Laboratory and the USGS Deep Continental Studies program is gratefully acknowledged.

### 3.7 References

- Ando, C.J., B.L. Czuchra, S.L. Klemperer, L.D. Brown, M.J. Cheadle, F.A. Cook, J.E. Oliver, S. Kaufman, T. Walsh, J.R. Thompson, J.B. Lyons, J.L. Rosenfeld, Crustal profile of a mountain belt: COCORP deep seismic reflection profile in New England and implications for architecture of convergent mountain chains, *Am. Assoc. Pet. Geol.*, 68, 819-837, 1984.
- Bohlen, S.R., J.W. Valley, and E.J. Essene, Metamorphism in the Adirondacks I. petrology, pressure and temperature, *Journal of Petrology*, 26, p. 971-992, 1985.
- Bohlen, S.R. and K. Mezger, Origin of granulite terranes and the formation of the lowermost continental crust, *Science*, 244, p. 326-329, 1989.
- Braile, L.W., W.J. Hinze, R.R.B. vonFrese, G.R. Keller, Seismic properties of the crust and uppermost mantle of the conterminous United States and adjacent Canada, in *Geophysical Framework of the Continental United States*, edited by L.C. Pakiser and W.D. Mooney, *Geol. Soc. Am. Memoir 172*, pp. 655-680, 1989.
- Brown, L.D., C.J. Ando, S. Klemperer, J.E. Oliver, S. Kaufman, B. Czuchra, T. Walsh, and Y.W. Isachsen, Adirondack-Appalachian crustal structure: The COCORP northeast traverse, *Geol. Soc. Am. Bull.*, 94, p. 1173-1184, 1983.
- Chiarenzelli, J.R. and J.M. McLelland, Age and regional relationships of granitoid rocks of the Adirondack Highlands, *Journal of Geology*, 99, p. 571-590, 1990.
- Coish, R.A., A. Bramley, T. Gavigan, and R. Mastiner, Progressive changes in volcanism during the Iapetan rift: comparison with the East African Rift System, *Geology*, 19, p. 1021-1024, 1991.
- Cosca, M.A., J.F. Sutter, and E.J. Essence, Cooling and inferred uplift/erosion history of the w orogeny, Ontario: constraints from  $^{40}\text{Ar}/^{39}\text{Ar}$  thermochronolgy, *Tectonics*, 10, p. 959-977, 1991.

Fountain, D.M, M.H. Salisbury, and J. Percival, Seismic structure of the continental crust based on rock velocity measurements from the Kapuskasing uplift, *J. Geophys. Res.*, 95, p. 1167-1186, 1990.

Fountain, D.M. and N.I. Christensen, Composition of the continental crust and upper mantle; a review, in *Geophysical Framework of the Continental United States*, edited by L.C. Pakiser and W.D. Mooney, *Geol. Soc. Am., Memoir 172*, p. 711-742, 1989.

Green, A.G., B. Milkereit, A. Davidson, C. Spencer, D.R. Hutchinson, W.F. Cannon, M.W. Lee, W.F. Agena, J.C. Behrendt, W.J. Hinze, Crustal structure of the Grenville front and adjacent terranes, *Geology*, 16, p. 788-792, 1988.

Hughes, S. and J.H. Luetgert, Crustal structure of the western New England Appalachians and the Adirondack Mountains, *J. Geophys. Res.*, 96, p. 16471-16494, 1991.

Hughes, S. and J.H. Luetgert, Crustal structure of the southeastern Grenville province, *J. Geophys. Res.*, in press.

Hutchinson, D.R., K.D. Klitgord, M.W. Lee, and A.M. Trehu, US Geological Survey deep seismic reflection profile across the Gulf of Maine, *Geol. Soc. Am. Bull.*, 100, p. 172-184, 1988.

Martignole J., Some questions about crustal thickening in the central part of the Grenville province, in *The Grenville province*, edited by J.M. Moore, A. Davidson and A.J. Baer, *Geol. Assoc. Can. Special Paper 31*, p. 61-74, 1986.

McHone, J.G. and J.R. Butler, Mesozoic igneous provinces of New England and the opening of the North Atlantic Ocean, *Geol. Soc. Am. Bull.*, 95, p. 757-765, 1984.

McLelland, J.M., S.R. Daly and J. Chiarenzelli, Sm-Nd and U-Pb Isotopic evidence of juvenile crust in the Adirondack Lowlands and

- implications for the evolution of the Adirondack Mts., *Journal of Geology*, in press.
- McLelland, J.M. and Y.W. Isachsen, Structural synthesis of the southern and central Adirondacks: A model for the Adirondacks as a whole and plate tectonics interpretations, *Geol. Soc. Am. Bull.*, 91, p. 208-292, 1980.
- Meisner, R., *The Continental Crust, A Geophysical Approach*, International Geophysics Series volume 34, Academic Press, New York, 426 p., 1986.
- Mezger, K., C. Rawnsley, S. Bohlen, and G. Hansen, U-Pb garnet, sphene, monzanite and rutile ages: implications for the duration of high grade metamorphism and cooling histories, Adirondack Mountains, New York, *Journal of Geology*, 99, p. 415-428, 1990.
- Mooney, W.D. and R. Meisner, Multi-genetic origin of crustal reflectivity: a review of seismic reflection profiling of the continental lower crust and Moho in *The Continental Lower Crust* edited by D.M. Fountain, R. Arculus and R. Kay, Elsevier, Holland, pp. 45-79, 1992.
- Nelson, K.D., A unified view of craton evolution motivated by recent deep seismic reflection and refraction results, *Geophys. J. Int.*, 105, p. 25-35, 1991.
- Owens, T.J., Crustal structure of the Adirondacks determined from broadband teleseismic waveform modeling, *J. Geophys. Res.*, 92, p. 6391-6401, 1987.
- Phinney, R.A. and K. Roy-Chowdhury, Reflection seismic studies in the eastern United States, in *Geophysical Framework of the Continental United States*, edited by L.C. Pakiser and W.D. Mooney, *Geol. Soc. Memoir 172*, pp. 613-653, 1989.
- Richardson, S.W. and P.C. England, Metamorphic consequences of crustal eclogite production in overthrust orogenic zones, *Earth and Planetary Science Letters*, 42, p. 183-190, 1979.

- Spencer, C., A. Green, P. Morel-a-l'Huissier, B. Milkereit, J.H. Luetgert, D.B. Stewart, J.D. Unger, and J.D. Philips, Allochthonous units in the Northern Appalachians: Results from the Quebec-Maine seismic reflection and refraction surveys, *Tectonics*, 8, p. 667-696, 1989.
- Stanley, R.S. and M.N. Ratcliffe, Tectonic synthesis of the Taconic orogeny in western New England, *Geol. Soc. Am. Bull.*, 96, 1227-1250, 1985.
- Stewart, D.B., B.E. Wright, J.D. Unger, J.D. Phillips, D.R. Hutchinson, J.H. Luetgert, W.A. Bothner, K.D. Klitgord, L.M. Liberty, C. Spencer, The Quebec-Maine-Gulf of Maine Transect, Southeastern Canada, Northeastern United States of America, Global Geoscience Transect 8, *U.S. Geological Survey Open File Report 91-353*, 1991.
- Thompson, J.B., W.A. Bothner, P. Robinson, Y.W. Isachsen, and K.D. Klitgord, A guide to the continent ocean transect E-1: Adirondacks to George's Bank, pp. 55, *in press*.
- Wynne-Edwards, H.R., The Grenville province, in *Variations in Tectonic Styles in Canada*, edited by R.A. Price and R.J.W. Douglas, *Geol. Assoc. Can. Special Paper 11*, p. 263-334, 1972.
- Zelt, C.A. and R.M. Ellis, Seismic structure of the crust and upper mantle in the Peace River Arch region, Canada, *J. Geophys. Res.*, 94, p. 5729-5744, 1989.

### 3.8 Captions

**Figure 3.1:** Simplified geologic map showing the location of the Ontario-New York-New England seismic refraction/wide-angle reflection profile. The profile traverses three crustal sub-divisions which are from west to east, the Central Metasedimentary Belt, the Central Granulite Terrane, and the western New England Appalachians.

**Figure 3.2:** Two-dimensional seismic velocity model derived from the Ontario-New York-New England seismic refraction/wide-angle reflection profile (Hughes and Luetgert, 1991; Hughes and Luetgert, *in press*) and interpretative geologic cross-section illustrating the major structural elements which comprise the southeastern Grenville province and the western New England Appalachians (Figure 3.1). Ray coverage is indicated by the shaded regions. All velocities are shown in km/s.

**Figure 3.3:** Wide-angle crustal-mantle reflections from the southeastern Grenville province (a) are characterized by multiple en-echelon reflection segments (stipple), suggesting broad-scale compositional interlayering across the crust-mantle boundary. The western New England Appalachians (b) are characterized by laterally coherent Moho reflections suggesting a sharp Moho. Cartoons illustrate possible models for the Moho. Velocities are shown in km/s (see Figure 3.2).

3.9 Figures

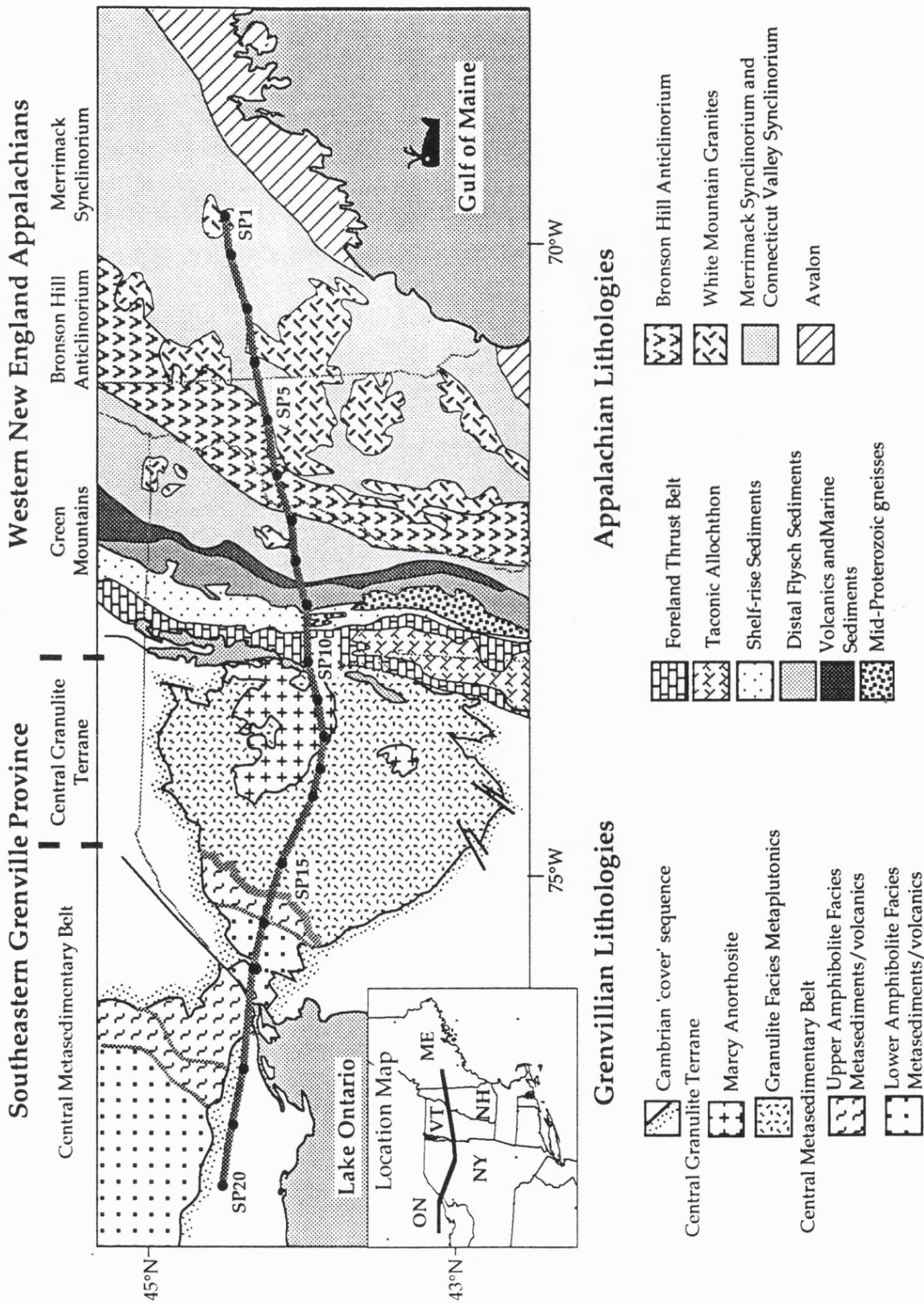


Figure 3.1

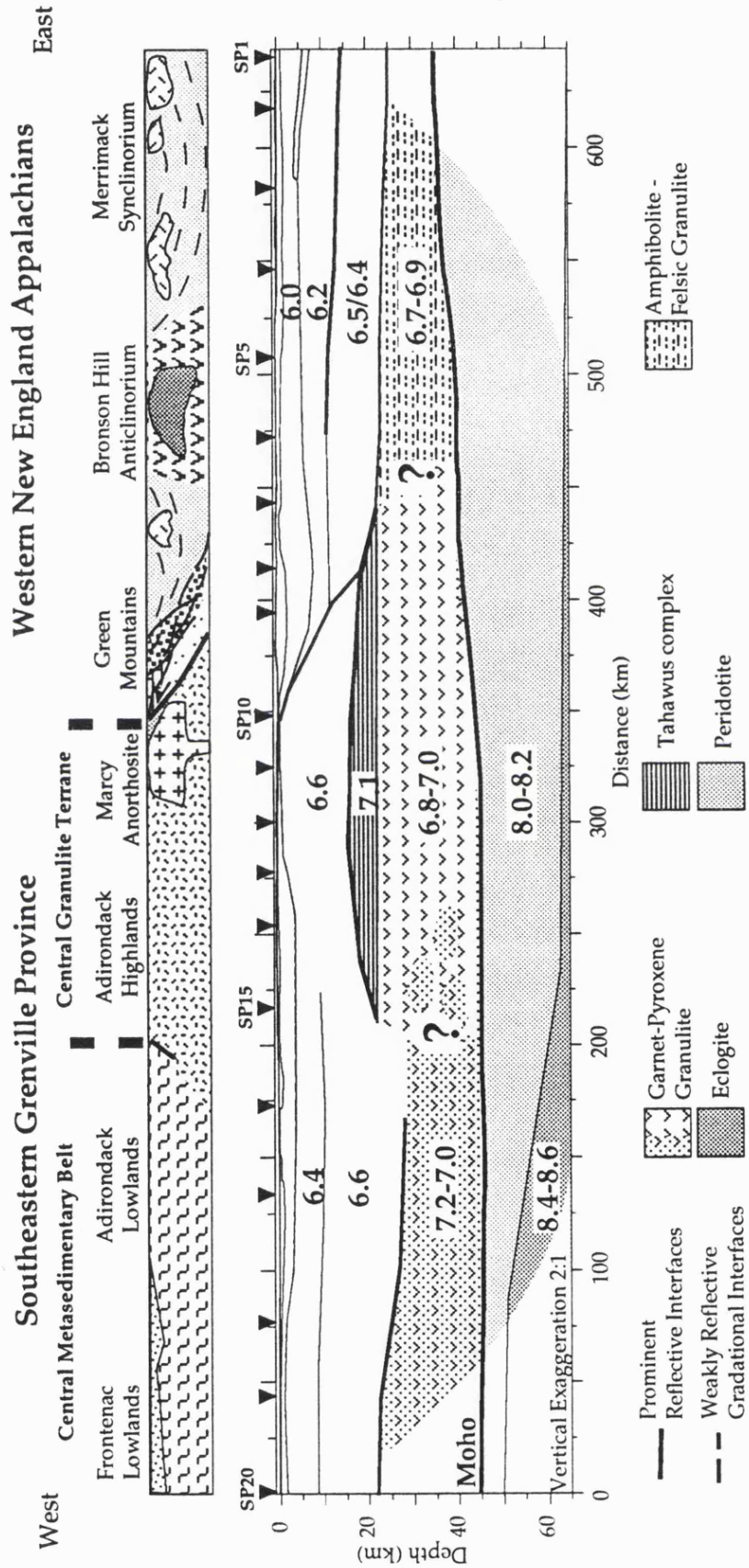


Figure 3.2

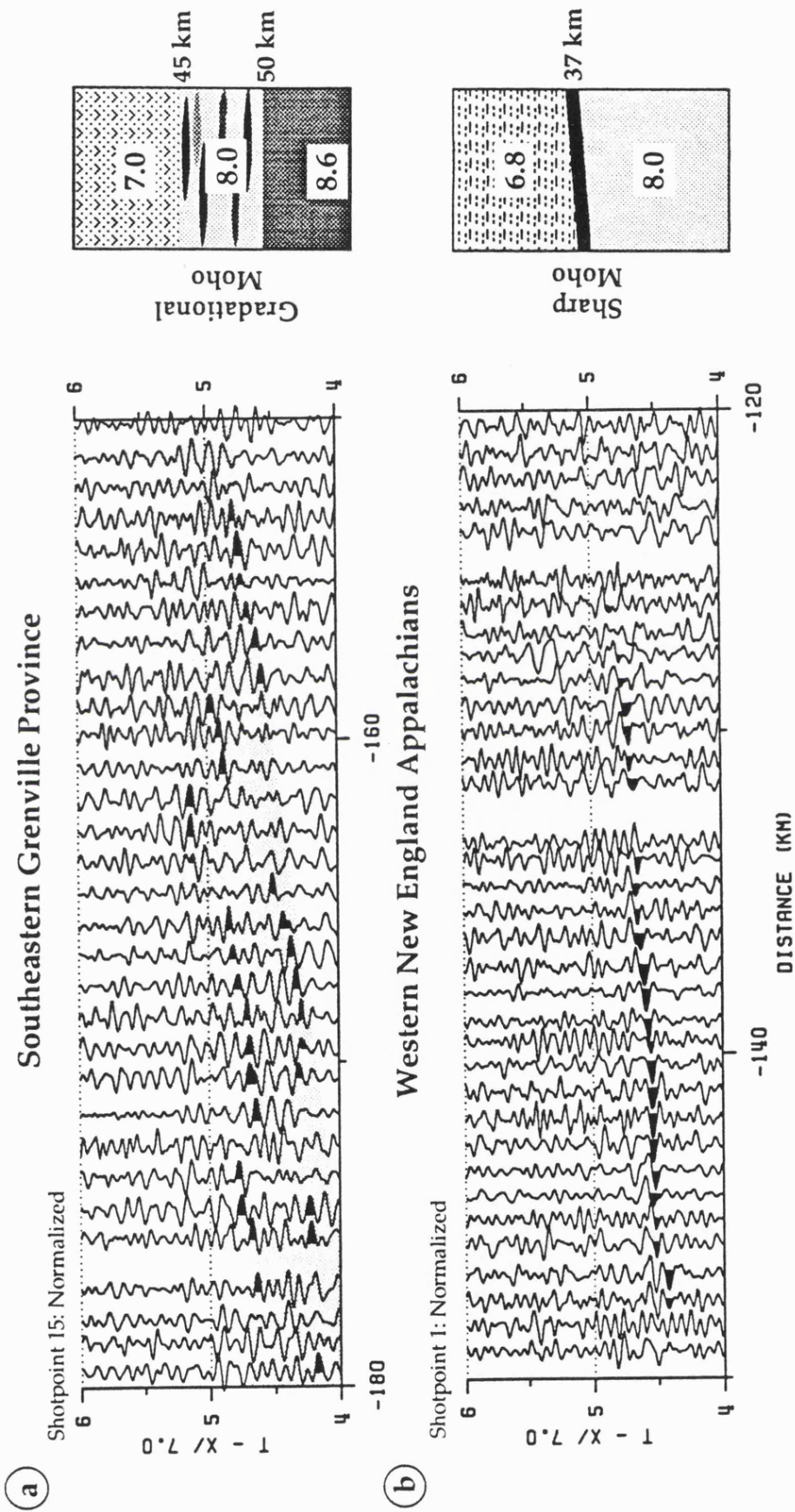


Figure 3.3

## **Seismic Anisotropy and Structural Inter-Relationships across the Grenvillian-Appalachian Boundary in New England**

### **4.1 Abstract**

The Grenvillian-Appalachian boundary is characterized by pervasive mylonitic deformation and retrogressive alteration of a suite of imbricated allochthonous and parautochthonous gneisses that were thrust upon the Grenvillian continental margin during the Lower Paleozoic. Seismic reflection profiling across this structural boundary zone reveals prominent dipping reflectors interpreted as overthrust basement slices (parautochthons) of the Green Mountain Anticlinorium. In contrast, a recent seismic refraction study of the Grenvillian-Appalachian boundary reveals a sub-horizontally layered seismic velocity model that is difficult to reconcile with the pronounced sub-vertical structures observed in the Green mountains. A suite of rock samples were collected from the Green Mountain Anticlinorium and measured at high pressures in the laboratory to determine the seismic properties of these allochthonous and parautochthonous gneisses. The mylonitic Green mountain gneisses display up to 12% anisotropy when measured in the high pressure laboratory. These measurements together with petrological analyses suggests that the retrograde metamorphic assemblages and imbricated structures of the Green mountain gneisses inhibits their resolution with

seismic refraction techniques. This is because refraction ray paths propagate normal to the sub-vertical foliation, and hence the 'slow' direction, with the result that resolution of the parautochthonous Green mountain gneisses is inhibited. In addition, re-metamorphism and hydration of the Green mountain par-autochthonous gneisses results in a further lowering of the seismic velocity of these rocks, so that they can not be readily correlated with their lithologic equivalents in the Adirondack Highlands.

## 4.2 Introduction

In western New England the Grenvillian-Appalachian boundary is characterized by pervasive mylonitic deformation and retrogressive alteration of a suite of imbricated allochthonous and parautochthonous gneisses that were thrust upon the Grenvillian continental margin during the Lower Paleozoic (Figure 4.1). Seismic studies of the Grenvillian-Appalachian boundary zone have sought to determine the deep structural inter-relationships within the juxtaposed litho-tectonic units of the western New England Appalachians, and hence to infer the mechanisms of crustal accretion during the Taconian (Devonian) and Acadian (Ordovician) orogenies. Structural interpretations of seismic reflection data acquired across the western New England Appalachians suggest that the Grenvillian-Appalachian boundary zone is characterized by an anastomosing system of folds and thrusts that encompass slices of autochthonous Grenvillian basement interposed within the allochthons of the western New England Appalachians (Ando *et al.*, 1984). In contrast, recent seismic refraction data that were acquired to investigate the structural inter-relationships across the Grenvillian-Appalachian boundary are difficult to reconcile with the complex imbricated structures observed in the western New England Appalachians (Hughes and Luetgert, 1991). Specifically, the resolution of a planar eastward dipping velocity interface separating the Grenville province from the allochthonous Appalachians appears to contradict the exposure of parautochthonous slices of Grenvillian basement to the east of the velocity interface in the Green Mountain Anticlinorium. In this study, we seek to reconcile the discrepancy between the observed lithologic juxtapositions within the Grenvillian-Appalachian boundary zone and the planar velocity structure inferred from seismic refraction data. Of particular importance to this objective are the seismic properties of the parautochthonous gneisses of the Green Mountain Anticlinorium (Figure 4.1).

The ability of geophysical techniques to resolve complex structural and lithologic discontinuities in the crust is a function of many intertwined parameters, most importantly amongst these are; (1) the physical properties (velocity and density) of the juxtaposed lithologies, (2) the principal structural grain (strike and dip) relative to the seismic profile, and (3) the spatial sampling of the seismic wavefield. Rock samples were collected from the western New England Appalachians and measured at high pressures in the laboratory to provide information on the physical properties of the juxtaposed lithologies exposed within the Grenvillian-Appalachian boundary zone. These measurements are used, together with structural information, to determine the anisotropic properties of the allochthonous and parautochthonous gneisses. In this manner, we seek to ascertain the affects of seismic anisotropy upon our ability to use *insitu* seismic refraction velocity measurements to resolve structural and lithologic inter-relationships. We begin with a detailed description of the lithologic and structural features of the western New England Appalachians which we present in terms of a tectonic model and a geologic cross section, in order, to emphasize the pervasive nature of the deformational fabrics. These structural fabrics play an important role in determining the anisotropic properties of the rock samples collected from the western New England Appalachians discussed in the proceeding sections.

### 4.3 Structural Framework of the Grenvillian-Appalachian Boundary

The resolution of the Grenvillian-Appalachian boundary by seismic refraction and reflection techniques provides a particularly exacting challenge due to the structural complexity and narrowness of the deformation zone in western New England (Figure 4.1). The autochthonous basement which underlies the obducted litho-tectonic units of the western New England Appalachians is exposed in the Adirondack

Highlands, where a suite of Mid-Proterozoic anorthosites, charnockites, syenites, and granitic gneisses are interleaved with quartzites and marbles (McLelland and Isachsen, 1986). The Grenvillian basement is characterized by hornblende-granulite facies metamorphism and large-scale recumbent (sub-horizontal) nappes which provide evidence for extensive ductile flow at mid-crustal depths prior to the unroofing of these crystalline rocks (Wiener *et al.*, 1984; McLelland and Isachsen, 1986). Substantial thicknesses of rift-volcanics, carbonates, and clastics were deposited along the Grenvillian continental shelf during a protracted period of extensional tectonism in the Late Proterozoic (Coish *et al.*, 1991). Outboard of the shelf-rise sequence, distal flysch deposits accumulated through the lowermost Paleozoic (Rowley and Kidd, 1980; Stanley and Ratcliffe, 1985). These sediments were incorporated into an accretionary complex that marked the location of an eastward dipping subduction system. Continued subduction in the Taconian orogeny (Mid-Upper Ordovician) led to the accretion of the Bronson Hill island-arc complex and the obduction of an eastward dipping wedge of accretionary sediments, slivers of oceanic crust and crystalline basement rocks against the Grenvillian continental margin (Figure 4.2).

In the later stages of the Taconian orogeny activation of the Champlain Thrust emplaced a slice of Mid-Proterozoic crystalline basement between the allochthonous shelf-rise sediments. The obduction of this autochthonous basement slice produced the Green Mountain Anticlinorium and its western counterpart the Middlebury Synclinorium (Stanley and Ratcliff, 1985). In central Vermont the core of the Green Mountain Anticlinorium is composed of two arcuate limbs which form the Lincoln massif (Figure 4.1). The Lincoln massif is composed of layered granitic gneisses and massive quartzites of the Mount Holly Complex. The western limb of the Lincoln massif is comparatively massive and competent, with only minor high-angle offset faulting of the recumbent anticlinal structure. The eastern limb

of the Lincoln massif is characterized by pervasive mylonitic schistosity resulting from extensive imbrication along a series of anastomosing thrust surfaces within an east to west stacked duplex structure (Figure 4.2-detail). Relic Grenvillian metamorphic fabrics in the paragneisses of the eastern limb suggest epidote-amphibolite/garnet zone conditions were prevalent at the time of obduction, locally attaining granulite facies conditions in the core of the Green Mountain Anticlinorium (DelloRusso and Stanley, 1986; Stanley, 1989). Flanking the Green mountains to the east, a series of distal flysch deposits are exposed that are characterized by amphibolite grade (garnet zone) metamorphism, pervasive imbrication and retrogressive fabrics (Stanley and Ratcliffe, 1985; DelloRusso and Stanley, 1986).

Uplift and erosion of the Taconian accretionary wedge and the obducted forearc material of the Bronson Hill Anticlinorium through Silurian and Devonian times led to the deposition of a sequence of low-grade clastics and volcanics in the extensional sub-basin of the Connecticut Valley Synclinorium (Figure 4.1). Reactivation of Taconian thrust surfaces in the Acadian orogeny (Devonian) is strongly suggested by tectonic synthesis of the New England orogen (Bradley, 1983; Stanley and Ratcliffe, 1985) further imbricating the Taconic allochthons against the Grenvillian continental margin. The New Hampshire Series granites (Knox Mountain and Barre plutons) were emplaced in the Late Devonian (Figure 4.1). The extent of deformation produced by the Alleghenian orogeny (Carboniferous) is thought to be relatively minor in the western New England Appalachians (Stewart *et al.*, 1991; Thompson *et al.*, *in press*).

#### 4.4 Geophysical Constraints on the Deep Crustal Structure

The Ontario-New York-New England seismic refraction/wide-angle reflection profile traverses the Adirondack massif and extends across the western New England Appalachians at an oblique angle, almost

perpendicular to the north-south trend of the principal litho-tectonic units (Figure 4.1). The distinct lithologic and structural characteristics of the Grenvillian and Appalachian provinces allow a seismic velocity discontinuity to be resolved that separates the Grenvillian upper crust from that of the western New England Appalachians (Hughes and Luetgert, 1991). This velocity discontinuity forms a ramp-like structure dipping eastwards beneath the western New England Appalachians (Grenvillian Ramp on Figure 4.3a). Interpretation of the Grenvillian ramp suggests that it is a zone of detachment that separates the autochthonous Grenvillian rocks and their Precambrian 'cover' sequence from the allochthonous Appalachian terranes (Hughes and Luetgert, 1991). However, the pronounced dipping structures recognized between the imbricated allochthons and parautochthonous rocks of the Green Mountain Anticlinorium are difficult to reconcile with the sub-horizontal velocity interfaces modeled in the region of the Green Mountain Anticlinorium (Figure 4.3a). In particular, the characterization of Grenvillian basement with high seismic velocities (6.55-6.65 km/s) is inconsistent with the seismic velocities of 5.95-6.05 km/s modeled beneath the Green Mountain Anticlinorium; where parautochthonous Grenvillian basement rocks should be readily resolved by their high apparent velocities. Thus, the Grenvillian ramp delineates a seismic boundary that is located 25 km west of the exposure of Grenvillian basement in the Green mountains (Figure 4.3a). The absence of resolvable travel-time features that might be correlated with the Green Mountain Anticlinorium raises questions concerning the seismic expression of the Grenvillian parautochthonous gneisses (Mount Holly Complex) which core the Green mountains.

Deep seismic reflection profiles acquired across the Adirondack Highlands and the western New England Appalachians provides an illuminating comparison with the seismic velocity model (Figure 4.3b). The seismic reflection profiles traverse the Adirondack Highlands, northern

New York State, and extends across the Taconic allochthon and the Green Mountain Anticlinorium in southern Vermont. The geology is remarkably similar along strike, so that comparisons may be readily drawn between the refraction model and the seismic reflection section. Although it should be noted that the Taconic Allochthon has been further eroded from the structurally deeper exposures in central Vermont. The seismic reflection profiles display a number of characteristic features that may be compared to the seismic velocity model (Figure 4.3). The Grenvillian basement is characteristically transparent, suggesting that the anorthosites, charnockites, syenites and granitic gneisses are relatively homogenous and lack significant internal structure (See 1 in Figure 4.3b). Eastwards across the Taconic Allochthon (Foreland Thrust Belt) a discontinuous sub-horizontal reflector was imaged at 1.0-1.5 seconds TWTT (See 2 in Figure 4.3b). A series of prominent sub-parallel dipping reflectors were imaged extending to approximately 5-6 seconds TWTT beneath the Connecticut Valley Synclinorium (See 3 in Figure 4.3b). These dipping reflectors splayed out into a zone of anastomosing reflections in the mid-lower crust (Brown *et al.*, 1983; Ando *et al.*, 1984). Interpretations of the seismic reflection profiles are numerous, and include; (1) thin-skin style 'flat-ramp-flat' structures, (2) ramp-anticlinal box structures, and (3) thick-skin planar crustal penetrating thrusts (Ando *et al.*, 1984; Phinney and Roy-Chowdhury, 1989; Thigpen, 1989). Although the seismic structures inferred between the obducted lithologic units are contentious, in each case, the buried edge of the Grenvillian crust is interpreted as a highly deformed thrust-imbricated zone. The Green mountains are commonly associated with back projected extrapolations of these imbricated thrust structures, suggesting that the Green Mountain Anticlinorium was obducted from the edge of the Grenvillian continental margin above a crustal penetrating décollement. These seismic reflection interpretations correlate with geologic observations

in the Green Mountain Anticlinorium (Stanley and Ratcliffe, 1985; DelloRusso and Stanley, 1986; Stanley, 1989) and suggest the Grenvillian-Appalachian boundary is characterized by complex compositional and structural inter-relationships, in sharp contrast to the seismic velocity model.

#### 4.5 Rock Samples

A suite of rock samples were collected in an attempt to resolve the apparent conflict between the geologic cross section, the seismic velocity model and the seismic reflection profile across the Green Mountain Anticlinorium. These samples were collected from the western New England Appalachians in the vicinity of the Ontario-New York-New England seismic refraction profile where it traverses central Vermont (Figure 4.1). Laboratory velocity measurements of the rock samples allow constraints to be placed on the interpretation of the velocity model by providing calibration with the lithologies traversed by the seismic refraction profile (Table 4.1). Three-mutually perpendicular cores were cut from these samples parallel and normal to the principal foliation (cleavage plane) and the structural lineation respectively. Each core was measured in the high pressure laboratory for seismic velocity at increasing pressure up to 1000 MPa. The samples display a characteristic rapid velocity increase up to pressures of 200-300 MPa associated with closing of micro-cracks and pore spaces in the samples. At pressures in excess of 200-300 MPa the seismic velocity increases linearly with pressure with mean velocities in the range 6.0-6.5 km/s (Figure 4.4a). Rock samples collected from the Adirondack Highlands (Birch, 1960; Manghnani *et al.*, 1974; Christensen and Fountain, 1975) are characterized by mean velocities in the range 6.2-7.2 km/s (Figure 4.4b). The Adirondack samples are characterized by compressional-wave

velocities that are approximately 0.5 km/s faster than that of samples collected from the western New England Appalachians (Figure 4.4).

The pervasive sub-vertical mylonitic schistosity associated with the imbricated litho-tectonic units of the Green Mountain Anticlinorium have significant effects upon the resolution of lateral velocity anomalies. The results obtained from the velocity measurements in the high pressure laboratory show that seismic velocities are reduced when transmitted (refracted) seismic energy propagates normal to the foliation. Seismic anisotropy of the samples varies from 2% in the massive granitic lithologies to as much as 12% in the schistose amphibolitic gneisses. In the Green Mountain Anticlinorium structural dips range from 60° through to sub-vertical (Figure 4.2). Thus, transmitted seismic energy which traverses the Green Mountain Anticlinorium propagates through a series of sub-vertical lithologic units which lie normal to the direction of propagation. Consequently, the minimum velocity measured in the high pressure laboratory (*i.e.*, normal to the foliation) is most representative of the *insitu* seismic velocity measured by the Ontario-New York-New England seismic refraction profile. Comparisons of the rock sample velocities with the seismic refraction model shows a scatter about the *insitu* velocity measurements, but in general, a broad agreement is attained between the two measurements (Figure 4.5). In particular, the minimum velocity of the anisotropic gneisses agrees most favorably with that obtained from the seismic refraction profile. Noticeably, the garnet-rich, biotite-plagioclase-quartz gneisses which form the core of the Green Mountain Anticlinorium (samples f and g) have a lower velocity compared to the amphibolitic gneisses, schists and phyllites (samples b and c) which mantle the Green mountains to the east (Figure 4.5). The association of low seismic velocities ( $5.9 \pm 0.1$  km/s) with the Grenvillian paragneisses of the Green Mountain

Anticlinorium is opposite to that observed within the Adirondack Highlands where velocities in excess of 6.5 km/s predominate.

#### 4.6 Discussion

Structurally complex regions, such as the Green Mountain Anticlinorium, are extremely difficult to image with regional seismic refraction techniques. Seismic velocities obtained from refraction profiling are frequently attributed to an aggregate of the lithological and structural variations along the seismic profile whose bulk properties tend to increase with depth resulting in a sub-horizontally stratified Earth model (Mooney, 1989). On first inspection such an interpretation for the velocity structure of the Green Mountain Anticlinorium appears to be satisfactory in the absence of resolvable seismic velocity evidence for complex interlayered structural fabrics associated with the obducted allochthons and parautochthons (Figure 4.3a). However, both structural geology and seismic reflection profiling in the Green Mountain Anticlinorium suggest that such an interpretation is grossly simplistic and inappropriate to these highly deformed paragneisses (Figure 4.3). Some additional factors must be affecting our ability to resolve the seismic velocity expression of the Green Mountain Anticlinorium.

*Composition:* The rocks which form the core of the Green Mountain Anticlinorium are lithologically equivalent to the Grenvillian 'basement' lithologies exposed in the Adirondack Highlands. Although extensive anorthosite, charnockite and syenite suites are absent in the Green mountains, one-to-one correlations can be made with the paragneisses and syn-tectonic granitoids exposed in the Green mountains (Mount Holly Complex) with those exposed in the Adirondack Highlands (Ratcliffe *et al.*, 1991). The Green mountains suffered extensive retrogressive metamorphism during the Taconian and Acadian orogenies. As a result all the lithologies exposed in the Green mountains are hydrated (1-2% H<sub>2</sub>O is

typical), pervasively refoliated and commonly display abundant chlorite-muscovite-epidote as retrogressive minerals formed during Taconian and Acadian re-metamorphism (DelloRusso and Stanley, 1986). From this petrological analysis it is clear that the mineralogical composition of the Green Mountain paragneisses has been substantially altered compared to their lithologic equivalents in the Adirondacks which remain relatively unscathed by Lower Paleozoic re-metamorphism. The retrogressive mineralogies observed in the Green mountains result in lowering the seismic velocity of the Mount Holly Complex. Complementary measurements for samples obtained from the Adirondack Highlands, that closely match the Mount Holly Complex in composition, have a seismic velocity about 0.5 km/s greater than those measured for the Green mountains (Figure 4.6). Thus, a primary reason for the absence of a resolvable velocity anomaly associated with the Green Mountain Anticlinorium is the re-metamorphism and hydration of the Grenvillian basement parautochthons.

*Structure and Anisotropy:* Brocher and Christensen [1990] showed that seismic velocity measurements vary as a function of dip relative to the azimuth of the seismic profile. For velocity measurements normal to the plane of the seismic profile, the maximum velocity is attained when the transmitted seismic energy is parallel to the foliation and the velocity decreases, as a sine of the dip angle, to a minimum when the foliation is normal to the transmitted energy. This observation is related to the preferential alignment of highly anisotropic minerals, such as micas and amphiboles in pervasively foliated gneisses (Fountain and Christensen, 1989; Brocher and Christensen, 1990). The Ontario-New York-New England seismic refraction profile provides a further demonstration of the relationship between seismic velocity and structural dip. From west to east across the Grenvillian-Appalachian boundary, the structural dip of the

'Adirondack' gneisses increases from sub-horizontal in the recumbent nappes of the Adirondack Highlands to sub-vertical in the core of the Green Mountain Anticlinorium (J.M. McLelland, *personnel communication*, 1992). Thus, lower seismic velocities would be expected across the Green mountains than across the Adirondack Highlands due to the anisotropic properties of the Mount Holly gneisses (Figure 4.7a). The absence of a resolvable velocity anomaly associated with the Grenvillian basement lithologies of the Green mountains must, in part, be due to the anisotropic lowering of the velocity of the steeply dipping mylonitized paragneisses (Figure 4.7b).

*Spatial Sampling:* A variety of geometrical factors also contribute to our ability to resolve regions of prominent structural fabric with regional seismic refraction techniques. The observation of travel time or amplitude features associated with the mylonitized gneisses of the Green mountains is inhibited by the 800 m receiver spacing and the 30-40 km shotpoint spacing. Thus, resolvable travel time anomalies are unlikely to be detected given the seismic properties of the Mount Holly Complex discussed above. In addition, the 8-10 Hz frequencies of the seismic refraction data further reduces the likelihood of identifying wide-angle reflections from the complex imbricated structures of the Green mountains. Indeed although *Hughes and Luetgert* [1991] were able to identify a series of high apparent velocity reflections in the vicinity of the Grenvillian ramp, these reflections were not amenable to 2-D raytrace modeling. Thus, the finely imbricated structures of the Green mountains do not permit the observation of back-scattered reflected energy, because the bulk velocity of the mylonitized paragneisses is insufficiently different from the mantling gneisses to permit their delineation with seismic refraction observations (Figure 4.7b).

#### 4.7 Conclusions

The Mid-Proterozoic parautochthonous rocks which form the core of the Green Mountain Anticlinorium were obducted from the edge of the Grenvillian continental shelf during the later stages of the Taconian orogeny (Stanley and Ratcliffe, 1985). Although the rock types quartzites, felsic gneisses and garnet-rich biotite-plagioclase-quartz gneisses are comparable in the Adirondacks and Green mountains the physical characteristics of these rock suites are sufficiently different so as to inhibit their seismic correlation. The secondary attributes (hydration, deformation) of the parautochthonous rock suites which form the core the Green Mountain Anticlinorium play an important role in affecting the resolution of velocity anomalies associated with the Mid-Proterozoic basement lithologies. Specifically, the anisotropic properties of the Green mountain paragneisses renders the transmission velocity insufficiently different from the surrounding amphibolitic lithologies to permit the imbricated basement structures to be distinguished by seismic refraction techniques alone. The application of high pressure laboratory measurements to the interpretation of regional seismic refraction data suggests that caution should be exercised in assigning seismic velocities in regions of high structural dip where the anisotropic properties of the deformed and mylonitized rocks are likely to be of paramount importance (Fountain and Christensen, 1989; Brocher and Christensen, 1990). Inferences of structural relationships from seismic refraction studies must be viewed with respect to the metamorphic, structural and anisotropic properties of the lithologies traversed by the seismic profile.

---

#### 4.8 Acknowledgments

The seismic data presented in this paper were collected by the US Geological Survey in collaboration with the Geological Survey of Canada and the US Air Force Geophysics Laboratory (AFGL). John Cipar (AFGL) kindly provided funding for the collection of the rock samples. We thank Dean Ballotti (Purdue University), for sample preparation and velocity measurements in the high pressure laboratory. Walter Mooney (USGS) and Tom Brocher (USGS) provided constructive reviews of early versions of this manuscript. Many thanks to Rolfe Stanley (University of Vermont), Nicholas Ratcliffe (USGS) and Dave Stewart (USGS) for their interest and encouragement.

#### 4.9 References

- Ando, C.J., B.L. Czuchra, S.L. Klemperer, L.D. Brown, M.J. Cheadle, F.A. Cook, J.E. Oliver, S. Kaufman, T. Walsh, J.R. Thompson, J.B. Lyons, J.L. Rosenfeld, Crustal profile of a mountain belt: COCORP's deep seismic reflection profile in New England and implications for architecture of convergent mountain chains, *Am. Assoc. Pet. Geol.*, 68, 819-837, 1984.
- Birch, F., The velocity of compressional waves in rocks at 10 Kbars part 1, *J. Geophys. Res.*, 65, 1083-1102, 1960.
- Blackwell, D.D., The thermal structure of the continental crust, in The Structure and Physical Properties of the Earth's crust, edited by Heacock J.G., *Am. Geophys. Un. Geophys. Monogr. Ser. 14*, pp. 169-184, 1971.
- Bradley, D.C., Tectonics of the Acadian orogeny in New England and adjacent Canada, *Journal of Geology*, 91, 381-400, 1983.
- Brocher, T.M. and Christensen N.I., Seismic anisotropy due to preferred mineral orientation observed in shallow crustal rocks in southern Alaska, *Geology*, 18, 737-740, 1990.
- Brown, L.D., C.J. Ando, S. Klemperer, J.E. Oliver, S. Kaufman, B. Czuchra, T. Walsh, and Y.W. Isachsen, Adirondack-Appalachian crustal structure: The COCORP northeast traverse, *Geol. Soc. Am. Bull.*, 94, 1173-1184, 1983.
- Christensen, N.I., Compressional-wave velocities in rocks at high temperatures and pressures, critical thermal gradients, and crustal low velocity zones, *J. Geophys. Res.*, 84, 6849-6857, 1979.
- Christensen, N.I. and Fountain D.M., Constitution of the lower continental crust based on experimental studies of seismic velocities in granulite, *Geol. Soc. Am. Bull.*, 86, 227-236, 1975.
- Coish, R.A., T. Bramley, T. Gavington, and R. Mastiner, Progressive changes in volcanism during Iapetan rifting: Comparisons with the East African rift-Red Sea system, *Geology*, 19, p. 1021-1024, 1991.

- DelloRusso, V. and R.S. Stanley, Bedrock geology of the northern part of the Lincoln Massif, Central Vermont, Special Bulletin 8, edited by C.A. Ratte, *Vermont Geological Survey*, 1986.
- Doll, C.G., W.M. Cady, J.B. Thompson, M.P. Billings, *Centennial geologic map of Vermont*, Vermont Geological Survey, 1961.
- Fountain, D.M. and N.I. Christensen, Composition of the continental crust and upper mantle; a review, in *Geophysical Framework of the Continental United States*, edited by L.C. Pakiser and W.D. Mooney, pp. 711-742, *Geol. Soc. Am. Memoir* 172, 1989.
- Hughes, S. and J.H. Luetgert, Crustal structure of the western Appalachians and the Adirondack Mountains, *J. Geophys. Res.*, 96, p. 16471-16494, 1991.
- Isachsen, Y.W. and D.W. Fisher, *Geologic Map of New York: Adirondack Sheet*, New York State museum and science services, map and chart series 15, 1970.
- Kern, H. and A. Richter, Temperature derivatives of compressional and shear wave velocities in crustal and mantle rocks at 6 Kbars confining pressure, *Journal of Geophysics*, 49, 47-56, 1981.
- Manghnani, M.H., R. Ramananantoandro and S.P. Clark, Compressional and shear wave velocities in granulite facies rocks and eclogites to 10 Kbars, *J. Geophys. Res.*, 79, 5427-5446, 1974.
- McLelland, J.M. and Y.W. Isachsen, Synthesis of geology of the Adirondack Mountains, New York, and their tectonic setting within the southwestern Grenville Province, in *The Grenville Province*, edited by J.M. Moore, A. Davidson and A.J. Baer, pp. 75-94, *Geological Association of Canada special paper* 31, 1986.
- Mooney, W.D., Seismic methods for determining earthquake source parameters and lithospheric structure, in *Geophysical Framework of*

*the Continental United States*, edited by L.C. Pakiser and W.D. Mooney, Geol. Soc. Memoir 172, pp. 11-34, 1989.

Phinney, R. A. and K. Roy-Chowdhury, Reflection seismic studies in the eastern United States, in *Geophysical Framework of the Continental United States*, edited by L.C. Pakiser and W.D. Mooney, Geol. Soc. Memoir 172, pp. 613-653, 1989.

Ratcliffe, N.M., J.M. Aleinikoff, W.C. Burton and P. Karibinos, Trondhjemitic, 1.35-1.31 Ga gneisses of the Mount Holly Complex of Vermont: evidence for an Elzevirian event in the Grenville basement of the United States Appalachians, *Can. J. Earth Sci.*, 28, 77-93, 1991.

Rowley, D.B. and W.S.F. Kidd, Stratigraphic relationships and detrital composition of the medial Ordovician flysch of western New England: Implications for the tectonic evolution of the Taconic orogeny, *Journal of Geology*, 89, 199-218, 1980.

Stanley, R.S. and M.N. Ratcliffe, Tectonic synthesis of the Taconic orogeny in western New England, *Geol. Soc. Am. Bull.*, 96, 1227-1250, 1985.

Stanley, R.S., A transect through the pre-Silurian foreland and hinterland of central Vermont, in *A transect through the New England Appalachians IGC 28 Fieldtrip guidebook T162*, edited by J.B. Lyons, and W.A. Bothner, pp. 15-29, A.G.U., 1989.

Stewart, D.B., B.E. Wright, J.D. Unger, J.D. Phillips, D.R. Hutchinson, J.H. Luetgert, W.A. Bothner, K.D. Klitgord, L.M. Liberty, C. Spencer, The Quebec-Maine-Gulf of Maine Transect, Southeastern Canada, Northeastern United States of America, Global Geoscience Transect 8, US Geological Survey Open File Report 91-353, 1991.

Thigpen, J.T., Seismic reflection evidence for imbricate basement slices in central New England, *unpublished MSc. Thesis, Cornell University*, pp. 95, 1989.

Thompson, J.B., W.A. Bothner, P. Robinson, Y.W. Isachsen and K.D.

Klitgord, A guide to the continent ocean transect E-1: Adirondacks to George's Bank, pp. 55, *in press*.

Wiener, R.W., J.M. McLelland, Y.W. Isachsen, and L.M. Hall, Stratigraphy and structural geology of the Adirondack Mountains, New York: review and synthesis, in *The Grenville Event in the Appalachians and Related Topics*, edited by M.J. Bartholomew, pp. 1-55, *Geol. Soc. Am. Special Paper 194*, 1984.

#### 4.10 Captions

**Table 4.1:** Location and composition of rock samples used in this study. Suffixes refer to the following references; (1) *Christensen and Fountain*, [1975], (2) *Manghnani et al.*, [1974] and (3) *Birch*, [1960].

**Figure 4.1:** Geologic map across the western New England Appalachians and the adjacent Adirondack Highlands. The Ontario-New York-New England seismic refraction/wide-angle reflection profile is shown by the bold line and shotpoints are indicated along the profile. The locations of rock samples collected from the western New England Appalachians are indicated by the letters a-i. The map has been simplified after the Vermont State geologic map compiled by *Doll et al.* [1961], and the New York State geologic map of *Isachsen and Fisher* [1970].

**Figure 4.2:** Geologic cross section along the Ontario-New York-New England seismic refraction/wide-angle reflection profile where it traverses the western New England Appalachians and the adjacent Adirondack Highlands. The seismic expression of the steeply dipping imbricated structures at the edge of the Grenvillian crust is examined by means of seismic refraction velocities (shotpoints indicated) and rock sample velocities (a through i). For key to lithologies see Figure 4.1. The cross section is simplified after *Doll et al.* [1961] and *Stanley* [1989].

**Figure 4.3:** Comparison between a seismic refraction velocity model (a) and deep seismic reflection sections (b) acquired across the Grenvillian-Appalachian boundary in New England. The seismic velocity model shows a steeply dipping ramp structure (Grenvillian ramp) dividing the western New England Appalachians from the Adirondack Highlands (*Hughes and Luetgert*, 1991). Note, the absence of velocity features which might be correlated with the parautochthonous Grenvillian rocks of the Green mountains. The geologic cross section is from *Stanley* [1989]. The seismic reflection profiles (b) acquired across the Green mountains and the

Taconic Allochthon in southern Vermont (Brown *et al.*, 1983; Ando *et al.*, 1984) display prominent dipping reflectors characteristic of mylonitized and imbricated structures at the edge of the Grenvillian craton. The seismic interpretation is from Ando *et al.* [1984]. The models are aligned with respect to Logan's Line (Champlain Thrust).

**Figure 4.4:** Comparison of mean laboratory velocity measurements for rock samples collected from the western New England Appalachians (a) and from the Adirondack Highlands (b). Note that the Adirondack rock samples have a compressional wave velocity that is 0.5 km/s faster than that of samples collected from the western New England Appalachians. Appalachian rock samples (a) were collected from localities shown in Figure 4.1, and additional Appalachian rock samples are from Birch [1960]. Adirondack rock samples (b) denoted by Samples #1-14 are from Manghnani *et al.* [1974] and samples 4, 5, 7 are from Christensen and Fountain [1975]. See Table 4.1 for location and composition of these rock samples. Laboratory data have been corrected for temperature using a geotherm of 15 °C/km (Blackwell, 1971) and an average thermal coefficient of  $2.0 \times 10^{-4}$  km/s°C<sup>-1</sup> (Christensen, 1979; Kern and Richter, 1981).

**Figure 4.5:** Rock Samples collected from the western New England Appalachians and measured for seismic velocity at 100 MPa in the high pressure laboratory. Sample velocities were measured parallel (slow direction) and normal (fast direction) to the principal foliation to enable comparison with the seismic velocity model. The graph shows that the laboratory velocities agree favorably with the seismic refraction velocities at 3 km (~100 MPa). Note that samples from the core of the Green Mountain Anticlinorium (f and g) have a lower velocity than the mantling amphibolitic gneisses (b and c). Sample localities and shotpoints are shown in Figure 4.1.

**Figure 4.6:** Comparison of laboratory measurements of seismic velocity for samples of Mid-Proterozoic gneisses from the Adirondack Highlands (Manghnani *et al.*, 1974) and from the Green Mountain Anticlinorium (Mount Holly Complex - samples f and g). The samples are compositional similar (garnet-rich biotite-plagioclase-quartz gneisses), but seismic velocities are significantly lower in the Green mountains than in the Adirondack Highlands. We conclude that retrogressive alteration (hydration) of the paragneisses from the Green Mountain Anticlinorium has an important effect in lowering the measured seismic velocity. One-dimensional velocity-depth functions for the Green mountains (SP9) and the Adirondack Highlands (SP11) are shown. A sample of Marcy Anorthosite is shown for reference.

**Figure 4.7:** The mylonitized gneisses of the Green Mountain Anticlinorium are characterized by 5% seismic anisotropy (a). Seismic refraction ray paths propagate approximately normal to the steeply dipping gneissic foliation (b). Consequently, the 'slow' velocity of the Mount Holly Complex gneisses is measured by the seismic refraction profile. The bulk velocity of the mylonitic gneisses of the Mount Holly Complex is insufficiently different from the mantling amphibolitic gneisses of the Green Mountain Anticlinorium to permit resolution of the imbricated basement structures with seismic refraction techniques. The observation of clear back-scattered energy (reflected raypaths) is inhibited by the finely imbricated structures within the Green Mountain Anticlinorium.

## 4.11 Table

Rock Samples

Sample Reference	Locality	Rock Type
Sample a	Barre, VT	Phyllitic schist
Sample b	Roxbury, Vt	Phyllite
Sample c	East Warren, Vt	Phyllitic schist
Sample e	Lincoln Gap, Vt	Mica schist
Sample f	South Lincoln, Vt	Granitic schist
Sample g	South Lincoln, Vt	Granitic gneiss
Sample h	East Middlebury, Vt	Quartzite
Sample i	Middlebury, Vt	Shaley limestone
Barre Granite 3	Barre, VT	Granite
Adirondack #1 2	Lake Placid, NY	Anorthosite
Adirondack #2 2	Tupper Lake, NY	Garnet-biotite-qtz-fldsp gneiss
Adirondack #3 2	Colton, NY	Migmatitic biotite-qtz-fldsp gneiss
Adirondack #4 2	Tupper Lake, NY	Ferrohypersthene granulite
Adirondack #5 2	Tupper Lake, NY	Charnockite
Adirondack #6 2	Willsboro, NY	Gabbroic anorthosite
Adirondack #7 2	Long Pond, NY	Gabbroic anorthosite
Adirondack #8 2	Saranac Lake, NY	Quartz mangerite
Adirondack #9 2	Saranac Lake, NY	Mangerite
Adirondack#10 <sup>2</sup>	Tupper Lake, NY	Microcline granulite
Adirondack#11 <sup>2</sup>	Everton, NY	Gabbroic granulite
Adirondack#12 <sup>2</sup>	Willsboro, NY	2-pyroxene-plagioclase granulite
Adirondack#13 <sup>2</sup>	Lake Placid, NY	Metasedimentary granulite
Adirondack#14 <sup>2</sup>	Everton, NY	Hornblende-pyroxene granulite
Adirondack#15 <sup>2</sup>	Everton, NY	Gabbroic granulite
Adirondack#16 <sup>2</sup>	Elizabethtown, NY	Almandine-CPX-Oligoclase granulite
Adirondack#17 <sup>2</sup>	Willsboro, NY	Almandine-pyroxenite gneiss
Sample 4 1	Saranac Lake, NY	Charnockite
Sample 5 1	Saranac Lake, NY	Charnockite
Sample 7 1	Saranac Lake, NY	Charnockite

Table 4.1

4.12 Figures

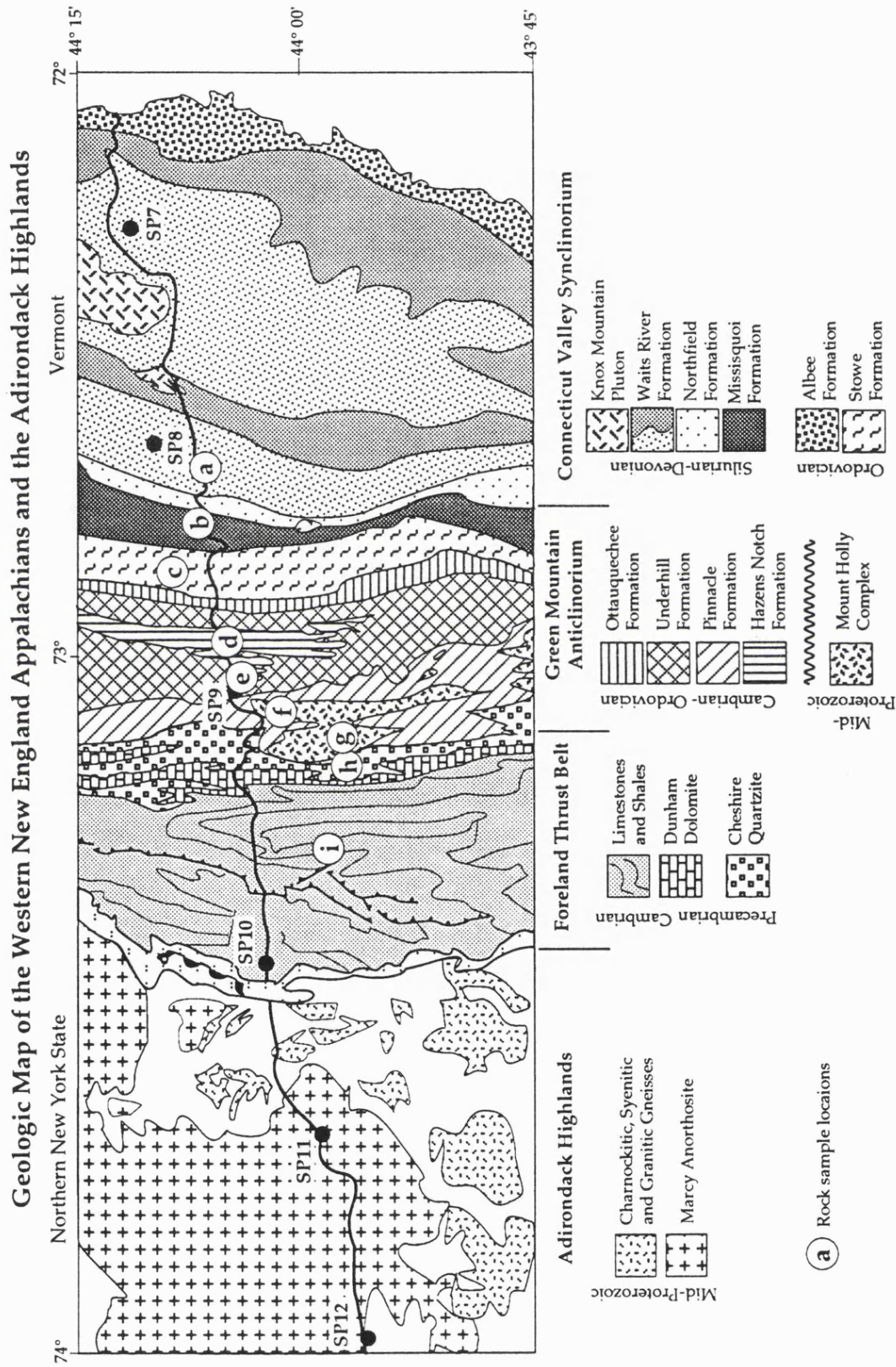


Figure 4.1



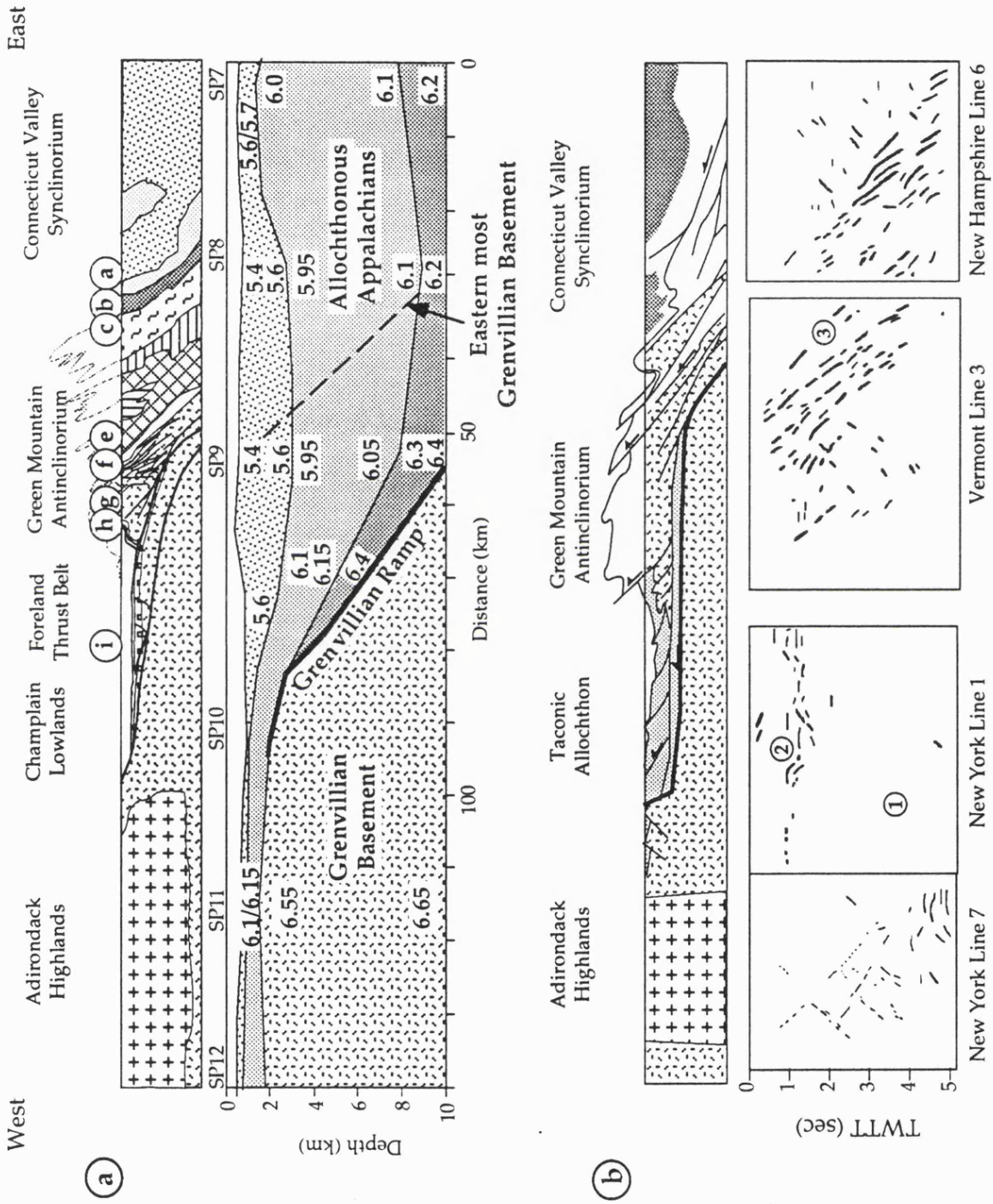


Figure 4.3

(a)

Western New England Appalachians

(b)

Adirondack Highlands

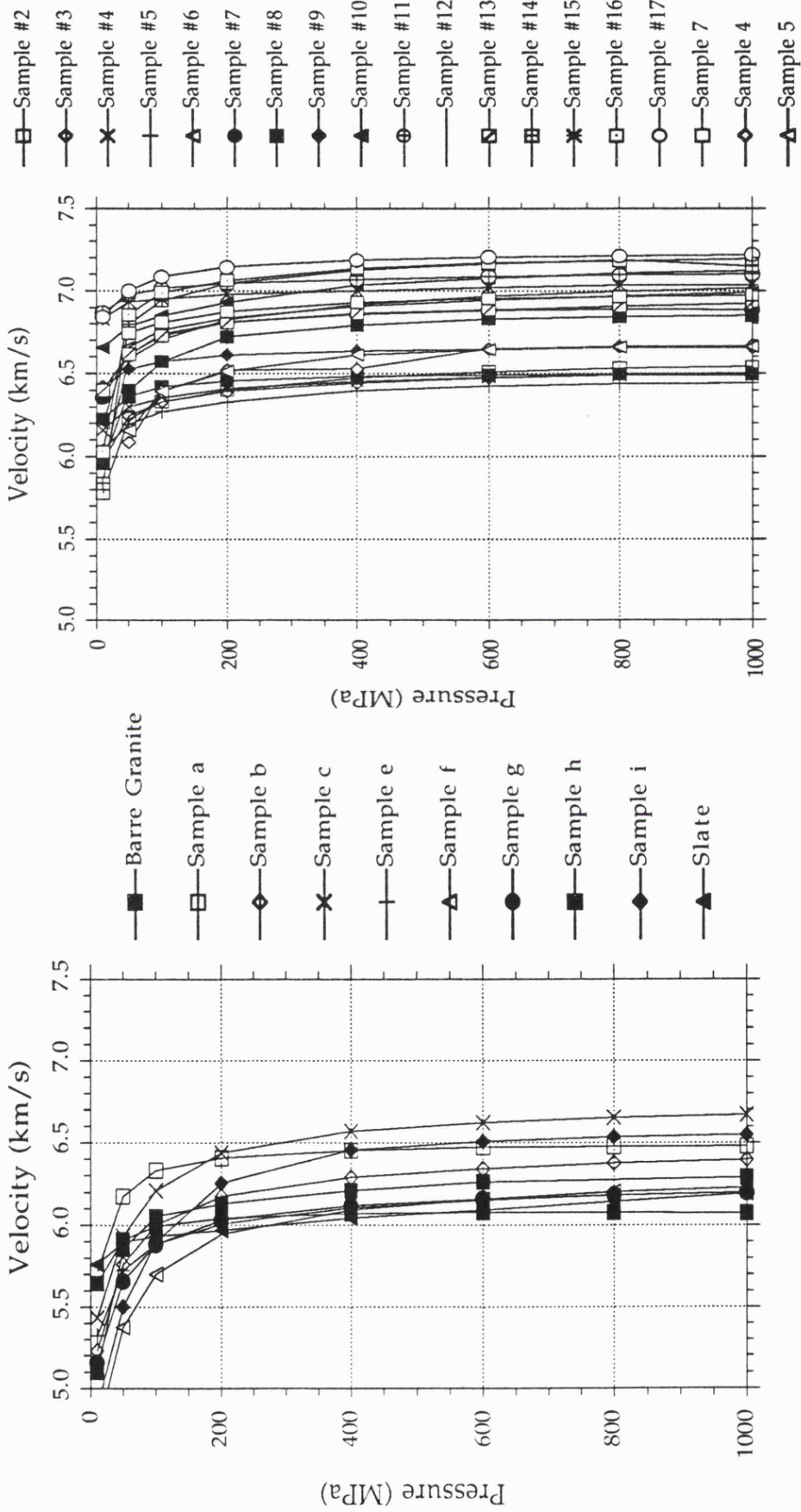


Figure 4.4

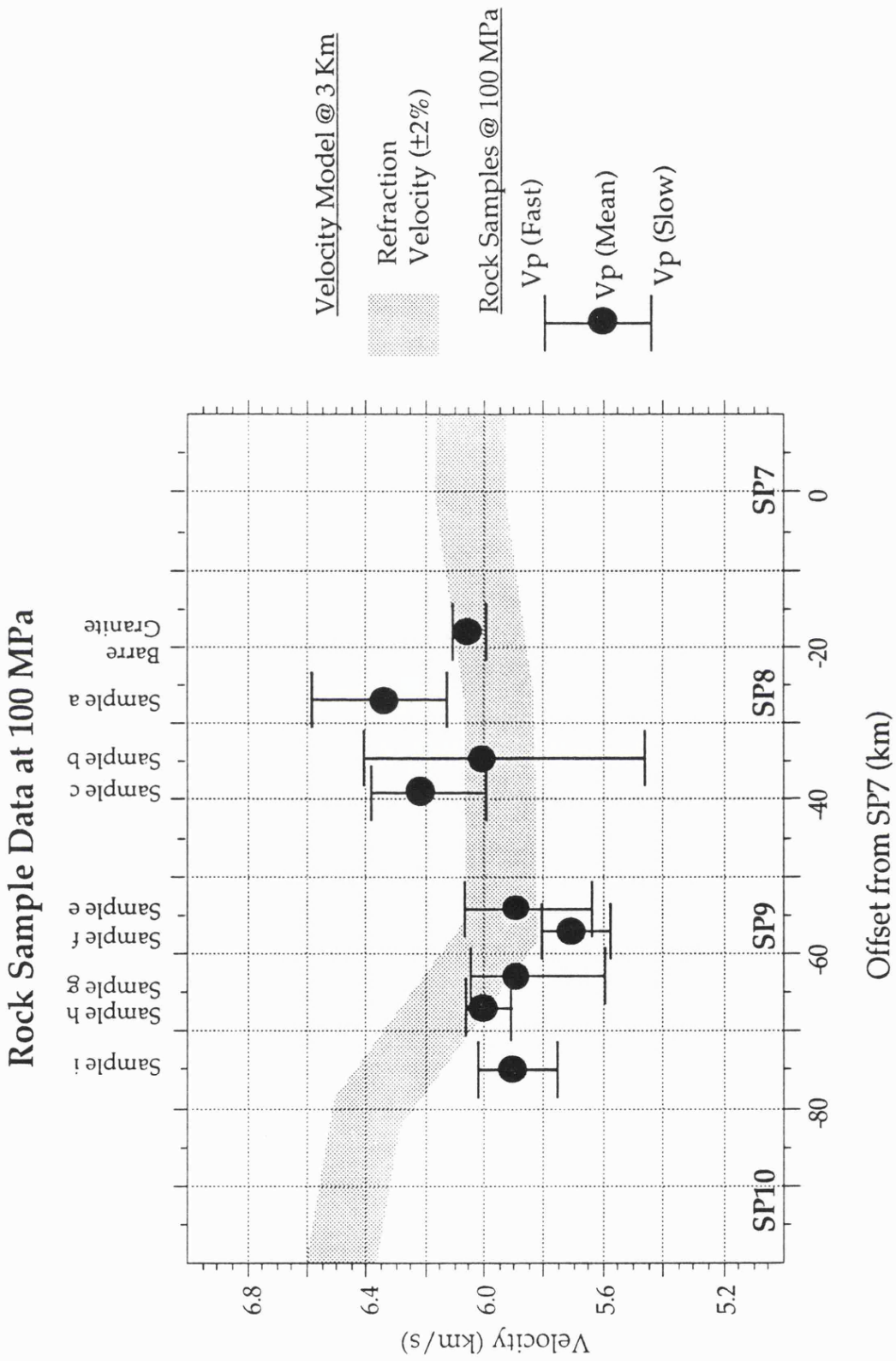


Figure 4.5

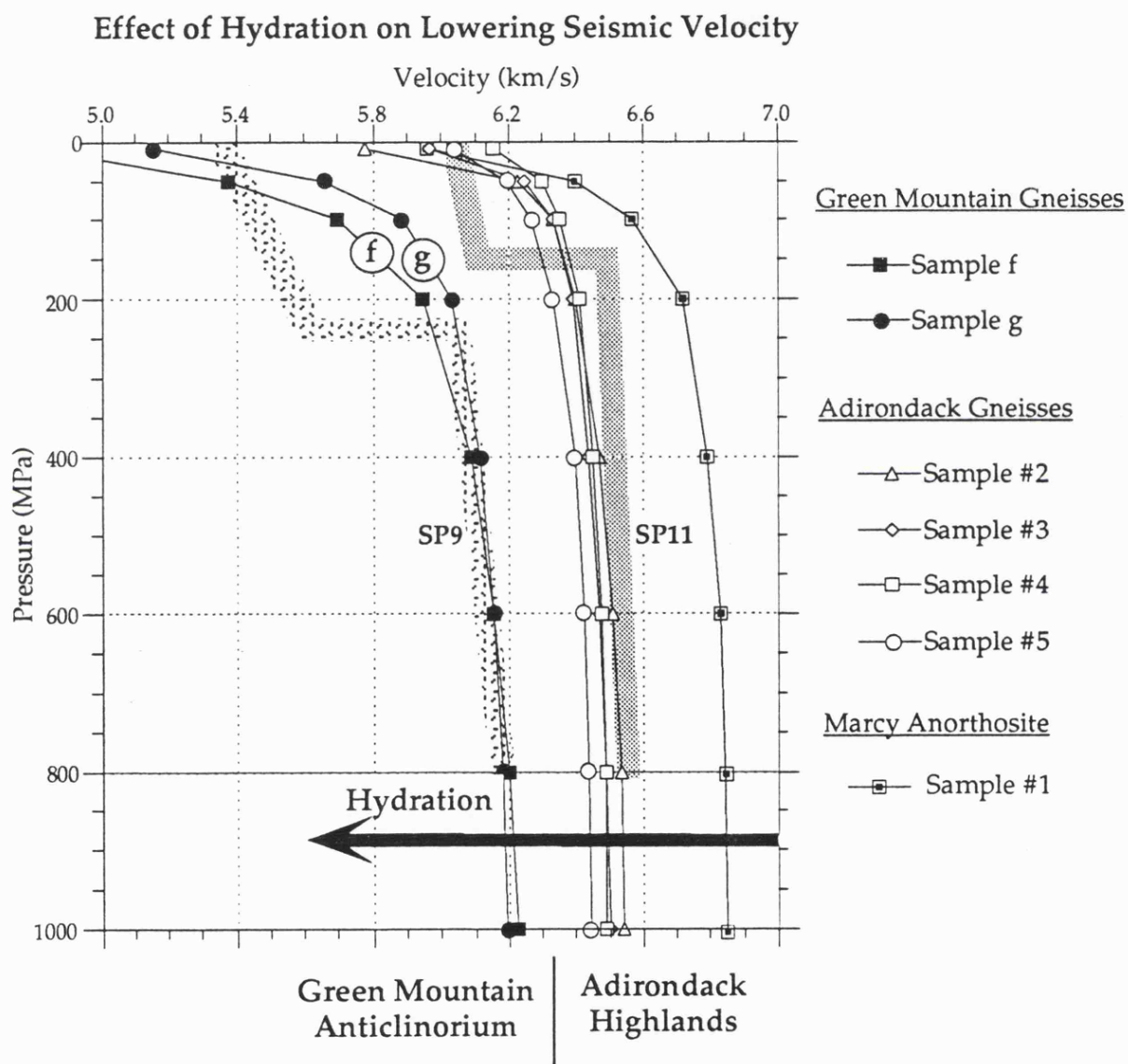


Figure 4.6

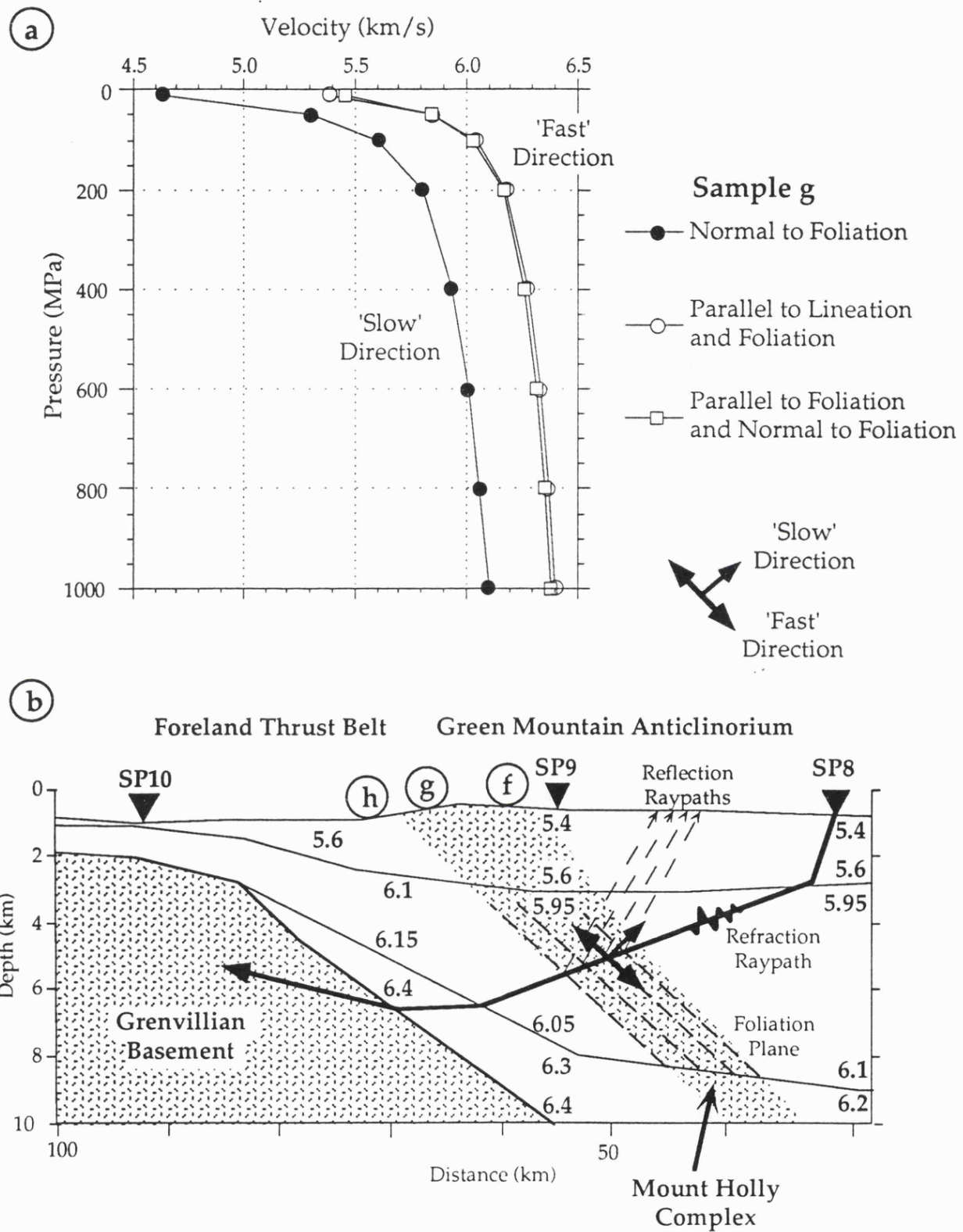


Figure 4.7



---

## **Data Report for the Ontario-New York-New England Seismic Refraction/Wide-Angle Reflection Experiment**

### **A.1 Introduction**

In September, 1988, the US Geological Survey (USGS), the US Air Force Geophysics Laboratory (AFGL), and the Geological Survey of Canada (GSC) conducted a seismic refraction/wide angle reflection experiment in southern Ontario, New York, and New England to investigate the crustal and upper mantle velocity structure and inter-relationships of the North American craton, the Adirondack massif, and the northern Appalachians. The primary line of the experiment extended east from Marmora, Ontario, Canada across the Adirondacks in upstate New York, and the northern Appalachians in Vermont and New Hampshire to Waterville, Maine. Portable seismographs were located along this line at intervals of 750-1000 m. Shotpoints were located at intervals ranging from 30 to 40 km. In addition to the linear profile data, three fan shotpoints, located to the south of the recording array, were fired to image deep crustal structures. A subsidiary line acutely transverse to the primary profile in Vermont was recorded at ~3 km spacing by instruments from AFGL and the USGS. A wide-angle reflection experiment was recorded with a modified cross array of 210 instruments recording shots at distances of 0, 70, and 100 km. Instrument spacing in the cross array was 100 meters.

This appendix is a compilation of the data collected by the USGS, AFGL and the GSC. The data have been archived at the National Geophysical Data Center in Boulder, Colorado. Tapes are available from:

U S Department of Commerce

National Oceanic and Atmospheric Administration

325 Broadway

Boulder, CO 80303

(303) 497-6472

## A.2 Background

USGS/GSC investigations of northern Appalachian crustal structure commenced in 1983 with the collection of magnetic, gravity, seismic reflection and seismic refraction data along a transect from southern Quebec across Maine and the Gulf of Maine to the continental slope (Stewart *et al.*, 1986; Murphy and Luetgert, 1986, 1987; Spencer *et al.*, 1989). The seismic refraction/wide-angle reflection experiment described here was initiated to further investigate northern Appalachian structure, the transition to the Grenville province and structure within the southeastern Grenville province. These data provide a partial link between the Quebec-Maine transect and the extensive data collected in the 1986 GLIMPCE experiment in the Great Lakes (Green *et al.*, 1989).

## A.3 Description of the Survey

Portable seismic recorders were laid out along the primary profile in a continuous linear pattern (Figure A.1). A total of 35 shots were fired at 20 locations along the profile (shotpoints 1-20) and at 3 locations south of the profile (Table A.1, Figure A.1). To achieve the total profile length of 650 km, instruments were deployed three times.

The first deployment of 120 USGS instruments and 150 GSC instruments extended from central Maine west to the New Hampshire/Vermont border. Instruments were placed at a nominal spacing of 800 meters. In addition, 31 AFGL portable recorders were placed along the westward extension of the line in upstate New York (Figure A.2).

The second deployment of instruments extended from the New Hampshire/Vermont border to the central Adirondacks at Long Lake, New York State. During this deployment, AFGL instruments and ten of the USGS instruments were located on a subsidiary 150-km-long profile line between SP10 at Lake Champlain and SP22 in southern New Hampshire (Figure A.3).

The third deployment of instruments extended from the central Adirondacks at Long Lake, New York State to Marmora, Ontario. During this deployment, AFGL instruments were located near USGS deployment 2 sites in the eastern Adirondacks (Figure A.4).

A subsidiary high-density wide-angle reflection experiment was recorded by placing USGS and GSC instruments in a Y-shaped array at 100 meter spacing and recording shots at shotpoints 4, 5, and 7 (Figures A.5 and A.6).

Recording instrument and shot point locations and elevations in the United States were determined using USGS 1:24000 and 1:62500 topographic maps. Shot point and instrument locations in Canada were determined using Canadian DEMR 1:50000 topographic maps. All the locations are estimated to be accurate to within 25 meters; elevations within 5 meters.

All shotpoints, except SP20 in Canada, were sited in 20 cm by 45 m drill holes (Table A.1). Ammonium nitrate explosive was detonated by electric caps, detonating cord, and boosters. The cap signal and two time-code signals, WWVB and IRIG-E, were recorded on paper strip-chart records, as described by *Healy et al.* [1982]. The shots were fired automatically and the origin times were read from the cap break on the paper record. The reported

shot times are accurate to within  $\pm 2$  milliseconds, assuming that the explosives detonated at the exact time of the cap break. SP20 was located in an abandoned, water filled quarry near Marmora, Ontario. Explosives were lowered to a depth of 195 m, connected to the surface with detonating cord and fired electrically from the shore. Shot instants are corrected for detonating cord delay.

#### A.4 Instrumentation and Data Reduction

*The Seismic Recorders:* The USGS seismic cassette recorders used in this seismic-refraction survey have been described by *Murphy* [1989]. Each instrument is connected to a Mark Products L4A 2-Hz vertical-component geophone. The signal from this geophone passes through three parallel amplifiers, each with an adjustable gain setting. The three seismic signals plus an internally generated time code (IRIG-E) and a fixed reference frequency are recorded as a multiplexed signal on analog cassette tape. A programmable memory board in each unit allows data to be recorded during ten predetermined time windows. Prior to recording the seismic data, the instrument records a geophone pulse, an amplification step, and 10-Hz sine-wave calibration signals at 1, 10, 100, and 1000 mv. The displacement frequency response curve for the system peaks at about 20 Hz (Figure A.7). Attenuation settings of every instrument have been checked against the calibration signals. Where calibration signals indicated a different dB setting than listed on the field sheets, the correct settings were calculated and entered into the computer. After checking for errors in clock drift and site locations, the analog data were digitized for 50 seconds, starting at (X/8-1) or (X/6-4) seconds prior to shot time, where X is the shot point to recorder distance in km. The sampling rate for digitizing was 200 samples per second.

The PRS-1 system used by the GSC also uses a Mark Products L4A 2-Hz vertical-component geophone. These digitally recording instruments have a total dynamic range of 126 dB. Curves showing displacement versus frequency for this system peak at approximately 17 Hz (Figure A.7). The PRS-1 system records data at a sample rate of 125 samples per second [I. Asudeh, personnel communication, 1987]. Data from these instruments have been resampled at 200 samples per second for merging with other data.

All AFGL data were recorded on automatic gain ranging Terra Technology DCS-302 portable digital cassette seismographs connected to either a Sprengnether Instruments S-6000, 2 Hz triaxial seismometer, or 3 Hall-Sears HS-10-1B, 1Hz seismometers. In standard configuration each DCS-302 recorded 3 channels of data at 100 samples per second with a 30 Hz anti-aliasing filter. Some stations were configured to record at 200 samples per second with a 70 Hz anti-aliasing filter. Calibration pulses for each seismometer were recorded on tape prior to each deployment. Each seismograph also recorded IRIG-H time code from WWVB receivers within each unit. Details of the AFGL instrumentation may be found in *Mangino and Cipar* [1990]. While the AFGL data was recorded with three components, only the vertical component has been used in this report for compatibility with the other data. All three components of the AFGL data may be found in *Mangino and Cipar* [1990].

The clocks of each recording unit were initially synchronized to a GOES master clock via a portable base receiver. Each unit was then deployed with programmable timers to initiate recording over the expected shot time window. After each deployment the GOES time signal was compared to the internal clocks for drift measurement. Most data were time corrected using the GOES data assuming a linear drift rate.

*Data Reduction:* Following the experiment, data from all groups was written in SEG-Y-LDS format and merged into shot gathers. All data have

been resampled (where necessary) to 200 samples per second and header information has been checked for accuracy and consistency.

*Record Sections:* For each shot a trace-normalized record section is presented (Plates 1-8). Since shots from shotpoints 4, 7, 10, 14, 17, 20 and 22 were recorded during multiple deployments, records from these shotpoints are concatenated to form single record sections.

All traces are normalized to their maximum deflection and plotted using reduced time, with a reduction velocity of 7.0 km/s. A few of the shot gathers were recorded in a fan geometry and, although time reduction is calculated using true offset distance, they are plotted versus distance from the endpoint of the recording array. All traces have been bandpass filtered from 2 to 18 Hz to attenuate high frequency noise bursts and ground roll. A few traces which recorded no data have been removed for clarity.

In order to make the record sections (Plates 1-8) easier to analyze, a few traces were deleted in areas where stations were close together or where a noisy trace obscured surrounding data.

## A.5 Description of the Plates

### Plate 1

Shotpoint 1 recorded by AFGL instruments in deployment 1.

Shotpoint 1 recorded by USGS/GSC instruments in deployment 1.

Shotpoint 2 recorded by AFGL instruments in deployment 1.

Shotpoint 2 recorded by USGS/GSC instruments in deployment 1.

Shotpoint 3 recorded by AFGL instruments in deployment 1.

Shotpoint 3 recorded by USGS/GSC instruments in deployment 1.

Shotpoint 4 recorded by AFGL instruments in deployment 1 and

USGS/GSC

instruments in deployments 1 & 2.

### Plate 2

Shotpoint 5 recorded by AFGL instruments in deployment 1.

Shotpoint 5 recorded by USGS/GSC instruments in deployment 1.

Shotpoint 6 recorded by AFGL instruments in deployment 1.

Shotpoint 6 recorded by USGS/GSC instruments in deployment 1.

Shotpoint 7 recorded by AFGL instruments in deployment 1 and  
USGS/GSC

instruments in deployments 1 & 2.

Shotpoint 8 recorded by USGS/GSC instruments in deployment 2.

Shotpoint 9 recorded by USGS/GSC instruments in deployment 2.

### **Plate 3**

Shotpoint 10 recorded by USGS/GSC instruments in deployments 1,2 & 3.

Shotpoint 11 recorded by USGS/GSC instruments in deployment 2.

Shotpoint 12 recorded by USGS/GSC instruments in deployment 2.

Shotpoint 13 recorded by USGS/GSC instruments in deployment 2.

Shotpoint 14 recorded by USGS/GSC instruments in deployments 1,2 & 3.

Shotpoint 14 recorded by AFGL instruments in deployments 1 & 3.

Shotpoint 10 recorded by AFGL instruments in deployments 1 & 3.

### **Plate 4**

Shotpoint 15 recorded by AFGL/USGS/GSC instruments in deployment 3.

Shotpoint 16 recorded by AFGL/USGS/GSC instruments in deployment 3.

Shotpoint 17 recorded by USGS/GSC instruments in deployments 2 & 3.

Shotpoint 18 recorded by AFGL/USGS/GSC instruments in deployment 3.

### **Plate 5**

Shotpoint 19 recorded by AFGL/USGS/GSC instruments in deployment 3.

Shotpoint 20 recorded by USGS/GSC instruments in deployments 2 & 3.

Shotpoint 20 recorded by AFGL instruments in deployment 3.

Shotpoint 21 recorded by USGS/GSC instruments in deployment 2 (fan).

Shotpoint 22 recorded by AFGL/USGS/GSC instruments in deployments 1  
& 2 (fan).

**Plate 6**

Shotpoint 23 recorded by AFGL instruments in deployment 1.

Shotpoint 23 recorded by USGS/GSC instruments in deployment 1 (fan).

Shotpoint 4 recorded by AFGL/USGS instruments in deployment 2 (fan).

Shotpoint 7 recorded by AFGL/USGS instruments in deployment 2 (fan).

Shotpoint 8 recorded by AFGL/USGS instruments in deployment 2 (fan).

Shotpoint 9 recorded by AFGL/USGS instruments in deployment 2 (fan).

Shotpoint 10 recorded by AFGL/USGS instruments in deployment 2.

Shotpoint 11 recorded by AFGL/USGS instruments in deployment 2.

**Plate 7**

Shotpoint 12 recorded by AFGL/USGS instruments in deployment 2.

Shotpoint 13 recorded by AFGL/USGS instruments in deployment 2.

Shotpoint 14 recorded by AFGL/USGS instruments in deployment 2.

Shotpoint 17 recorded by AFGL/USGS instruments in deployment 2.

Shotpoint 20 recorded by AFGL/USGS instruments in deployment 2.

Shotpoint 21 recorded by AFGL/USGS instruments in deployment 2 (fan).

Shotpoint 22 recorded by AFGL/USGS instruments in deployment 2.

**Plate 8**

Shotpoint 4 recorded by USGS/GSC instruments in reflection experiment

Shotpoint 4 recorded by USGS/GSC instruments in reflection experiment  
(fan).

Shotpoint 5 recorded by USGS/GSC instruments in reflection experiment

Shotpoint 5 recorded by USGS/GSC instruments in reflection experiment  
(fan).

Shotpoint 7 recorded by USGS/GSC instruments in reflection experiment

Shotpoint 7 recorded by USGS/GSC instruments in reflection experiment

---

## A.6 Acknowledgments

The authors would like to express their appreciation to the many members of the USGS, GSC and AFGL field crews for their assistance in making the field operations successful.

In addition, we would like to thank the following individuals and institutions for their valuable assistance and cooperation. Mr. Larry Rathman of the SUNY Biological Station; Boise-Cascade Corporation; Whitney Lumber Industries; Mr. Phillip Capone of New York Department of Environmental Conservation; Dr. C. Spencer of the GSC; Dr. P. Young and Dr. C. Thomson of Queen's University at Kingston, Ontario.

Funding for this work has come from the US Geological Survey, the US Air Force Geophysics Laboratory, the Geological Survey of Canada, and the Electric Power Research Institute.

---

**A.7 References**

- Green, A.G., W.F. Cannon, B. Milkereit, D.R. Hutchinson, A. Davidson, J.C. Behrendt, C. Spencer, M.W. Lee, P. Morel-a-l'Huissier, and W.F. Agena, A "GLIMPCE" of the deep crust beneath the Great Lakes, in *Properties and Processes of Earth's Lower Crust*, edited by R.F. Mereu, S. Muller, and D.M. Fountain, Am. Geophys. Un., Washington D.C., Geophysical Monograph 51, 65-80, 1989.
- Mangino, S. and J. Cipar, Data Report for the 1988 Ontario-New York-New England Seismic Refraction Experiment: Three-Component Profiles, Air Force Geophysics Laboratory Open File Report GL-TR-90-0039, 1990.
- Murphy, J.M. and J.H. Luetgert, Data report for the Maine-Quebec cross-strike seismic-refraction profile, *USGS Open-file Report 86-47*, U S Geol. Surv., 1986.
- Murphy, J.M. and J.H. Luetgert, Data report for the Maine-Quebec along-strike seismic-refraction profiles, *USGS Open-file Report 87-133*, U S Geol. Surv., 1987.
- Murphy, J.M., USGS FM cassette seismic-refraction recording system, *USGS Open-file Report 88-570*, U S Geol. Surv., 1989.
- Spencer C., A. Green, P. Morel-a-l'Huissier, B. Milkereit, J.H. Luetgert, D.B. Stewart, J.D. Unger, and J.D. Phillips, The extension of the Grenville basement beneath the Northern Appalachians: results from the Quebec-Maine Seismic reflection and refraction surveys, *Tectonics*, 8, 677-696, 1989.
- Spencer C., A. Green, and J.H. Luetgert, More seismic evidence on the location of the Grenville basement beneath the Appalachians of Quebec-Maine, *Geophys. J. R. Astron. Soc.*, 89, 177-182, 1987.
- Stewart D.B., J.D. Unger, J.D. Phillips, R. Goldsmith, W.H. Poole, C.P. Spencer, A.G. Green, M.C. Loiselle, P. St-Julien, The Quebec-Western Maine Seismic Reflection Profile: Setting and first year

results, in *Reflection Seismology: The Continental Crust*. *Geodyn.* 14, edited by M. Barazangi and L.D. Brown, pp. 189-199, AGU, Washington, D.C., 1986.

## A.8 Captions

### Table A.1: Master Shot List

**Figure A.1:** Shotpoints Fired During the Experiment

**Figure A.2:** Recording Sites and Shotpoints for Deployment 1

**Figure A.3:** Recording Sites and Shotpoints for Deployment 2

**Figure A.4:** Recording Sites and Shotpoints for Deployment 3

**Figure A.5:** The High Density, Wide-Angle Reflection Experiment

**Figure A.6:** Recording Sites for Reflection Experiment

**Figure A.7:** Response Curves for Instruments

A.9 Table

Shot No.	Shot Point	Date	Shot Time Day:Hr:Mn:Sec	Size (kg)	Latitude (deg, min)	Longitude (deg, min)	Elev. (m)
1	2	1988/9/16	261:04:00:00.006	1011.5	44 33.795N	70 02.672W	122
2	5	1988/9/16	261:04:02:00.009	997.9	44 20.173N	71 23.098W	516
3	7	1988/9/16	261:04:04:00.006	1224.7	44 10.708N	72 14.192W	460
4	22	1988/9/16	261:04:06:00.008	907.2	43 14.165N	71 51.534W	325
5	14	1988/9/16	261:04:08:00.006	1360.8	43 59.969N	74 29.266W	530
6	6	1988/9/16	261:06:00:00.006	907.2	44 16.857N	71 49.785W	329
7	4	1988/9/16	261:06:02:00.010	986.6	44 24.686N	70 58.175W	317
8	1	1988/9/16	261:06:04:00.006	2091.1	44 35.409N	69 44.766W	95
9	3	1988/9/16	261:08:00:00.011	1020.6	44 27.537N	70 31.360W	277
10	23	1988/9/16	261:08:02:00.010	1029.7	43 26.947N	70 40.309W	79
11	10	1988/9/16	261:08:04:00.010	1360.8	44 03.217N	73 23.188W	35
12	4	1988/9/19	264:19:00:00.011	476.3	44 24.686N	70 58.175W	317
13	7	1988/9/19	264:19:04:00.006	158.8	44 10.708N	72 14.192W	460
14	5	1988/9/19	264:20:02:00.007	340.2	44 20.173N	71 23.098W	516
15	8	1988/9/23	268:04:00:00.009	907.2	44 09.047N	72 34.595W	433
16	9	1988/9/23	268:04:02:00.006	907.2	44 04.409N	72 55.955W	671
17	12	1988/9/23	268:04:04:00.007	952.5	43 56.259N	73 58.960W	535
18	22	1988/9/23	268:04:06:00.007	907.2	43 14.165N	71 51.534W	325
19	20	1988/9/23	268:04:07:59.970	1360.8	44 28.661N	77 39.485W	0
20	7	1988/9/23	268:06:00:00.009	1224.7	44 10.708N	72 14.192W	460
21	17	1988/9/23	268:06:02:00.010	1156.7	44 17.825N	75 55.547W	94
22	13	1988/9/23	268:06:04:00.007	1043.3	43 58.078N	74 15.689W	524
23	10	1988/9/23	268:06:06:00.006	907.2	44 03.217N	73 23.188W	35
24	14	1988/9/23	268:08:00:00.007	1247.2	43 59.969N	74 29.266W	530
25	11	1988/9/23	268:08:02:00.006	975.2	43 59.532N	73 39.668W	287
26	21	1988/9/23	268:08:04:00.007	907.2	43 03.415N	72 56.287W	710
27	4	1988/9/23	268:08:06:00.011	1224.7	44 24.686N	70 58.175W	317
28	20	1988/9/29	274:03:59:59.969	907.2	44 28.661N	77 39.485W	0
29	18	1988/9/29	274:04:01:59.990	907.2	44 21.156N	76 41.066W	143
30	17	1988/9/29	274:04:04:00.009	272.2	44 17.825N	75 55.547W	94
31	14	1988/9/29	274:04:06:00.010	1134.0	43 59.969N	74 29.266W	530
32	19	1988/9/29	274:05:59:59.996	907.2	44 25.211N	77 09.508W	180
33	16	1988/9/29	274:06:02:00.007	884.5	44 14.635N	75 31.696W	175
34	15	1988/9/29	274:06:04:00.006	816.5	44 09.337N	75 00.946W	427
35	10	1988/9/29	274:06:06:00.005	1360.8	44 03.217N	73 23.188W	35

Table A.1

A.10 Figures

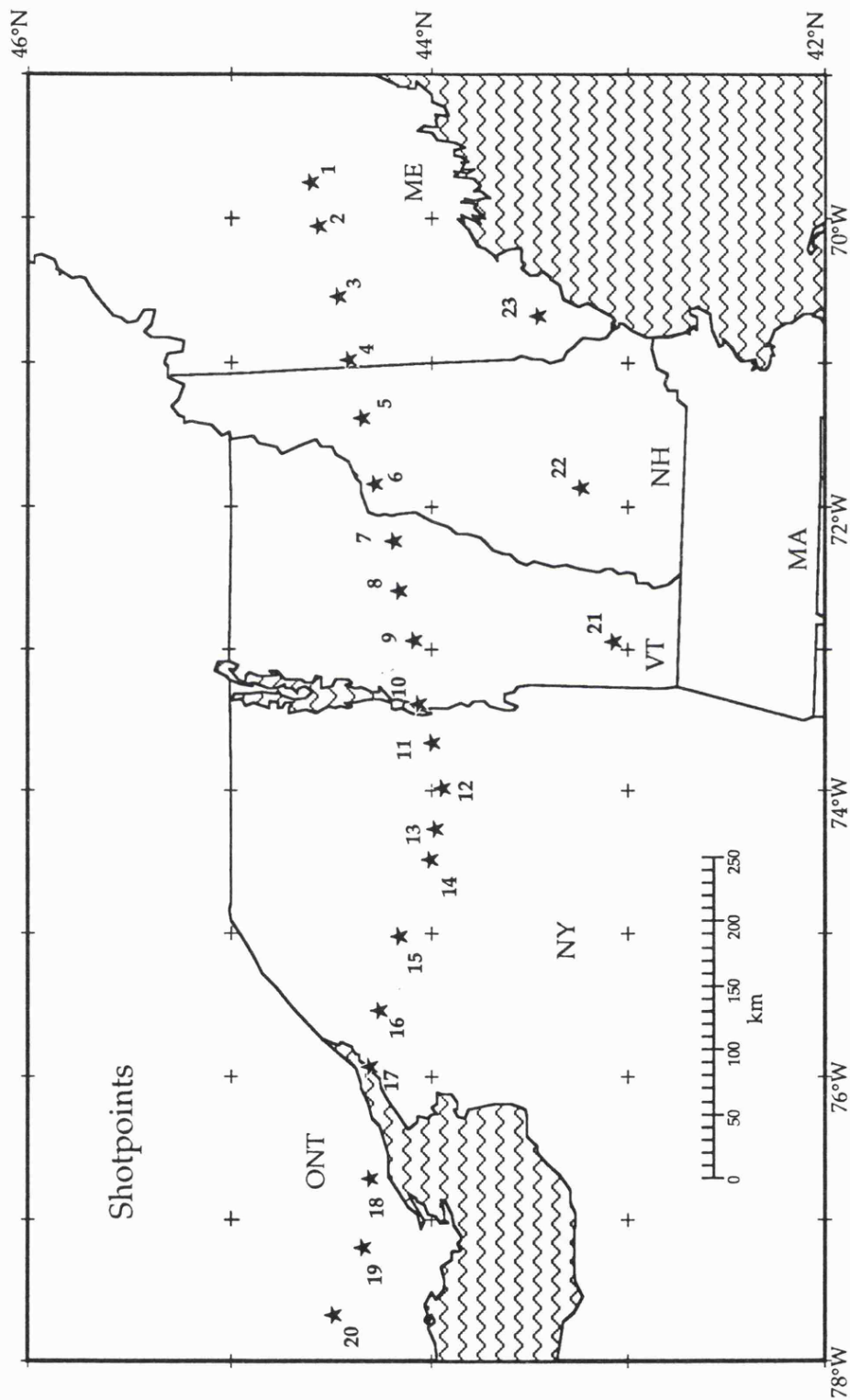


Figure A.1

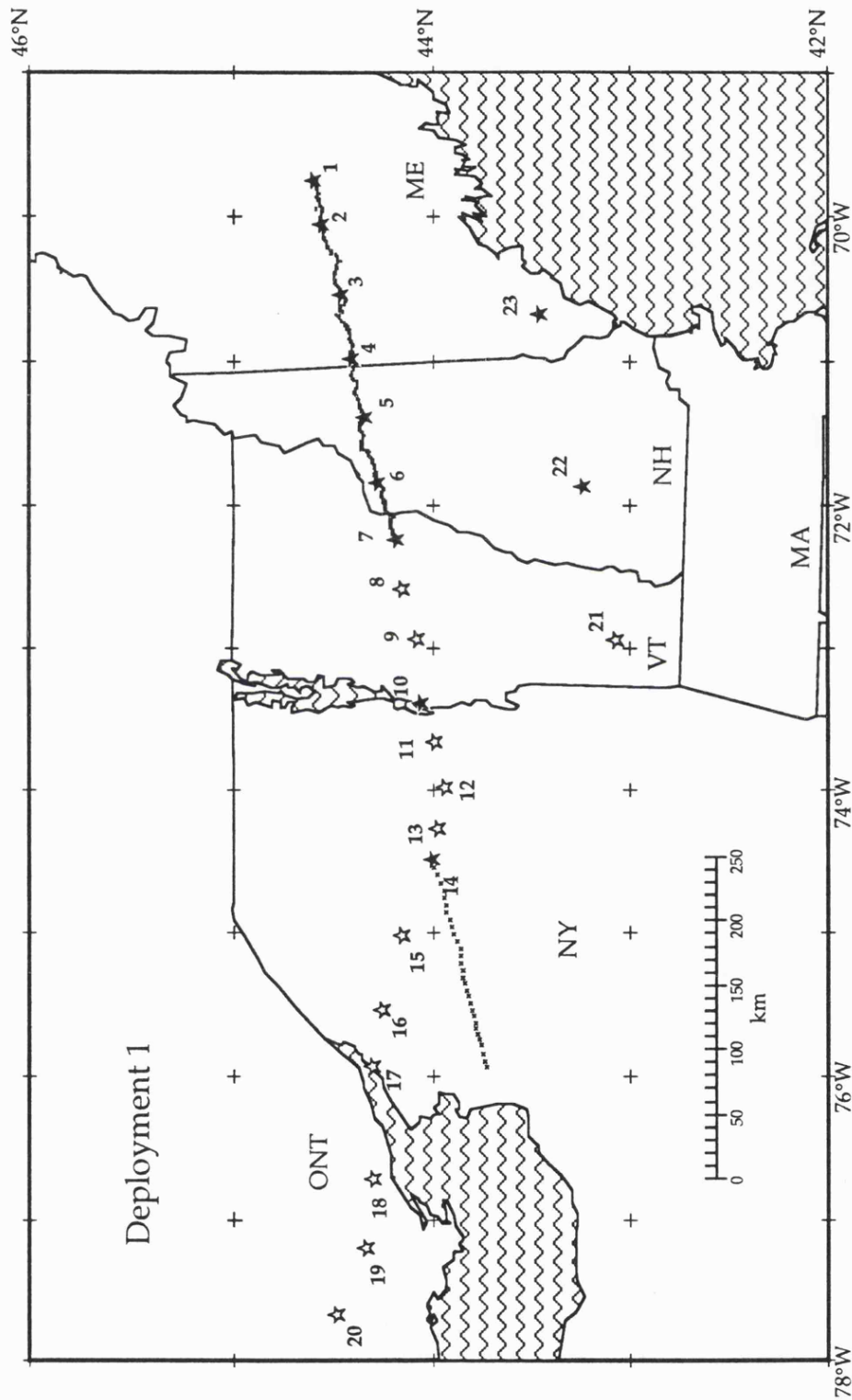


Figure A.2

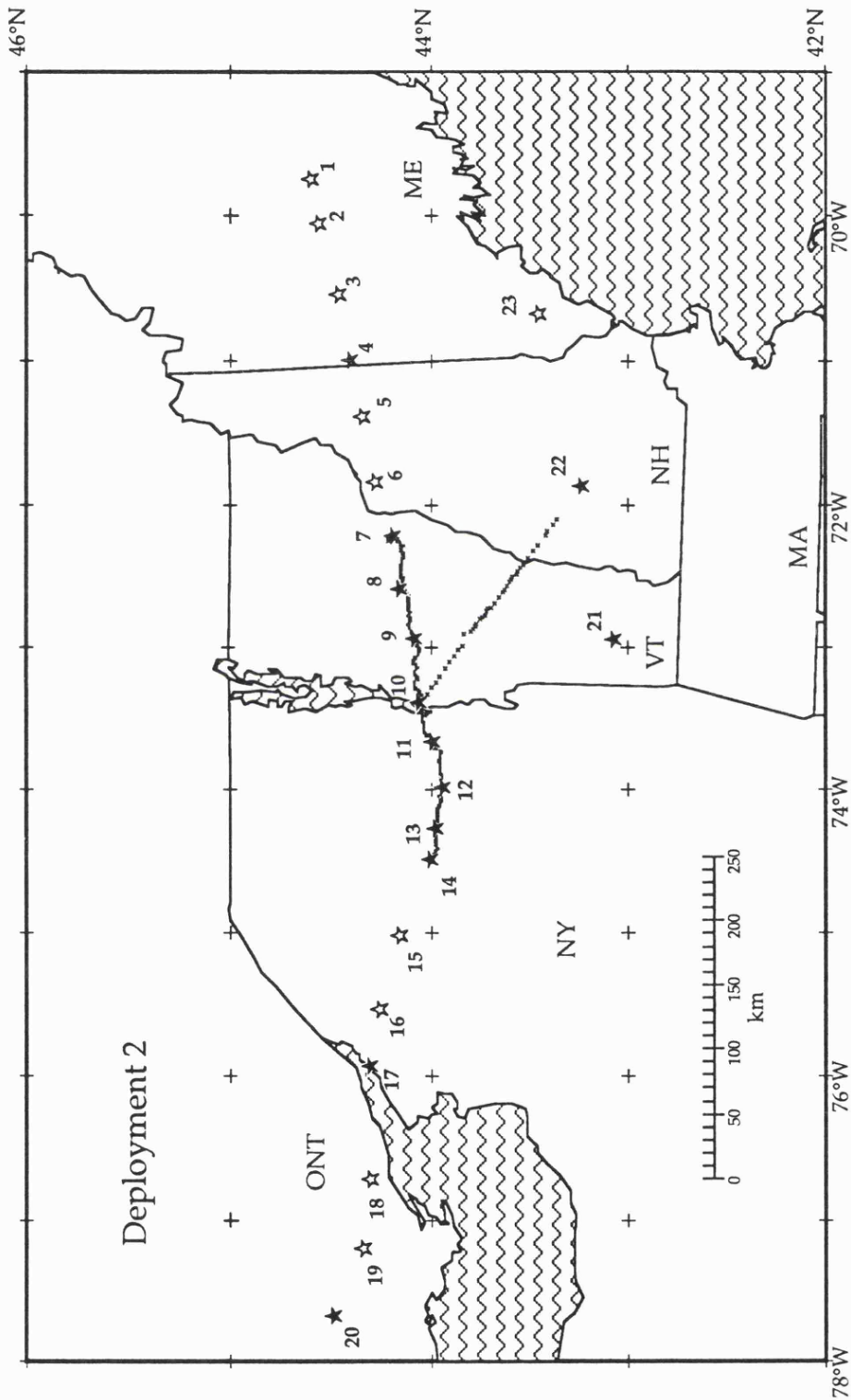


Figure A.3

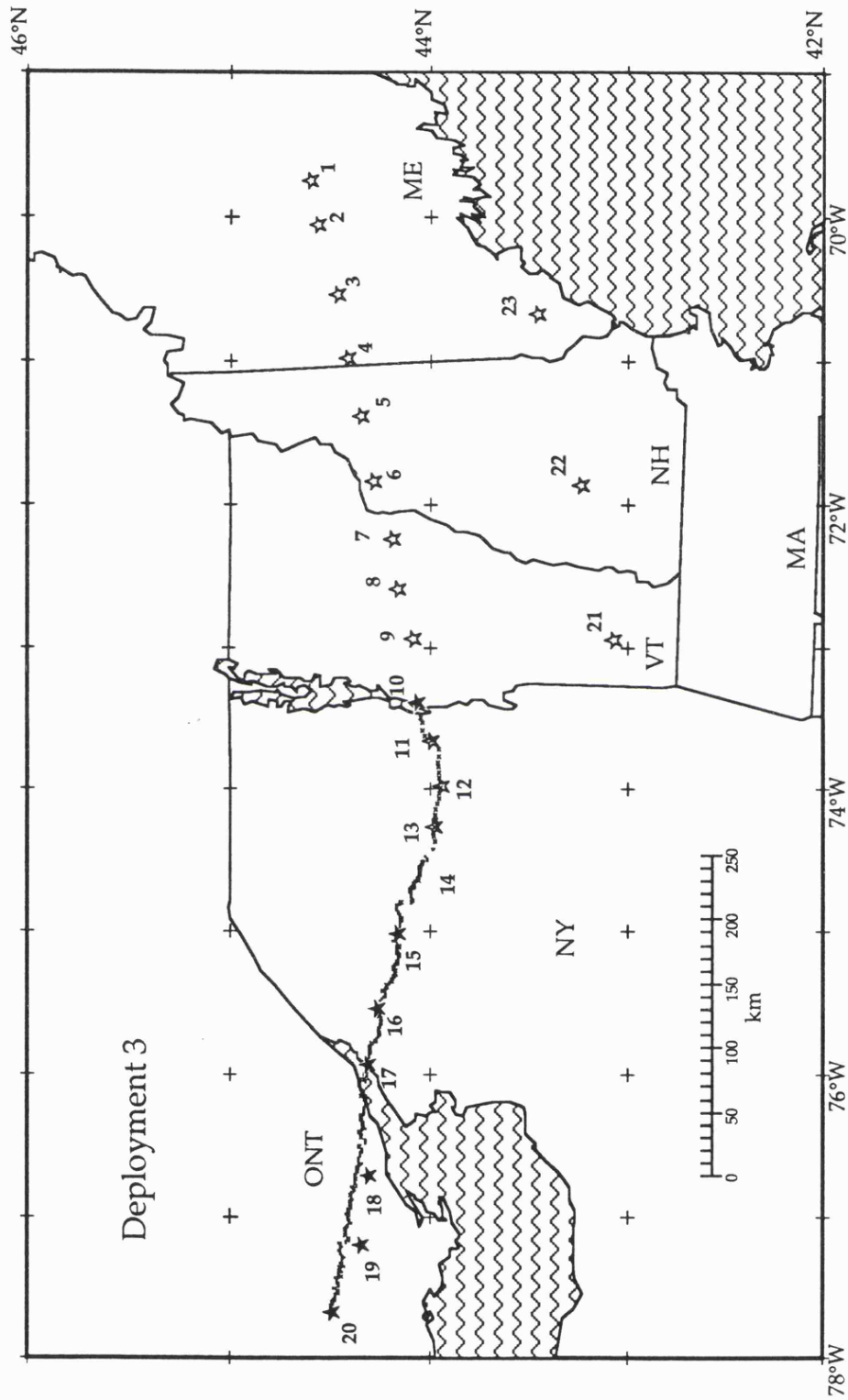


Figure A.4

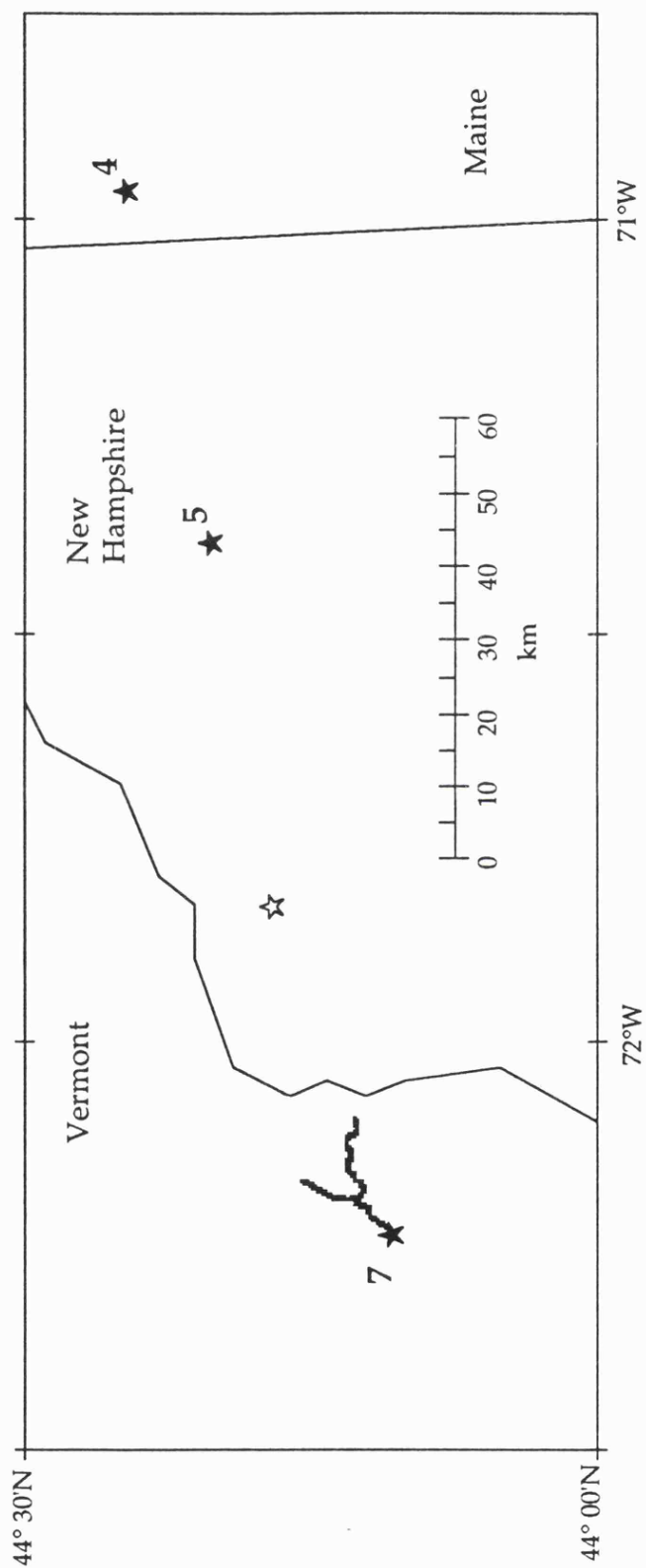


Figure A.5

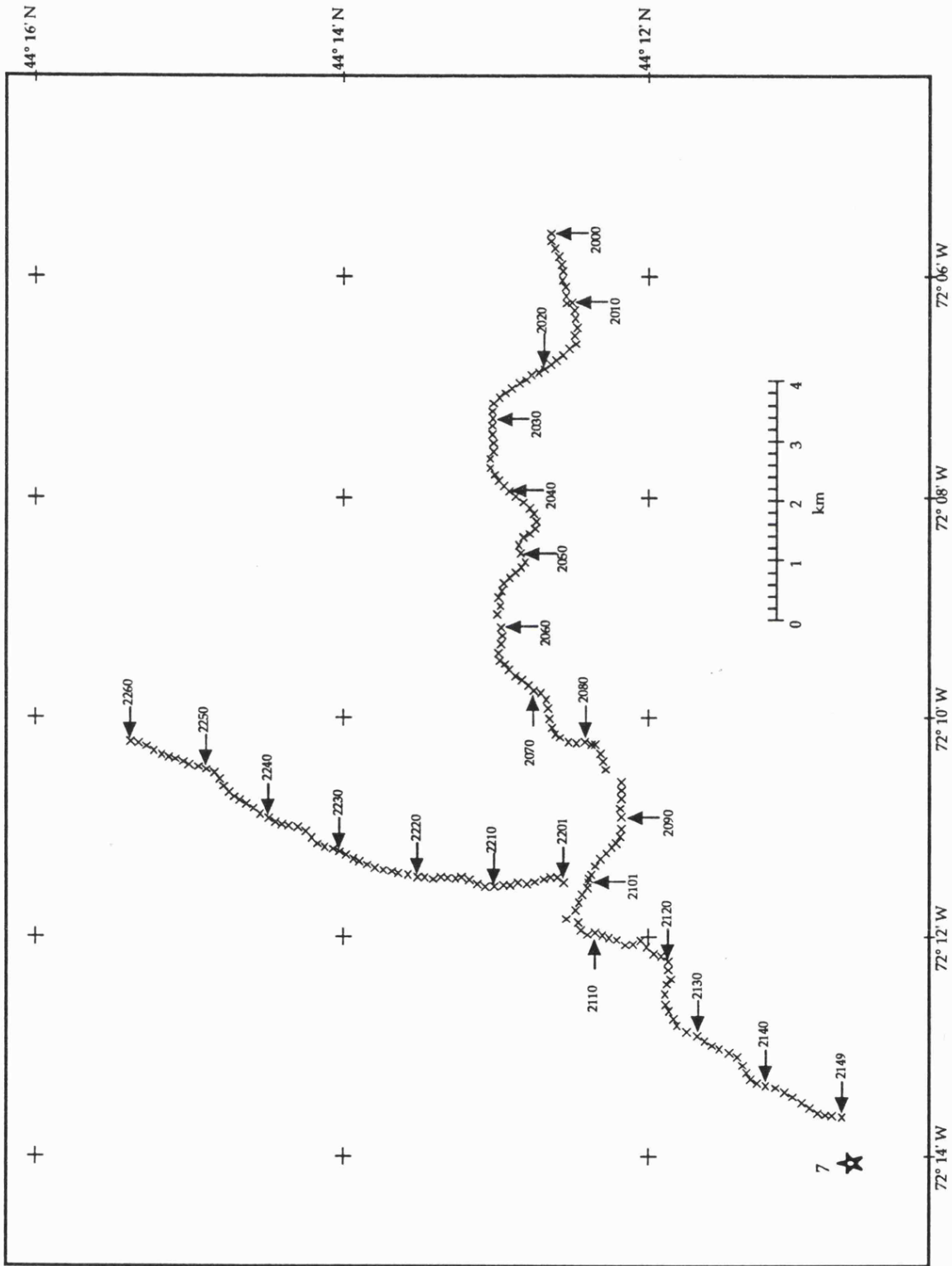


Figure A.6

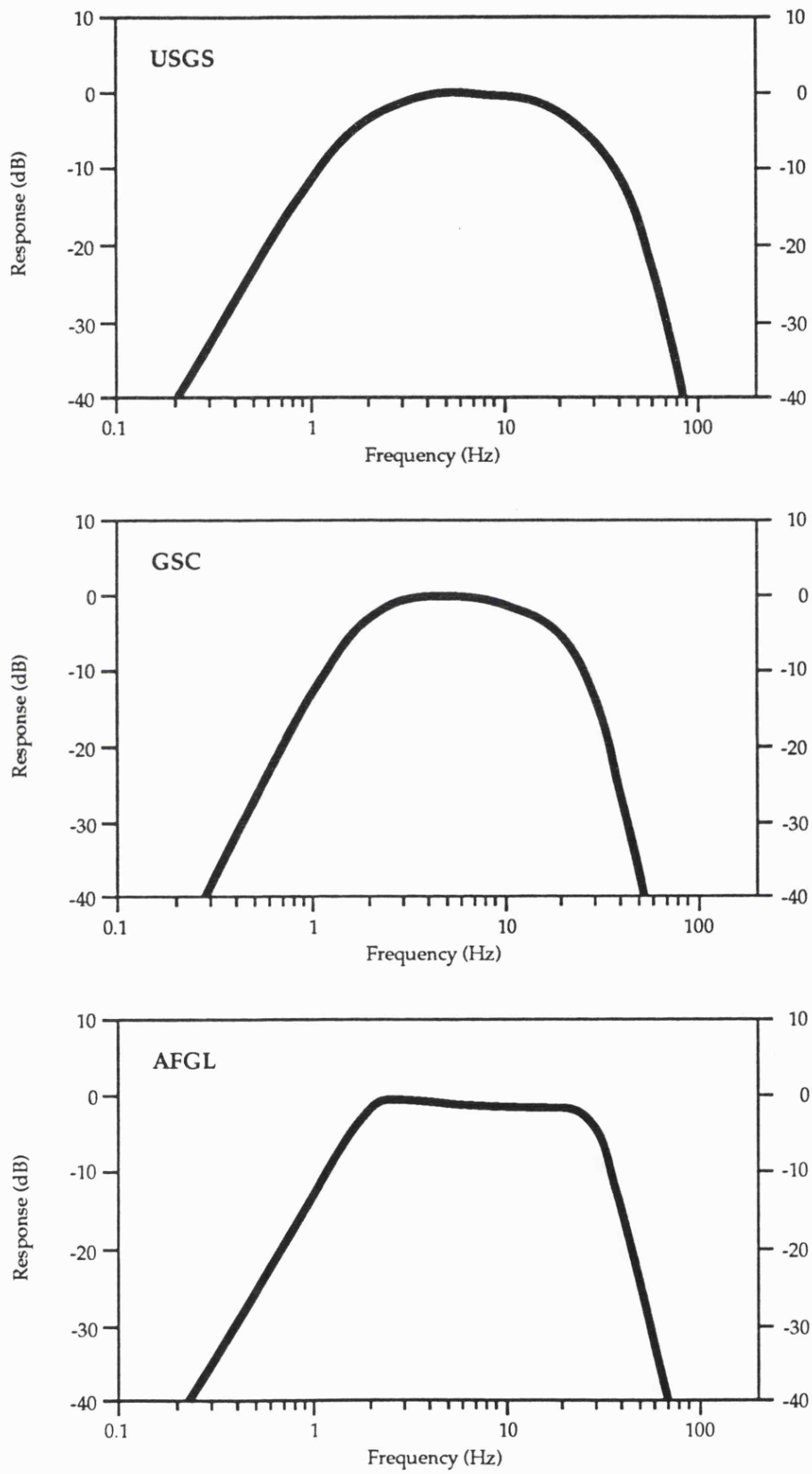


Figure A.7

# -B-

---

## **Travel Time Modeling of Seismic Refraction/Wide-Angle Reflection Data: Forward and Inverse Methods**

### **B.1 Introduction**

The seismic refraction/wide-angle reflection data used in this thesis were analyzed by a variety of travel time and synthetic amplitude algorithms that attempt to replicate the physical properties of the Earth's crust through the construction of numerical models in the computer. At the core of the analysis procedure lies an appreciation of forward and inverse methodologies. In the forward method the theoretical response of a model is calculated and compared with the observed data. Model convergence is obtained through trial and error iterative modeling. In the inverse method an estimation of the theoretical Earth model is sought directly from the observed data by minimizing the discrepancy between the theoretical and observed data sets. The forward step is used as a precursor to the inversion to enable the appropriate model adjustments to be calculated. Since neither forward nor inverse methods can provide a definitive assessment of the Earth's structure these methods were used in tandem to construct a 'best fitting' model.

## **B.2 Assumptions and Restrictions**

The interpretation of seismic refraction/wide-angle reflection data is non-intuitive. The seismic wave field is a complicated amalgamation of refracted, reflected, multiple and scattered energy which inhibits the interpreter from extracting information directly from the record sections. It is for this reason that a number of assumptions are made to minimize the complexity of the interpretation and subsequent computational analysis. The fundamental assumption underlying nearly all analyses of seismic data is that the Earth is composed of a series of planar sub-horizontal layers. On a macroscopic scale this assumption appears reasonable, but clearly in areas of complex geology such as at plate margins, or in fold-thrust belts this assumption is not valid. In this regard the importance of incorporating geologic observations into the modeling procedure can not be over stressed. It is assumed that the seismic energy is contained within a vertical plane, and correspondingly the interpretation is limited to two-dimensional features. Lateral velocity variations are assumed to be smaller than vertical variations in the Earth's structure.

## **B.3 Reduction of the Seismic Data**

Computational analysis of seismic refraction/wide-angle reflection data requires that the wave field data is reduced to a series of distance/travel time picks. Correct identification and correlation of individual seismic phases on the record sections is of primary importance. Factors affecting the correct identification of seismic phases include the signal to noise ratio (ambient noise), spatial sampling (signal coherency), and multiple/converted phases which can obscure the primary seismic phase. These factors all contribute a significant bias to the analysis; a mis-identified or incorrectly correlated phase will result in a poorly constrained velocity model (Mooney, 1989).

It is vital to obtain an overview of the entire data set before attempting to pick the travel time data. Phase identification is enhanced by applying a reduction velocity to the record sections that maximizes the angular separation between phases with apparent velocities corresponding to the reduction velocity. A travel time pick is made either at the peak amplitude, or at the maximum change in gradient as the seismic energy arrives at the receiver. In either case the same point on a particular phase must be picked throughout. Reciprocal travel times are used to constrain the travel time correlations for overlapping shot gathers.

#### **B.4 The Forward Method - Iterative Ray Trace Modeling**

In the forward method the interpreter constructs a velocity model through which rays are propagated in order to calculate the theoretical response of a particular model parameterization. The seismic velocity model is composed of a series of velocity layers each of which relate to a phase(s) on the record sections. The model parameterization is adjusted until the theoretical response matches the observed phase. The seismic velocity model presented in chapter one was derived using ray trace forward modeling (Cerveny *et al.*, 1977; Luetgert, 1988).

*Model Parameterization:* The seismic velocity model is constructed from a series of parameter nodes which specify the velocity and interface at a given point in the model. An interface is built up of a series of linked linear segments which traverse the model. Layers are constructed from successive pairs of interfaces, which enclose a series of isotropic velocity trapezoids. Each layer must extend fully across the model. Vertical interfaces can not be readily included in the model. The velocity must be continuous within any layer, but interfaces may 'pinch out' to describe lateral velocity discontinuities. Step or gradational velocity discontinuities may occur at the interfaces. At any point in the seismic velocity model, the velocity is

given by a linear combination of the four adjacent velocity nodes (Figure B.1a).

*The Raytrace Algorithm:* Once the seismic velocity model is parameterized rays are propagated from a specified source location in the model to estimate the travel time of a particular seismic phase. A ray is traced from its source through the model by means of a series of discrete linear steps which add up to produce a ray path. For any given point in the velocity field the direction of ray propagation is a function of the angle of incidence and the gradient of the velocity field. Thus, because the seismic velocity model is known, the direction of propagation can be calculated. The ray trace algorithm calculates the propagation of rays within a layer by stepwise integration of the system of first order differential equations,

$$\begin{aligned}\frac{dX(t)}{dt} &= V(x,z)\sin(\phi) \\ \frac{dZ(t)}{dt} &= V(x,z)\cos(\phi) \\ \frac{d\phi(t)}{dt} &= \frac{dV}{dx}\cos(\phi) - \frac{dV}{dz}\sin(\phi)\end{aligned}$$

where,  $\phi$  is the ray's angle from the vertical and  $z$  is positive downwards (Figure B.1a).

The total travel time along a ray path is calculated by summing each incremental step through the velocity model. The precision of the calculated travel time is dependent upon the size of the integration step, and the gradient of the velocity field. Large integration steps through areas of high seismic gradients result in imprecise travel time calculations because the ray path will be composed of a limited number of linear segments, which poorly approximate the curved trajectory of the 'real' ray. The integration step must be adjusted in accordance with the parameterization of the model, and the desired numerical precision (Luetgert, 1988).

The propagation of the ray through the velocity model is controlled by a numerical ray code which specifies the sequence of layers through which the ray travels. When the ray encounters an interface the ray code is referred to in order to decide whether the ray should be refracted or reflected through the interface. In either case Snell's law is applied to calculate the angle of refraction or reflection through the interface (Figure B.1b). The stepwise integration continues along the new propagation direction until a new interface is encountered and the process is repeated. The ray is terminated if it leaves the model boundaries, or if it has returned to the surface.

*Errors and Model Uniqueness:* Estimates of relative errors may be achieved by applying a series of perturbations to the model parameters, and comparing the perturbed model with the 'final' model. This procedure is inherent in the modeling process, so that the interpreter often has a very thorough knowledge of the possible bounds on his model, and a sense of the uniqueness of his particular model parameterization. Nevertheless, it is extremely difficult to estimate absolute errors in depth to interfaces and layer velocities. Sources of error that are difficult to quantify include (1) a mis-identified phase, (2) non two-dimensional features, (3) assuming a straight line for the receiver geometry, (4) using an inappropriate model parameterization, and (5) using a homogeneous isotropic velocity model to represent a complex heterogeneous structure. Amplitude modeling can often provide enhanced constraint on the vertical seismic gradients within a layer, and on the magnitude of velocity discontinuities at interfaces (McMechan and Mooney, 1980).

A useful means of illustrating the uniqueness of a particular model parameterization is to apply a series of perturbations to the final velocity model. In this manner the bounds on a particular interface position or velocity specification may be estimated by comparing the final model with

the perturbed model. Important features of the perturbed model which must be considered include; (1) travel time fits to lie within  $\pm 0.1$  s for the upper crust, (2) ray propagation and (3) physical and geologic properties of the perturbed model. In the following example an estimate of the uniqueness of the Grenvillian Ramp structure, discussed in chapter 1, is sought by applying a series of 'end-member' perturbations to the model to place constraints on the velocity structure of this interface. The perturbed models illustrated in the following discussion should be compared to Figure B.2 which shows the final model for the Grenvillian Ramp and uses shotpoints 11 and 8 to illustrate the reversed ray-coverage (note, Figure B.2 replicates Figure 1.11 and is shown here for comparison purposes). These shotpoints were chosen as representative examples of the ray-coverage obtained for the ramp structure, but it must be emphasized that the final model utilizes information from all the shotpoints traversing the Grenvillian-Appalachian boundary. The Grenvillian Ramp structure is modeled as a planar velocity interface which dips eastwards at  $15^\circ$ . The upper edge of this dipping velocity interface is labeled 'Hinge' on the velocity model, and may be correlated with an apparent velocity transition observed on the seismic travel time data (see chapter 1). The lateral position of the ramp is explored first by considering a dipping interface parallel to the Grenvillian Ramp but displaced 10 km either side of the final model. Following this analysis the dipping geometry of the ramp structure is explored by pivoting the final model by  $+10^\circ$  and  $-5^\circ$  about the 'Hinge' point. These model perturbations will be investigated by a series of velocity models each with a discrete dipping interface referred to as Ramp 1 to 4, respectively. Discussion concerning the laminated structure of the ramp is focused upon a series of reflections observed on the seismic record sections.

*The Lateral Position of the Grenvillian Ramp Structure:* A lateral velocity transition is indicated by the seismic data in the vicinity of receiver

number 510 and may be correlated across individual record sections to within 5 km, or 6 seismic traces at an average station spacing of 800 m (see Appendix A). This receiver position fixes the location of the velocity transition in the uppermost layer of the velocity model, and is marked 'Hinge' on Figure B.2. Reversed ray coverage in the upper crust provides further constraint on the position of the 'Hinge' in the velocity model. In the following two examples deviations of  $\pm 10$  km in the position of the ramp structure are shown to produce unacceptably large mislocations of the velocity transition.

*Ramp 1:* Consider a dipping velocity interface parallel to the Grenvillian Ramp but displaced 10 km to the east. Let this dipping velocity interface be denoted Ramp 1 as shown in Figure B.3a. For shotpoints west of Ramp 1 (*i.e.*, Shotpoint 11) the 'Hinge' point is mislocated to model coordinate 20 km, or approximately 10 km east of its position in the final model (Figure B.3a). Furthermore, rays propagate through a greater volume of the 6.6 km/s Grenvillian crust, so that travel times are advanced by up to 0.1 seconds (Figure B.3a). For progressively larger eastward displacements of the ramp the travel time mis-match is increased. For shotpoints east of Ramp 1 (*i.e.*, Shotpoint 8) rays propagate through the Appalachian crust and successfully fit the travel time data up to the position of Ramp 1. However, once rays are refracted through the 6.6 km/s Grenvillian crust the calculated travel times are advanced by 0.1 seconds, corresponding to the eastward displacement of the ramp (Figure B.3b). Because Ramp 1 is displaced eastwards (closer to shotpoint 8) the crossover from the Appalachian arrival branch to the Grenvillian branch is mislocated 10 km to the east.

*Ramp 2:* Considering the case where the ramp structure is displaced 10 km to the west of the Grenvillian ramp, travel times are systematically delayed and the 'Hinge' is mislocated in the opposite sense to that of Ramp 1. For shotpoints west of Ramp 2 (*i.e.*, Shotpoint 11), rays propagate through

a greater volume of the low velocity 6.0 km/s Appalachian crust, so that calculated travel times are delayed relative to the seismic data. Moreover, the position of the velocity transition from the 6.6 km/s crust to the 6.0 km/s crust is mislocated 10 km to the west (Figure B.3c). For shotpoint 8 calculated travel times are delayed by 0.1 seconds for rays refracted through Ramp 2. Displacing the ramp 10 km to the west introduces a further problem in terms of propagating rays through the model. For Ramp 2 refracted arrivals from shotpoint 8 cannot be fitted at offsets close to the 'Hinge' (model coordinates -10 to 10 km). This is because rays cannot be refracted through Ramp 2 and return back to the surface without introducing unrealistically high seismic velocity gradients (see 'travel time gap' in Figure B.3d).

The planar geometry of the ramp is controlled by shotpoints at successively larger offsets which provide reversed ray-coverage for successively deeper portions of the ramp. Shotpoints east of the 'Hinge' provide ray-coverage for discrete portions of the velocity interface (e.g., shotpoint 8 controls the interface between 8-10 km depth). Specifically, shotpoint 9 controls the geometry of the upper portion of the ramp between 4-6 km depth, and necessitates that the ramp structure forms a 'sharp' corner below the point marked 'Hinge'. This corner feature of the model is reversed by shotpoints to the west of the 'Hinge' (Figure B.2a). However, the 'sharp' corner modeled below the 'Hinge' results in a 'travel time gap' where rays are unable to bend through the Ramp as shown in Figure B.3d. The model parameterization selected for the Grenvillian Ramp is based upon a summation of information from all the shotpoints, and necessitates that a 'trade-off' is made between the precision of the travel time fits and the ability to propagate rays to all travel time observations.

Displacing the ramp structure by 10 km to the west or east degrades the travel time fits by up to 0.1 seconds, and furthermore mislocates the

position of the lateral velocity transition observed on the seismic record sections. The location of the velocity transition on the seismic record sections is replicated by travel time modeling which shows that the 'Hinge' point marked on Figure B.2 is a fully reversed feature of the velocity model. Given that the 'Hinge' point may be located with confidence to  $\pm 5$  km the dipping geometry of the ramp structure must be considered with respect to the 'Hinge' point as a pivot through which the dipping interface may rotate.

*The Dipping Geometry of the Grenvillian Ramp Structure:* For the general case of a dipping refractor, the apparent velocity of the refracted arrival branch is lower than the refraction velocity for rays propagating down dip, and higher than the refraction velocity for rays propagating up dip. Thus, for increasing refractor dip, the apparent velocity of rays propagating down dip will show a corresponding decrease. This effect controls the apparent velocity of the refracted arrivals through the Grenvillian Ramp structure as discussed below.

*Ramp 3:* Consider the case where the velocity interface is more steeply dipping than the Grenvillian Ramp structure. Figure B.4a shows Ramp 3 which dips eastwards at  $25^\circ$  from its uppermost edge labeled 'Hinge'. In this model the 'Hinge' point is located correctly at the position of receiver 510, so that rays which propagate through the upper 2-3 km of the crust successfully fit the observed velocity transition (Figure B.4a). For shotpoints west of Ramp 3 where rays propagate down dip, the apparent velocity of the arrivals refracted through Ramp 3 is decreased relative to the final model because of the increased dip of this interface (Figure B.4a). This is due to the longer travel time paths for rays which propagate through the deeper portions of Ramp 3 (greater than 5 km depth), resulting in longer travel times and consequently a delay in the refracted arrival times. A similar travel time delay is observed for shotpoints east of Ramp 3 (Figure B.4b).

*Ramp 4*: The alternate case where the velocity interface is less steeply dipping than the Grenvillian Ramp structure is illustrated by Ramp 4 which dips at  $10^\circ$  from the 'Hinge' point. For shotpoints west of Ramp 4, rays propagate down a less steeply dipping interface, so that the apparent velocity of the arrivals refracted through Ramp 4 is increased relative to that calculated for the Grenvillian Ramp structure (Figure B.4c). This is due to the shorter travel time paths for rays which propagate through the deeper portions of Ramp 4 (greater than 5 km depth), resulting in shorter travel times and consequently an advance in the refracted arrival times. A similar travel time advance is observed for shotpoints east of Ramp 4 (Figure B.4d).

The detailed forwarding modeling performed for the Grenvillian Ramp structure illustrates that this velocity boundary is a well constrained and fully reversed feature of the upper crust. Data redundancy provided by reversing shot gathers (shotpoints 14 through 7) across the Grenvillian-Appalachian boundary permits a seismic interface to be located to within  $\pm 5$  km in the velocity model at the point labeled 'Hinge'. Lateral displacements of the Grenvillian Ramp structure of 10 km produce calculated travel time mis-matches in excess of 0.1 seconds, which lies beyond the range of acceptable travel time fits. The dip of the ramp structure is less precisely resolved but is unlikely to lie outside of  $\pm 5^\circ$  of the final model, with a maximum permissible variation in the dipping geometry of  $\pm 10^\circ$ . The  $15^\circ$  eastward dipping geometry of the ramp structure is essential to permit rays to be propagated through the velocity model with the observed apparent velocities. Ray-coverage is limited at depths greater than 15 km so that the portion of the dipping velocity interface which soles out at 25 km depth is least well constrained. The Grenvillian Ramp structure discussed in chapter 1 produces travel time fits which lie within  $\pm 0.1$  seconds of the observed seismic data. Thus, the Grenvillian ramp

structure produces a quantitatively superior travel time fit to the seismic data than any of the perturbed models discussed above.

*Internal Structure of the Grenvillian Ramp Structure:* The internal velocity structure of the Grenvillian/Appalachian boundary is not readily resolved with regional-scale seismic refraction data such as collected by the Ontario-New York-New England seismic refraction/wide-angle reflection experiment. Indications of a complex laminated velocity structure at the edge of the Grenvillian craton are strongly implied by wide-angle reflections observed on shotpoints immediately east of the Grenvillian Ramp structure (see Figure B.2b). Reflections in the vicinity of the Grenvillian ramp are characterized by short en-echelon segments with high apparent velocities (e.g. Figure 1.10). These reflection segments are of insufficient lateral continuity to permit them to be correlated between adjacent shot gathers, suggesting that they are localized features which cannot be readily delineated by ray trace techniques. The incorporation of such localized and discrete reflection events into the velocity model is not justified because they produce a negligible effect upon the travel time paths of the 1-km-wavelength seismic sources used in this study. The ray trace modeling performed on the Ontario-New York-New England seismic refraction/wide-angle reflection data was used to derive a first-order velocity model which replicates the gross petro-physical properties of the crust. Geologic interpretations of the Grenvillian Ramp however are not restricted to the idiosyncrasies of the ray-method and may include the reflection segments as evidence for a complex imbricated structural detachment at the edge of the Grenvillian craton. The most likely cause of these wide-angle reflection segments is a series of alternating velocity lamellae such as might be produced by mylonite zones in the Green Mountain Anticlinorium.

*Practical Application:* It is often impossible to fit all the features of the seismic data with equal weight. The interpreter must prioritize the quality

of his fits (*i.e.* it is more important to fit critical reflections than post critical reflections). In addition the interpreter must decide upon a 'cut-off' point at which modeling stops, this is a highly subjective decision. The interpreter must decide upon the quality of his travel time picks, and make a subjective assessment of which parts of the model are well constrained by the data. A perfect fit to all the phases observed on the record section is impossible because the seismic wave field contains many non two-dimensional features.

The forward method allows the interpreter to inject intuition, experience and a fair amount of common sense into the interpretation process. Known geologic and geophysical constraints may readily be entered into the model. However, the interpreter's methodology and pre-conceived notions create an a priori subjectivity inherent in the forward modeling procedure. In practice raytrace forward modeling is a laborious and tedious task which is compounded by the inherent subjectivity of the method.

### **B.5 The Inverse Method - Linearized Travel Time Inversion**

Seismic travel time inversions seek to minimize the discrepancy between the observed travel time data and the theoretical travel times obtained via the seismic velocity model. Because of the non-linearity of the seismic travel time problem a starting model and iterative approach is required to optimize the seismic velocity model. The inversion scheme used in chapter two utilizes a least squares technique to update the velocity model following a forward step which utilizes an adapted ray trace algorithm (Zelt and Smith, 1992). Least squares inversion algorithms are suitable for the inversion of seismic travel time data because of their robustness when dealing with imperfect and incomplete data sets (Lines and Treitel, 1984).

*Least Squares Inversion Theory:* Travel time is a non-linear function of seismic velocity. In this case, the dependent travel time variable,  $t$  is functionally related to the independent velocity variable,  $V$ .

$$t = f(V)$$

The first step in the least squares travel time inversion is to linearize the velocity function. Travel time,  $t$  can be linearized by using the Taylor Series Expansion,

$$t = f(V_0) + f'(V_0)dv + 1/2f''(V_0)dv^2 + \text{higher order terms}$$

where,

$$f'(V_0) = \partial V_0 / \partial t$$

We can neglect second order and higher terms because an iterative approach is used to optimize the velocity model. Hence,

$$t \approx f(V_0) + f'(V_0)dv$$

Where,

$t_0$  is the theoretical travel time calculated through the starting velocity,  $V_0$ . Substituting  $t_0 = f(V_0)$  and rearranging we get,

$$t - t_0 \approx f'(V_0)dv$$

Now we can define the travel time residual,  $r$  as the difference between the observed travel time,  $t$  and the calculated travel time,  $t_0$ , so that,

$$r \approx f'(V_0)dv$$

This is the least squares equation. By minimizing,  $r$  with respect to the starting model,  $V_0$  we can optimize the velocity model.

The general principle which lies behind a least squares inversion is shown in Figure B.6. In this simplified example we consider a starting model which has been parameterized with the value,  $V_0$ . Rays are then traced through the starting model as in the forward method describe previously to give a starting time  $t_0$ . In the inverse method however, an additional step is required to calculate the partial derivative  $f'(V_0)$ , this is done analytically whilst ray tracing (Figure B.6a). After ray tracing the

parameter adjustment value,  $d\mathbf{v}$  is solved for using the least squares equation and applied to the starting model,  $\mathbf{V}_0$  to produce an updated model,  $\mathbf{V}_1$  (Figure B.6b). Rays are then re-traced through the updated model, and the new theoretical travel times are calculated,  $t_1$ . The procedure is repeated until a satisfactory fit to the observed data is achieved. In practice the incremental adjustment to the velocity model will become negligibly small for increasing numbers of iterations, so a stopping criteria is often applied (Figure B.6c).

In the case of the real Earth there are  $i$  observed travel times, from which we wish to construct a complex model consisting of  $j$  parameter nodes each of which must be optimized. In vector notation the least squares equation becomes;

$$\Delta\mathbf{t} = \mathbf{A}\Delta\mathbf{m}$$

where,

$\Delta\mathbf{t}$  is the travel time residual vector,

$\mathbf{A}$  is the partial derivative matrix containing the elements  $\partial t_i / \partial m_j$

where  $t_i$  is the  $i^{\text{th}}$  observed travel time, and  $m_j$  is the  $j^{\text{th}}$  model parameter selected for adjustment in the inversion, and

$\Delta\mathbf{m}$  is the model parameter adjustment vector.

In general, not all the travel time observations will fit the velocity model due to errors in the travel time data and inadequate knowledge of the velocity function, so an error term is introduced into the least squares equation. A damping parameter is included to increase the stability of the inversion. The damped least squares equation can thus be rewritten in the form;

$$\Delta\mathbf{m} = (\mathbf{A}^T \mathbf{C}_t^{-1} \mathbf{A} + \mathbf{D} \mathbf{C}_m^{-1})^{-1} \mathbf{A}^T \mathbf{C}_t^{-1} \Delta\mathbf{t}$$

where,

$\mathbf{C}_t = \text{diag} \{ \sigma_i^2 \}$  is the estimated data covariance,

$\mathbf{C}_m = \text{diag} \{ \sigma_j^2 \}$  is the estimated model covariance, and

$D$  is the damping parameter.

The standard deviation  $\sigma_i$  is the estimated uncertainty of the  $i^{\text{th}}$  travel time measurement. The value of  $\sigma_j$  is an a priori estimate of the uncertainty of the  $j^{\text{th}}$  model parameter (Zelt and Smith, 1992). The relative sizes of the data and model covariances determine the trade off between the size of the velocity and interface adjustments in the inversion (Figure B.7). The damping parameter controls the trade-off between resolution and uncertainty of the model parameters, as well as the size of the parameter adjustments (Lutter *et al.*, 1990; Zelt and Smith, 1992). The damping parameter must be chosen to minimize the trade-off curve between the spread of resolution and the size of covariance (Figure B.7).

A variety of techniques can be used to perform the damped least squares inversion, and hence solve for the parameter adjustment vector,  $\Delta m$ . Both the travel time residual vector and the partial derivative matrix are calculated analytically while ray tracing. The matrix inversion is performed by using a singular valued decomposition - a standard method that eliminates the need to calculate the inverse term in the damped least squares equation (Benz, 1982). Hence the parameter adjustment vector can be solved for and applied to update the model. This procedure is repeated until a prescribed fit is achieved, or a stopping criteria is satisfied.

*Resolution:* The model resolution is given by Zelt and Smith [1992];

$$R = (A^T C_t^{-1} A + D C_m^{-1})^{-1} A^T C_t^{-1} A$$

The resolution values range between zero and unity, with unity indicating a perfect resolution. Physically the parameter resolution,  $R$  can be thought of as an indication of the relative ray coverage that samples each model parameter. A high resolution implies overall consistency through the data set, rather than any indication of model uniqueness. Clearly, the parameter resolution is functionally related to the number of data points, the number of rays, and the number of nodes used in an inversion. *Zelt and Smith*

[1992] used synthetic data to specify that reliable nodal parameterizations are achieved when the resolution value exceeds 0.6.

*Errors and Model Uniqueness:* The inversion scheme calculates the standard errors or uncertainty of the model parameters by taking the square root of the diagonal elements of the covariance matrix (Zelt and Smith, 1992). The calculated parameter uncertainties are a function of the estimated travel time pick uncertainties, so they do not account for all possible sources of error. It is thus the case that the uncertainty estimates should be used in a relative sense rather than an absolute sense. Model uniqueness is best estimated by performing a series of perturbations as described for the forward method. The inversion scheme allows a quantitative assessment of the dependence of a particular nodal parameterization on the final velocity model.

*Practical Application:* In practice the inverse step is restricted by the idiosyncrasies of the ray method. Reliable inversions are obtained only if the nodal parameterization is vastly over constrained (in chapter two for example 3026 data points were used to resolve 61 parameter nodes). The automated ray tracing routine used to implement the forward step can 'hang up' if the velocity model becomes too complex, or if an interface with a corner is encountered. This means that the model must remain relatively smooth to allow rays to be propagated through the velocity model. Consequently, it is often very difficult to construct complex laterally heterogeneous velocity structures.

The inverse method supplies the interpreter with a useful and fast convergence to a given model parameterization. This increased modeling power, is set back by the need to assess the affect of a particular model parameterization on the updated model. This amounts to an application of trial-and-error modeling using an automated forward step. A comparison of the forward and inverse methods is summarized in the Table B.1.

## B.6 Discussion and Conclusions

A successful interpretation of a seismic refraction/wide-angle reflection data set is in effect a numerical encoding of the Earth's seismic response function. Whilst the utilization of numerical modeling procedures has the potential to enhance our understanding of the Earth's structure these methods can be used incorrectly to resolve features smaller than the imaging wavelength, or in extreme cases to mis-interpret the seismic data through the incorrect identification of the seismic wave field. In this respect the complexity of the model is largely a function of the interpreters judgment - how much one can accurately see in the data. It has been shown that a variety of different interpretations are not only possible but probable for a given seismic record section (Mooney, 1989).

The seismic refraction/wide-angle reflection data which forms the core of this thesis exposes many of the intricacies and subtleties of the ray trace method. The  $\approx 1$  km spatial sampling of the Ontario-New York-New England data set reveals complexities in the seismic phases which can not be replicated by a homogeneous layered Earth model. In this thesis the seismic data have been grossly over simplified, complex laterally heterogeneous structures have been reduced to a homogeneous isotropic approximation. In this respect the traditional interpretation technique coined by Mohorovicic of matching a set of travel-time hyperbolae to a seismic record section is shown to be unsatisfactory.

Recently a great deal of play has been made of the ability of linearized inversion methods to eliminate the subjectivity inherent in forward modeling (Lutter *at al.*, 1990; Zelt and Smith, 1992). This is far from being the case; the 'final' model still remains the product of the input travel time data and of the model parameterization. The inverted velocity model is obtained from a reduced subset of the seismic wave field which has been picked using highly subjective criteria based mostly on the interpreter's

---

intuition and experience. Furthermore, the success of an inversion depends critically on the parameterization of the model, so that a given inversion is equally as non-unique as its forward modeled counterpart.

---

**B.7 References**

- Benz, H.M., Simultaneous Inversion for lateral velocity variations and hypocenters in the Yellowstone region using earthquake and seismic refraction data, *Unpublished Masters Thesis*, University of Utah, pp. 105, 1982.
- Cerveny, V., I.A. Molotkov, I. Psencik, Ray Method in Seismology, Karlova Univ. Press, Prague, 214 pp., 1977.
- Lines L.R. and S. Treitel, Tutorial: A review of least squares inversion and its application to geophysical problems, *Geophysical Prospecting*, 32, 159-186, 1984.
- Luetgert, J.H., Users Manual for RAY83/R83PLT: Interactive two-dimensional ray tracing /synthetic seismogram package, *U.S. Geol. Surv. Open File Report 88-238*, 1988.
- Lutter W.J., R.L. Nowack , and W.L. Braile, Seismic imaging of upper crustal using travel times from the PASSCAL Ouachita Experiment, *J. Geophys. Res.*, 95, 4621-4631, 1990.
- Mooney, W.D., Seismic methods for determining earthquake source parameters and lithospheric structure, in *Geophysical Framework of the Continental United States*, edited by L.C. Pakiser and W.D. Mooney, *Geol. Soc. Am., Memoir 172*, pp. 11-34, 1989.
- McMechan, G.A. and W.D. Mooney , Asymptotic ray theory and synthetic seismograms for laterally varying structures: theory and application to Imperial Valley, California, *Bull. Seismo. Soc. Am.* 70, 2021-2035, 1980.
- Zelt, C.A. and R.B. Smith, Seismic travel time inversion for 2-D crustal velocity structure, *Geophysical Journal International*, 108, 16-34, 1992.

---

**B.8 Captions**

**Table B.1.** A summary of the advantages and disadvantages inherent in the forward and inverse methods.

**Figure B.1.** An example of the model parameterization used in ray trace modeling. A ray path traversing an isotropic velocity trapezoid is shown (a). Snell's Law is applied at an interface (b).

**Figure B.2:** Travel time diagrams for the Grenvillian Ramp structure. This figure is a replica of Figure 1.11 in chapter 1. Travel time picks are shown by the small squares, and calculated travel times are shown by the crosses. The ray diagrams are labeled with reference to features described in the text. Note, irregularities in the ray paths are due to the plotting software, and not due to irregularities in the velocity field.

**Figure B.3:** Travel time diagrams for Ramp 1 (a and b) and Ramp 2 (c and d), showing the effects of perturbing the Grenvillian Ramp model 10 km to the east and west, respectively. Plotting parameters as Figure B.2.

**Figure B.4:** Travel time diagrams for Ramp 3 (a and b) and Ramp 4 (c and d), showing the effect of a rotating the Grenvillian Ramp structure by  $10^\circ$  for Ramp 3 and  $-5^\circ$  for Ramp 4 about the 'Hinge' point. Plotting parameters as Figure B.2.

**Figure B.5:** A simplified example of a linear travel time inversion scheme, using a raytrace forward step and a least squares minimization technique.

**Figure B.6:** The damping factor must be chosen to optimize the trade off between parameter resolution and model stability.

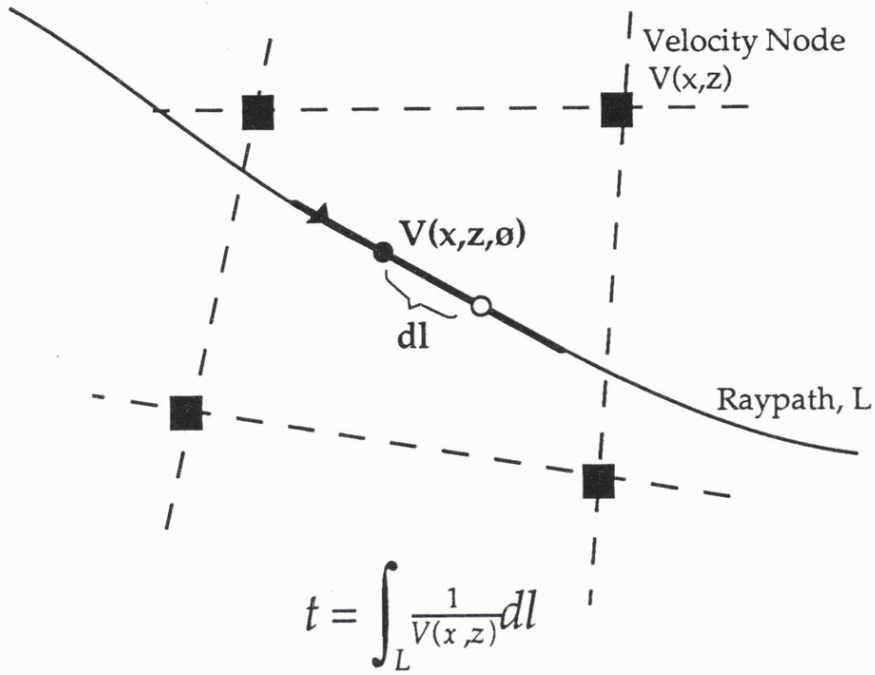
B.9 Table

	<b>Raytrace Forward Modeling</b>	<b>Linearized Travel Time Inversion</b>
<b>Advantages</b>	<ul style="list-style-type: none"> <li>• Simple to construct and edit model.</li> <li>• Easy to input known geologic / geophysical constraints.</li> </ul>	<ul style="list-style-type: none"> <li>• Fast convergence to a local minimum.</li> </ul>
<b>Disadvantages</b>	<ul style="list-style-type: none"> <li>• Extremely slow and tedious</li> <li>• Assessment of 'fit' is highly subjective.</li> </ul>	<ul style="list-style-type: none"> <li>• Difficult to assess sensitivity of model parameterization.</li> <li>• Ray coverage must be uniform.</li> </ul>
<b>Model Parameter-ization</b>	<ul style="list-style-type: none"> <li>• Isotropic velocity trapezoids.</li> <li>• Adjusting an interface changes velocity gradient.</li> </ul>	<ul style="list-style-type: none"> <li>• As forward model</li> </ul>
<b>Data Input</b>	<ul style="list-style-type: none"> <li>• Easily adjusted and changed</li> <li>• Can be smoothed by 'eye'.</li> </ul>	<ul style="list-style-type: none"> <li>• Phase correlations are tied to a particular parameterization</li> </ul>
<b>Estimation of Errors</b>	<ul style="list-style-type: none"> <li>• Absolute error determinations are extremely difficult.</li> </ul>	<ul style="list-style-type: none"> <li>• Estimation of parameter resolution and uncertainty.</li> </ul>

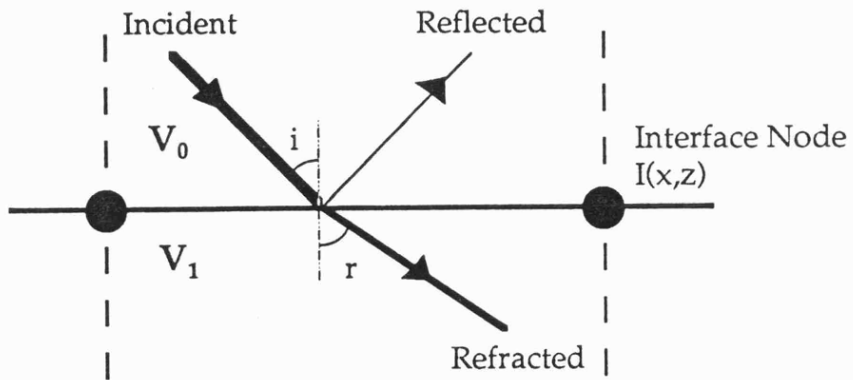
Table B.1

B.10 Figures

a) Model Parametization



b) Interfaces



$$\frac{V_0}{V_1} = \frac{\text{Sini}}{\text{Sinr}}$$

Figure B.1

Travel Time Diagrams for the Grenvillian Ramp Structure

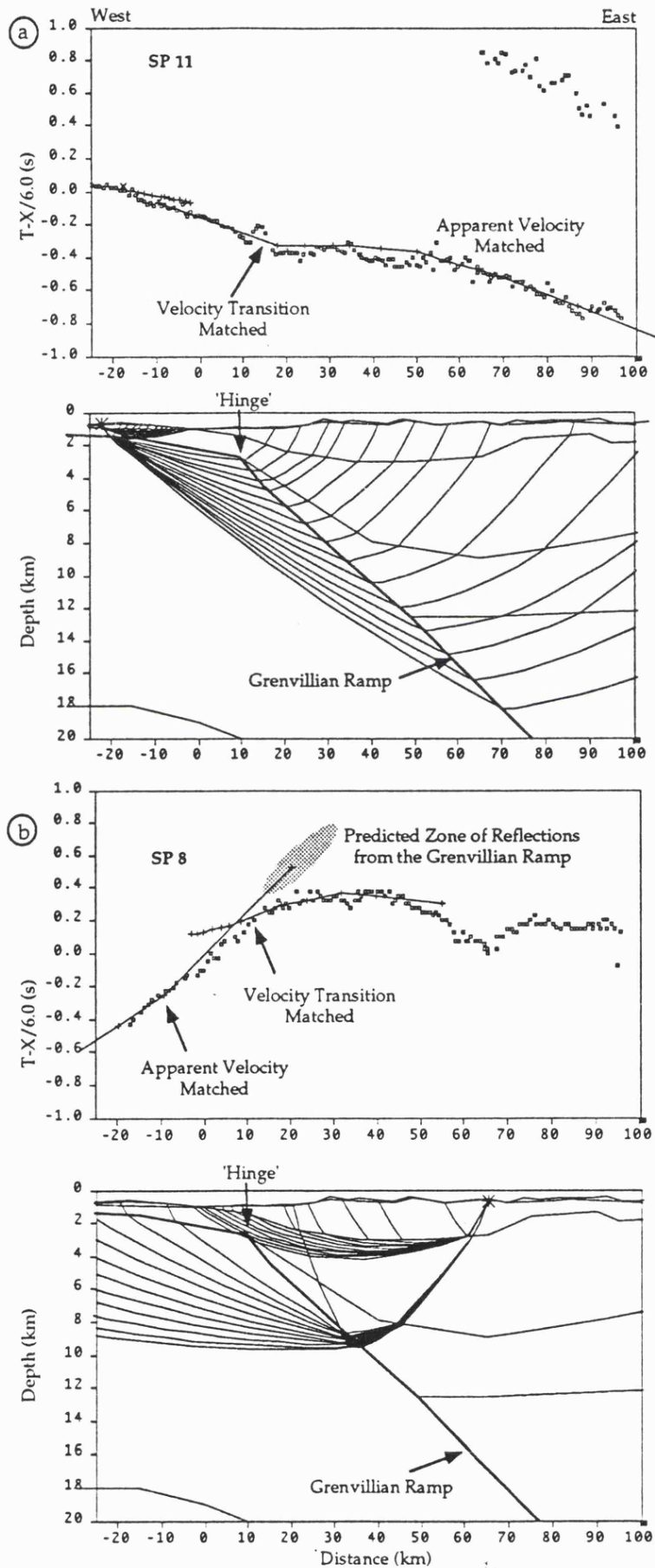


Figure B.2

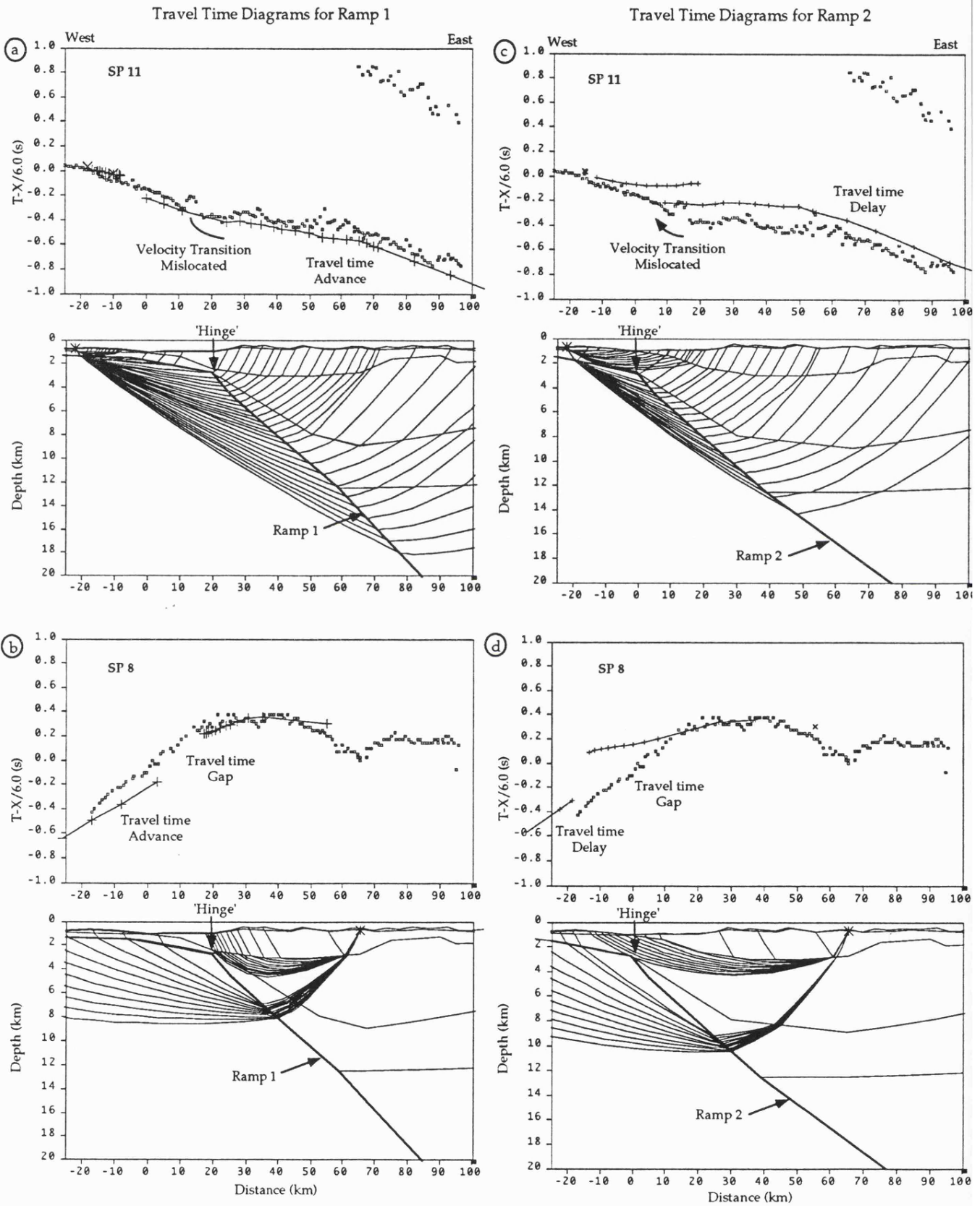


Figure B.3

Travel Time Diagrams for Ramp 3

Travel Time Diagrams for Ramp 4

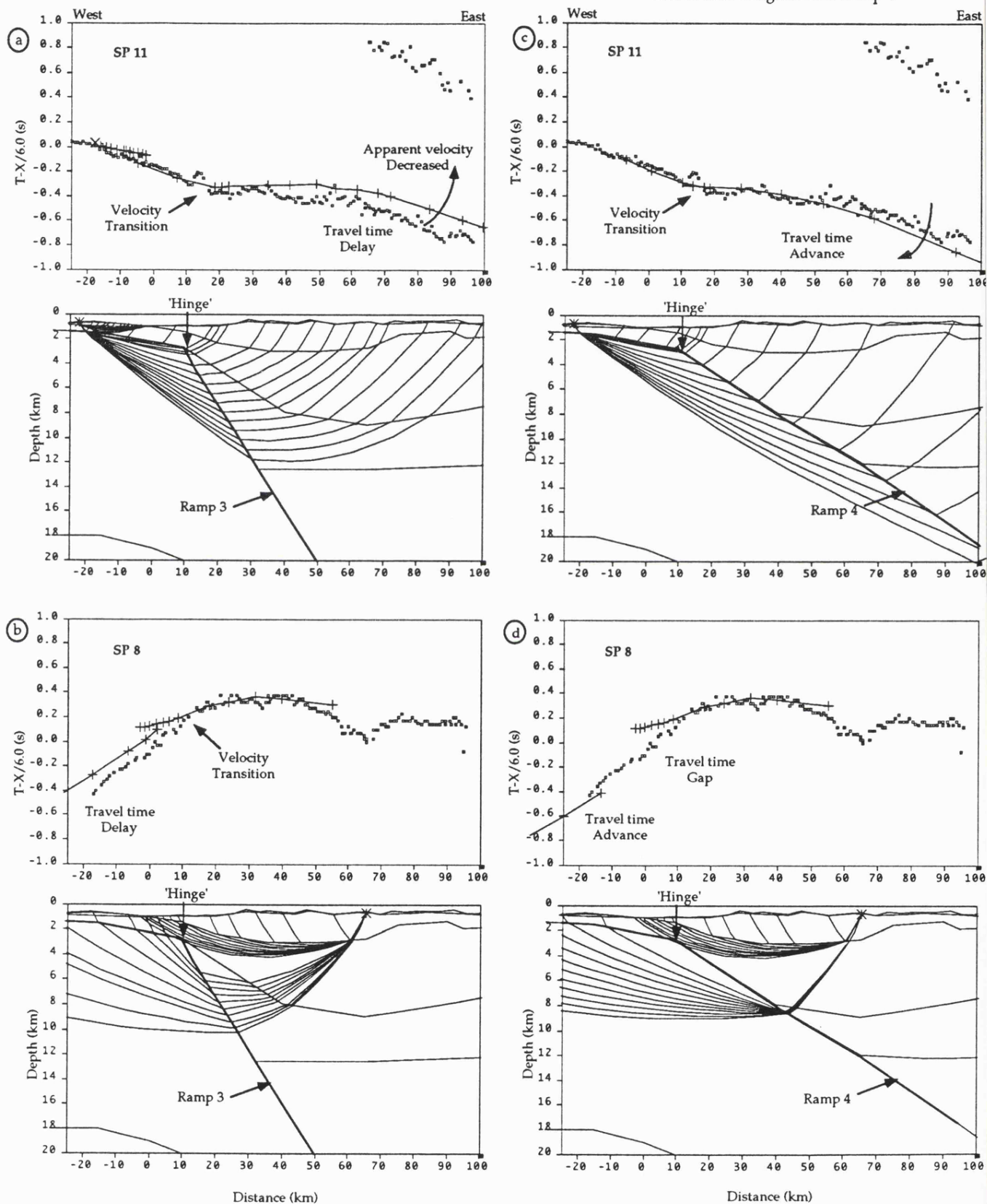
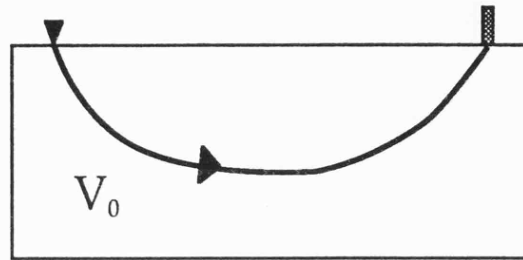


Figure B.4

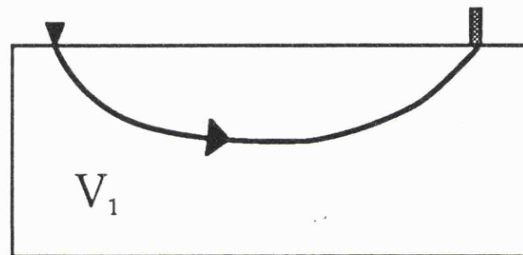
**a) Starting Model,  $V_0$**



Calculated travel time,  $t_0$

Apply the least squares equation,  $t - t_0 = f'(V_0)dv$

**b) Updated Model,  $V_1 = V_0 + dv$**



Calculated travel time,  $t_1$

Reapply the least squares equation,  $t - t_1 = f'(V_1)dv$

**c) Minimize the travel time residual,  $r$**

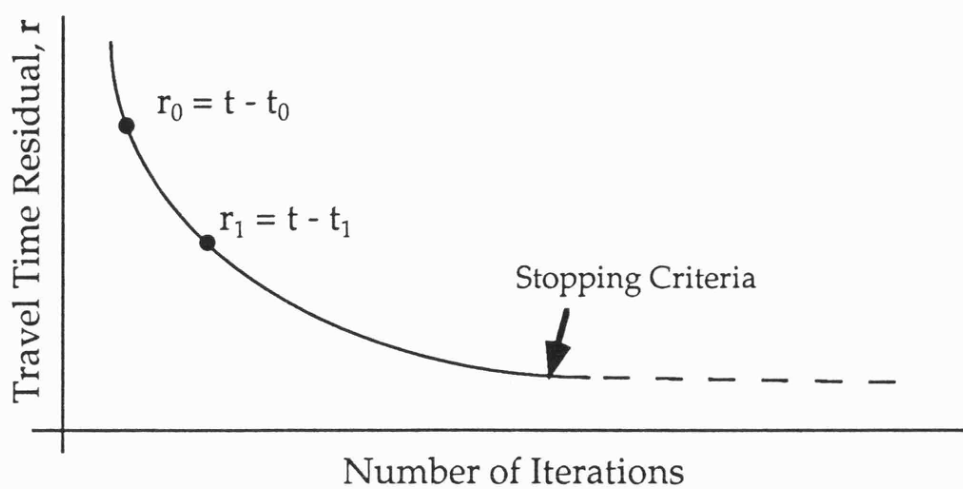


Figure B.5

Trade-off between Resolution and Damping

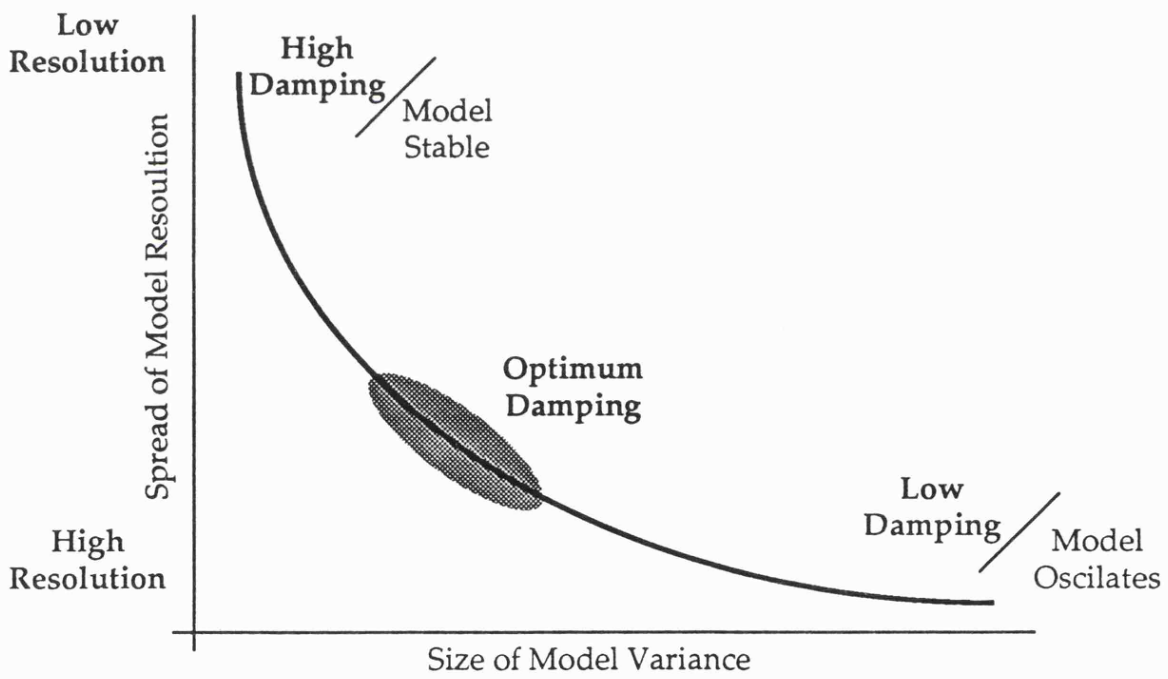


Figure B.6



---

## Rock Sample Data

### C.1 Introduction

The rock sample data presented in Chapter 4 were collected from road cut exposures in the vicinity of the Ontario-New York-New England seismic refraction/wide-angle reflection profile where it traverses central Vermont. Oriented samples about the size of a football were collected from the Champlain Lowlands, the Green Mountain Anticlinorium and the Connecticut Valley Synclinorium. Three mutually perpendicular cores were cut from each of these rock samples. The compressional-wave velocity was measured for each core using a pulsed electronic transducer and receiver arrangement held at elevated pressures using a hydraulic pressure vessel. A description of the laboratory apparatus and methodology is presented by *Christensen* [1965]. The compressional-wave velocity data are shown in Table C.1.

### C.2 Description of the Rock Samples

**Sample a:** Waits River Formation, Barton Member. Lower Devonian

*Description:* Gray fine grained phyllitic schist. Prominent lustrous cleavage surface 220°/40°W.

*Location:* SW of Barre. Second large road cut on route 63 west, located 1.6 miles east of junction with Interstate 89. Sample locality is 87m west of 55 mph sign.

**Sample b:** Missisquoi Formation, Cram Hill Member. Upper Ordovician

*Description:* Gray/green phyllite, foliation striking 210°/sub-vertical.

*Location:* NE of Roxbury. Large road cut on route 12a, 0.5 miles east of railway bridge and immediately west of golf course.

**Sample c:** Stowe Formation. Lower Ordovician

*Description:* Quartz-sericite-chlorite phyllite and schist. vertical cleavage, striking north-south. Rock is weathered.

*Location:* Roxbury Mountain dirt road between Roxbury and East Warren.

Sample collected from second bluff at the top of Roxbury Hill, 2.1 miles east of T-junction at East Warren.

**Sample d** (unable to core this sample): Hazen's Notch Formation.

Cambrian

*Location:* West of Warren. 0.4 miles west of turn off for Lincoln Gap at Warren. Small bluff opposite from 'No Parking' sign.

*Description:* Gray/green quartz-sericite-chlorite-biotite schist. In places, gneissic - quartz partings in a foliated mica schist.

**Sample e:** Underhill Formation. Cambrian

*Location:* Top of Lincoln Gap. Sample collected from large road cut on south side.

*Description:* Dark mica schist with fine silvery micaceous partings.

220°/050°E.

**Sample f:** Mount Holly Complex. Precambrian

*Description:* Muscovite granitic gneiss, weathers to a pale grayish white.

*Location:* South Lincoln. Road cut is 1.3 miles south on fork to South Lincoln, beneath first bridge over Haven River.

**Sample g:** Mount Holly Complex. Precambrian

*Description:* Granitic gneiss, with large blocky quartzite intrusions.

*Location:* Ripton. Road cut is 0.1 miles west of Ripton Store on route 125.

**Sample h:** Cheshire quartzite. Cambrian

*Description:* Pink massive quartzite.

*Location:* East Middlebury. Large roadcut 500m east of bridge on route 125

**Sample i:** Middlebury Limestone. Cambrian

*Description:* Gray massively bedded limestone and interbedded shaley limestones. Buff dolomite exposed in places along roadcut.

*Location:* Middlebury. Large roadcuts on route 125 west of Middlebury.

### C.3 Reference

Christensen, N.I., Compressional-wave velocities in metamorphic rocks at pressures to 10 Kbars, *J. Geophys. Res.*, 70, p. 6147-6164, 1965.

### C.4 Caption

**Table C.1** Seismic velocity measurements of rock samples collected from the western New England Appalachians at elevated pressures. Core A is taken normal to the gneissic foliation (slow direction), core B is taken parallel to the lineation and the foliation (fast direction) and core C is taken parallel to the foliation and perpendicular to the lineation.

C.5 Table

	Core	Density (g/cc)	Velocity (km/s) @ Pressure (MPa)							
			10	50	100	200	400	600	800	1000
Sample a Phyllitic Schist	A	2.741	5.501	5.954	6.123	6.217	6.285	6.324	6.352	6.374
	B	2.728	6.086	6.449	6.583	6.662	6.723	6.758	6.784	6.803
	C	2.739	5.574	6.131	6.308	6.397	6.466	6.506	6.534	6.557
	Mean	2.736	5.720	6.178	6.338	6.425	6.491	6.530	6.557	6.578
Sample b Phyllite	A	2.705	4.731	5.146	5.466	5.677	5.843	5.941	6.011	6.066
	B	2.719	5.560	5.948	6.158	6.343	6.476	6.540	6.586	6.621
	C	2.720	5.765	6.200	6.404	6.554	6.662	6.722	6.765	6.799
	Mean	2.715	5.232	5.765	6.009	6.192	6.327	6.401	6.454	6.459
Sample c Phyllitic Schist	A	2.587	5.031	5.649	5.994	6.287	6.476	6.565	6.627	6.675
	B	2.862	5.643	6.125	6.383	6.588	6.715	6.776	6.819	6.853
	C	2.859	5.632	6.042	6.280	6.496	6.640	6.703	6.745	6.777
	Mean	2.769	5.435	5.939	6.219	6.457	6.611	6.681	6.730	6.769
Sample e Mica Schist	A	2.677	4.909	5.453	5.645	5.793	5.936	6.021	6.082	6.130
	B	2.706	5.590	5.921	6.068	6.183	6.277	6.331	6.369	6.399
	C	2.675	5.471	5.812	5.970	6.103	6.214	6.278	6.324	6.360
	Mean	2.686	5.323	5.729	5.894	6.026	6.142	6.210	6.258	6.296
Sample f Granitic Schist	A	2.670	4.635	5.248	5.586	5.873	6.063	6.154	6.219	6.269
	B	2.666	4.653	5.378	5.734	5.992	6.165	6.260	6.328	6.381
	C	2.682	4.927	5.515	5.809	6.025	6.166	6.240	6.294	6.335
	Mean	2.673	4.738	5.381	5.710	5.963	6.131	6.218	6.280	6.328
Sample g Granitic Gneiss	A	2.752	4.636	5.299	5.604	5.806	5.937	6.009	6.061	6.102
	B	2.727	5.381	5.847	6.048	6.181	6.277	6.332	6.371	6.401
	C	2.741	5.456	5.845	6.030	6.165	6.261	6.314	6.352	6.381
	Mean	2.740	5.158	5.664	5.894	6.051	6.159	6.218	6.261	6.295
Sample h Quartzite	A	2.639	5.575	5.938	6.043	6.105	6.161	6.194	6.217	6.236
	B	2.641	5.640	5.842	5.923	5.973	6.011	6.033	6.049	6.061
	C	2.642	5.729	5.965	6.048	6.105	6.155	6.185	6.206	6.222
	Mean	2.641	5.648	5.915	6.004	6.061	6.109	6.137	6.157	6.173
Sample i Shaley Limestone	A	2.693	5.116	5.668	6.024	6.345	6.525	6.583	6.619	6.647
	B	2.690	4.637	5.308	5.768	6.216	6.484	6.562	6.605	6.636
	C	2.685	4.907	5.544	5.922	6.259	6.471	6.559	6.618	6.665
	Mean	2.689	4.887	5.507	5.905	6.273	6.493	6.568	6.614	6.649

Table C.1